PHOTODISSOCIATION AND PHOTOIONIZATION OF CARBON AND CARBIDE CLUSTERS

by

BRIAN WESLEY TICKNOR

(Under the Direction of Michael A. Duncan)

ABSTRACT

Clusters of carbon, noble metal (Cu, Au) carbide, and silicon carbide are produced in the gas phase as cations in a molecular beam using laser vaporization in a pulsed nozzle cluster source and are detected with time-of-flight mass spectrometry. Neutral clusters of carbon are produced in a similar source and are studied by vacuum ultraviolet photoionization mass spectrometry. Cationic carbon clusters are mass selected and photodissociated using the third (355 nm) harmonic of a Nd:YAG laser or the tunable output of a dye laser. Dissociation proceeds by elimination of C_3, and resonance enhanced photodissociation (REPD) is used to collect spectra for C_6^+ and C_8^+ from 620 – 660 nm. Some transitions are detected which may aid in the future gas phase spectroscopy of these species.

Mass selected carbides are studied by photodissociation at 355 nm. Small copper and gold carbide clusters with an odd number of carbons fragment by losing the entire carbon cluster, while species with an even number of carbons show significant loss of neutral C_3. This even-odd alternation, with the even clusters having mixed fragments, holds true for sizes as large as CuC_{30}^+. In the silicon carbide studies, Si_3C^+ is especially abundant in the mass spectrum, and is also a common fragment from larger clusters, suggesting that it has high relative stability. The

$Si_{7-10}C^+$ clusters lose neutral Si_2C and Si_3C, which are concluded to be stable neutral leaving groups.

Neutral carbon clusters (C_n, n = 2 – 15) produced in a laser vaporization molecular beam source are studied by vacuum ultraviolet (VUV) photoionization mass spectrometry using tunable VUV light from the Advanced Light Source (ALS) at the Lawrence Berkeley National Laboratory. The mass spectra, recorded by single photon ionization at different energies, reveal the distribution of neutral carbon clusters grown from a laser vaporization source. Ionization threshold spectra are recorded from 8 – 12 eV for C_{4-15}, and comparison to theory allows the assignment of isomeric structures for some cluster sizes. The data suggests the presence primarily of a linear structure for C_7, C_9, C_{11}, and C_{13}, and of a cyclic structure for C_{10}.

INDEX WORDS: Laser Vaporization, Molecular Beams, Mass Spectrometry, Photodissociation, Carbon Clusters, Metal Carbide Clusters, Silicon Carbide Clusters, Vacuum Ultraviolet Photoionization

PHOTODISSOCIATION AND PHOTOIONIZATION OF CARBON AND CARBIDE CLUSTERS

by

BRIAN WESLEY TICKNOR

B.S. Furman University, 2002

A Dissertation Submitted to the Graduate Faculty of The University of Georgia in Partial Fulfillment of the Requirements for the Degree

DOCTOR OF PHILOSOPHY

ATHENS, GEORGIA

2008

PHOTODISSOCIATION AND PHOTOIONIZATION OF CARBON AND CARBIDE CLUSTERS

by

BRIAN WESLEY TICKNOR

Major Professor:	Michael A. Duncan
Committee:	Nigel G. Adams Geoffrey D. Smith

Electronic Version Approved:

Maureen Grasso
Dean of the Graduate School
The University of Georgia
May 2008

DEDICATION

This dissertation is dedicated to my mother and father, Jenny Young Ticknor and Robert William Ticknor, who have always, since day one, encouraged the advancement of my education.

ACKNOWLEDGEMENTS

The most important acknowledgement I think any graduate student can make is to their research advisor, so I would like to first thank Dr. Michael A. Duncan. He is always a teacher before he is a boss, and that is something that I have valued and admired very much in my graduate career. His talent and enthusiasm for science is incredible, and it has been a privilege to learn as much from him as I have.

I also want to thank Dr. Lon B. Knight, Jr., my research advisor at Furman University. He is really the reason that I ended up in graduate school and came to Mike's lab at UGA. I think he knew better than I ever did how good of a fit this lab would be for me. Dr. Knight also taught me a couple of things about chemistry that I will never forget. First, he taught me that physical chemists are really just glorified plumbers, and truer words have never been spoken. Second, when asked about the reasons for studying a certain molecule or cluster, and possible applications of this type of research, he gave the standard response any good molecular spectroscopist would give about catalysis and nanoeletronics and so on. Then he said, "And sometimes, it's just because the mountain has never been climbed." It took me a few years before I really understood how profound a driving force in science that seemingly clichéd statement really is. Being the first person to ever measure or study something in the little (or big!) corner of the world that you have chosen for your research is truly an exciting experience.

My family has obviously been an extremely important part of my life, both in graduate school and out, and I want to thank them as well. I don't think I ever would have become a

chemist if my Dad hadn't majored in chemistry at the Air Force Academy. He never really used his degree for science, but it inspired me when I was a kid, and still inspires me now. I usually feel like my Dad knows more about everything than I do, but I think I can finally say that I know more about chemistry than he does. And Mom, I know that you never really understood all this chemistry stuff, but you always supported me in it. Thank you so much for that.

To my brothers, Bobby and John, I think it's safe to say that you have simultaneously driven me crazy and kept me sane. At the end of the day, I know that you both will always be there for me if I ever needed anything, and for that I am grateful. Maybe I will not make you call me Dr. Ticknor.

I would also like to thank everyone I have worked with in the Duncan Lab. In no particular order (in case I messed up): Greg Grieves, Nick Walker, Todd Jaeger, Richard Walters, Tim Ayers, Jared Jaeger, Dinesh Pillai, Karen Molek, Joe Velasquez, Prosser Carnegie, Zack Reed, Tim Cheng, Gary Douberly, Allen Ricks, and Biswajit Bandyopadhyay.

I would also like to give a special thanks John Reddic, who spent a lot of time teaching me about dye lasers, which often involved answering the same questions over and over. It is amazing to me that I can call John up now, almost 10 years after he graduated, and he can still give me details about the ScanMate off the top of his head. John's help was instrumental in generating the data reported in Chapter 3 of this dissertation.

My final word of thanks goes out the guys at the Chemical Dynamics Beamline of the Advanced Light Source, specifically Leonid Belau and Musa Ahmed. From June 2006 to February 2007 I took three trips to Berkeley and spent almost a month and a half out there. I had a great time, and learned a lot too. The data presented in Chapter 6 of this dissertation would not have been possible without the hard work of both of them.

TABLE OF CONTENTS

Page

LIST OF TABLES

Page

LIST OF FIGURES

Page

CHAPTER 1

INTRODUCTION

1.1 CARBON AND CARBIDES IN THE BULK

The study of pure carbon,[1-3] as well as the closely associated transition metal and silicon carbide species, reaches over an extremely wide range of scientific disciplines. The presence of carbon and carbides is ubiquitous throughout areas such as combustion,[4] refractory materials,[5] catalysis,[8-11] electronics,[12] and astrophysics.[13-26] Simply understanding the chemical bonding in these species has long posed a challenge, and developing a better understanding of the chemistry that leads to the multitude of useful properties of these materials would be advantageous to many areas of science.

Bulk carbon exists in two major allotropic forms. Graphite, thermodynamically the most stable form of carbon, is made up of sp^2 hybridized atoms, creating a two dimensional hexagonal crystal structure.[12] The remaining valence electron on each atom creates weak interplanar bonding that allows graphite to stack in sheets, and also gives it electrical conductivity. Diamond, however, adopts sp^3 hybridized bonding, leading to a three dimensional, tetrahedral crystal structure. Diamond is an insulator with a large conduction gap (5.5 eV). Both forms of carbon display strong covalent bonding and are among the stiffest (graphite) and hardest (diamond) naturally occurring materials. Carbon also has the highest melting point of any element, and despite the differences in electrical conductivity between graphite and diamond, both are excellent thermal conductors.[12] Because of these properties, due mainly to the unique chemical bonding, carbon has found uses in a wide variety of industrial applications.

Doping metal atoms into carbon, or conversely, doping carbon into metals, has long been recognized as a way to change the physical properties of a material. Perhaps the best known example of this is the addition of a small percentage of carbon to iron in

the steel making process. Careful control of the exact amount of carbon mixed with the iron allows for the selection of a number of different physical properties, including hardness, ductility, and tensile strength. Additionally, the intercalation of metals between graphite sheets offers one method of altering the electrical conductivity characteristics of the material, which is often critical in the semiconductor industry.[12]

The term carbide technically refers to compounds of carbon with elements that possess a lower electronegativity.[27] The alkaline, alkaline earth, and main group metals tend to form salt-like carbides, in which the bonding is regarded as mostly ionic. Transition metals, on the other hand, form interstitial compounds, in which the carbon occupies the octahedral sites in the face centered metal lattice.[6-8,27] Thus the insertion of the carbon atom creates little change in the metallic bonding network, serving mainly to stabilize the lattice. This explains the refractory properties of these materials, as well as their retention of metallic characteristics, such as high electrical conductivity. Finally, silicon and boron are both known to form covalent bonds with carbon, and thus represent the class of compounds known as covalent carbides.[27] The bonding in silicon carbide is tetrahedral, and each carbon atom is surrounded by four silicon atoms, and vice versa, which continues infinitely in three dimensional arrays. Despite the differences in their chemical bonding, both interstitial and covalent carbides are characterized by their extreme hardness and high melting points. As noted above, however, the metallic lattice structure of interstitial carbides makes them electrical conductors, while covalent carbides are semiconducting. The band gap of silicon carbide varies with the exact crystal structure but is on the order of 2.4 – 3.3 eV.[22]

The hardness and high melting point of interstitial carbides have led to their utilization in many materials science applications, including cutting tools, and they are classified as nonoxidic ceramic materials.[6] They are known to be very active as catalysts for reactions such as hydrogenolysis, hydrogenation, dehydrogenation, methanation, hydrodesulfurization, hydrodenitrogenation, and ammonia synthesis.[6-11] In some cases their catalytic activity approaches that of the considerably more expensive platinum group metals, and there are also indications that they are more resilient to poisoning from sulfur and nitrogen contamination.[8] The catalytic activity of these species is thought to be closely tied to their electronic structure, as are many of their physical characteristics. Thus studying the structure of small, isolated pieces of these substances may help reveal the genesis of their desirable properties.

Carbon and silicon are also known to be two of the most abundant elements in interstellar space, as well as in stellar atmospheres.[1,2,13-21] Carbon species were detected in astrophysical sources more than 100 years ago, and have been found in comets, stars, and interstellar clouds.[2] Many of the molecules which have been detected by spectroscopic searches of space are made up of carbon chains combined with various main group elements, including silicon.[18] Carbon chains have also been suggested as possible carriers of the diffuse interstellar bands (DIBS), which are unassigned absorption bands in the visible region of the spectrum detected in space.[2,13,19-21] Recent spectroscopic work by Maier has proven that small neutral carbon molecules are not the carriers of the DIBs,[19,20] but many other types of carbon and carbide molecules, likely present in astrophysical conditions, have yet to be studied in the laboratory. Additionally, through the study of meteorites, metal and silicon carbide species are known to be present

in presolar grains that are left over from the formation of the solar system,[24,25] and titanium carbide nanocrystals have been assigned as the carrier of the 21 μm band observed in the atmospheres of some stars.[26] Thus the study of carbon and carbide species may aid astrophysics by identifying potential candidates detection, and providing laboratory comparisons to astronomical data.

1.2 CLUSTERS

Many of the bulk properties described in the discussion above are intimately related to the electronic structure and chemical bonding present in a particular material, as well as the doping level in the composites. One method for investigating the chemical origin of bulk physical properties is by studying very small particles, or clusters, of the material.[28-31] Clusters can be made up of anywhere from two or three to several hundred atoms or molecules, and exist in the nanometer size range. Metallic and semiconductor clusters are now recognized to have structures and properties that may differ significantly from the bulk material, but at increasing sizes their chemical and physical behavior should approach that of the bulk.[30] Thus clusters represent an intermediate step between isolated atoms and molecules and solid materials. The structure and reactivity of clusters, as well as their optical and electrical properties, can depend strongly on their size. The study of clusters thus allows the examination of these properties on as a function of size.[30] In this way clusters with interesting properties, such as unusual reactivity or stability, can be identified. Elucidating the specific properties of clusters thus has implications for applied fields such as catalysis[6-11] and nanoelectronics.[12] Great scientific

interest remains, however, in studying the nature of the unique bonding present in small clusters and in watching the emergence of bulk characteristics with increasing size.

Cluster science has led to the discovery several remarkable species with unusual geometries and properties. The most famous example of this is the production of a cluster containing sixty carbon atoms. Smalley and co-workers, in 1985, were studying carbon clusters produced by laser vaporization of a graphite disc by mass spectrometry.[32,33] A mass peak corresponding to 720 atomic mass units, or 60 carbon atoms, was extremely prominent. Subsequent experiments showed C_{60} to have a unique geometry. It is a spherical shell of carbon atoms, which has sp^2 hybridized bonding, similar to graphite.[12,33] The molecule was named buckminsterfullerene, and since the initial discovery many other larger and smaller molecules in the fullerene family have been found.[12] Fullerenes are characterized by high chemical stability, and were isolated in the condensed phase in macroscopic quantities by 1990.[34] Interest in these molecules quickly led to the generation of long tubes of fullerenes, commonly called carbon nanotubes, which, like C_{60}, have attracted an incredible amount of scientific attention due to their unique physical and chemical properties.[35]

A similar story exists in the study of transition metal carbide clusters. In 1992 Castleman and co-workers, using mass spectrometry, observed the formation of clusters with the general form M_8C_{12}, which were dubbed metallocarbohedrenes, or met-cars.[36] The clusters are created by the combination of metal and carbon in a laser plasma, and show extremely high relative stability. Most of the early transition metals are reactive enough to form met-cars clusters, and numerous examples have been produced in the gas phase. Duncan and co-workers expanded on the initial discovery and identified larger

metal carbide clusters with stiochiometries of $M_{14}C_{13}$.[37] Laser photodissociation studies indicated that these larger nanocrytal clusters have a rock salt lattice structure. Met-cars have yet to be synthesized in the condensed phase, which has limited the ways in which they can be studied and has prevented their use in a wider range of chemical and materials science experiments, as compared to fullerenes.

The illustrations of C_{60} and met-cars above represent just two particular examples of interesting results of cluster studies. Undoubtedly more such systems still await discovery, and research in cluster science remains a very active area. Clusters can be produced by a wide variety of experimental methods, and many novel cluster generation techniques have been developed over the years.

1.3 CLUSTER PRODUCTION AND DETECTION

Early studies of clusters relied on high temperature Knudsen oven effusion mass spectrometric techniques. Experiments by Chupak,[38] Inghram,[38,39] and Drowart[39] made clusters of carbon by heating graphite in tungsten or tantalum ovens. Only small species are produced in these oven techniques, on the order of $C_{4\text{-}5}$, even though carbon is now known to form clusters more readily than most other elements.[30] Similar techniques were applied to metal carbides. These experiments recorded ionization efficiency curves and generated appearance potentials as well as estimates of the dissociation energy, heat of formation, and atomization energies of small clusters.[40-44] Berkowitz and co-workers,[40] in a study focusing on aluminum, gallium, and lanthanum, predominately observed the formation of the dicarbide and tetracarbide species. Later experiments by Gingerich and

co-workers did observe the larger MC_3^+, MC_5^+, and MC_6^+ species, but the ion intensities were considerably less than for MC_2^+ and MC_4^+.[44]

It is now understood that cluster growth occurs by gas phase collisions of vaporized atoms or molecules.[31] These early studies were limited by the concentrations they could achieve from oven vaporization sources. Additionally, extremely high temperatures are required to produce vapor from graphite or carbides, making the atoms or molecules produced in this way very hot. These experiments lacked additional collision partners in the vapor to quench condensation energy, which heats up a cluster as bonds are formed between species in the vapor. The presence of a collision gas, which lowers the internal energy, allows larger species to form and helps prevents fragmentation.[28,31]

Ion sputtering has also been employed to produce metal carbide and silicon clusters.[31,45-48] In this experiment, a fast ion beam of an inert gas, typically argon, is accelerated to around 10 keV and used to bombard a target of the sample material. As with the oven experiments, this technique is also limited in the cluster sizes it can produce. The ions are also internally hot, as the main cooling mechanism is evaporation. Only species with high relative stability are likely to survive this growth process, so studying a wide distribution of clusters is difficult.[31]

The advent of the laser ablation source by Smalley and co-workers in 1981 led to a very efficient method for vaporizing metal and growing clusters.[49] In this method, a pulsed laser is focused onto a solid sample and the material is vaporized instantly. Essentially any solid material can be produced in the gas phase by laser vaporization. These sources are generally coupled to supersonic expansions from a pulsed nozzle to

produce clusters in a molecular beam. A pulse of the carrier gas, typically an inert gas such as helium or argon, rapidly quenches the laser generated vapor and promotes aggregation by taking away internal energy through three body collisions. The fast cooling in these sources permits the formation of a wide distribution of cluster sizes. Fragmentation processes are limited because collisions do not occur after the expansion and cooling has taken place. Clusters produced in a laser vaporization source may be neutral or ionic, enabling the study of many different systems. This technique also offers the advantage that ligands of interest may be seeded directly into the expansion gas, which can produce both weakly bound metal-ion ligand complexes[50] or strongly bound species such as metal oxides [51] and metal carbides.[37]

The clusters produced in the sources described above are generally detected by mass spectrometers. This requires some sort of ionization process, however. Electron impact ionization (EI) was the ionization method used in most of the early oven vapor experiments.[38-44] This process can be efficient when the energy of the electron is above the ionization potential (IP) of the species.[52] Excess energy above the IP can be deposited in the cluster, however, leading to internal heating and fragmentation. One alternative is laser photoionization, which uses laser light to ionize neutral clusters. The IPs of C_3 and Si_3, however, are both fairly high, 11.61 eV[53] and 7.9 eV,[54] respectively. Thus the use of common ultraviolet laser lines at 355 nm (3.49 eV) or 193 nm (6.42 eV) would require the absorption of multiple photons to ionize these small neutral species. As with EI, multiphoton absorption can leave significant internal energy in the clusters and cause fragmentation. Even the use of vacuum ultraviolet (VUV) photoionization at 118 nm (10.5 eV) cannot ionize C_3 with a single photon. An added complication is that

the photon absorption cross sections can be energy and cluster size dependent, so some clusters may absorb more efficiently than others. This potential bias in the ionization process makes it difficult to determine nascent cluster distributions. Recent experiments at the Advanced Light Source, detailed in Chapter 6 of this dissertation for carbon clusters, have overcome some of these limitations by utilizing tunable VUV light to ionize carbon species at threshold.[53,55,56] This experiment is relatively new, however, and requires synchrotron radiation, so it has not yet come into common use. One method for avoiding detection bias, commonly employed in our lab, is to measure cations produced directly by the laser vaporization in the supersonic expansion.

1.4 PREVIOUS WORK ON CLUSTERS OF CARBON AND CARBIDES

As described above, many of the early experiments used the Knudsen effusion oven mass spectrometric technique, but the cluster sizes attained in the experiments were fairly small.[40-44] Other experiments trapped species produced by vaporization in ovens in rare gas matrices to study both infrared and visible spectroscopy.[57] Trapping carbon species in matrices allows for higher concentrations than is possible in the gas phase, and recombination events are possible under these conditions. Thus larger clusters were grown, and spectroscopy was measured on clusters as large as C_9.

The study of clusters of this sort was greatly accelerated by the advent of the laser vaporization pulsed nozzle cluster source,[49] as described above. Many mass spectrometry experiments have studied carbon clusters produced from laser ablation of graphite in a helium expansion.[1,2,32,33,58-64] Neutral clusters,[63,64] as well as cations[58-62] and

anions,[1,2] are all produced simultaneously in these experiments. Clusters with enhanced abundances have been seen, most famously $C_{60,}$ as mentioned above,[1,2,32,33] but other cluster sizes may also be prominent depending on the specifics of the experiment. Photodissociation,[62,65-68] metastable ion decay,[69,70] and collision induced dissociation (CID)[66,71] have been used to study the fragmentation behavior of carbon clusters. All these experiments show that small clusters ($C_n^{+/-}$, n< 30) fragment predominately by the loss of neutral C_3. The larger fullerene clusters however, lose either C_2 or C atom.[1,2,65,67] Fourier transform ion cyclotron resonance (FT-ICR) mass spectrometry has measured the IPs of small carbon clusters by charge-transfer bracketing reactions.[72] Ion mobility experiments by Bowers and co-workers on mass selected ions have detected both linear chain and cyclic ring isomers at small sizes and fullerenes appear at C_{30}^+ and larger sizes.[71] These experiments also concluded that the linear chains were much more reactive than the rings.

Neutral carbon molecules have been studied by electronic,[1,2,81] infrared,[1,2,57,82-88] and Raman[89,90] matrix isolation spectroscopy, but only a few gas phase measurements have been made.[1,2,90-94] Terahertz spectroscopy has also been employed.[95] Anions have been studied with resonance-enhanced photodetachment spectroscopy,[2,96,97] photoelectron spectroscopy,[2,98-100] and matrix isolation infrared spectroscopy.[101] Carbon cluster cations have proven more difficult to study with spectroscopy, which is largely limited to several recent studies by Maier and coworkers which reported the electronic and infrared absorption spectra of the C_6^+ ion in a neon matrix, and the electronic spectra for $C_{7\text{-}9}^+$ isolated in a matrix.[102] Much theoretical work on the neutral[1,2,103-118] and

charged[119-130] species has guided the spectroscopic studies and helped to confirm the structures and energetics of these clusters.

Transition metal carbide clusters have also been studied extensively. The pioneering work by Castleman and coworkers and Duncan and coworkers on met-cars, described above,[36,37] has led to many other experimental inveistigations.[131] Fragmentation of these clusters has been studied by photodissociation,[37,132] CID,[133] and metastable decay.[134] Ion mobility[135] experiments by Bowers and co-workers and photoelectron[136] spectroscopy by Wang and co-workers, along with numerous theoretical studies,[131,137-140] have helped reveal the structures of both met-cars and nanocrystals. More recently, infrared multi-photon ionization spectroscopy with a tunable free electron laser was used to measure the infrared spectrum of these species, confirming the cubic rock salt lattice structure for the nanocrystal.[141]

Metal carbides have been produced by oven sources,[40-44,142] laser photolysis of organometallic vapor,[143] and laser vaporization sources,[144-149] and studied by mass spectrometry. Ion mobility has also been used by Jarrold and co-workers in experiments focused on smaller metal carbide clusters as well as the formation of larger metallofullerenes.[150]

Neutral diatomic transition metal carbide molecules have been studied spectroscopically by laser induced fluorescence,[151-154] resonant two photon ionization,[155] dispersed fluorescence,[156] and millimeter wave spectroscopy.[157] Matrix isolation has been used to measure the vibrational spectra of a variety of small metal carbides.[158] Metha and co-workers studied tantalum carbide clusters of the type Ta_mC_n (m = 1-6, n = 1-7) with multiphoton ionization in a reflectron time of flight mass spectrometer.[159]

Anionic metal carbide clusters have also been studied in the gas phase by photoelectron spectroscopy,[160-163] ion mobility,[164] and FT-ICR mass spectrometry coupled with CID.[143]

An extensive amount of computational work has been conducted specifically on met-cars clusters.[131,137-140] Smaller clusters have also been studied, and as with the experimental work, much of the theoretical work consists of studies of the early transition metals.[165-170] In the course of studying met-cars, theoretical investigations of small metal carbide clusters have also been conducted.[131,171-190] Diatomic neutral carbides of the 3d,[188,189] 4d,[190a] and 5d[190b] transition metals have been the subject of studies analyzing the changes in the bonding as d electrons are added going across the periodic table. Largo and co-workers have additionally looked at the neutral[191a] and cationic[191b] dicarbides of the first row transition metals in order to study the structure and bonding in these systems.

Silicon carbide has also been studied by many of the same techniques listed above. Mass spectroscopy experiments have looked at the products of both laser vaporization[192-194] and ion sputtering.[47,48] The cations have been investigated by photodissociation,[195] but no spectroscopy exists. The anionic clusters have been studied mainly by photoelectron spectroscopy.[196,197] Spectroscopy of the neutrals is more abundant, and they have been studied by infrared spectroscopy in the gas phase[198] as well as in matrices.[199] Microwave and millimeter wave spectroscopy[200] has also been used extensively on these species. Theory has also studied these clusters as both cations[201-205] and neturals.[206-219]

Despite the tremendous amount of previous work on all of these cluster systems, much remains unknown. Spectroscopy of many of the cation systems is sparse, and is

often non-exsitent in the gas phase, where comparison to astronomical data may be relevant. Addtionally, many of the studies on metal carbide clusters examined met-cars but ignored smaller mixed clusters formed from the later transition metal with carbon, so the structure and bonding motifs in these clusters are not well known. Photodissociation has been shown by our group to be an effective way to study relative stabilities and fragmentation channels of strongly bound metal-oxide[51], met-cars,[37,132], and metal-silicon[219] systems. This technique can reveal fragmentation channels, which give insight into structure and bonding, as well as identify stable speciess, either by detecting charged fragments or by inferring neutral elimination products. Resonance enhanced photodissociation can also be used to meausure spectrostroscopy of ions by monitoring fragmentation as a function of laser wavelength.[50] The work presented here applies photodissociation to clusters of carbon, noble metal (Cu, Au) carbide, and silicon carbide. Resonance enhanced dissociation spectra of carbon clusters are also reported for the first time. Finally, the VUV photoionization behavior of neutral carbon clusters is studied using single photon ionization at the Advanced Light Source.

1.5 REFERENCES

(1) Weltner, Jr., W.; Van Zee, R. J. *Chem. Rev.* **1994**, *89*, 1713.

(2) Van Orden, A.; Saykally, R. J. *Chem. Rev.* **1998**, 98, 2313.

(3) Lifshitz, C. *Int. J. Mass Spectrom.* **2000**, *200,* 423**.**

(4) Gardiner, W. C. *Combustion Chemistry*; Springer-Verlag: New York, 1984.

(5) Oyama, S. T., Ed. *The Chemistry of Transition Metal Carbides and Nitrides***;** Blackie: Glasgow, 1996.

(6) Oyama, S. T. *Catal. Today* **1992**, *15*, 179.

(7) Johansson, L. I. *Surf. Sci. Rep.* **1995**, *21*, 177.

(8) Chen, J. G. *Chem. Rev*. **1996**, *96*, 1477.

(9) Chen, J. G. *Surf. Sci. Rep.* **1997**, *30*, 1.

(10) Furimsky, E. *App. Catal. A* **2003**, *240*, 1.

(11) Delannoy, L.; Giraudon, J.-M.; Granger, P.; Leclercq, L.; Leclercq, G *Catal. Today* **2000**, *59*, 231.

(12) Dresselhaus, M. S.; Dresselhaus, G.; Eklund, P. C. *Science of Fullerenes and Carbon Nanotubes;* Academic Press: San Diego, CA, 1996.

(13) Tielens, A.G.G.M., Snow, T. P., Eds., *The Diffuse Interstellar Bands;* Kluwer: Dordrecht, The Netherlands, 1995.

(14) Hartquist, T. W.; Williams, D. A., Eds., *The Molecular Astrophysics of Stars and Galaxies;* Oxford University Press: New York, 1998.

(15) Heath, J. R.; Van Orden, A.; Hwang, H. J.; Kuo, E. W.; Tanaka, K.; Saykally, R. J. *Adv. Space Res.* **1995**, *15*, 25.

(16) Maier, J. P. *J. Phys. Chem. A* **1998,** *102*, 3462.

(17) Kirkwood, D. A.; Linnartz, H.; Grutter, M.; Dopfer, O.; Motylewski, C. T.; Pachkov, M.; Tulej, M.; Wyss, M.; Maier, J. P. *Faraday Discuss.* **1998,** *109*, 109.

(18) Thaddeus, P.; McCarthy, M. C., *Spectrochimica Acta A* **2001,** *57A*, 757.

(19) Maier, J. P.; Walker, G. A. H.; Bohlender, D. A. *Astrophys. J.* **2004,** *602*, 286.

(20) Maier, J. P.; Electronic Spectroscopy of Carbon Chains and Their Relevance to Astrophysics. In *The Dense Interstellar Medium in Galaxies*; Pfalzner, S., Kramer, C., Staubmeier, C., Heithausen, A., Eds.; Springer Proceedings in Physics 91; Springer Verlag: Berlin, 2004; pp 55-60.

(21) Boguslavskiy, A. E.; Dzhonson, A.; Maier, J. P.; The Electronic Spectra of Carbon Chains, Rings, and Ions of Astrophysical Interest. In *Astrochemisty: From Laboratory Studies to Astronomical Observations*; Kaiser, R. I., Bernath, P., Osamura, Y., Petrie, S., Mebel, A. M., Eds.; AIP Conference Proceedings 855, American Institute of Physics: Melville, New York, 2006; pp 201-208.

(22) Henning, T.; Mutschke, H. *Spectrochim. Acta, Part A* **2001**, *57*, 815.

(23) Cataldo, F. *Int. J. Astrobiol.* **2003**, *2*, 51.

(24) Kimura, Y.; Kaiton, C. *Mon. Not. R. Astron. Soc.* **2003**, *343*, 385.

(25) Clayton, D. D.; Nittler, L. R. *Annu. Rev. Astron. Astrophys*. **2004**, *42*, 39.

(26) von Helden, G.; Tielens, A. G. G. M.; van Heijnsbergen, D.; Duncan, M. A.; Hony, S.; Waters, L. B. F. M.; Meijer, G. *Science* **2000**, *288*, 313.

(27) Cotton, F. A.; Wilkinson, G.; Murillo, C. A.; Bochmann, M. *Advanced Inorganic Chemistry*, 6th ed.; Wiley & Sons: New York, 1999.

(28) Mingos, M. P.; Wales, D. J. *Introduction to Cluster Chemistry*; Prentice Hall: Englewood Cliffs, New Jersey, 1990.

(29) Duncan, M. A. Ed. *Advances in Metal and Semiconductor Clusters, Vol. 1*, JAI Press: Greenwich, Connecticut, 1993.

(30) Haberland, H. Ed. *Clusters of Atoms and Molecules I: Theory, Experiment, and Clusters of Atoms;* Springer-Verlag: Berlin, 1995.

(31) Johnson, R. L. *Atomic and Molecular Clusters*; Taylor and Francis: London, 2002.

(32) Kroto, H. W.; Heath, J. R.; O'Brien, S. C.; Curl, R. F.; Smalley, R. E. *Nature* **1985**, *318*, 162.

(33) Kroto, H. W.; Allaf, A. W.; Balm, S. P. *Chem. Rev.* **1991**, *91*, 1213.

(34) Kratchmer, W.; Lamb, L.; Fostiropoulos, D. K.; Huffman, D. *Nature* **1990**, *347*, 354.

(35) (a) Iijima, S. *Nature* **1991**, *354*, 56. (b) Iijima, S. *Nature* **1993**, *363*, 603.

(36) (a) Guo, B. C.; Kerns, K. P.; Castleman, A. W. Jr. *Science* **1992**, *255*, 1411. (b) Guo, B. C.; Wei, S.; Purnell, J.; Buzza, S.; Castleman, A. W. Jr. *Science* **1992**, *256*, 515. (c) Wei, S.; Guo, B. C.; Purnell, J.; Buzza, S.; Castleman, A. W. Jr. *Science* **1992**, *256*, 818. (d) Leskiw, B. D.; Castleman, A. W. Jr. *C. R. Physique* **2002**, *3*, 251.

(37) (a) Pilgrim, J. S.; Duncan, M. A. *J. Am. Chem. Soc.* **1993**, *115*, 6958. (b) Pilgrim, J. S.; Duncan, M. A. *J. Am. Chem. Soc.* **1993**, *115*, 9724. (c) Pilgrim, J. S.; Duncan, M. A. Metal-Carbon Clusters: The Construction of Cages and Crystals. In *Advances in Metal and Semiconductor Clusters*; Duncan, M. A., Ed.; JAI Press: London, 1995; Vol. 3. (d) Duncan, M. A. *J. Clust. Sci* **1997**, *8*, 239.

(38) (a) Chupka, W. A.; Inghram, M. G. *J. Chem. Phys.* **1953**, *21*, 371. (b) Chupka, W. A.; Inghram, M. G. *J. Chem. Phys.* **1953**, *21*, 1313. (c) Chupka, W. A.; Inghram, M. G. *J. Chem. Phys.* **1954**, *22*, 1472. (d) Chupka, W. A.; Inghram, M. G. *J. Phys. Chem.* **1955**, *59*, 100. (e) Chupka, W. A.; Inghram, M. G. *Mem. Soc. Roy. Liege* **1955**, *15*, 373.

(39) Drowart, J.; Burns, R. P.; DeMaria, G.; Inghram, M. G. *J. Chem. Phys.* **1959**, *31*, 1131.

(40) Chupka, W. A.; Berkowitz, J.; Giese, C. F.; Inghram, M. G. *J. Phys. Chem.* **1958**, *62*, 611.

(41) De Maria, G.; Guido, M.; Malaspina, L.; Pesce, B. *J. Chem. Phys.* **1965**, *43*, 4449.

(42) Vander Auwera-Mahieu, A.; Drowart, J. *Chem. Phys. Lett.* **1967**, *1*, 311.

(43) Kohl, F. J.; Stearns, C. A. *J. Phys. Chem.* **1970**, *74*, 2714.

(44) (a) Haque, R.; Gingerich, K. A. *J. Chem. Phys.* **1981**, *74*, 6407. (b) Gupta, S. K.; Nappi, B. M.; Gingerich, K. A. *J. Phys. Chem.* **1981**, *85*, 971. (c) Pelino, M.; Haque, R.; Bencivenni, L.; Gingerich, K. A. *J. Chem. Phys.* **1988**, *88*, 6534. (d) Meloni, G.; Thomson, L. M.; Gingerich, K. A. *J. Chem. Phys.* **2001**, *115*, 4496.

(45) Hofer, W. O. *Sputtering by Particle Bombardment III*; Springer-Verlag: Berlin, 1991.

(46) (a) Leleyter, M.; Ortoli, S.; Joyes, P. *Sur. Sci.* **1981**, *106*, 293. (b) Leleyter, M.; Joyes, P. *Sur. Sci.* **1985**, *156*, 800. (c) Leleyter, M. *J. Phys. II France* **1991**, *1*, 1179.

(47) Yamamoto, H.; Asaoka, H. *Appl. Surf. Sci.* **2001**, *169-170* , 305.

(48) Belykh, S.F.; Rasulev, U. K.; Samartsev, A.V.; Stroev, L.V. ; Zinoviev, A.V. *Vacuum* **2000**, *56*, 257.

(49) (a) Dietz, T. G.; Duncan, M. A.; Powers, D. E.; Smalley, R. E. *J. Chem. Phys.* **1981**, *74*, 6511. (b) Powers, D. E.; Hansen, S. H.; Geusic, M. E.; Puiu, A. C.; Hopkins, J. B.; Dietz, T. G. Duncan, M. A.; Langridge-Smith, P. R. R.; Smalley, R. E. *J. Phys. Chem.* **1982**, *86*, 2556.

(50) (a) Duncan, M. A.; *Int. J. Mass Spectro*. **2000**, *200*, 545. (b) Duncan, M. A.; *Int. Rev. Phys. Chem.* **2003**, *2*, 407.

(51) (a) France, M. R.; Buchanan, J. W.; Robinson, J. C.; Pullins, S. H.; Tucker, J. L.;

King, R. B.; Duncan, M. A. J. *Phys. Chem. A* **1997**, *101*, 6214. (b) Molek, K. S.; Jaeger, T. D.; Duncan, M. A. *J. Chem. Phys.* **2005**, *123*, 144313. (c) Molek, K. S.; Reed, Z. M.; Ricks, A. M.; Duncan, M. A. *J. Phys. Chem. A* **2007**, *111*, 8080. (d) Reed, Z. A.; Duncan, M. A. *J. Phys. Chem. A*, in press. (e) Molek, K. S.; Anfuso-Cleary, C.; Duncan, M. A. *Phys. Chem. A*, in press.

(52) Massey, H. S. W. Electron Collisions with Molecules and Photoionization; Oxford University Press, Oxford, 1969.

(53) Nicolas, C.; Shu, J.; Peterka, D. S.; Hochlaf, M.; Poisson, L.; Leone, S. R.; Ahmed, M. *J. Am. Chem. Soc.* **2006**, *128*, 220

(54) Raghavachari, K.; Logovinsky, V. *Phys. Rev. Lett.* **1985**, *55*, 2853.

(55) Metz, R. B.; Ahmed, M.; Leone, S. R. *J. Chem. Phys.* **2005**, *123*, 114313.

(56) Belau, L.; Wheeler, S. E.; Ticknor, B. W.; Ahmed, M.; Leone, S. R.; Allen, W. D.; Schaefer, H. F. III; Duncan, M. A. *J. Am. Chem. Soc.* **2007**, *129*, 10229.

(57) (a) Weltner, W., Jr.; Walsh, P. N. *J. Chem. Phys.* **1962**, *37*, 1153. (b) Weltner, W., Jr.; Walsh, P. N.; Angell, C. L. *J. Chem. Phys.***1964**, *40*, 1299. (c) Weltner, W, Jr.; McLeod, D., Jr.; Angell, C. L. *J. Chem. Phys.* **1964**, *40*, 1305. (d) Weltner, W. Jr.; MeLeod, D. Jr. *J. Chem. Phys.* **1966**, *45*, 3096. (e) Weltner, W., Jr.; Thompson, K. R.; DeKock, R. L. *J. Am. Chem. Soc.* **1971**, *93*, 4688.

(58) Rohlfing, E. A. *J. Chem. Phys.* **1990**, *93*, 7851.

(59) Moriwaki, T.; Kobayashi, K.; Osaka, M.; Ohara, M.; Shiromaru, H.; Achiba, Y. *J. Chem. Phys.* **1997**, *107*, 8927.

(60) Choi, Y.-K.; Im, H.-S.; Jung, K.-W. *Int. J. Mass Spectrom.* **1999**, *189*, 115.

(61) Bae, C. H.; Park, S. M. *J. Chem. Phys.* **2002**, *117*, 5347.

(62) (a) Geusic, M. E.; Jarrold, M. F.; McIlrath, T. J.; Bloomfield, L. A.; Freeman, R. R.; Brown, W. L. *Z. Phys. D: At., Mol. Clusters* **1986**, *3*, 309. (b) Geusic, M. E.; McIlrath, T. J.; Jarrold, M. F.; Bloomfield, L. A.; Freeman, R. R.; Brown, W. L. *J. Chem. Phys.* **1986**, *84*, 2421. (c) Geusic, M. E.; Jarrold, M. F.; McIlrath, T. J.; Freeman, R. R.; Brown, W. L. *J. Chem. Phys.* **1987**, *86*, 3862.

(63) Kaizu, K.; Kohno, M.; Suzuki, S.; Shiromaru, H.; Moriwaki, T.; Achiba, Y. *J. Chem. Phys.* **1997**, *106*, 9954.

(64) (a) Wakabayashi, T.; Momose, T.; Shida, T. *J. Chem. Phys.* **1999**, *111*, 6260. (b) Kato, Y.; Wakabayashi, T.; Momose, T. *J. Chem. Phys.* **2003**, *118*, 5390.

(65) O'Brien, S. C.; Heath, J. R.; Curl, R. F.; Smalley, R. E. *J. Chem. Phys.* **1988**, *88*, 220.

(66) Sowa, M. B.; Hintz, P. A.; Anderson, S. L. *J. Chem. Phys.* **1991**, *95*, 4719.

(67) Bouyer, R.; Roussel, F.; Monchicourt, P.; Perdix, M.; Pradel, P. *J. Chem. Phys.* **1994**, *100*, 8912.

(68) (a) Pozniak, B. P.; Dunbar, R. C. *Int. J. Mass Spectrom. Ion Processes* **1997**, *165*/*166*, 299. (b) Pozniak, B.; Dunbar, R. C. *Int. J. Mass Spectrom. Ion Processes* **1994**, *133*, 97.

(69) Radi, P. P.; Bunn, T. L.; Kemper, P. R.; Molchan, M. E.; Bowers, M. T. *J. Chem. Phys.* **1988**, *88*, 2809.

(70) (a) Gluch, K.; Matt-Leubner, S.; Echt, O.; Concina, B.; Scheier, P.; Mark, T. D. *J. Chem. Phys.* **2004**, *121*, 2137. (b) Concina, B.; Gluch, K.; Matt-Leubner, S.; Echt, O.; Scheier, P.; Mark, T. D. *Chem. Phys. Lett.* **2005**, *407*, 464.

(71) Sowa-Resat, M. B.; Hintz, P. A.; Anderson, S. L. *J. Phys. Chem.* **1995**, *99*,

10736.

(72) (a) Bach, S. B. H.; Eyler, J. R. *J. Chem. Phys.* **1990**, *92*, 358. (b) Ramanathan, R.; Zimmerman, J. A.; Eyler, J. R. *J. Chem. Phys.* **1993**, *98*, 7838.

(73) (a) von Helden, G.; Hsu, M. T.; Kemper, P. R.; Bowers, M. T. *J. Chem. Phys.* **1991**, *95*, 3835. (b) von Helden, G.; Hsu, M. T.; Gotts, N.; Bowers, M. T. *J. Phys. Chem.* **1993**, *97*, 8182. (c) von Helden, G.; Gotts, N. G.; Bowers, M. T. *J. Am. Chem. Soc.* **1993**, *115*, 4363. (d) von Helden, G.; Gotts, N. G.; Bowers, M. T. *Chem. Phys. Lett.* **1993**, *212*, 241. (e) von Helden, G.; Palke, W. E.; Bowers, M. T. *Chem. Phys. Lett*. **1993**, *212*, 247. (f) Gotts, N. G.; von Helden, G.; Bowers, M. T. *Int. J. Mass Spectrom. Ion Processes* **1995**, *149/150*, 217.

(80) (a) Hunter, J. M.; Fye, J. L.; Roskamp, E. J.; Jarrold, M. F. *J. Phys. Chem.* **1994**, *98*, 1810. (b) Shvartsburg, A. A.; Hudgins, R. R.; Dugourd, P.; Gutierrez, R.; Frauenheim, T.; Jarrold, M. F. *Phys. Rev. Lett.* **2000**, *84*, 2421.

(81) (a) Forney, D.; Fulara, J.; Freivogel, P.; Jakobi, M.; Lessen, D.; Maier, J. P. *J. Chem. Phys.* **1995**, *103*, 48. (b) Freivogel, P.; Fulara, J.; Jakobi, M.; Forney, D.; Maier, J. P. *J. Chem. Phys.* **1995**, *103*, 54. (c) Forney, D.; Freivogel, P.; Grutter, M.; Maier, J. P. *J. Chem. Phys.* **1996**, *104*, 4954. (d) Freivogel, P.; Grutter, M.; Forney, D.; Maier, J. P. *Chem. Phys. Lett.* **1996**, *249*, 191. (e) Grutter, M.; Freivogel, P.; Forney, D.; Maier, J. P. *J. Chem. Phys.* **1997**, *107*, 5356. (f) Wyss, M.; Grutter, M.; Maier, J. P. *Chem. Phys. Lett.* **1999**, *304*, 35. (g) Grutter, M.; Wyss, M.; Riaplov, E.; Maier, J. P.; Peyerimhoff, S. D.; Hanrath, M. *J. Chem. Phys.* **1999**, *111*, 7397.

(82) Monninger, G.; Förderer, M.; Gurtler, P.; Kalhofer, S.; Petersen, S.; Nemes, L.;

Szalay, P. G.; Kratschmer, W. *J. Phys. Chem. A* **2002**, *106*, 5779.

(83) (a) Vala, M.; Chandrasekhar, T. M.; Szczepanski, J.; Van Zee, R.; Weltner, W., Jr. *J. Chem. Phys.* **1989**, *90*, 595. Szczepanski, J.; Vala, M. *J. Chem. Phys.* **1993**, *99*, 7371. (b) Szczepanski, J.; Ekern, S.; Chapo, C.; Vala, M. *Chem. Phys.* **1996**, *211*, 359. (c) Lapinski, L.; Vala, M. *Chem. Phys. Lett.* **1999**, *300*, 195.

(84) (a) Shen, L. N.; Graham, W. R. M. *J. Chem. Phys.* **1989**, *91*, 5115. (b) Shen, L. N.; Withey, P. A.; Graham, W. R. M. *J. Chem. Phys.* **1991**, *94*, 2395. (c) Kranze, R. H.; Withey, P. A.; Rittby, C. M. L.; Graham, W. R. M. *J. Chem. Phys.* **1995**, *103*, 6841. (d) Kranze, R. H.; Rittby, C. M. L.; Graham, W. R. M. *J. Chem. Phys.* **1996**, *105*, 5313. (e) Wang, S. L.; Rittby, C. M. L.; Graham, W. R. M. *J. Chem. Phys.* **1997**, *107*, 6032. (f) Wang, S. L.; Rittby, C. M. L.; Graham, W. R. M. *J. Chem. Phys.* **1997**, *107*, 7025. (g) Wang, S. L.; Rittby, C. M. L.; Graham, W. R. M. *J. Chem. Phys.* **2000**, *112*, 1457. (h) Ding, X. D.; Wang, S. L.; Rittby, C. M. L.; Graham, W. R. M. *J. Chem. Phys.* **2000**, *112*, 5113.

(85) Miki, M.; Wakabayashi, T.; Momose, T.; Shida, T. *J. Phys. Chem.* **1996**, *100*, 12135.

(86) Freivogel, P.; Grutter, M.; Forney, D.; Maier, J. P. *Chem. Phys*. **1997**, *216*, 401.

(87) (a) Presilla-Marquez, J. D.; Sheehy, J. A.; Mills, J. D.; Carrick, P. G.; Larson, C. W. *Chem. Phys. Lett.* **1997**, *274*, 439. (b) Presilla-Marquez, J. D.; Harper, J.; Sheehy, J. A.; Carrick, P. G.; Larson, C. W. *Chem. Phys. Lett.* **1999**, *300*, 719.

(88) Tam, S.; Macler, M.; Fajardo, M. E. *J. Chem. Phys.* **1997**, *106*, 8955.

(89) (a) Ott, A. K.; Rechtsteiner, G. A.; Felix, C.; Hampe, O.; Jarrold, M. F.; Van

Duyne, R. P.; Raghavachari, K. *J. Chem. Phys.* **1998**, *109*, 9652. (b) Dechtsteiner, G. A.; Felix, C.; Ott, A. K.; Hampe, O.; Van Duyne, R. P.; Jarrold, M. F.; Raghavachari, K. *J. Phys. Chem. A* **2001**, *105*, 3029.

(90) Moazzen-Ahmadi, N.; Thong, J. J.; McKellar, A. R. W. *J. Chem. Phys.* **1994**, *100*, 4033.

(91) (a) Van Orden, A.; Provencal, R. A.; Keutsch, F. N.; Saykally, R. J. *J. Chem. Phys*. **1996**, *105*, 6111. (b) Giesen, T. F.; Berndt, U.; Yamada, K. M. T.; Fuchs, G.; Schieder, R.; Winnewisser, G.; Provencal, R. A.; Keutsch, F. N.; Van Orden, A.; Saykally, R. J. *Chem. Phys. Chem* **2001**, *2*, 242.

(92) Neubauer-Guenther, P.; Giesen, T. F.; Berndt, U.; Fuchs, G.; Winnewisser, G. *Spectrochim. Acta Part A* **2003**, *59*, 431.

(93) Balfour, W. J.; Cao, J. Y.; Prasad, C. V. V.; Qian, C. X. W. *J. Chem. Phys.* **1994**, *101*, 10343.

(94) (a) Motylewski, T.; Vaizert, O.; Giesen, T. F.; Linnartz, H.; Maier, J. P. *J. Chem. Phys.* **1999**, *111*, 6161. (b) Linnartz, H.; Vaizert, O.; Motylewski, T.; Maier, J. P. *J. Chem. Phys.* **2000**, *112*, 9777. (c) Boguslavskiy, A. E.; Ding, H.; Maier, J. P. *J. Chem. Phys.* **2005**, *123*, 034305. (d) Boguslavskiy, A. E.; Maier, J. P. *J. Chem. Phys.* **2006**, *125*, 094308. (e) Maier, J. P.; Boguslavskiy, A. E.; Ding, H.; Walker, G. A. H.; Bohlender, D. A. *Astrophys. J*. **2006**, *640*, 369. (f) Ding, H.; Maier, J. P. *J. Phys.Conf. Ser.* **2007**, *61*, 252. (g) Boguslavskiy, A. E.; Maier, J. P. *Phys. Chem. Chem. Phys.* **2007**, *9*, 127.

(95) (a) Giesen, T. F.; Van Orden, A. O.; Cruzan, J. D.; Provencal, R. A.; Saykally, R.

J.; Gendriesch, R.; Lewen, F.; Winnewisser, G. *Astrophys. J.* **2001**, *551*, L181. (b) Gendriesch, R.; Pehl, K.; Giesen, T.; Winnewisser, G.; Lewen, F. *Z. Naturforsch.* **2003**, *58a*, 129.

(96) (a) Ohara, M.; Suwa, M.; Ishigaki, T.; Shiromaru, H.; Achiba, Y.; Kratschmer, W. *J. Chem. Phys.* **1998**, *109*, 1329. (b) Ohara, M.; Kasuya, D.; Shiromaru, H.; Achiba, Y. *J. Phys. Chem. A* **2000**, *104*, 8622.

(97) (a) Lakin, N. M.; Pachkov, M.; Tulej, M.; Maier, J. P.; Chambaud, G.; Rosmus, P. *J. Chem. Phys.* **2000**, *113*, 9586. (b) Lakin, N. M.; Guthe, F.; Tulej, M.; Pachkov, M.; Maier, J. P. *Faraday Discuss.* **2000**, *115*, 383.

(98) Kohno, M.; Suzuki, S.; Shiromaru, H.; Moriwaki, T.; Achiba, Y. *Chem. Phys. Lett.* **1998**, *282*, 330.

(99) Fromherz, R.; Gantefor, G.; Shvartsburg, A. A. *Phys. Rev. Lett.* **2002**, *89*, 083001.

(100) (a) Arnold, D. W.; Bradforth, S. E.; Kitsopoulos, T. N.; Neumark, D. M. *J. Chem. Phys.* **1991**, *95*, 8753. (b) Xu, C.; Burton, G. R.; Taylor, T. R.; Neumark, D. M. *J. Chem. Phys.* **1997**, *107*, 3428. (c) Frischkorn, C.; Bragg, A. E.; Davis, A. V.; Wester, R.; Neumark, D. M. *J. Chem. Phys.* **2001**, *115*, 11185.

(101) Szczepanski, J.; Hodyss, R.; Vala, M. *J. Phys. Chem. A* **1998**, *102*, 8300.

(102) (a) Fulara, J.; Riaplov, E.; Batalov, A.; Shnitko, I.; Maier, J. P. *J. Chem. Phys.* **2004**, *120*, 7520. (b) Fulara, J.; Shnitko, I.; Batalov, A.; Maier, J. P. *J. Chem. Phys.* **2005**, *123*, 044305.

(103) (a) Magers, D. H.; Harrison, R. J.; Bartlett, R. J. *J. Chem. Phys.* **1986**, *84*, 3284.

(b) Watts, J. D.; Gauss, J.; Stanton, J. F.; Bartlett, R. J. *J. Chem. Phys.* **1992**, *97*, 8372.

(104) (a) Raghavachari, K.; Whiteside, R. A.; Pople, J. A. *J. Chem. Phys.* **1986**, *85*, 6623. (b) Raghavachari, K.; Binkley, J. S. *J. Chem. Phys.* **1987**, *87*, 2191.

(105) (a) Martin, J. M. L.; Francois, J-P.; Gijbels, R. *J. Chem. Phys.* **1989**, *90*, 3403. (b) Martin, J. M. L.; Francois, J.-P.; Gijbels, R. *J. Chem. Phys.* **1990**, *93*, 8850. (c) Martin, J. M. L.; Francois, J.-P.; Gijbels, R. *J. Chem. Phys.* **1991**, *94*, 3753. (d) Martin, J. M. L.; Francois, J.-P.; Gijbels, R. *J. Chem. Phys.* **1991**, *95*, 9420.

(106) Parasuk, V.; Almlof, J. *J. Chem. Phys.* **1989**, *91*, 1137.

(107) (a) Liang, C.; Schaefer, H. F. *Chem. Phys. Lett.* **1990**, *169*, 150. (b) Liang, C.; Schaefer, H. F. *J. Chem. Phys.* **1990**, *93*, 8844.

(108) Ortiz, J. V.; Zakrzewski, V. G. *J. Chem. Phys.* **1994**, *100*, 6614.

(109) Hutter, J.; Luthi, H. P.; Diederich, F. *J. Am. Chem. Soc.* **1994**, *116*, 750.

(110) Schmatz, S.; Botschwina, P. *Chem. Phys. Lett.* **1995**, *235*, 5.

(111) (a) Martin, J. M. L.; Taylor, P. R. *Chem. Phys. Lett.* **1995**, *240*, 521. (b) Martin, J. M. L.; Elyazal, J.; Francois, J.-P. *Chem. Phys. Lett.* **1995**, *242*, 570. (c) Martin, J. M. L.; Taylor, P. R. *J. Chem. Phys.* **1995**, *102*, 8270. (d) Martin, J. M. L.; Taylor, P. R. *J. Phys. Chem.* **1996**, *100*, 6047. (e) Martin, J. M. L.; Schwenke, D. W.; Lee, T. J.; Taylor, P. R. *J. Chem. Phys.* **1996**, *104*, 4657.

(112) Martin, J. M. L.; El-Yazal, J.; Francois, J.-P. *Chem. Phys. Lett.* **1996**, *252*, 9.

(113) Ohno, M.; Zakrzewski, V. G.; Ortiz, J. V.; von Niessen, W. *J. Chem. Phys.* **1997**, *106*, 3258.

(114) Valdes, E. A.; De La Mora, P.; Castro, M.; Keller, J. *Int. J. Quantum Chem.*

1997, *65*, 867.

(115) (a) Hanrath, M.; Peyerimhoff, S. D.; Grein, F. *Chem. Phys.* **1999**, *249*, 121. (b) Muhlhauser, M.; Froudakis, G. E.; Hanrath, M.; Peyerimhoff, S. D. *Chem. Phys. Lett.* **2000**, *324*, 195. (c) Muhlhauser, M.; Froudakis, G. E.; Peyerimhoff, S. D. *Chem. Phys. Lett.* **2001**, *336*, 171. (d) Grein, F.; Franz, J.; Hanrath, M.; Peyerimhoff, S. D. *Chem. Phys.* **2001**, *263*, 55. (e) Muhlhauser, M.; Froudakis, G. E.; Peyerimhoff, S. D. *Phys. Chem. Chem. Phys.* **2001**, *3*, 3913. (f) Hanrath, M.; Peyerimhoff, S. D. *Chem. Phys. Lett.* **2001**, *337*, 368. (g) Cao, Z. X.; Muhlhauser, M.; Hanrath, M.; Peyerimhoff, S. D. *Chem. Phys. Lett.* **2002**, *351*, 327.

(116) Giuffreda, M. G.; Deleuze, M. S.; Francois, J.-P.; Trofimov, A. B. *Int. J. Quantum Chem.* **2001**, *85*, 475.

(116) Jo, C.; Lee, K. *J. Korean Phys. Soc.* **2002**, *41*, 200.

(118) Baranovski, V. I. *Chem. Phys. Lett.* **2005**, *408*, 429.

(119) Martin, J. M. L.; Francois, J. P.; Gijbels, R. *J. Chem. Phys.* **1990**, *93*, 5037.

(120) Scuseria, G. E. *Chem. Phys. Lett.* **1991**, *176*, 27.

(121) Watts, J. D.; Stanton, J. F.; Gauss, J.; Bartlett, R. J. *J. Chem. Phys.* **1991**, *94*, 4320.

(122) (a) Schnell, M.; Muhlhauser, M.; Froudakis, G. E.; Peyerimhoff, S. D. *Chem. Phys. Lett.* **2001**, *340*, 559. (b) Haubrich, J.; Muhlhauser, M.; Peyerimhoff, S. D. *Phys. Chem. Chem. Phys.* **2002**, *4*, 2891. (c) Haubrich, J.; Muhlhauser, M.; Peyerimhoff, S. D. *J. Mol. Spec.* **2004**, *228*, 31.

(123) Gillery, C.; Rosmus, P.; Werner, H. J.; Stoll, H.; Maier, J. P. *Mol. Phys.* **2004**,

102, 2227.

(124) (a) Giuffreda, M. G.; Deleuze, M. S.; Francois, J.-P. *J. Phys. Chem. A* **1999**, *103*, 5137. (b) Deleuze, M. S.; Giuffreda, M. G.; Francois, J.-P.; Cederbaum, L. S. *J. Chem. Phys.* **1999**, *111*, 5851. (c) Deleuze, M. S.; Giuffreda, M. G.; Francois, J.-P.; Cederbaum, L. S. *J. Chem. Phys.* **2000**, *112*, 5325. (d) Deleuze, M. S.; Giuffreda, M. G.; Francois, J.-P. *J. Phys. Chem. A* **2002**, *106*, 5626.

(125) Diaz-Tendero, S.; Martin, F.; Alcami, M. *J. Phys. Chem. A* **2002**, *106*, 10782

(126) Orlova, G.; Goddard, J. D. *Chem. Phys. Lett.* **2002**, *363*, 486.

(127) Schmatz, S.; Botschwina, P. *Int. J. Mass Spectrom. Ion Processes* **1995**, *150*, 621.

(128) Cao, Z. X.; Peyerimhoff, S. D.; Grein, F.; Zhang, Q. *J. Chem. Phys.* **2001**, *115*, 2062.

(129) Lepine, F.; Allouche, A. R.; Baguenard, B.; Bordas, C.; Aubert-Frecon, M. *J. Phys. Chem. A* **2002**, *106*, 7177.

(130) Giuffreda, M. G.; Deleuze, M. S.; Francois, J.-P. *J. Phys. Chem. A* **2002**, *106*, 8569.

(131) Rohmer, M. M.; Benard, M. *Chem. Rev.* **2000**, *100*, 495.

(132) (a) Pilgrim, J. S.; Duncan, M. A. *J. Am. Chem. Soc.* **1993**, *115*, 4395. (b) Pilgrim, J. S.; Duncan, M. A. *Int. J. Mass Spect. Ion Proc.* **1994**, *138*, 283. (c) Pilgrim, J. S.; Brock, L. R.; Duncan, M. A. *J. Phys. Chem* **1995**, *99*, 544.

(133) (a) Kerns, K. P.; Guo, B. C.; Deng, H. T.; Castleman, A. W. Jr. *J. Chem. Phys.* **1994**, *101*, 8529. (b) Kerns, K. P.; Guo, B. C.; Deng, H. T.; Castleman, A. W. Jr. *J. Phys. Chem.* **1996**, *100*, 16821.

(134) (a) Wei, S.; Guo, B. C.; Purnell, J.; Buzza, S. A.; Castleman, A. W. Jr. *J. Phys. Chem.* **1993**, *97*, 9559. (b) Purnell, J.; Wei, S.; Castleman, A. W. Jr. *Chem. Phys. Lett*. **1994**, *229*, 105. (c) Stairs, J. R.; Davis, K. M.; Castleman, A. W. Jr. *J. Chem. Phys.* **2002**, *117*, 4371.

(135) (a) Bowers, M. T. *Acc. Chem. Res.* **1994**, *27*, 324. (b) Lee, S.; Gotts, N. G.; von Helden, G.; Bowers, M. T. *Science* **1995**, *267*, 999.

(136) (a) Wang, L. S.; Li, S.; Wu, H. *J. Phys. Chem.* **1996**, *100*, 19211. (b) Li, S.; Wu, H.; Wang, L. S. *J. Am. Chem. Soc.* **1997**, *119*, 7417.

(137) Zhang, Q.; Lewis, S. P. *Chem. Phys. Lett.* **2003**, *372*, 836.

(138) (a) Hou, H.; Muckerman, J. T.; Liu, P.; Rodriguez, J. A. *J. Phys. Chem. A* **2003**, *107*, 9344. (b) Liu, P.; Rodriguez, J. A. *J. Chem. Phys.* **2003**, *120*, 5414. (c) Liu, P.; Rodriguez, J. A.; Muckerman, J. T. *J. Chem. Phys.* **2004**, *121*, 10321.

(139) Martinez, J. I.; Castro, A.; Rubio, A.; Poblet, J. M.; Alonso, J. A. *Chem. Phys. Lett.* **2004**, *389*, 292.

(140) (a) Varganov, S. A.; Gordon, M. S. *Chem. Phys.* **2006**, *326*, 97. (b) Varganov, S. A.; Dudley, T. J.; Gordon, M. S. *Chem. Phys. Lett.* **2006**, *429*, 49.

(141) (a) van Heijnsbergen, D.; von Helden, G.; Duncan, M. A.; van Roij, A. J. A.; Meijer, G. *Phys. Rev. Lett.* **1999**, *83*, 4983. (b) von Helden, G.; van Heijnsbergen, D.; Duncan, M. A.; Meijer, G. *Chem. Phys. Lett.* **2001**, *333*, 350. (c) van Heijnsbergen, D.; Duncan, M. A.; Meijer, G. ; von Helden, G. *Chem. Phys. Lett.* **2001**, *349*, 220.

(142) Yamada, Y.; Castleman, A. W. Jr. *Chem. Phys. Lett.* **1993**, *204*, 133.

(143) Jin, C.; Haufler, R. E.; Hettich, R.L.; Barshick, C. M.; Compton, R. N.; Puretzky, A. A.; Dem'yanenko, A. V.; Tuinman, A. A. *Science* **1994**, *263*, 68.

(144) Dietze, H. J.; Becker, S. *Int. J. Mass Spectrom. and Ion Process*. **1988**, *82*, 47.

(145) (a) Teghil, R.; Giardini-Guidoni, A.; Piccirillo, S.; Mele, A.; Polla-Mattiot, F. *Appl. Sur. Sci.* **1990**, *46*, 220. (b) Mele, A.; Giardini-Guidoni, A.; Teghil, R. *Proc. Indian Acad. Sci. (Chem. Sci.)* **1993**, *105*, 715. (c) Teghil, R.; D'Alessio, L.; Zaccagnino, M.; Marotta, V.; Ferro, D.; De Maria, G. *Appl. Sur. Sci.* **2001**, *173*, 233.

(146) (a) McElvany, S. W.; Cassady, C. J. *J. Phys. Chem.* **1990**, *94*, 2057. (b) Cassady, C. J.; McElvany, S. W. *J. Am. Chem. Soc.* **1990**, *112*, 4788.

(147) Reddic, J. E.; Duncan, M. A. *Chem. Phys. Lett.* **1997**, *264*, 157.

(148) Gibson, J. K. *J. Vac. Sci. Technol. A* **1998**, *16*, 653.

(149) Zhang, R.; Achiba, Y.; Fisher, K. J.; Gadd, G. E.; Hopwood, F. G.; Ishigaki, T.; Smith, D. R.; Suzuki, S.; Willett, G. D. *J. Phys. Chem. B* **1999**, *103*, 9450.

(150) (a) Clemmer, D. E.; Shelimov, K. B.; Jarrold, M. F. *J. Am. Chem. Soc.* **1994**, *116*, 5971. (b) Clemmer, D. E.; Jarrold, M. F. *J. Am. Chem. Soc.* **1994**, *116*, 8841. (c) Shelimov, K. B.; Clemmer, D. E.; Jarrold, M. F. *J. Phys. Chem.* **1995**, *99*, 11376. (d) Shelimov, K. B.; Jarrold, M. F. *J. Phys. Chem.* **1995**, *99*, 17677. (e) Shelimov, K. B.; Jarrold, M. F. *J. Am. Chem. Soc.* **1996**, *118*, 1139. (f) Shelimov, K. B.; Clemmer, D. E.; Jarrold, M. F. *J. Chem. Soc., Dalton Trans.* **1996**, *5*, 567.

(151) (a) Steimle, T. C.; Jung, K. Y.; Li, B. –Z. *J. Chem. Phys.* **1995**, *102*, 5937. (b) Beaton, S. A.; Steimle, T. C. *J. Chem. Phys.* **1999**, *111*, 10876,

(152) Balfour, W. J.; Cao, J.; Prassad, C. V. V.; Qian, C. X. W. *J. Chem. Phys.* **1995**, *103*, 4046.

(153) Barnes, M.; Merer, A. J.; Metha, G. F. *J. Chem. Phys.* **1995**, *103*, 8360.

(154) Adam, A. G.; Peers, J. R. D. *J. Mol. Spec.* **1997**, *181*, 24.

(155) (a) Brugh, D. J.; Morse, M. D. *J. Chem. Phys.* **1997**, *107*, 9772. (b) Brugh,D. J.; Ronningen, T. J.; Morse, M. D. *J. Chem. Phys.* **1998**, *109*, 7851. (c) Langenberg, J. D.; DaBell, R. S.; Shao, L.; Dreessen, D.; Morse, M. D. " *J. Chem. Phys.* **1998**, *109*, 7863. (d) Langenberg, J. D.; Shao, L.; Morse, M. D *J. Chem. Phys.* **1999**, *111*, 4077. (e) Sickafoose, S. M.; Smith, A. W.; Morse, M. D. *J. Chem. Phys.* 2002, **116**, 993. (f) Brugh, D. J.; Morse, M. D. *J. Chem. Phys.* **2002**, *117*, 10703. (g) Lindholm, N. F.; Hales, D. A.; Ober, L. A.; Morse, M. D. *J. Chem. Phys*. **2004**, *121*, 6855.

(156) DaBell, R. S.; Meyer, R. G.; Morse, M. D. *J. Chem. Phys.* **2001**, *114*, 2938.

(157) (a) Allen, M. D.; Pesch, T. C.; Ziurys L. M. *Astrophys. J.* **1996**, *472*, L57. (b) Brewster, M. A.; Ziurys, L. M. *Astrophys. J.* **2001**, *559*, L163. (c) Sheridan, P. M.; Ziurys, L. M.; Hirano, T. *Astrophys. J.* **2003**, *593*, L141.

(158) (a) Robbins, D. L.; Rittby, C. M. L.; Graham, W. R. M. *J. Chem. Phys.* **2001**, *114*, 3570. (b) Robbins, D. L.; Chen, K. C.; Rittby, C. M. L.; Graham, W. R. M. *J. Chem. Phys.* **2004**, *120*, 4664. (c) Gonzalez, E.; Rittby, C. M. L.; Graham, W. R. M. *J. Chem. Phys.* **2006**, 125, 044550. (d) Bates, S. A.; Rittby, C. M. L.; Graham, W. R. M. *J. Chem. Phys.* **2006**, 125, 074506. (e) Kinzer, R. E. Jr.; Rittby, C. M. L.; Graham, W. R. M. *J. Chem. Phys.* **2006**, 125, 074531. (f) Bates, S. A.; Rhodes, J. A.; Rittby, C. M. L.; Graham, W. R. M. *J. Chem. Phys.* **2007**, *127*,

064506. (g) Kinzer, R. E.; Rittby, C. M. L.; Graham, W. R. M. *J. Chem. Phys.* **2008**, *128*, 064312.

(159) (a) Heaven, M. W.; Stewart, G. M.; Buntine, M. A.; Metha, G. F. *J. Phys. Chem. A* **2000**, *104*, 3308. (b) Dryza, V.; Addicoat, M. A.; Gascooke, J. R.; Buntine, M. A.; Metha, G. F. *J. Phys. Chem. A* **2005**, *109*, 11180.

(160) (a) Wang, X. B.; Ding, C. F.; Wang, L. S. *J. Phys. Chem.* A **1997**, *101*, 7699. (b) Li X.; Wang, L. S. *J. Chem. Phys.* **1999**, *111*, 8389. (c) Wang, L. S.; Li, X. *J. Chem. Phys.* **2000**, *112*, 3602. (d) Zhai, H. J.; Wang, L. S.; Jena, P.; Gutsev, G. L.; Bauschlicher, C. W. Jr. *J. Chem. Phys.* **2004**, *120*, 8996. (e) Alexandrova, A. N.; Boldyrev, A. I.; Zhai, H. J.; Wang, L. S. *J. Phys. Chem. A* **2005**, *109*, 562.

(161) (a) Suzuki, S.; Kohno, M.; Shiromaru, H.; Achiba, Y.; Kietzmann, H.; Kessler, B.; Gantefor, G.; Eberhardt, W. *Z. Phys. D* **1997,** *40*, 407. (b) Kohno, M.; Suzuki, S.; Shiromaru, H.; Kobayashi, K.; Nagase, S.; Achiba, Y.; Kietzmann, H.; Kessler, B.; Gantefor, G.; Eberhardt, W. *J. Electron Spec. and Rel. Phen.* **2000,** *112*, 163.

(162) Tono, K.; Terasaki, A.; Ohta, T.; Kondow, T. *J. Chem. Phys.* **2002**, *117*, 7010.

(163) Knappenberger, K. L. Jr.; Jones, C. E. Jr.; Sobhy, M. A.; Iordanov, I.; Sofo, J.; Castleman, A. W. Jr. *J. Phys. Chem. A* **2006**, *110*, 12814.

(164) von Helden, G.; Gotts N. G.; Maitre, P.; Bowers, M. T. *Chem. Phys. Lett.* **1994** *227*, 601.

(165) Roszak, S.; Majumdar, D.; Balasubramanian, K. *J. Chem. Phys.* **2002**, *116*, 10238.

(166) (a) Redondo, P.; Barrientos, C.; Largo, A. J. *Phys. Chem. A* **2005**, *109*, 8594. (b) Redondo, P.; Barrientos, C.; Largo, A. *J. Phys. Chem. A* **2006**, *110*, 4057.

(167) Strout, D. L.; Hall, M. B. *J. Phys. Chem*. **1996**, *100*, 18007.

(168) Puzzarini, C.; Peterson, K.A. *J. Chem. Phys.* **2005**, *122*, 084323.

(169) Roszak, S.; Balasubramanian, K. *J. Chem. Phys.* **1997**, *106*, 158.

(170) Strout, D. L.; Hall, M. B. *J. Phys. Chem. A* **1998**, *102*, 641.

(171) (a) Sumathi, R; Hendrickx, M. *J. Phys. Chem. A* **1998**, *102*, 7308. (b) Sumathi, R.; Hendrickx, M. *J. Phys. Chem. A* **1998**, *102*, 4883.

(172) Bauschlicher, C. W. Jr. *Theor. Chem. Acc*. **2003**, *110*, 153.

(173) (a) Rayón, V. M.; Redondo, P.; Barrientos, C.; Largo, A. *Chem. Phys. Lett.* **2006**, *422*, 289. (b) Largo, L.; Cimas, A.; Redondo, P.; Rayón, V. M.; Barrientos, C. *Chem. Phys.* **2006**, *330*, 431.

(174) Sosa, R. M.; Gardiol, P.; Beltrame, G. *Int. J. Quantum Chem.* **1997**, *65*, 919.

(175) Majumdar, D.; Roszak, S.; Balasubramanian, K. *J. Chem. Phys.* **2003**, *118*, 130.

(176) (a) Redondo, P.; Barrientos, C.; Largo, A. *J. Chem. Theory Comput.* **2006**, *2*, 885. (b) Redondo, P.; Barrientos, C.; Largo, A. *J. Mol. Struct. (THEOCHEM)* **2006**, *769*, 225. (c) Redondo, P.; Barrientos, C.; Largo, A. *Int. J. Mass Spectrom.* **2007**, *263*, 101.

(177) (a) Dai, D.; Roszak, S.; Balasubramanian, K. *J. Phys. Chem.* **2000**, *104*, 5861. (b) Dai, D.; Roszak, S.; Balasubramanian, K. *J. Phys. Chem.* **2000**, *104*, 9760.

(178) Harris, H.; Dance, I. *J. Phys. Chem. A* **2001**, *105*, 3340.

(179) Noya, E. G.; Longo, R. C.; Gallego, L. J. *J. Chem. Phys.* **2003**, *119*, 11130.

(180) Ryzhkov, M.; Ivanovskii, A. L.; Delley, B. T. *Chem. Phys. Lett.* **2005**, *404*, 400.

(181) Harris, H. H.; Dance, I. G. *Polyhedron* **2007**, *26*, 250.

(182) Arbuznikov, A. V.; Hendrickx, M. *Chem. Phys. Lett.* **2000**, *320*, 575.

(183) Froudakis, G. E.; Mühlhäuser, M.; Andriotis, A. N.; Menon, M. *Phys. Rev. B* **2001**, *64*, 241401.

(184) Longo, R. C.; Alemany, M. M. G.; Fernández, B.; Gallego, L. J. *Phys. Rev. B* **2003**, *68*, 167401.

(185) Roszak, S.; Balasubramanian, K. *J. Chem. Phys.* **1997**, *106*, 4008.

(186) (a) Strout, D. L.; Miller III, T. F.; Hall, M. B. *J. Phys. Chem. A* **1998**, *102*, 6307. (b) Miller III, T. F.; Hall, M. B. *J. Am. Chem. Soc* **1999**, *121*, 7389.

(187) Barrientos, C.; Redondo, P.; Largo, A. *J. Chem. Theory Comput.* **2007**, *3,* 657.

(188) Gutsev, G. L.; Andrews, L.; Bauschlicher, C. W. Jr. *Theor. Chem. Acc.* **2003**, *109*, 298.

(189) Harrison, J. F. *Chem. Rev.* **2000**, *100*, 679.

(190) (a) Wang, J.; Sun, X.; Wu, Z. *Chem. Phys. Lett.* **2006**, *426*, 141. (b) Wang, J.; Sun, X.; Wu, Z. *J. Cluster Sci.* **2006**, *426*, 141.

(191) (a) Rayón, V. M.; Redondo, P.; Barrientos, C.; Largo, A. *Chem. Eur. J.* **2006**, 12, 6963. (b) Rayón, V. M.; Redondo, P.; Barrientos, C.; Largo, A. *J. Phys. Chem. A.* **2007**, *111*, 6345.

(192) Capano, M. A. *J. Appl. Phys.* **1995**, *78*, 4790.

(193) Kimura, T.; Nakamura, T.; Ishikawa, K.; Kokai, F.; Koga, Y. *Chem. Phys. Lett.* **2001**, *340*, 296.

(194) Nam, S. H.; Park, S. M. *Appl. Phys. A.* **2004**, *79*, 1117.

(195) Pellarin, M., Ray, C. ; Mélinon, P.; Lermé, J.; Vialle, J. L.; Kéghélian, P.; Perez, A. Broyer, M. *Chem. Phys. Lett.* **1997**, *277*, 96.

(196) Nakajima, A.; Taguwa, T.; Nakao, K.; Gomei, M.; Kishi, R.; Iwata, S.; Kaya, K. *J.*

Chem. Phys. **1995**, *103*, 2051.

(197) Duan, X.; Burggraf, L. W.; Weeks, D. E.; Davico, G. E.; Schwartz, R. L.; Lineberger, W. C. *J. Chem. Phys*. **2002**, *116*, 3601.

(198) (a) Van Orden, A.; Giesen, T. F.; Provencal, R. A.; Hwang, H.J.; Saykally, R. J. *J. Chem. Phys.* **1994**, *101*, 10237. (b) Van Orden, A.; Provencal, R. A.; Giesen, T. F.; Saykally, R. J. *Chem. Phys. Lett.* **1995**, *237*, 77. (c) Van Orden, A., Provencal, R. A.; Giesen, T. F.; Saykally, R. J. *Chem. Phys Lett.* **1995**, *237*, 77.

(199) (a) Presilla-Márquez, J. D.; Graham, W. R. M. *J. Chem. Phys.* **1990**, *93*, 5424. (b) Presilla-Márquez, J. D.; Graham, W. R. M. *J. Chem. Phys.* **1991**, *95*, 5612. (c) Withey, P. A.; Graham, W. R. M. *J. Chem. Phys.* **1992**, *96*, 4068. (d) Presilla-Márquez, J. D.; Graham, W. R. M. *J. Chem. Phys.* **1992**, *96*, 6509. (e) Presilla-Márquez, J. D.; Graham, W. R. M. *J. Chem. Phys.* **1994**, *100*, 181. (f) Presilla-Márquez, J. D.; Gay, S.C.; Rittby, C. M. L.; Graham, W. R. M. *J. Chem. Phys.* **1995**, *102*, 6354. (g) Presilla-Márquez, J. D.; Rittby, C. M. L.; Graham, W. R. M. *J. Chem. Phys.* **1996**, *104*, 2818. (h) Presilla-Márquez, J. D.; Rittby, C. M. L.; Graham, W. R. M. *J. Chem. Phys.* **1997**, *106*, 8367. (i) Ding, X. D.; Wang, S. L.; Rittby, C. M. L.; Graham, W. R. M. *J. Chem. Phys.* **1999**, *110*, 11214.

(200) (a) Apponi, A. J.; McCarthy, M. C.; Gottlieb, C. A.; Thaddeus, P. *J. Chem. Phys.* **1999**, *111*, 3911. (b) McCarthy, M. C.; Apponi, A. J.;Thaddeus, P. *J. Chem. Phys.* **1999**, *111*, 7175. (c) Gordon, V. D.; Nathan, E. S.; Apponi, A. J.; McCarthy, M. C.; Thaddeus, Botschwina, P. P. *J. Chem. Phys.* **2000**, *113*, 5311. (d) McCarthy, M. C.; Apponi, A. J.; Gottlieb, C. A.; Thaddeus, P. *Astrophys. J.* **2000**, *538*, 766.

(201) Bruna, P. J.; Petrongolo, C., Buenker, R. J.; Peyerimhoff, S. D. *J. Chem. Phys.* **1981**, *74*, 4611.

(202) Ignatyev, I. S.; Schaefer, H. F. III *J. Chem. Phys.* **1995**, *103*, 7025.

(203) (a) Pascoli, G.; Lavendy, H. *Int. J. Mass Spec.* **1998**, *177*, 31. (b) Pascoli, G.; Lavendy, H. *Eur. Phys. J. D* **2002**, *19*, 339.

(204) (a) Wu, H.; Jiang, Z.; Xu, X.; Zhang, F.; Jin, Z. *J. Mol. Struc.* **2003**, *620*, 9. (b) Jiang, Z.; Xu, X.; Wu, H.; Zhang, F.; Jin, Z. *J. Mol. Struc*. **2003**, *624*, 61.

(205) Li, G.; Tang, Z. J. *Phys. Chem. A.* **2003**, *107*, 5317.

(206) Bauschlicher, C. W. Jr.; Langhoff, S. R. *J. Chem. Phys.* **1987**, *87*, 2919.

(207) Martin, J. M. L.; Francois, J. P.; Gijbels, R. *J. Chem. Phys.* **1990**, *92*, 6655.

(208) Rittby, C. M. L. *J. Chem. Phys.* **1994**, *100*, 175.

(209) (a) Froudakis, G.; Zdetsis, A. D; Mühlhäuser, M.; Engels, B.; Peyerimhoff, S. D. *J. Chem. Phys.* **1994**, *101*, 6790. (b) Froudakis, G.; Mühlhäuser, M.; Zdetsis, A. D *Chem. Phys. Lett.* **1995**, *233*, 619. (c) Zdetsis, A. D; Froudakis, G.; Mühlhäuser, M.; Thümnel, H. *J. Chem. Phys.* **1996**, *104*, 2566. (d) Zdetsis, A. D; Engels, B.; M. Hanrath, Peyerimhoff, S. D. *Chem. Phys. Lett.* **1999**, *302*, 288. (e) Mühlhäuser, M.; Froudakis, G.; Zdetsis, A. D. *J. Mol. Spec.* **2004**, *223*, 96.

(210) Boldyrev, A. I.; Simons, J.; Zakrzewski, V. G.; von Niessen, W. *J. Phys. Chem.* **1994**, *98*, 1427.

(211) (a) Kishi, R.; Gomei, M.; Nakajima, A.; Iwata, S.; Kaya, K. *J. Chem. Phys.* **1996**, *104*, 8593. (b) Gomei, M.; Kishi, R.; Nakajima, A.; Iwata, S.; Kaya, K. *J. Chem. Phys.* **1997**, *107*, 10051.

(212) Hunsicker, S.; Jones, R. O. *J. Chem. Phys.* **1996**, *105*, 5048.

(213) (a) Bertolus, M.; Brenner, V.; Millié, P. *Eur. Phys. J. D.* **1998**, *1*, 197. (b) Bertolus, M.; Finocchi, F.; Millié, P. *J. Chem. Phys.* **2004**, *120*, 4333.

(214) Robles, J.; Mayorga, O. *NanoStructured Mat.* **1998**, *10*, 1317.

(215) Erkoc, S.; Türker, L. *Physica E* **2000**, *8*, 50.

(216) Reddy, R. R.; Ahammed, Y. N.; Gopal, K. R.; Azeem, P. A.; Rao, T. V. R. *J. Qual. Spec. and Rad. Trans.* **2000**, *67*, 85.

(217) Stanton, J. F.; Gauss, J.; Christiansen, O. *J. Chem. Phys.* **2001**, *114*, 2993.

(218) Jiang, Z. Y.; Xu, X. H.; Wu, H. S.; Jin, Z. H. *J. Phys. Chem. A* **2003**, *107*, 10126.

(219) Jaeger, J. B.; Jaeger, T. D.; Duncan, M. A. *J. Phys. Chem. A.* **2006**, *110*, 9310.

CHAPTER 2

EXPERIMENTAL

Clusters in these experiments are produced by laser vaporization in a Smalley-type laser ablation source[1,2] and studied by mass spectrometry in a custom built molecular beam machine,[3-17] depicted schematically in Figure 2.1. The machine consists of two differentially pumped vacuum chambers connected by a gate valve. The first chamber, called the "source chamber," is where the clusters to be studied are created by a laser ablation pulsed nozzle cluster source. The second chamber, called the "mass spectrometer chamber," contains a reflectron time-of-flight mass spectrometer (RTOF-MS), where the clusters produced by the source are mass analyzed and, if desired, laser photodissociation studies may be conducted.

The sample rods used in these experiments are either 1/2 inch carbon (99.9% purity, Glass Supply) or 1/2 inch silicon (99.999%, ESPI). Experiments on pure carbon and silicon carbide require no further preparation and are loaded as is into the source chamber. The experiments on metal carbides, however, require that metal coatings be deposited on the sample rod. This is done in a vacuum deposition chamber. The rod is placed in the vacuum chamber, and a tungsten oven source is loaded with approximately 0.3 grams of the metal that will be coated. The pressure in the deposition chamber is kept at better than 10^{-5} torr for the course of the deposition. The tungsten is resistively heated to vaporize the metal, which then deposits onto the carbon rod. The rod is rotated throughout the process to ensure an even coating. The metal coated carbon rod is then placed in the source chamber of the molecular beam machine, as described below.

The source chamber pressure is maintained at approximately 10^{-5}-10^{-6} torr by a Varian VHS-10 diffusion pump, capable of pumping 6,600 liters/second of helium. A schematic of our laser vaporization cluster source is shown in Figure 2.2. The second

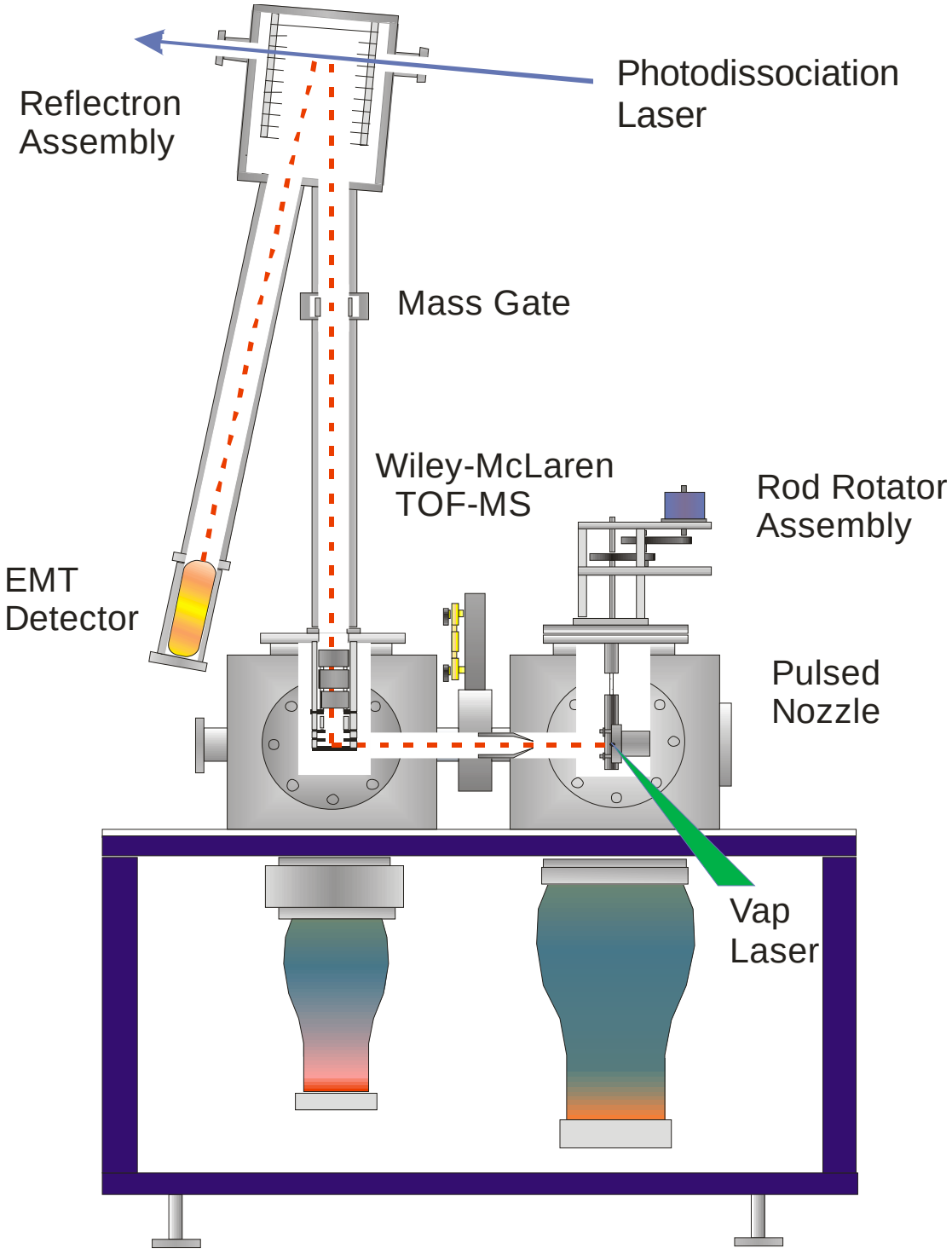

Figure 2.1: Laser vaporization pulsed molecular beam reflectron time-of-flight mass spectrometer (TOF-MS).

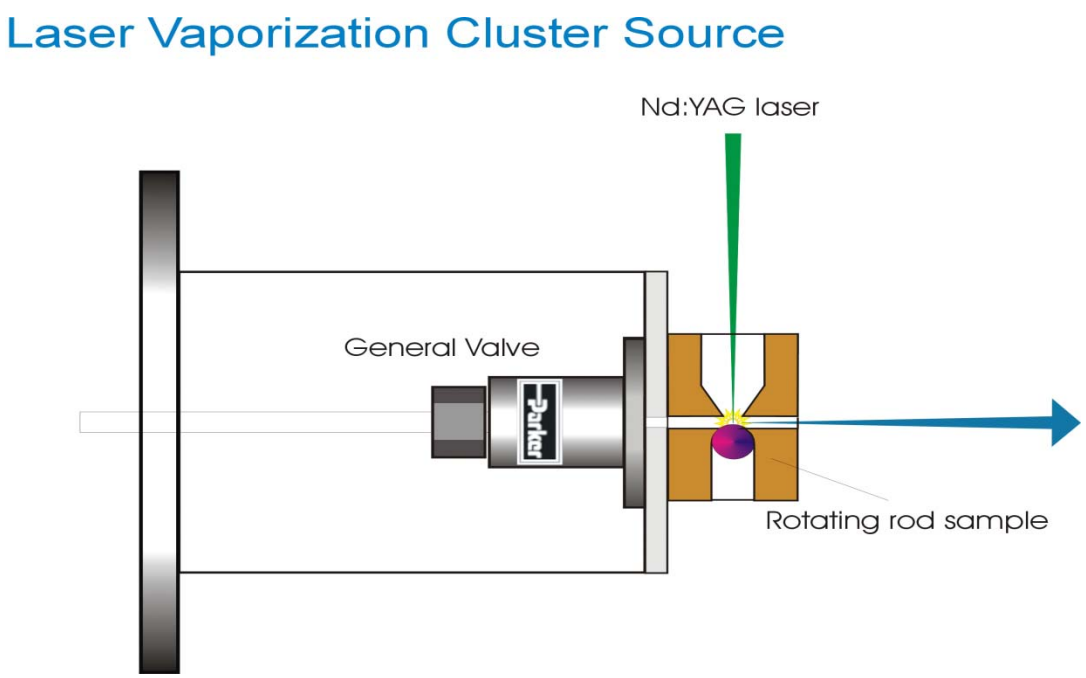

Figure 2.2: Laser ablation cluster source with pulsed Series 9 General Valve nozzle, rotating sample rod, and homemade rod holder.

(532 nm) or third (355 nm) harmonic of a Nd:YAG laser is focused onto a sample rod which is held in a homemade rod holder. The laser is operated at 10 Hz and emits a pulse 5 nanoseconds in duration with an energy of 1 – 20 mJ / pulse. Rotating and translating the rod ensures that a fresh surface of material is available for every laser shot. The carrier gas, typically helium, is pulsed by a Series 9 General Valve nozzle with a 1 mm orifice. The nozzle produces a gas pulse with a 200 – 400 μsec width and is backed by 20 – 100 psig of pressure. The timing of the experiment is controlled by digital delay generators (Stanford Research Systems DG535) such that the timing of the laser pulse can be adjusted relative to the gas pulse coming from the nozzle.

The laser vaporizes the sample rod and creates a hot plasma which is nominally neutral but contains both cations and anions, as well as free electrons and neutral species. The plasma is quenched by a pulse of the carrier gas which is brought to the vaporization spot by a 2 mm diameter channel in the rod holder. The vaporized species (carbon, metals, or silicon) are entrained in the carrier gas. Clusters grow via three body collisions between the helium and the various vaporization products. Simultaneous with growth, the clusters may be cooled in internal degrees of freedom by two body collisions with the helium. The extent of this cooling is dependent on the amount of collisional energy transfer between the clusters and the carrier gas. Translational to translational energy transfer is very efficient and thus leads to a low translational temperature, which is the equivalent of a narrow velocity distribution of the species in the molecular beam.[18] Because of the close spacing of rotational levels, energy in rotational degrees of freedom is also efficiently quenched by two body collisions in the expansion, leading to low rotational temperatures on the order of 10 K. Rare gases such as helium, neon,

and argon have no vibrational degrees of freedom with which to absorb energy, however, so the dissipation of internal vibrational energy in the clusters by efficient vibrational to vibrational energy transfer is not possible. Vibrational to translational collisonal energy transfer, which is possible here, can be inefficient, especially for high frequency vibrations.[18] Significant amounts of internal energy may thus be left in the vibrations of the clusters, which can lead to vibrational temperatures on the order of 50 – 300 K.

The growth of larger clusters requires multiple three body collisions between the recombining atomic or molecular species and the carrier gas. A true adiabatic, or free, expansion would limit the number of collisions of the vaporized species with each other and inhibit growth. Thus to grow bigger clusters this collision rate must be increased. This is done with a 4 mm diameter channel, contained in the rod holder but downstream from the vaporization point. The channel spoils the free expansion by confining the plasma. The concentration of the ablated species is kept high for a longer time, which helps to foster multiple collisions. Cluster aggregation is facilitated by allowing for more recombination of the vaporized species. The length of the second channel can be adjusted by adding a "growth" channel of the desired length to the end of the rod holder. A longer channel confines the gas pulse and the vaporization products for a longer time and also creates some turbulence in the gas flow, both leading to more collisions. This is necessary to form strongly bound clusters such as carbon and carbides, which have high condensation energies. The plasma then exits the channel and expands from a region of high pressure into the vacuum, and additional collisions with the carrier gas help to cool the clusters after their synthesis. This creates a supersonic molecular beam of cold clusters.

The molecular beam passes through a 3 mm skimmer cone (Beam Dynamics) approximately 15 cm downstream of the nozzle, which serves to collimate the beam. It then enters the differentially pumped mass spectrometer chamber. The pressure in this chamber is maintained at 10^{-8}-10^{-7} torr by a Varian VHS-6 diffusion pump, capable of pumping 1930 liters/second of helium. In this chamber the beam enters the extraction region of a Wiley-McLaren type time-of-flight (TOF) mass spectrometer.[19] A schematic of the mass spectrometer is shown in Figure 2.3. The source of the TOF consists of three acceleration plates. The bottom and middle plates, the repeller, and draw out grid (DOG), are pulsed to approximately 1000 V and 900 V, respectively, while the top plate is constantly held at ground (0 V). The molecular beam passes between the repeller and DOG plates, and cations are pulse extracted from the molecular beam and accelerated perpendicular to the beam axis. As mentioned above, the beam also contains neutral and anionic species, but by pulsing positive voltage on the plates, only positively charged cations are accelerated perpendicularly into the first flight tube. The timing of the pulses is controlled by a digital delay generator so that the plates are pulsed at a precise time after the nozzle and the laser have fired. The fast switching time of the high voltage on the repeller and DOG is achieved by using fast high voltage transistor switches (Behlke HTS-50, 50 nsec rise time). The difference in the voltage and the spacing of the plates creates an electric field gradient which can be optimized to increase the mass resolution of the instrument by compressing the ion packet spatially. Additional deflection plates are used in the first flight tube to compensate for any remaining velocity in the initial molecular beam direction. The deflection plates are especially critical for the detection of larger clusters, which due to their high mass are more likely to retain velocity in the

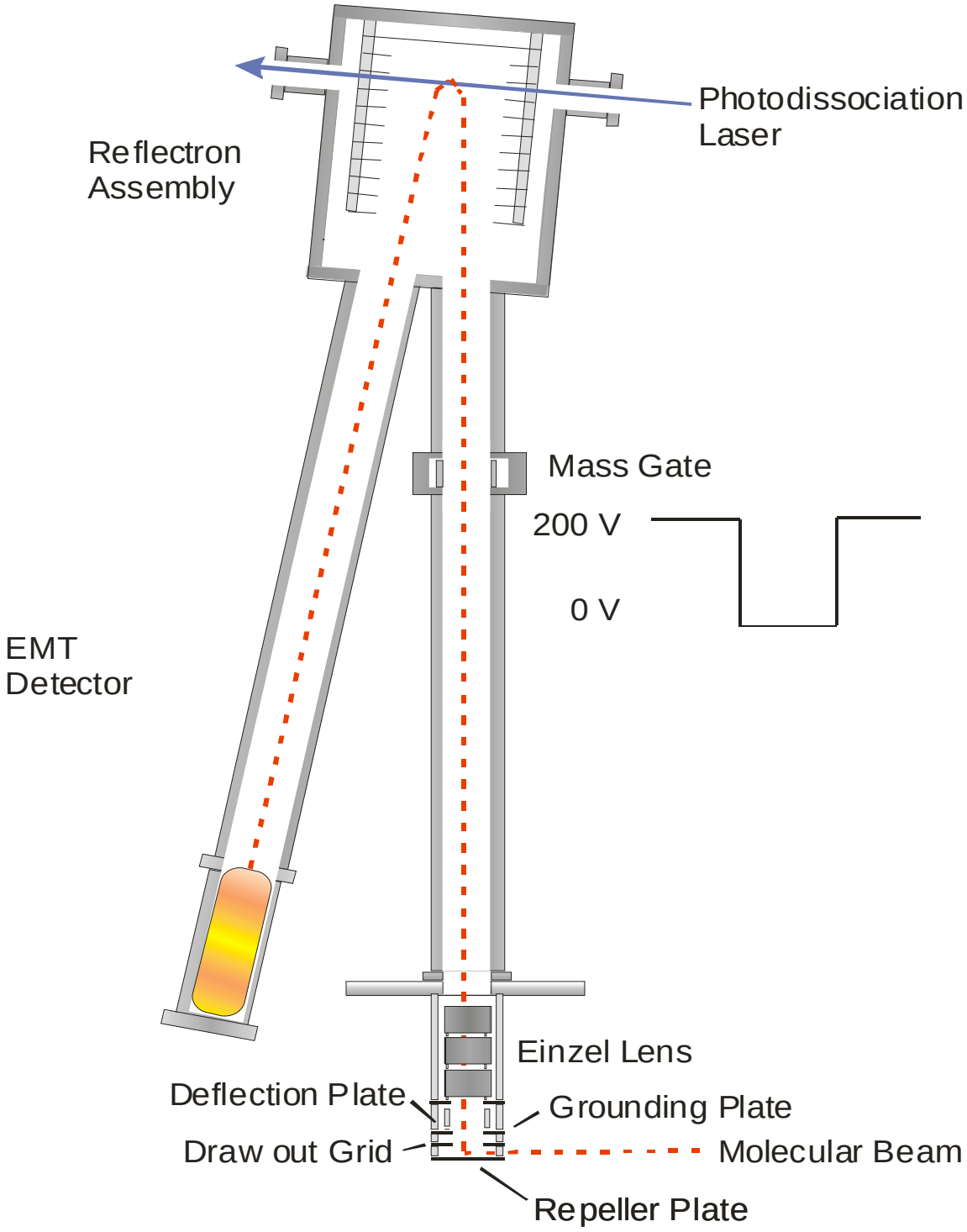

Figure 2.3: Reflectron time-of-flight mass spectrometer

initial direction of the beam. This flight tube also contains an einzel lens to help focus the ions axially onto the detector, limiting the spread of the ions away from the molecular beam direction. It consists of three cylinders, the middle of which is held at about +400 V while the outer two are kept grounded. The focal length of the lens is adjusted by changing the voltage on the center cylinder, and the optimal voltage varies with the mass of the ions being focused.

When the ions are accelerated by the mass spectrometer plates into the first flight tube, they all receive a "push," corresponding to the kinetic energy imparted on them by the electric fields created by pulsing the voltage on the plates. The ions begin to separate based on their mass to charge ratio in the field free drift region of the flight tube. If all the ions are singly charged, the separation is simply based on the mass. This can be seen in equations 2.1 and 2.2, where the kinetic energy (*KE*) and the mass (*m*) of an ion is related to its velocity (*v*). Because all the cluster ions are given the same kinetic

$$KE = \frac{1}{2} mv^2 \qquad (2.1)$$

$$\sqrt{\frac{2KE}{m}} = v \qquad (2.2)$$

energy, the lighter clusters (smaller *m*) will have a greater velocity than heavier clusters (larger *m*). This difference in velocity means that clusters with different masses will take different amounts of time to move down the flight tube, with the slower (heavier) species taking a longer time to traverse the tube and reach the detector. Equation 2.3 shows that velocity can be defined as a distance (*d*) divided by a time (*t*). In this case, *d* corresponds to the length of the flight tube, and *t* then corresponds to the flight time down the tube. In equation 2.2, KE is equal for all ions, and these two expressions reduce to equation 2.4.

$$v = \frac{d}{t} \tag{2.3}$$

The time of flight for an ion is thus proportional to the distance traveled multiplied by the square root of the mass. It follows from this that a longer flight tube will result in better separation between clusters with different masses by creating a greater separation in their

$$d\sqrt{m} \propto t \tag{2.4}$$

flight time. The difference in flight time between two ions with different masses, m_1 and m_2, along the same flight tube with distance *d* can be seen in equation 2.5 and 2.6. The first flight tube in the instrument is about 1 meter long, which provides sufficient time

$$m_1 \left(\frac{1}{t_1}\right)^2 = m_2 \left(\frac{1}{t_2}\right)^2 \tag{2.5}$$

$$m_2 = m_1 \left(\frac{t_2}{t_1}\right)^2 \tag{2.6}$$

separation between clusters to resolve most masses in the ranges examined in this study. A time of flight mass spectrum generated by detecting ion arrival times can be mass assigned using equation 2.6 if the arrival time of one mass is already known.

The separation of ions down the flight tube also allows for the use of a "mass gate," which is a set of two plates located in the first flight tube. If both of the plates are grounded, all clusters pass through unperturbed and the entire mass spectrum is detected. Selection of a particular cluster size for further experiments can be achieved by holding the mass gate at a constant 200 V. Ions that pass through the gate when the voltage is applied are deflected out of the beam and are not detected. Some separation of the ions has already been achieved based on their flight time from the extraction plates to the mass gate. Because of this, the voltage on the gate can very quickly be switched to 0 V

to allow a single cluster size of interest to pass with no deflection, and then be switched back to 200 V to deflect all ions coming later. The inset of Figure 2.3 shows the mass gate pulse. This form of mass selection is very well suited for experiments such a photodissociation, to be described below.

When the clusters reach the end of the first flight tube, they enter the reflectron, where they are slowed down to almost zero velocity, and then reaccelerated down a second flight tube. The reflectron in this experiment is a series of eleven steel plates that have rectangular holes cut in them. The front plates are grounded, while the other nine plates are connected in series by 200 kΩ resistors. A potential of about 1400 V is applied to the back plate, and the voltage drop across each resistor produces a voltage gradient that decreases moving toward the front plate. The electric field from the plates gradually slows ions that enter the reflectron to near zero velocity by converting their kinetic energy into potential energy. The ions are then reaccelerated down the second flight tube of the apparatus toward the detector. A reflectron can improve mass resolution by helping to compensate for the initial energy spread of the ions, but it also provides another benefit for laser photodissociation experiments. At the turning point of the ion trajectory, inside the reflectron, the ions briefly have zero velocity in the vertical direction. The precise moment when the ions are slowed in the turning region of the reflectron provides an excellent opportunity to overlap a photodissociation laser pulse with the ion packet. A laser pulse 5 nanoseconds in duration is typically used in these experiments, while the ions are in the turning region for 2 -3 μsec, so they move very little on the laser time scale laser. Thus both the temporal and spatial overlap of the dissociation laser with the ion packet is easily achieved at this point. Both the parent ions

and any daughter ions that result from photofragmentation are then reaccelerated by the reflectron down the second drift tube, and are again mass separated based on their flight times.

The ions are detected at the end of the second flight tube with an electron multiplier tube detector (Hamamatsu R595), or EMT, which amplifies the ion current by a factor of 10^6. This signal is then passed through a preamplifier (Stanford Research Systems 445A), which amplifies the signal by an additional factor of 5 or 25. The signals are recorded with a digital oscilloscope (LeCroy 9310 and LeCroy Waverunner) and transferred to a PC via an IEEE-488 interface. The mass spectrum is assigned on the PC using the equations described above.

Figure 2.4 shows two different mass spectra of carbon cluster cations produced in this experiment. The carbon rod was vaporized with 5 mJ/pulse of 532 nm light in an expansion of pure helium and clusters were grown in the regular rod holder configuration, with no growth channel. The upper trace shows a distribution of small carbon clusters, peaked at the C_7^+ cluster, while the bottom trace is peaked at C_{15}^+ and contains clusters of much larger size. The differences in the two mass spectra come about because of subtle variations in the experimental conditions. This includes changes in the delay between the gas pulse from the nozzle and the firing of the vaporization laser, changes in the width of the gas pulse, and changes in the alignment of the vaporization laser on the ablation rod. Adjusting these factors cause slight changes in the laser plasma because the plasma is being ignited by the laser at different times and at different areas within the gas pulse. As can be seen here, these very small changes can have a dramatic impact on the cluster distribution produced.

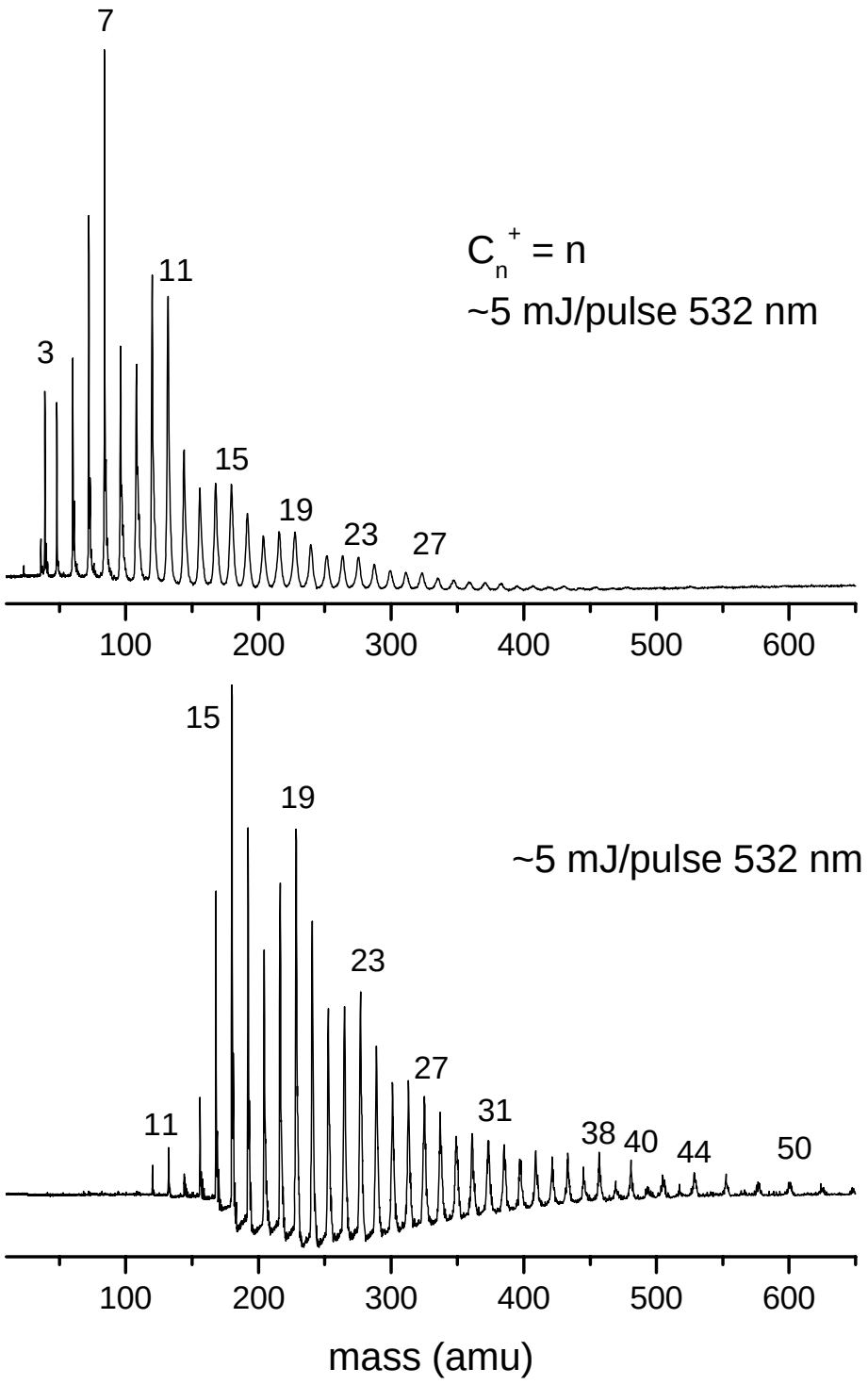

Figure 2.4: Time-of-flight mass spectrum of carbon clusters with experimental conditions optimized for smaller clusters (top) or larger clusters (bottom).

Additionally, the voltages on the deflection plates and the einzel lens must be changed to ensure the detection of all the clusters. Because heavier species have more momentum in the initial direction of the molecular beam before pulse extraction into the mass spectrometer, a higher voltage on the deflection is plates is required to ensure the trajectory of the ions is such that they arrive at the detector. As described above, the einzel lens also helps to focus the ion beam to ensure better detection as well. These small differences in the dynamics of the cluster growth process and ion focusing optics explain the dramatic differences in the cluster distributions between the upper and lower traces in Figure 2.4.

As mentioned above, photodissociation experiments of mass selected clusters are also conducted using this apparatus. In these experiments, the mass gate is used to select out one particular cluster size of interest. All other ions are deflected and do not reach the detector. At the precise time that the cluster ion of interest is in the turning point of the reflectron, the beam is excited by the third harmonic (355 nm) of an Nd:YAG (Spectra Physics DCR-3 or DCR-11). If the clusters absorb the light, then photofragmentation may occur. At this point both the parent ion and any resulting daughter ions are reaccelerated by the reflectron into the second flight tube and are detected simultaneously by the EMT. Both the parent and daughter ions have zero kinetic energy in the turning region, so when they are reaccelerated they will receive the same kinetic energy "push" from the electric fields in the reflectron. This allows the parent and fragment ions to be mass separated by their flight times down the second tube in the same manner as described above.

Figure 2.5 shows how photodissociation mass spectra can then be collected. The upper trace of Figure 2.5 is the mass selected C_{10}^+ cluster, with the photodissociation laser off. The presence of just the one desired cluster is seen in the mass spectrum, with no peaks to lower mass. A small peak likely corresponding to hydrogen contamination can be seen to the high mass side of the selected peak, but this small amount of signal that was not completely rejected by the mass gate does not pose a serious problem here. The complete mass selection achieved by the mass gate allows for the detection of fragment ions on a zero background. The middle trace in Figure 2.5 shows the mass spectrum when the cluster beam is excited by the photodissociation laser. Fragmentation of the parent occurs, and both parent and daughter ions are detected. In this case, the C_7^+ cluster is detected as a fragment, and by mass conservation it can be inferred that C_{10}^+ eliminated neutral C_3. The lower trace in Figure 2.5 is a difference mass spectrum, where the mass spectrum with the laser on is subtracted from the mass spectrum with the laser off. The positive going peak shows the appearance of the fragment, while the negative going peak shows the depletion of the parent. The integrated areas of the fragment peaks should theoretically be exactly equal to the area of the parent depletion peak, displaying charge conservation. This is not always the case, however. Mass discrimination in our instrument due to ion focusing effects prevents the simultaneous detection of both parent and fragment ions with equal sensitivity, and in some cases all of the parent or daughter ions may not be detected.[3] Generally we concentrate on focusing the fragment ions at the detector to prevent any strong bias in the observed fragmentation channels. Due to these

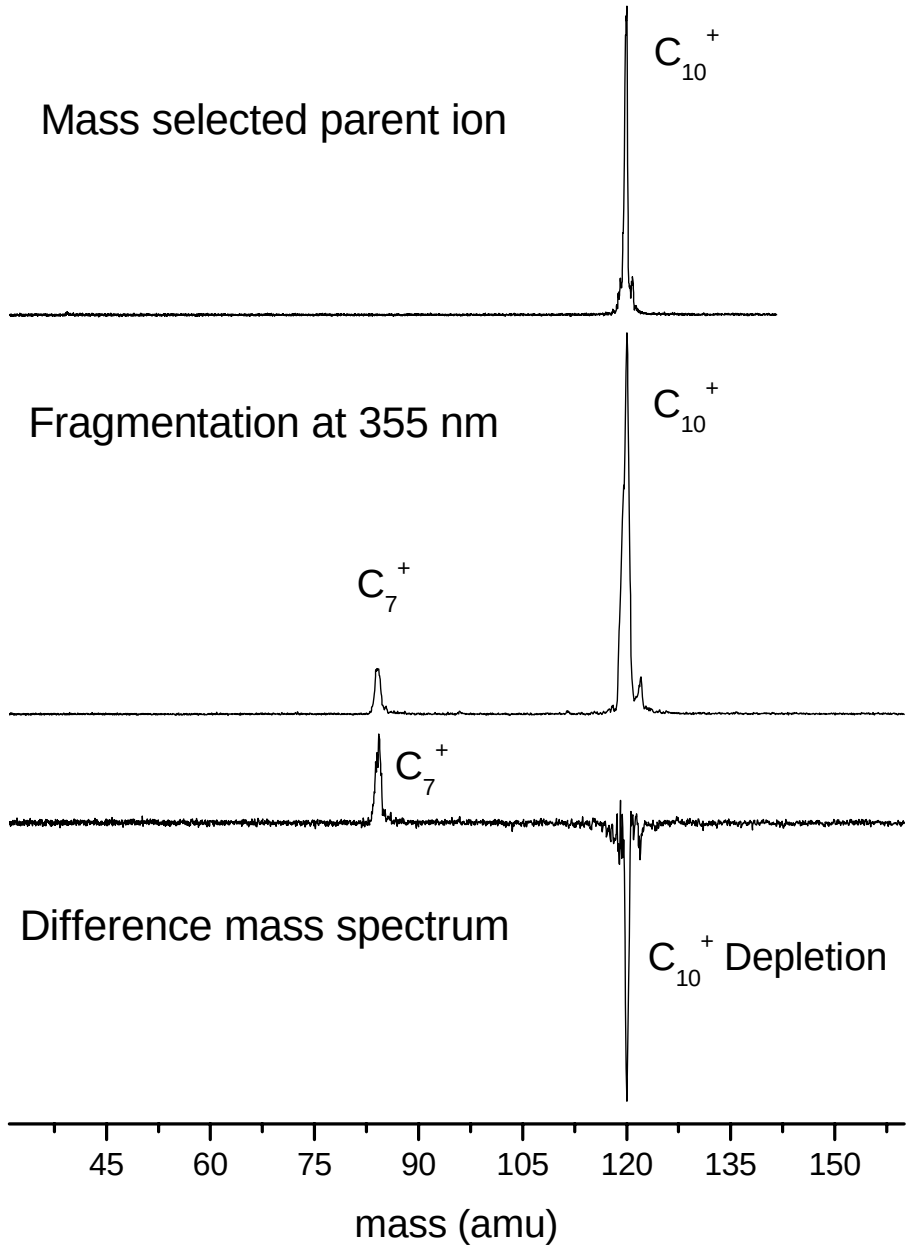

Figure 2.5: Photodissociation mass spectrum of C_{10}^{+}. The upper trace shows the mass selected parent ion (laser off), the middle traced shows the parent and the fragment ions (laser on), and the bottom trace is a difference mass spectrum, showing positive appearance of the fragment and negative depletion of the parent.

instrumental limitations, however, branching ratios are not reported, and fragmentation mass peaks are simply distinguished as either strong or weak.

Unimolecular kinetics described by RRKM theory can be used to explain the photodissociation of polyatomic molecules or clusters.[20,21] An implicit assumption with this theory is that vibrational excitation of the electronic ground state can occur if photon absorption is followed by fast internal vibrational energy redistribution in an excited electronic state. The system may then undergo internal conversion back to the ground state. Dissociation takes place when the cluster internal energy is higher than that of the lowest energy fragmentation channel of the ground state. Thus the weakest bond in a cluster is expected to break first. For strongly bound clusters, where the energy of a single photon is below the dissociation energy, photon absorption followed by energy redistribution may be repeated several times before enough energy is transferred to the dissociative coordinate to break a bond. Multiple photon absorption events are possible, and sometimes necessary to fragment strongly bound clusters. This may lead to fragments with high internal energy, but it greatly increases the rate of dissociation by raising the internal energy of the cluster above the dissociation threshold. The rate depends on both the amount of excess energy absorbed by the cluster above its dissociation threshold and on the density of states near the level where excitation occurs. Higher laser fluences increase the probability of multiphoton events, favoring unimolecular dissociation by providing higher internal cluster energy. A drawback, however, is that high laser fluences also create the possibility that fragments from the original parent ion may also absorb multiple photons, leading to sequential dissociation.

Fragmentation laser power dependence studies can help determine if sequential dissociation events are occurring. Lowering the laser power allows fewer multiphoton absorption events, so sequential dissociation (fragmentation of the fragments) is less likely to happen. Thus fragment mass peaks which correspond to this process should disappear. Figure 2.6 shows this process for C_{10}^+. The upper trace shows a photodissociation mass spectrum taken when 45 mJ/pulse of 355 nm light is used to excite the cluster beam. Extensive fragmentation occurs, and detected fragment masses range from C_2^+ up to C_7^+, with C_4^+ and C_7^+ being the largest fragments. In the lower trace 10 mJ/pulse of 355 nm light is used to dissociate C_{10}^+, and only a single fragment, C_7^+, is observed. By mass conservation the inferred neutral loss is C_3. From Figure 2.6, it is clear that loss of C_3 to form C_7^+ is the dominant fragmentation channel of the C_{10}^+ cluster, and the other fragment peaks are present due to subsequent dissociation events, and notably the intensity of the C_4^+ peak very likely corresponds to the sequential loss of C_3 from the original C_7^+ fragment.

Photodissociation can be a very useful experimental tool to study the bonding and energetics of clusters, especially in cases where spectroscopic information is unavailable. As discussed above, the weakest bond generally breaks first, so the relative bond strengths within a cluster can be studied by examination of the fragmentation channels. Charge conservation in the fragmentation of cations also ensures that one of the products from a given dissociation event will contain a charge. In this case, the charge is expected to remain on the fragment with the lower ionization potential (IP). Thus the relative IP's of the fragments, both charged and the inferred neutrals, may also be determined. Comparison to measured or calculated IP data for certain fragments may set upper or

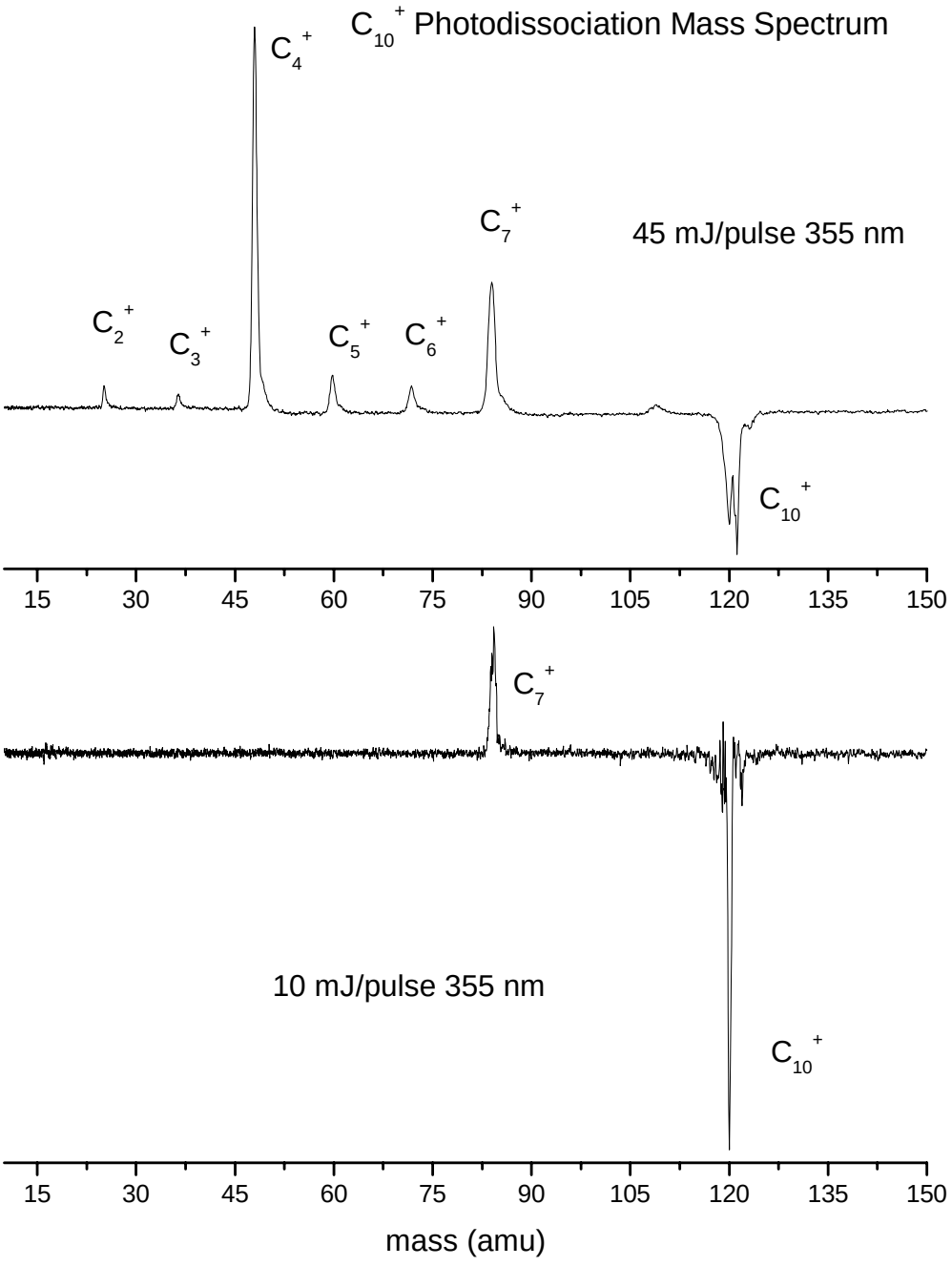

Figure 2.6: Photodissociation mass spectrum of C_{10}^+ at high and low laser power limits with 355 nm light.

lower levels for their IPs. For some carbon and carbide clusters IPs can be a sensitive measure of the structure, so bracketing the IP of a fragment may reveal that one isomer is present while another is not. Finally, if certain stoichiometries repeatedly appear as cation or neutral fragments from a variety of different clusters, this is an indication that these common fragment species enjoy enhanced stability. They may possibly be potential building blocks for larger clusters, and the recognition of their enhanced stability may identify them as interesting targets for both spectroscopy and theory, aiding in the ever advancing understanding of chemical bonding. The experimental apparatus described here has been used to study the photodissociation of metal carbide,[4-10] metal oxide,[11-15] silicon carbide,[16] and metal silicon species.[17]

2.1 REFERENCES

(1) Dietz, T. G.; Duncan, M. A.; Powers, D. E.; Smalley, R. E. *J. Chem. Phys.* **1981**, *74*, 6511.

(2) Powers, D. E.; Hansen, S. H.; Geusic, M. E.; Puiu, A. C.; Hopkins, J. B.; Dietz, T. G. Duncan, M. A.; Langridge-Smith, P. R. R.; Smalley, R. E. *J. Phys. Chem.* **1982**, ***86,*** 2556.

(3) Cornett, D. S.; Peschke, M.; Laihing, K.; Cheng, P. Y.; Willey, K. F.; Duncan, M. A. *Rev. Sci. Instrum.* **1992**, *63*, 2177.

(4) Pilgrim, J. S.; Duncan, M. A. *J. Am. Chem. Soc.* **1993**, *115*, 4395.

(5) Pilgrim, J. S.; Duncan, M. A. *J. Am. Chem. Soc.* **1993**, *115*, 6958.

(6) Pilgrim, J. S.; Duncan, M. A. *J. Am. Chem. Soc.* **1993**, *115*, 9724.

(7) Pilgrim, J. S.; Duncan, M. A. *Int. J. Mass Spect. Ion Proc.* **1994**, *138*, 283.

(8) Pilgrim, J. S.; Brock, L. R.; Duncan, M. A. *J. Phys. Chem* **1995**, *99*, 544.

(9) Duncan, M.A. *J. Clust. Sci.* **1997**, *8*, 239.

(10) Ticknor, B. W.; Bandyopadhyay, B.; Duncan, M. A. *J. Phys. Chem. A* to be submitted.

(11) France, M. R.; Buchanan, J. W.; Robinson, J. C.; Pullins, S. H.; Tucker, J. L.; King, R. B.; Duncan, M. A. J. *Phys. Chem. A* **1997**, *101*, 6214.

(12) Molek, K. S.; Jaeger, T. D.; Duncan, M. A. J. Chem. Phys. 2005, 123, 144313.

(13) Molek, K. S.; Reed, Z. M.; Ricks, A. M.; Duncan, M. A. *J. Phys. Chem. A* **2007**, *111*, 8080.

(14) Reed, Z. A.; Duncan, M. A. *J. Phys. Chem. A*, in press.

(15) Molek, K. S.; Anfuso-Cleary, C.; Duncan, M. A. *J. Phys. Chem. A*, in press.

(16) Ticknor, B. W.; Duncan, M. A. *Chem. Phys. Lett.* **2005**, *405*, 214.

(17) Jaeger, J. B.; Jaeger, T. D.; Duncan, M. A. *J. Phys. Chem. A.* **2006**, *110*, 9310.

(18) Yardley, J. T. *Introduction to Molecular Energy Transfer*; Academic Press: New York, 1980.

(19) Wiley, W. C.; McLaren, I. H. *Rev. Sci. Instrum.* **1955**, *26*, 1150.

(20) Lethokov, V. S. Ed. *Laser Spectroscopy of Highly Vibrationally Excited Molecules;* Hilger: London, 1989.

(21) Baer, T.; Hase, W. *Unimolecular Reaction Dynamics*; Oxford University Press: New York, 1996.

CHAPTER 3

VISIBLE AND INFRARED PHOTODISSOCAITION STUDIES OF CARBON CLUSTER CATIONS

3.1 ABSTRACT

Carbon cation clusters are produced by laser vaporization in a pulsed molecular beam and detected with time-of-flight mass spectrometry. Specific sizes are mass selected and photodissociated. Spectra for the C_6^+ and C_8^+ were collected from 620 – 660 nm, and several broad resonances are detected. Complications from cluster dissociation energies and high internal energies prevent assignments of the observed transitions, but C_6^+ does show a resonance at 648 nm, near the 645.8 nm band previously measured in a neon matrix. The resonances in both species are close to several known diffuse interstellar bands, and thus these preliminary experiments may serve as a guide for future high resolution gas phase spectroscopic searches. Attempts to measure infrared photodissociation spectra from 2000 – 4000 cm^{-1} were unsuccessful, but several experimental improvements are underway which may allow the eventual realization of this goal.

3.2 INTRODUCTION

The clusters of pure carbon have generated a staggering number of experimental and theoretical studies,[1-3] especially since the discovery of fullerenes by Smalley and co-workers in 1985.[4,5] The study of carbon clusters has implications in areas as varied as combustion chemistry,[6,7] nanomaterials,[8-12] and astrophysics,[13-21] and understanding the molecular structure and bonding in these systems is an ongoing challenge to experiment

and theory. The measurement of both electronic and vibrational spectra for these species would greatly advance the current knowledge of these systems. The present work represents a preliminary attempt to use photodissociation spectroscopy with tunable visible and infrared laser systems to probe the electronic and vibrational spectra of mass selected carbon cation clusters.

Many mass spectrometry experiments have studied carbon clusters produced from laser ablation of graphite in a helium expansion.[4,22-31] Neutral species, as well as cations and anions, are all produced simultaneously in these experiments. Clusters with enhanced abundances have been seen, most famously C_{60},[4,5] but other sizes may also be prominent depending on the specifics of the experiment. For the cations, the cluster sizes C_3^+, C_7^+, C_{11}^+, C_{15}^+, and C_{19}^+ have been seen with enhanced abundances.[1,2] This pattern fits a 4n – 1 relationship for sizes with enhanced intensity, corresponding to every fourth cluster. Whether the enhanced abundance of these species is due to greater relative stability or simply lower ionization potentials is still a subject of debate. Anions have also been studied by mass spectrometry, and seem to favor C_n^- (n = even) cluster sizes, with C_{10}^-, C_{12}^-, and C_{14}^- seen as the most prominent.[1,2] Several groups have used 10.5 eV light to photoionize neutral carbon clusters in molecular beams, and C_{10}^+, C_{12}^+, and C_{14}^+ were seen as the most prominent, similar to the anion experiments.[26-29] Multiphoton ionization at 355 nm, however, shows C_{11}^+, C_{15}^+, and C_{19}^+ to be prominent, the same as seen in the cation experiments.[30] A recent study by Duncan and co-workers, described in detail in Chapter 6 of this dissertation, used single photon ionization with tunable vacuum ultraviolet light to study the distribution of neutral carbon clusters produced in a laser plasma and also to measure ionization thresholds for individual sizes.[32] The study found

that, when using photon energies above the ionization potential of C_3 (11.6 eV),[33] C_3^+dominated the mass spectrum, and that C_{10}^+, C_{12}^+, and C_{14}^+ , although considerably smaller than C_3^+, were also prominent. The high IP of C_3 had thus previously prevented its detection by single photon ionization at 10.5 eV.[26-29] This finding then raises questions about photon energy and the size dependence of the photoionization cross sections, ionization potentials (IPs), and electron affinities (EAs) in the earlier experiments. Fragmentation events likely also play a role in the growth of both the ionic and neutral clusters. Because of these issues, clusters seen to be abundant in any of these mass spectrometry experiments cannot be confidently said to exhibit enhanced stability, with the notable exception of fullerenes, the stability of which numerous experiments have confirmed.

To circumvent some of these issues, experiments have been performed on mass selected cluster ions. In this way, regardless of the mechanism of growth and ionization, a single ionic cluster size may be studied and the results interpreted independently of the problems described above. Fragmentation channels and dissociation energies may be measured directly without the complication of possible photofragmentation of larger species and variations in the ionization cross section, IP, and EA with size. Photodissociation,[34-41] metastable ion decay,[42-45] and collision induced dissociation (CID)[38,46] have been used to study carbon clusters. All these dissociation experiments have found that small clusters ($C_n^{+/-}$, $n< 30$) fragment predominately by the loss of neutral C_3. The larger fullerenes, however, lose either C_2 or C atom, depending on the size, allowing a closed spherical shell structure to be maintained.[37] This very distinct change in fragmentation behavior was observed for C_{32}^+, while other photodissociation

experiments showed an increase in dissociation energy at C_{30}^+.[39] Both experiments thus suggest the onset of fullerene formation in this size regime. Additionally, the CID experiment determined dissociation energies for the small clusters, and indeed C_3^+, C_7^+, C_{11}^+, C_{15}^+, and C_{19}^+ were all seen to have higher dissociation energies than surrounding sizes.[38,46] Fourier transform ion cyclotron resonance mass spectrometry has also been used to bracket the ionization potentials of small carbon clusters by reacting mass selected ions with neutral molecules of known IPs.[47,48] Bowers and co-workers have conducted ion mobility experiments on mass selected ions.[49] Depending on the size, both linear chain and cyclic ring isomers were seen at small sizes, while fullerenes appeared at C_{30}^+ and larger sizes. These experiments also concluded that the linear chains were much more reactive than the rings.

The spectroscopy of carbon clusters has also been an extremely active area of research, both in the laboratory and in astronomical searches of space. Neutral carbon molecules of many sizes have been quite extensively characterized by electronic[1,2,50-56] and infrared[1,2,59-76] and Raman[77,78] matrix isolation spectroscopy, but only a few gas phase measurements have been made.[1,2,79-90] More recently terahertz spectroscopy has been employed.[91,92] So far, however, C_3 remains the biggest pure carbon molecule identified in diffuse interstellar clouds.[2,91,93-95] Searches for C_4 and C_5 in interstellar space have failed,[95,96] although C_5 has been observed in the circumstellar shell of a carbon star.[2] There is also a large body of theoretical work on the neutral species that has guided the spectroscopic studies and helped to confirm the structures and energetics of these molecules.[1,2,96-128] Small neutral carbon clusters with an odd number of carbon atoms (C_3, C_5, C_7, C_9) are almost certainly linear chains in the ground state, with the cyclic

isomers lying somewhat higher in energy.[2] The even numbered carbon species (C_4, C_6, C_8) have both linear and cyclic structures lying very close in energy and even high level quantum mechanical calculations struggle with issue of determining the lowest energy isomer, although computations tend to prefer the cyclic structures.[2] In the laboratory, however, the linear chains have proven easier to detect spectroscopically in both the gas phase and in matrices, and thus the vast majority of the experimental literature deals with the this isomer.[2] At sizes between C_{10} - C_{20}, the lowest energy structure is always predicted to be a monocyclic ring, while with sizes above C_{20} polycyclic rings, bowls, graphitic sheets, and fullerenes are all possible.[2]

Carbon cluster cations, like their neutral counterparts, have generated considerable interest but have proven more difficult to study spectroscopically. As described above, mass spectroscopy experiments utilizing various dissociation methods,[34-46] have revealed important energetic information for these species. Vala and coworkers reported the infrared spectra of cyclic C_5^+ in an argon matrix,[129] but later reassigned the observed vibrational bands to the C_3•H_2O species.[130] Recently, Maier and coworkers recorded the electronic and infrared absorption spectra of the C_6^+ ion in a neon matrix, the first spectroscopic study of a pure carbon cation chain larger than the dimer.[131] This was followed by the measurement of electronic spectra for $C_{7\text{-}9}^+$ isolated in a matrix, which detected multiple transitions for both the linear and cyclic isomers of C_7^+ and C_8^+, and a single transition for the linear isomer of C_9^+.[132] Numerous theoretical studies[133-144] have been conducted on these species, complementing experiment by helping to identify structural and energetic information of these clusters.

Carbon clusters, both neutral and charged, have been suggested as possible carriers for the diffuse interstellar bands (DIBs).[13-17,19-21] Carbon is known to be abundant in both stellar and interstellar environments, and many of the species which have been detected in space contain carbon. Carbon chains are also predicted to have intense electronic transitions throughout the visible region of the spectrum, some of which might correspond to certain DIBs. Extensive work by John Maier has lead to the conclusion that small neutral chains can be excluded as carriers, but larger species, specifically sizes C_{15-31} with an odd number of carbon atoms, will have electronic transitions with appreciable oscillator strength in the correct region of the spectrum.[21] The spectroscopy of carbon cluster cations is less well characterized, however, and they have not yet been ruled out as a potential source of the DIBs. Gas phase measurements of the electronic spectra of these ions will be essential for comparison to astronomical observations. It would also serve as a rigorous test of computational chemical methods, as spectroscopy may determine the structures of these molecules unambiguously.

Photodissociation serves as a possible method to measure the spectroscopy of these species. This technique has been used previously in our laboratory and others to measure both electronic[145] and infrared[145,146] spectroscopy of size selected cations. In the present study, carbon cluster cations produced by laser vaporization in a pulsed molecular beam are studied with mass selected photodissociation. Attempts to measure both electronic and infrared resonance enhanced photodissociation spectra are described, and preliminary measurements of the gas phase electronic photodissociation spectra of C_6^+ and C_8^+ in the 620 nm – 650 nm region, both with possible resonances near the position

of numerous DIBs, including the very prominent 628.4 nm band, are reported for the first time.

3.3 EXPERIMENTAL

Pure carbon cation clusters are produced in the pulsed nozzle laser vaporization source and molecular beam machine described in detail in Chapter 2 of this dissertation. Briefly, the second harmonic (532 nm) of a Spectra Physics Nd:YAG laser (Quanta Ray GCR-11) is used to vaporize a rotating and translating carbon rod (Glass Supply 99.9% purity). A Series 9 General Valve with a 1 mm orifice pulses helium at 300 μsec and a backing pressure of 50 psi. The vaporization ignites a plasma and the clusters are grown in a rod holder with a 4 mm diameter channel, before being cooled by supersonic expansion into the source chamber.

The molecular beam is then skimmed into the differentially pumped mass spectrometer chamber. Cations present in the molecular beam are pulse extracted into the time-of-flight mass spectrometer. The cluster size of interest is mass selected by pulsed deflection plates before entering the reflectron. The ions are slowed to near zero velocity in the turning region of the reflectron, where they are intersected with the output of a tunable dye laser to excite electronic transitions or with infrared light to excite vibrational transitions. Resonant excitation of the clusters occurs, and if enough energy is absorbed photodissociation will occur. Alternately, the third harmonic (355 nm) of an Nd:YAG laser (Spectra Physics DCR-3) may be used to dissociate the clusters using high laser power at a single frequency. Mass separation of the parent ion and photofragments is

achieved by flight times through the second drift tube before arriving at the electron multiplier detector. The output of the detector is recorded with a digital oscilloscope (LeCroy WaveRunner 341) connected to a PC with an IEE-488 interface. The resonance enhanced photodissociation (REPD) spectra are recorded by monitoring the fragmentation yield as a function of dissociation laser wavelength.

For electronic transitions in the visible or ultraviolet region of the spectrum, the excitation laser is a tunable dye laser (Lambda Physik Scanmate-2E) pumped by the second harmonic (532 nm) of an Nd:YAG laser (Spectra Physics GCR-170). Approximately 3 mJ/pulse of power is used in these experiments, with step sizes of .05 nm. Vibrational transitions in the infrared region of the spectrum are probed by light from a Laser Vision IR OPO/OPA (optical parametric oscillator / optical parametric amplifier) pumped by a Continuum 8000 seeded Nd:YAG. This system produces tunable laser light from 2000 - 4500 cm^{-1} with typical pulse energies between 2 - 15 mJ/pulse and laser linewidths on the order of 0.3 cm^{-1}.

3.4 RESULTS AND DISSCUSSION

Figure 3.1 shows mass spectra of carbon cluster cations produced in the pulsed laser ablation source. The mass spectrum in the upper trace, collected with a vaporization laser power of 15 mJ/pulse of 532 nm light, contains mainly small species and is peaked at C_6^+. Sharp drop offs in intensity are observed after cluster sizes C_7^+, C_{11}^+, C_{15}^+, and C_{19}^+. This pattern of enhanced abundances for clusters satisfying the 4n – 1 relationship (every fourth cluster) has been seen before in many mass spectrometry experiments on

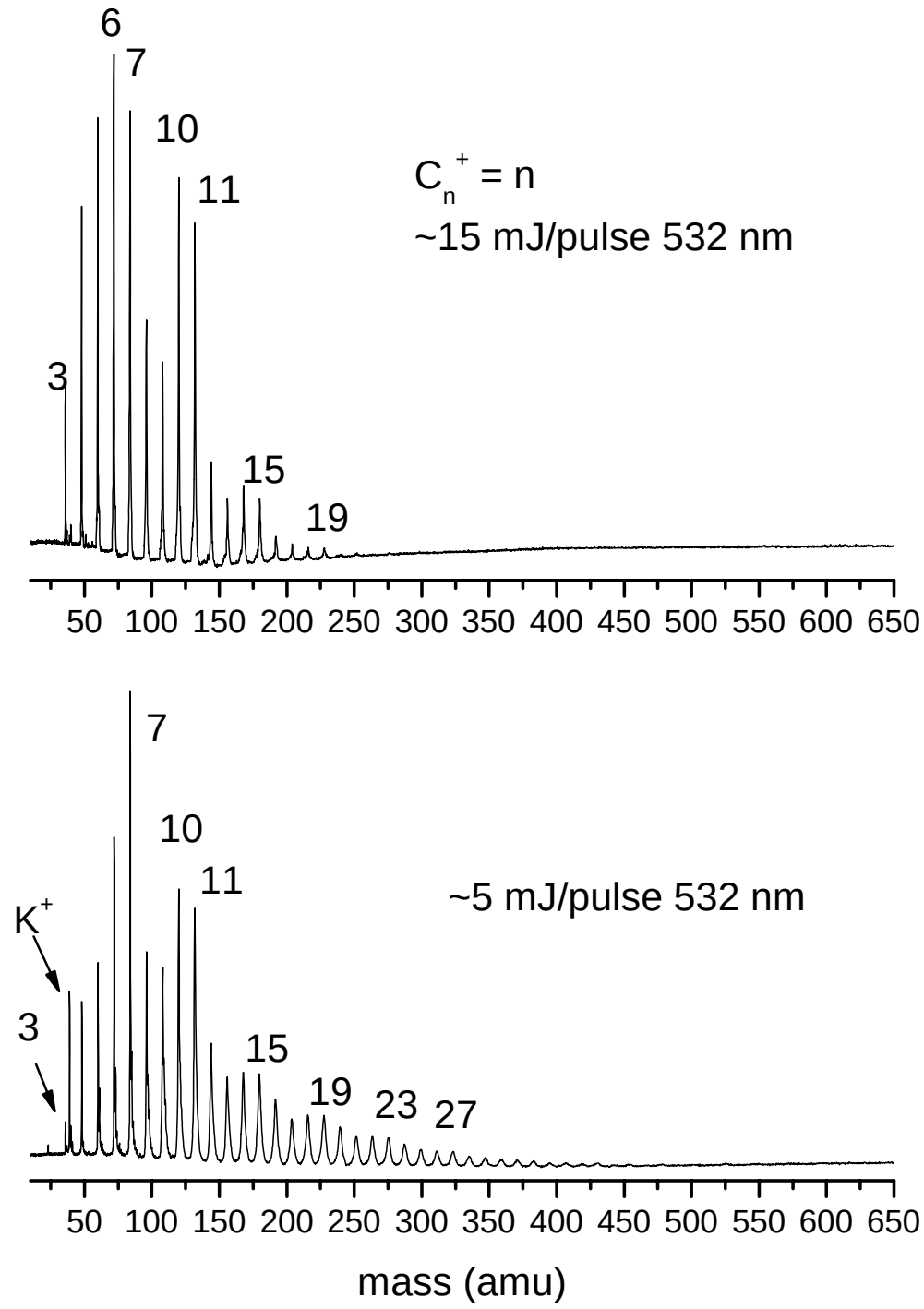

Figure 3.1: Time-of-flight mass spectrum of carbon clusters, produced with vaporization laser powers of 15 mJ/pulse (top) or 5 mJ/pulse (bottom) at 532 nm.

carbon cations, as described above.[1,2] The bottom trace of figure 3.1 was collected under similar experimental conditions but with lower laser power, 5 mJ/pulse. The mass spectrum here is peaked at C_7^+. The same 4n - 1 cluster series is observed with enhanced abundances, but the increase in intensity is not as dramatic. Additionally, much bigger speciess are present here, and the intensity of the smaller cluster peaks is lower than in the top trace. C_3^+ especially is much more prominent in the upper trace. A mass peak corresponding to the potassium atomic ion, a common impurity, is much larger than C_3^+ in the lower trace, while in the upper trace the opposite is true. The experimental conditions for generating both mass spectra are essentially the same, and the differences in the two mass spectra can be explained by a difference in the laser power used to ablate the sample rod and grow the clusters.

Laser vaporization of carbon is known to produce a high density of C_3[32] and carbon aggregates very efficiently in the gas phase. Thus in both experiments, large carbon cations are likely formed initially. With high laser power, however, the larger clusters undergo fragmentation events, either from multiphoton absorption of the 532 nm wavelength utilized in the vaporization or from high energy collisions that occur in the plasma. Either way, the larger species do not survive the higher energy growth conditions present in the upper trace, and they fragment to form the smaller clusters. This explains the absence of the larger clusters in the upper trace.

Examining the fragmentation channels for some of these larger clusters then makes clear the reasons for the greater relative intensities found for all the smaller carbon peaks, especially C_3^+. Figures 3.2 and 3.3 shows representative photodissocation mass spectra generated for some intermediate carbon cluster cation sizes. Experiments of this

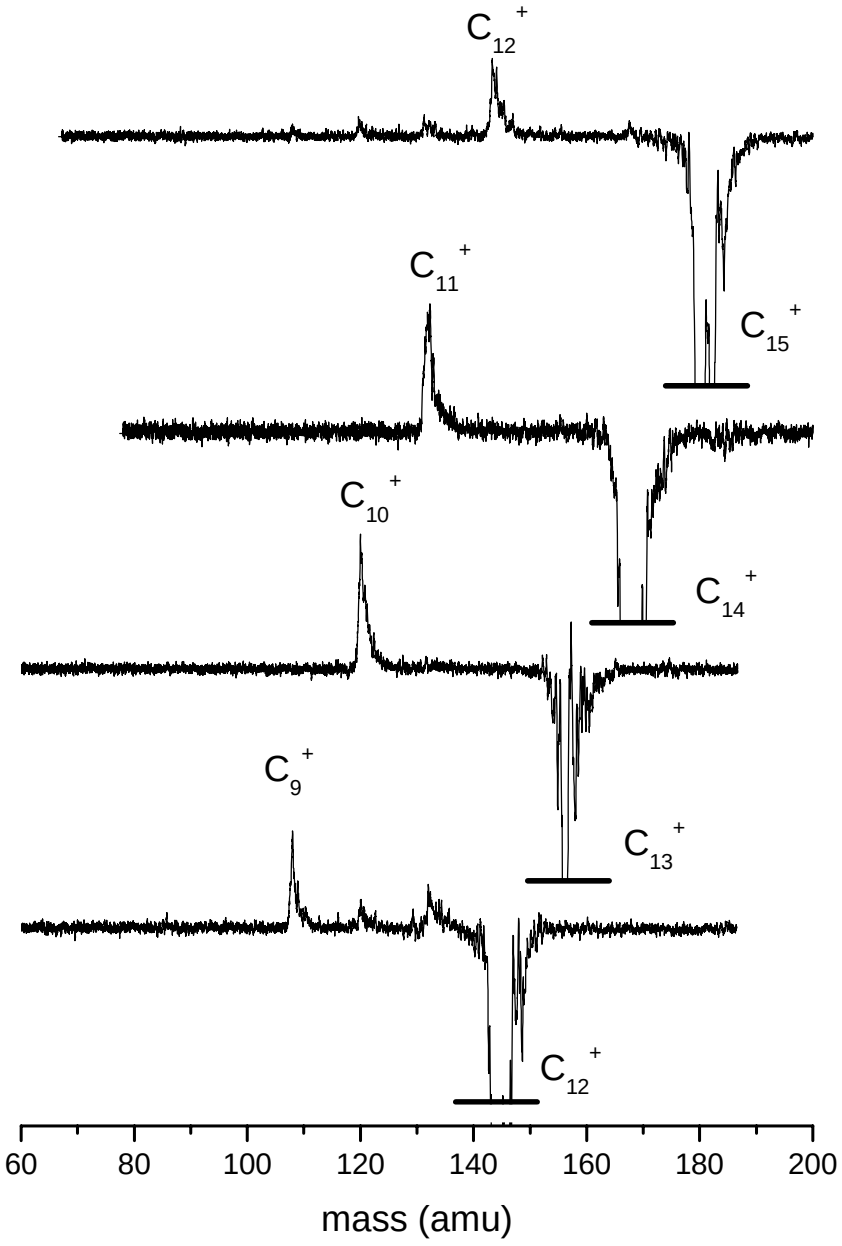

Figure 3.2: Photodissociation mass spectra of $C_{12\text{-}15}^{+}$ clusters with 10 mJ/pulse of dissociation laser power at 355 nm.

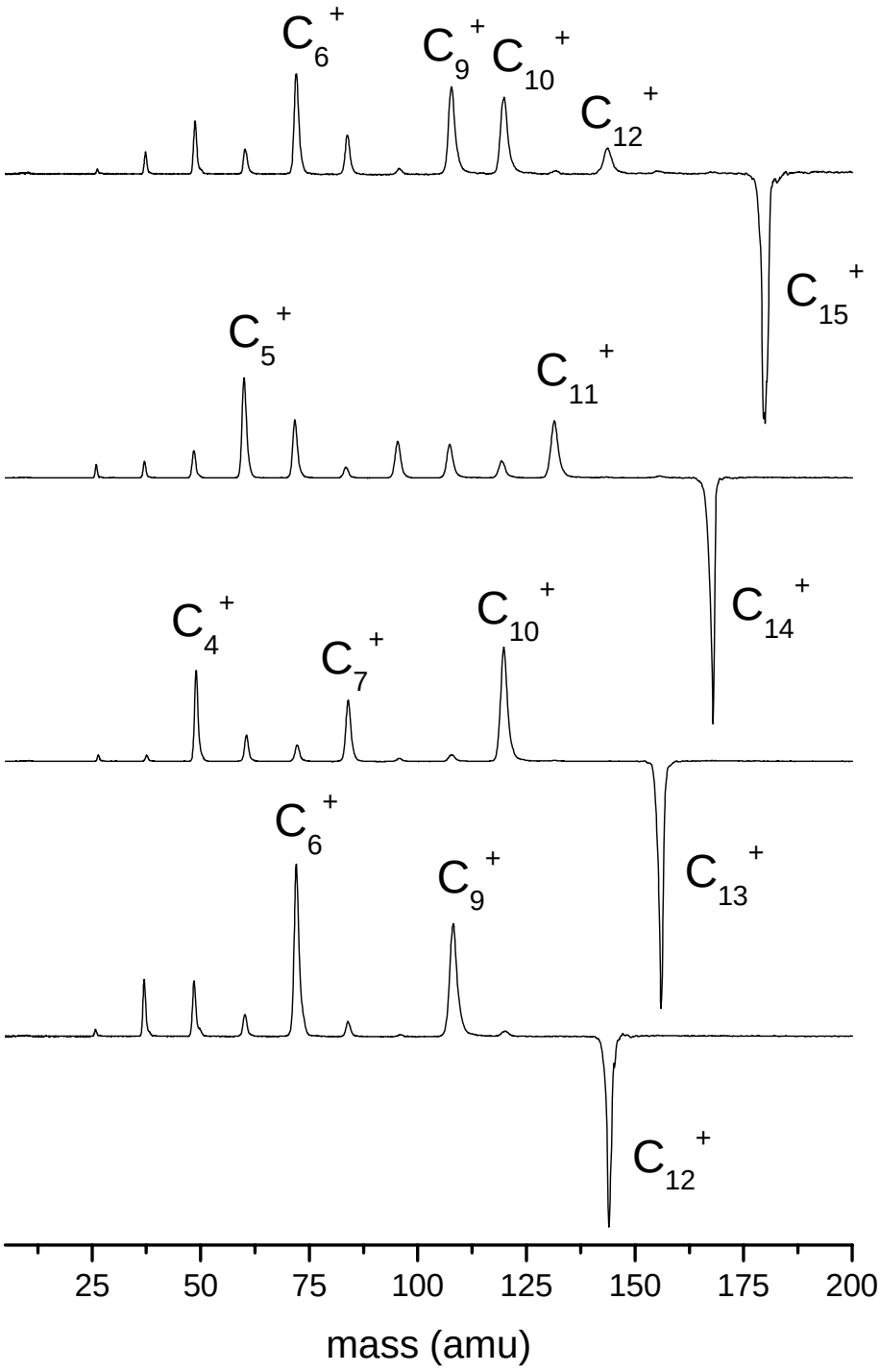

Figure 3.3: Photodissociation mass spectra of $C_{12\text{-}15}^{+}$ clusters with 45 mJ/pulse of dissociation laser power at 355 nm.

sort have been performed previously on carbon cations,[34-41] and the results reported here are entirely consistent with those experiments. These mass spectra are generated by the difference method described in detail in Chapter 2 of this dissertation. A particular cluster size of interest is mass selected and intersected with a laser in the turning region of the reflectron. Photodissociation occurs if the species absorbs enough energy. The dissociation mass spectra then represent the difference of a mass spectrum collected with the dissociation laser on minus a mass spectrum collected with the laser off. The positive peaks represent the appearance of the fragments, while the negative peaks represent the depletion of the parent ion. The dissociation mass spectra shown in Figure 3.2 were collected using 355 nm light with 10 mJ/pulse, while those in Figure 3.3 were collected with 45 mJ/pulse. As described in Chapter 2 and depicted in Figure 2.6, power dependence studies of photodissociation pathways helps in the determination of parallel versus sequential fragmentation events. In Figure 3.2, at low laser power conditions, one fragment peak is predominate for each cluster size, corresponding to the loss of neutral C_3 from each parent. The loss of C and C_2 from the C_{12} parent has been seen previously and is thought to represent dissociation from an unrelaxed fraction of the ions rather than from additional fragmentation channels opened by multiple photon absorption.[41] Besides this, however, C_3 elimination is clearly the favored fragmentation channel. Figure 3.3, taken at high laser power, shows significant fragmentation for every cluster size, very much beyond the simple loss of C_3 seen in Figure 3.2. Because of the differences in Figure 3.2 and 3.3, we can conclude that the use of high laser power dramatically increases the chances for multiphoton absorption and the observed fragmentation patterns correspond to sequential and not parallel channels. The photofragmentation pathways

seen here give insight into the fragmentation of the carbon clusters that may occur when high ablation laser power is used to grow the them.

As shown in Figure 3.3, extensive dissociation of carbon clusters, including sequential fragmentation events, is possible with high laser power. Clearly, many different daughter ions are produced by the fragmentation of one cluster size. When the dissociation channels of many different clusters are all combined, a variety of smaller sizes will result. Because of possible mass discrimination issues that occur with the experimental apparatus, as well as the extremely high photon flux used here, the measurement of branching ratios is not appropriate here. However, the fragmentation patterns for all cluster sizes do show significant fragmentation by the inferred loss of C_3 neutral. Even sequential fragmentation events favor this loss channel. In the laser plasma, then, fragmentation of larger clusters forms smaller cations species and neutral C_3. The C_3 may subsequently be ionized in the plasma, and then C_3^+ would be detected. This pathway for C_3^+ formation may explain its increased abundance in the upper trace of Figure 3.1. Alternatively, the ionization potential of C_3 (11.6 eV)[33] is known to be higher than that of the larger carbon clusters. C_3 may thus already be present in good intensity in the laser generated carbon plume, but only in the hot plasma conditions which occur when high laser power is used does it become ionized. Some combination of both these factors may be at work here. Regardless, the photodissociation data measured for carbon cations helps rationalize the differences between the two mass spectra shown in Figure 3.1.

The formation process of these clusters can lead to complications in spectroscopy experiments, however. Species formed by fragmentation of larger clusters are likely to

contain significant internal energy, possibly just below the dissociation energy. Strongly bound clusters of this type also have high condensation energies which can leave significant internal energy leftover from the growth process. This is especially true for larger clusters, which can contain energy in many different vibrations. As described in Chapter 2 of this dissertation, the quenching of vibrational energy by collisions in a supersonic expansion can be inefficient. High internal energy has implications for measuring resonance enhanced photodissociation spectra. Population may be spread over a number of low lying excited states and isomers, and dissociation may become efficient even without resonance enhancement.

Pure carbon cations, as mentioned above, have never been previously studied spectroscopically in the gas phase, so very precise knowledge of the location of transitions in these species is unavailable. Maier's work on matrix isolated C_n^+ (n = 6-9) [131,132] clusters is the best available guide for the location of the electronic transitions for these clusters. Some available data on these species, both experimental and theoretical, is collected in Table 3.1. In a neon matrix, linear C_6^+, which has $D_{\infty h}$ symmetry, has a $^2\Pi_g \leftarrow X^2\Pi_u$ electronic transition with an origin band at 646 nm. The initial assignment of the spectrum was achieved with the aid of MRD-CI calculations.[136] The agreement of theory with experiment is fairly poor, however, as theory overestimates the transition by more than 0.5 eV. A second theoretical study on excited electronic states of C_6^+ [138] showed the transition intensity for both the linear and cyclic isomers is spread over a number of low lying states. Strong coupling among these states makes the prediction of relative intensities and a simulation of the electronic spectrum very problematic from a theoretical point of view.

Using Maier's matrix spectra as a guide,[131] we conducted a search for transitions corresponding to the C_6^+ cation in the area of 645 nm. Figure 3.4 shows fragmentation mass spectra for C_6^+ collected with both 355 nm (3.49 eV) light and 630 nm (1.96 eV) light. The fragmentation patterns are similar, with C_3^+ (and inferred loss of neutral C_3) production the major fragmentation channel at both wavelengths. Photodissociation of this species at 630 nm has not been previously reported. Before this investigation it was not certain that fragmentation would occur in this wavelength range at all, even on resonance. The dissociation energy of this species has been measured by CID to be 5.2 eV,[38,46] meaning that fragmentation from the ground state of the cluster would be at least a three photon process at this wavelength. The similarity of the fragmentation pattern as compared to that seen with 355 nm light suggests that sequential fragmentation events are not occuring. Observing fragmentation at this wavelength is extemely problematic, however, because it suggests that dissociation may not be wavelength dependent, which would complicate the measurement of resonance enhanced photodissociation spectra. In fact, initial scans of the spectrum showed background fragmentation everywhere and no signs of enhancement of the fragmentation signal corresponding to changes in the excitation wavelength. This might be due to the fragmentation of an internally hot fraction of the C_6^+ ions in the beam, which, as described above, is plausible for clusters produced from this source. Another possibility is that the clusters absorb so strongly that multiphoton processes are unavoidable, even without resonance enhancement. It is likely that only species which already have significant internal energy are fragmenting, and any resonant processes aree obscured by this. It might be possible to probe a colder portion

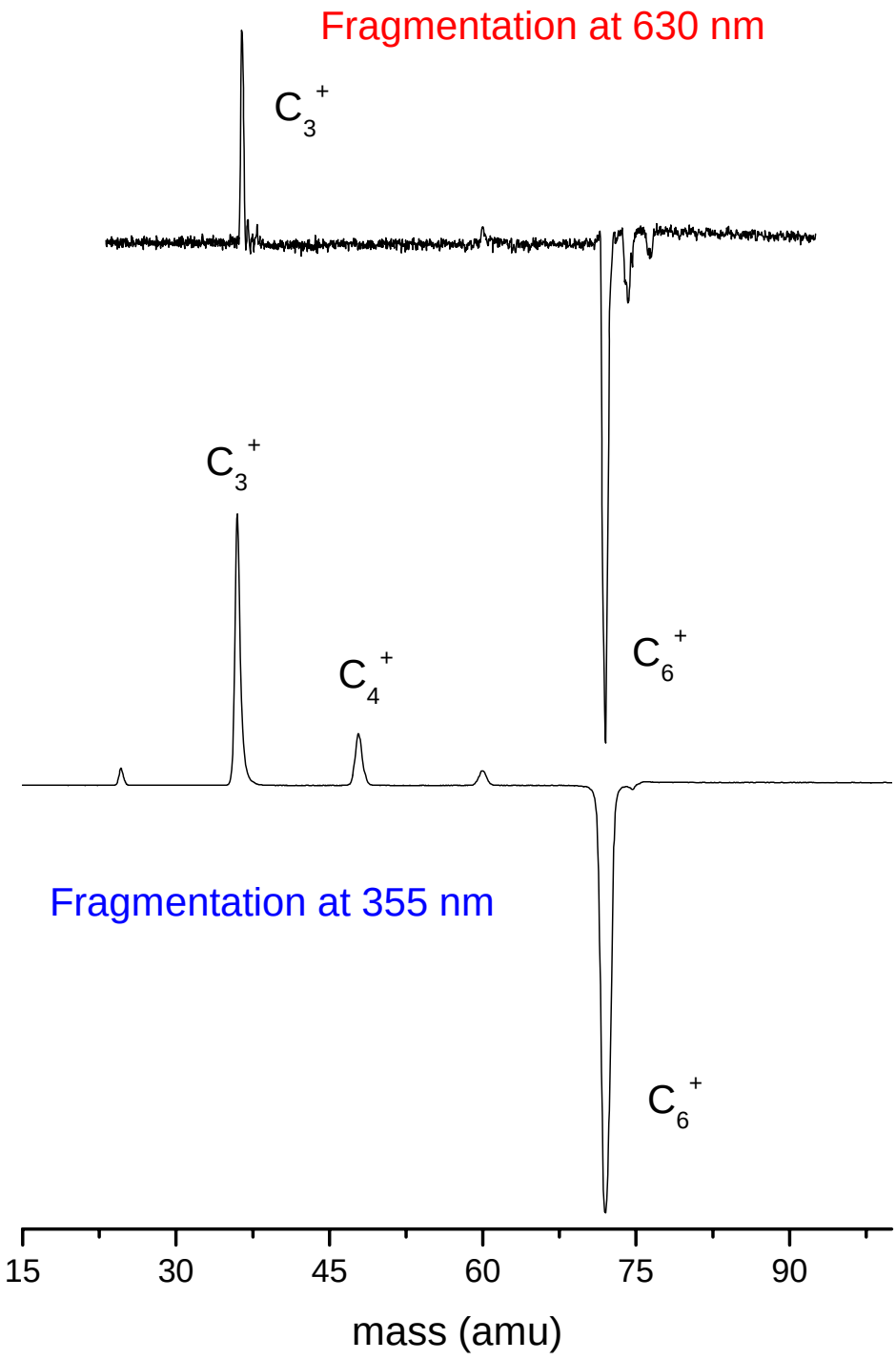

Figure 3.4: Photodissociation mass spectra of C_6^+ at 630 nm (top) and 355 nm (bottom).

of the clusters, however, which would not dissociate with red light alone. To attempt this, the visible laser was frequency doubled to generate ultraviolet light. The residual red light was not filtered out but instead both the UV and the visible light were allowed to intersect the cluster beam. The idea is that the ions would resonantly absorb one photon of the red light and then subsequently absorb the higher energy UV photons. In this way the clusters may absorb enough energy to exceed their dissociation threshold. At low photon flux, the ions should only dissociate if the initial visible photon is resonant with an electronic transition. Thus if a portion of the clusters in the beam have low internal energy, this approach may provide a way to probe them.

Figure 3.5 shows the photodissociation spectrum measured for mass selected C_6^+ from 620 – 660 nm, with ultraviolet light, corresponding to half the wavelength of the visible light, also used. The spectrum was collected by monitoring the appearance of the C_3^+ fragment versus laser wavelength. The fragment signal intensity was corrected versus the parent intensity to account for instability in the cluster source. Low laser power (~3 mJ/pulse) was used and the beam was expanded, both to try and limit background fragmentation that was not wavelength dependent. Unfortunately, some fragmentation was still observed across the entire spectrum. The spectrum appears to show some enhancement in fragmentation intensity in the regions around 633 nm and 648 nm. The second peak is very close to the origin band observed in the matrix at 645.8 nm,[131] These peaks are broad, possibly indicating that the clusters probed still contain significant internal energy. No assignments for the transitions are suggested, because as mentioned above the electronic spectrum of this ion is very complicated, with significant mixing possible between large numbers of low lying excited states.[138] The preliminary

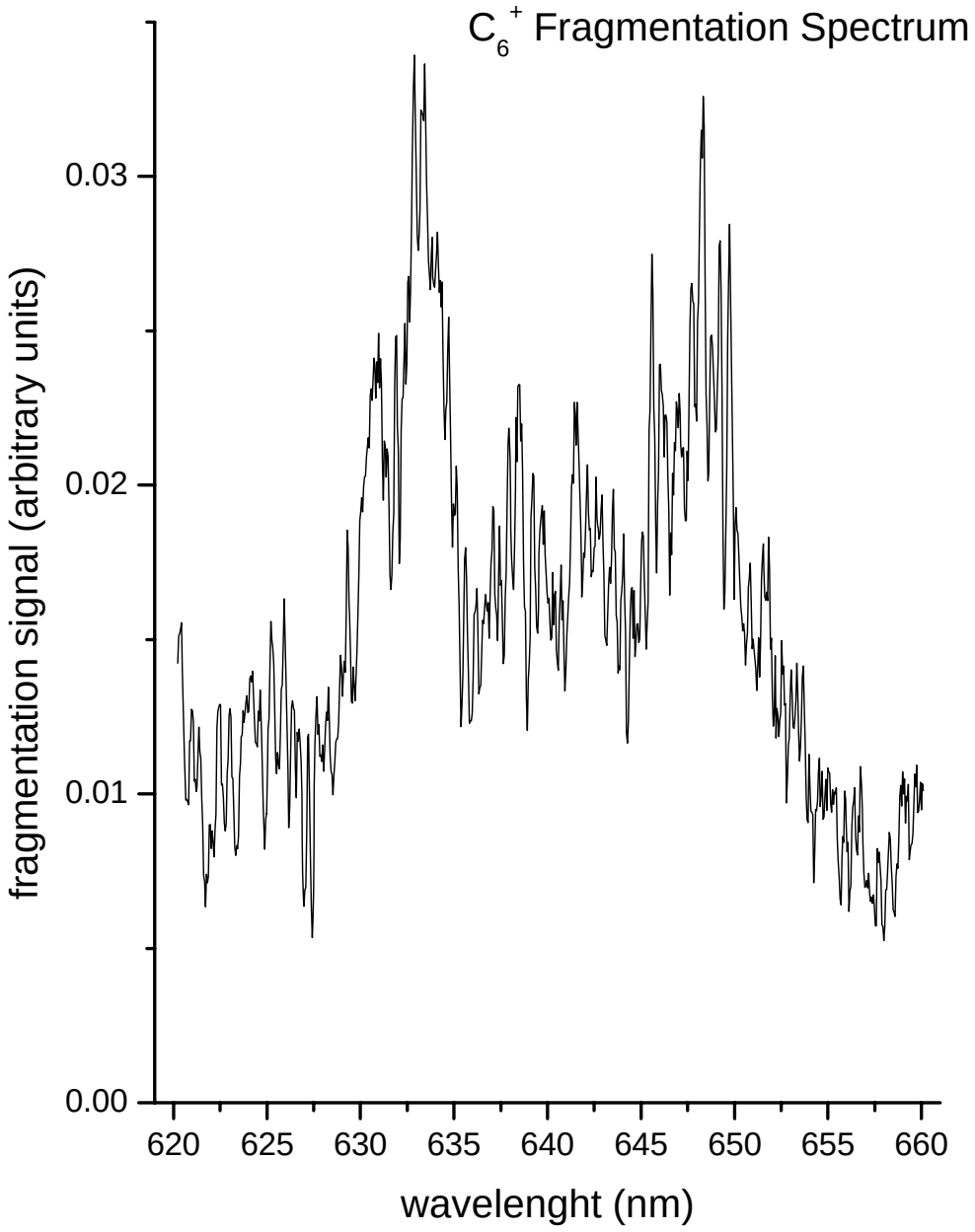

Figure 3.5: Photodissociation spectrum of mass selected C_6^+ from 620 – 660 nm.

spectrum shown in Figure 3.5, reported here for the first time, may help to guide future gas phase searches for the electronic spectrum of this ion.

Figure 3.6 shows the photodissociation spectrum measured for the mass selected C_8^+ ion from 620-650 nm. Initial scans showed some fragmentation at all wavelengths, likely due to clusters with high internal energy. This spectrum was collected in the same manner described above for C_6^+, using the visible light to absorb one photon on resonance, and subsequent absorption of ultraviolet photons causing dissociation. Recently, Maier and coworkers trapped C_8^+ in a neon matrix and measured five electronic transitions from both the linear and cyclic isomers.[132] Both isomers have transitions in the region around 687 nm. The cyclic structure is predicted to lie lower in energy by as much as 20 kcal/mol,[32] but even at this energy both isomers are likely to be populated in our experiment. The measured spectrum shows several possible resonances. The most intense peaks are centered around 624 and 654 nm. Again, all these peaks are broad, and the spectrum is collected on top of a constant fragmentation signal. No bands were observed in the matrix at these wavelengths, and no assignments of the transitions observed here are made. This ion has many low lying excited electronic states with considerable state mixing possible, leading at a potentially very complex spectrum.[135] This is the first reported photodissociation spectrum of the C_8^+ species, and this work may help to guide future spectroscopic searches for the electronic spectrum of this ion.

We have also attempted to measure the vibrational spectra of carbon cations in the gas phase. The only previous experimental observation of the infrared spectrum of a carbon cation was the IR absorption spectrum of C_6^+ recored by Maier and coworkers in a neon matrix.[131] The observed infrared fundamentals modes were at 2092 cm^{-1} for the

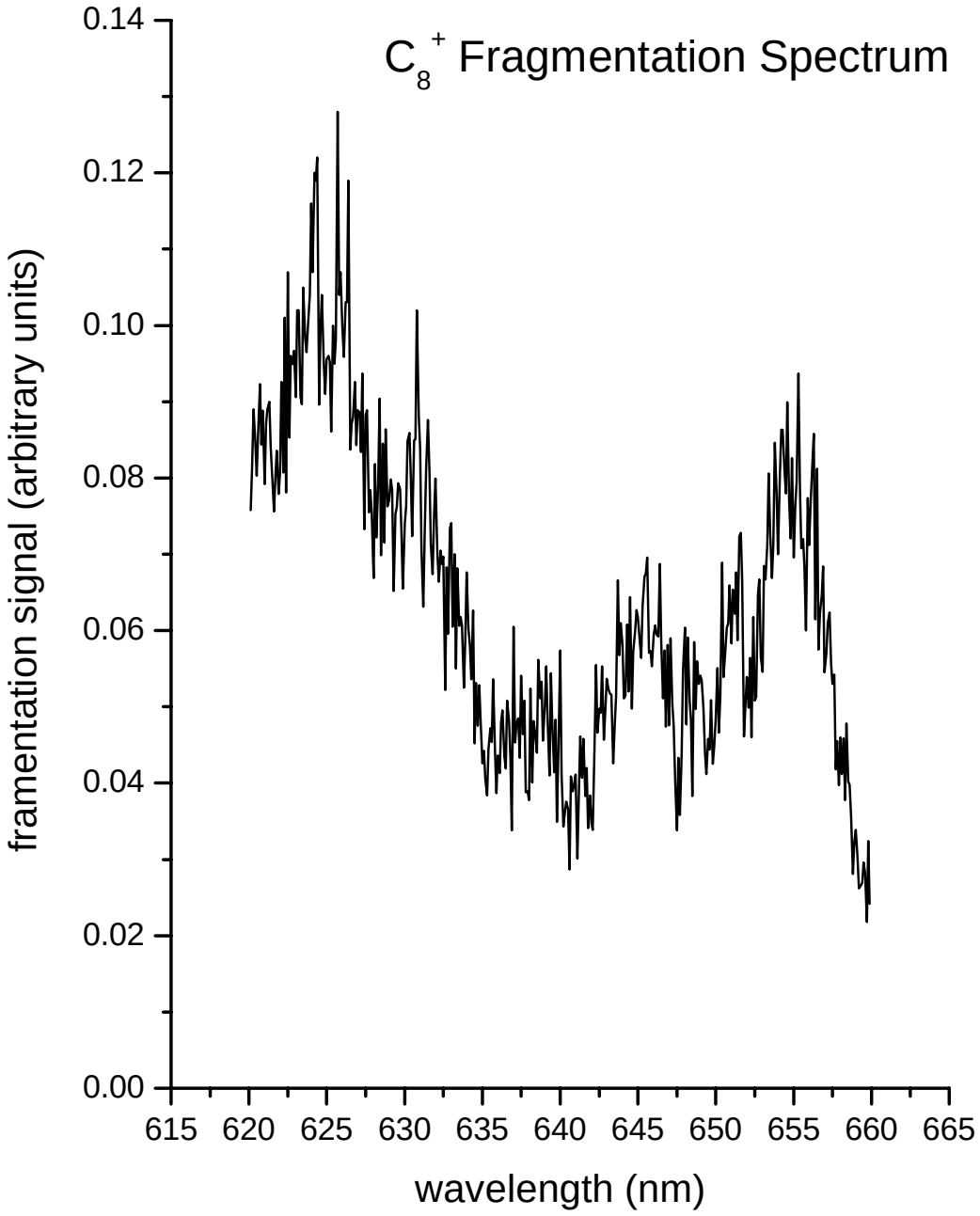

Figure 3.6: Photodissociation spectrum of mass selected C_8^+ from 620 – 660 nm.

linear structure and 1972 cm^{-1} for the cyclic structure, corresponding to the ν_4 asymmetric stretching mode and the ν_9, respectively. Gas phase laboratory measurements are non-existent for C_6^+ or any other carbon cation. There have been theoretical predictions on the infrared spectra of these molecules,[139] however, which indicate that a number of different carbon clusters have vibrations with sizable IR intensities above 2000 cm^{-1}, a region within the tuning range of our OPO laser. The results of these calculations, obtained using DFT methods with the B3LYP functional and cc-pVDZ basis set, are listed in Table 3.2, which also includes the experimental matrix values for C_6^+. Based on Table 3.2, C_5^+ appears to be an excellent candidate for infrared spectroscopy. For C_5^+, the linear structure is very low lying compared to the cyclic structure, with almost 31 kcal/mol of energy separating the isomers.[32] Thus bands from two different isomers are unlikely to complicate the spectrum. The C_5^+ cluster also has the highest vibrational frequency calculated for any of the clusters examined in this study. The calculated vibration, at 2249 cm^{-1}, corresponds to the asymmetric stretching mode of the linear structure. The IR intensity of the vibration is also calculated to be large (1802 km/mol) which should aid in the spectroscopic detection of the cluster.

However, just as for the electronic spectroscopy, dissociation energies for these species may present a problem for photodissocation experiments. CID has measured the dissociation energy of C_5^+ at about 6.0 eV.[38,46] These clusters are much more strongly bound than the metal ion – ligand complexes previously studied by infrared REPD in our lab,[146] and in fact would likely require resonant multiphoton absorption for fragmentation to occur. Multiphoton conditions are possible with the infrared laser employed here, but these processes are expected to be extremely inefficient at the photon flux achieveable.

As mentioned above, however, we believe that at least some fraction of the clusters produced in the experiment contain significant internal energy. If the internal energy of a cluster is only slightly below the dissociation energy, absorption of one (or two) photons, even in the low energy infrared region of the spectrum, may cause fragmentation. Thus infrared spectra might still be generated by resonance enhanced photodissociation.

With this in mind, C_5^+ and C_7^+ were scanned from 2000 – 4000 cm^{-1}, but no dissociation was observed. This is likely due to the binding energies, as outlined above. Even if the clusters are internally hot, the dissociation energies are still high enough and the flux of infrared photons low enough that dissociation does not occur. In this case, a much higher power laser, such as a free electron laser, might be necessary to generate the photon flux necessary for resonance enhanced multiphoton dissociation. Several other scenarios may also explain the lack of dissociation observed. First, the intensity of the infrared transition may be too weak for efficient absorption and dissociation to take place. Second, the calculated spectra may be inaccurate, and the vibrational frequency for the asymmetric stretching mode we searched for here may be below the tuning range of the laser employed in this experiment. And finally, the higher energy cyclic isomers may be populated. The frequencies for these isomers are almost certainly below the range of our laser, and the IR intensities for the cyclic vibrations are much lower than for the linear isomers. The negative results from this experiment have shown that the gas phase infrared spectra of carbon cations will likely require more sensitive detection schemes and more broadly tunable lasers.

3.5 CONCLUSIONS

Gas phase spectroscopic measurements on carbon cluster cations represent a sizeable hole in the understanding of these systems. This initial study has shown the ability to produce and study carbon clusters with photodissociation. Preliminary spectra of C_6^+ and C_8^+ in the 620 – 660 nm region have been collected, but the complicated manifold of low lying excited states and the possibly of significant internal energy in these clusters prevents meaningful conclusions to be drawn about the electronic spectra of these species. The possible appearance of resonances in both clusters near the DIB at 628.4 nm is a very tantalizing result, however, and certainly warrants the development of better experimental methods to produce and spectroscopically study these systems.

Attempts to measure the vibrational spectra of C_5^+ and C_7^+ in the gas phase via photodissociation were unsuccessful. The high dissociation energies of these species likely prevents fragmentation. A second complication is that many isomers of the carbon cations have predicted vibrations below 2000 cm^{-1}, which could not be measured in the experimental configuration described here. Both of these issues are currently being addressed in our laboratory. We have recently acquired a $AgGaSe_2$ crystal which extends the wavelength range of the infrared laser down to approximately 650 cm^{-1}. All the small carbon clusters will have infrared active vibrations in the spectral region currently accessible with this crystal. Additionally, a "cold" source is under development which should allow the growth of carbon clusters with lower internal energy by precooling the expansion gas and cooling the rod holder. This may allow the use of the rare gas tagging technique, which has been successfully utilized in several laboratories,[145-149] to measure

infrared spectra of species with dissociation energies larger than the vibrational frequencies being probed. This technique works by attaching a weakly bound species, such as a rare gas atom, to the cluster. Upon vibrational excitation, intramolecular vibrational energy redistribution takes places, and dissociation via the loss of the rare gas atom may occur. The bonding of the rare gas atom to the cluster, expected to be weak, will lead to efficient resonance enhanced dissociation. The infrared spectrum can then be measured by monitoring the appearance of the rare gas atom fragment versus laser wavelength.

The production of internally cold clusters will also aid in future spectroscopic searches for electronic transitions in carbon cations. Wavelength independent fragmentation, likely due to high internal energy, presented an obstacle to the measurement of resonance enhanced dissociation spectra. Better quenching of the cluster internal energy will make this technique more sensitive. Additionally, cooler clusters will be less likely to have population spread across multiple states and isomers, leading to better resolved transitions and less complicated spectra. High resolution spectra will allow better comparisons to the previous matrix measurements and will be absolutely necessary for comparisons to astronomical data measured for the DIBs.

Table 3.1: Major Electronic Transitions in Carbon Cluster Cations

Species	MRD-CI	CASSCF[d]	Matrix (Ne)[e]
C_5^+			
linear $D_{\infty h}$	$^2\Sigma_g^+ \leftarrow X^2\Sigma_u^+ = 0.05$ eV[a]		
	$^2\Pi_g^+ \leftarrow X^2\Sigma_u^+ = 0.24$ eV[a]		
	$^2\Pi_g^+ \leftarrow X^2\Sigma_u^+ = 2.62$ eV (473 nm)[a]		
	$^2\Sigma_g^+ \leftarrow X^2\Sigma_u^+ = 3.36$ eV (369 nm)[a]		
C_6^+			
linear $D_{\infty h}$	$^2\Pi \leftarrow X^2\Pi_u = 2.57$eV (482 nm)[b]	2.58 eV (481 nm)	1.92 eV (646nm)
	$3^2\Pi_g \leftarrow X^2\Pi_u = 5.80$eV (214 nm)[b]		
cyclic C_{2v}	$2^2B_2 \leftarrow X^2A_1 = 3.08$ eV (403 nm)[b]	3.26 eV (380 nm)	2.17 eV (570 nm)
	$3^2A_1 \leftarrow X^2A_1 = 3.59$ eV (345 nm)[b]	3.68 eV (337 nm)	
	$3^2B_2 \leftarrow X^2A_1 = 3.69$ eV (336 nm)[b]	4.04 eV (307 nm)	
C_8^+			
cyclic C_{4h}	$1^2B_g \leftarrow X^2B_u = 0.77$ eV[c]		
	$2^2B_g \leftarrow X^2B_u = 1.83$ eV (678 nm)[c]		1.57 eV (791 nm)
	$1^2E_g \leftarrow X^2B_u = 4.20$ eV (295 nm)[c]		3.69 eV (336 nm)
linear $D_{\infty h}$	$^2\Delta_u \leftarrow X^2\Pi_g = 1.69$ eV (734 nm)[c]		bands measured, but assignments uncertain
	$^2\Pi_u \leftarrow X^2\Pi_g = 5.45$ eV (228 nm)[c]		

[a]Ref. 135, [b]Ref. 136, [c]Ref. 137, [d]Ref. 138, [e]Ref. 131,132

Table 3.2: Infrared Active Vibrations of Carbon Cations

Species	B3LYP/cc-pVDZ energy (kcal/mol)[a]	B3LYP/cc-pVDZ vibrations (IR intensities, km/mol)[a]	Matrix (Ne)[b]
C_4^+			
linear $D_{\infty h}$ doublet	0 kcal/mol	1330 cm^{-1} (632)	
cyclic D_{2h} doublet	1.2 kcal/mol	620 cm^{-1} (64)	
C_5^+			
linear $C_{\infty v}$ doublet	0 kcal/mol	2249 cm^{-1} (1802)	
linear $D_{\infty h}$ quartet	30.9 kcal/mol	1964 cm^{-1} (881)	
C_6^+			
linear $D_{\infty h}$ doublet	0 kcal/mol	2068 cm^{-1} (1225)	2092 cm^{-1}
linear $C_{\infty v}$ quartet	7.3 kcal/mol	1975 cm^{-1} (305), 2131 cm^{-1} (384)	
cyclic C_{2v} doublet	11.2 kcal/mol	2076 cm^{-1} (600)	1972 cm^{-1}
C_7^+			
cyclic C_s doublet	0 kcal/mol	1760 cm^{-1} (145), 1775 cm^{-1} (138)	
linear $C_{\infty v}$ doublet	19.6 kcal/mol	2182 cm^{-1} (835), 2244 cm^{-1} (2189)	
C_8^+			
cyclic C_s doublet	0 kcal/mol	1803 cm^{-1} (389, 396, 32)	
linear $D_{\infty h}$	5.1 kcal/mol	2171 cm^{-1} (2420)	
C_9^+			
cyclic C_{2v} doublet	0 kcal/mol	1955 cm^{-1} (341), 2001 cm^{-1} (163)	
linear $C_{\infty v}$ doublet	1.7 kcal/mol	1833 cm^{-1} (4191), 2108 cm^{-1} (2122)	

[a]Ref. 139, [b]Ref. 131

3.6 REFERENCES

(1) Weltner, Jr., W.; Van Zee, R. J. *Chem. Rev.* **1994**, *89*, 1713.

(2) Van Orden, A.; Saykally, R. J. *Chem. Rev*. **1998**, *98*, 2313.

(3) Lifshitz, C. *Int. J. Mass Spectrom. 2000,* **200,** ***423.***

(4) Kroto, H. W.; Heath, J. R.; O'Brien, S. C.; Curl, R. F.; Smalley, R. E. *Nature* **1985**, *318*, 162.

(5) Kroto, H. W.; Allaf, A. W.; Balm, S. P. *Chem. Rev.* **1991**, *91*, 1213.

(6) Gardiner, W. C. *Combustion Chemistry*; Springer-Verlag: New York, 1984.

(7) Ebert, L. B. *Science* **1990**, *247*, 1468.

(8) Kroto, H. W.; Allaf, A. W.; Balm, S. P. *Chem. Rev.* **1991**, *91*, 1213.

(9) Dresselhaus, M. S.; Dresselhaus, G.; Eklund, P. C. *Science of Fullerenes and Carbon Nanotubes;* Academic Press: San Diego, CA, 1996.

(10) Strout, D. L.; Scuseria, G. E. *J. Phys. Chem.* **1996**, *100*, 6492.

(11) Zheng, G.; Irle, S.; Elstner, M.; Morokuma, K. *J. Phys. Chem. A* **2004**, *108*, 3182.

(12) Irle, S.; Zheng, G.; Wang, Z.; Morokuma, K. *J. Phys. Chem. B* **2006**, *110*, 14531.

(13) Tielens, A.G.G.M., Snow, T. P., Eds., *The Diffuse Interstellar Bands;* Kluwer: Dordrecht, The Netherlands, 1995.

(14) Hartquist, T. W.; Williams, D. A., Eds., *The Molecular Astrophysics of Stars and Galaxies;* Oxford University Press: New York, 1998.

(15) Heath, J. R.; Van Orden, A.; Hwang, H. J.; Kuo, E. W.; Tanaka, K.; Saykally, R.

J. *Adv. Space Res.* **1995**, *15*, 25.

(16) Maier, J. P. *J. Phys. Chem. A* **1998,** *102*, 3462.

(17) Kirkwood, D. A.; Linnartz, H.; Grutter, M.; Dopfer, O.; Motylewski, C. T.; Pachkov, M.; Tulej, M.; Wyss, M.; Maier, J. P. *Faraday Discuss.* **1998,** *109*, 109.

(18) Thaddeus, P.; McCarthy, M. C., *Spectrochimica Acta A.* **2001,** *57A*, 757.

(19) Maier, J. P.; Walker, G. A. H.; Bohlender, D. A., *Astrophys. J.* **2004,** *602*, 286.

(20) Maier, J. P.; Electronic Spectroscopy of Carbon Chains and Their Relevance to Astrophysics. In *The Dense Interstellar Medium in Galaxies*; Pfalzner, S., Kramer, C., Staubmeier, C., Heithausen, A., Eds.; Springer Proceedings in Physics 91; Springer Verlag: Berlin, 2004;, pp 55-60.

(21) Boguslavskiy, A. E.; Dzhonson, A.; Maier, J. P.; The Electronic Spectra of Carbon Chains, Rings, and Ions of Astrophysical Interest. In *Astrochemisty: From Laboratory Studies to Astronomical Observations*; Kaiser, R. I., Bernath, P., Osamura, Y., Petrie, S., Mebel, A. M., Eds.; AIP Conference Proceedings 855, American Institute of Physics: Melville, New York, 2006; pp 201-208.

(22) Rohlfing, E. A.; Cox, D. M.; Kaldor, A. *J. Chem. Phys.* **1984**, *81*, 3322.

(23) Curl, R. F.; Smalley, R. E. *Science* **1988**, *242*, 1017.

(24) Hahn, M. Y.; Honea, E. C.; Paguia, A. J.; Schriver, K. E.; Camarena, A. M.; Whetten, R. L. *Chem. Phys. Lett.* **1986**, *130*, 12.

(25) Rohlfing, E. A. *J. Chem. Phys.* **1990**, *93*, 7851.

(26) Kaizu, K.; Kohno, M.; Suzuki, S.; Shiromaru, H.; Moriwaki, T.; Achiba, Y. *J. Chem. Phys.* **1997**, *106*, 9954.

(27) Moriwaki, T.; Kobayashi, K.; Osaka, M.; Ohara, M.; Shiromaru, H.; Achiba, Y. *J. Chem. Phys.* **1997**, *107*, 8927.

(28) Wakabayashi, T.; Momose, T.; Shida, T. *J. Chem. Phys.* **1999**, *111*, 6260.

(29) Kato, Y.; Wakabayashi, T.; Momose, T. *J. Chem. Phys.* **2003**, *118*, 5390.

(30) Choi, Y.-K.; Im, H.-S.; Jung, K.-W. *Int. J. Mass Spectrom.* **1999**, *189*, 115.

(31) Bae, C. H.; Park, S. M. *J. Chem. Phys.* **2002**, *117*, 5347.

(32) Belau, L.; Wheeler, S. E.; Ticknor, B. W.; Ahmed, M.; Leone, S. R.; Allen, W. D.; Schaefer, H. F. III; Duncan, M. A. *J. Am. Chem. Soc.* **2007**, *129*, 10229.

(33) Nicolas, C.; Shu, J.; Peterka, D. S.; Hochlaf, M.; Poisson, L.; Leone, S. R.; Ahmed, M. *J. Am. Chem. Soc.* **2006**, *128*, 220.

(34) Geusic, M. E.; Jarrold, M. F.; McIlrath, T. J.; Bloomfield, L. A.; Freeman, R. R.; Brown, W. L. *Z. Phys. D: At. Mol. Clusters* **1986,** *3*, 309.

(35) Geusic, M. E.; McIlrath, T. J.; Jarrold, M. F.; Bloomfield, L. A.; Freeman, R. R.; Brown, W. L. *J. Chem. Phys.* **1986,** *84*, 2421.

(36) Geusic, M. E.; Jarrold, M. F.; McIlrath, T. J.; Freeman, R. R.; Brown, W. L. *J. Chem. Phys.* **1987,** *86*, 3862.

(37) O'Brien, S. C.; Heath, J. R.; Curl, R. F.; Smalley, R. E. *J. Chem. Phys.* **1988**, *88*, 220.

(38) Sowa, M. B.; Hintz, P. A.; Anderson, S. L. *J. Chem. Phys.* **1991**, *95*, 4719.

(39) Bouyer, R.; Roussel, F.; Monchicourt, P.; Perdix, M.; Pradel, P. *J. Chem. Phys.* **1994,** *100*, 8912.

(40) Pozniak, B.; Dunbar, R. C. *Int. J. Mass Spectrom. Ion Processes* **1994**, *133*, 97.

(41) Pozniak, B. P.; Dunbar, R. C. *Int. J. Mass Spectrom. Ion Processes* **1997**, *165/166*, 29.

(42) Radi, P. P.; Bunn, T. L.; Kemper, P. R.; Molchan, M. E.; Bowers, M. T. *J. Chem. Phys.* **1988**, *88*, 2809.

(43) Radi, P. P.; Hsu, M. T.; Brodbelt-Lustig, J.; Ricon, M.; M. E.; Bowers, M. T. *J. Chem. Phys.* **1990**, *92*, 4817.

(44) Gluch, K.; Matt-Leubner, S.; Echt, O.; Concina, B.; Scheier, P.; Märk, T. D. *J. Chem. Phys.* **2004**, *121*, 2137.

(45) Concina, B.; Gluch, K.; Matt-Leubner, S.; Echt, O.; Scheier, P.; Märk, T. D. *Chem. Phys. Lett.* **2005**, *407*, 464.

(46) Sowa-Resat, M. B.; Hintz, P. A.; Anderson, S. L. *J. Phys. Chem.* **1995**, *99*, 10736.

(47) Bach, S. B. H.; Eyler, J. R. *J. Chem. Phys.* **1990**, *92*, 358.

(48) Ramanathan, R.; Zimmerman, J. A.; Eyler, J. R. *J. Chem. Phys.* **1993**, *98*, 7838.

(49) von Helden, G.; Hsu, M. T.; Gotts, N.; Bowers, M. T. *J. Phys. Chem.* **1993**, *97*, 8182.

(50) Forney, D.; Fulara, J.; Freivogel, P.; Jakobi, M.; Lessen, D.; Maier, J. P. *J. Chem. Phys.* **1995**, *103*, 48.

(51) Freivogel, P.; Fulara, J.; Jakobi, M.; Forney, D.; Maier, J. P. *J. Chem. Phys.* **1995**, *103*, 54.

(52) Forney, D.; Freivogel, P.; Grutter, M.; Maier, J. P. *J. Chem. Phys.* **1996**, *104*, 4954.

(53) Freivogel, P.; Grutter, M.; Forney, D.; Maier, J. P. *Chem. Phys. Lett.* **1996**, *249*, 191.

(54) Grutter, M.; Freivogel, P.; Forney, D.; Maier, J. P. *J. Chem. Phys.* **1997**, *107*, 5356.

(55) Wyss, M.; Grutter, M.; Maier, J. P. *Chem. Phys. Lett.* **1999**, *304*, 35.

(56) Grutter, M.; Wyss, M.; Riaplov, E.; Maier, J. P.; Peyerimhoff, S. D.; Hanrath, M. *J. Chem. Phys.* **1999**, *111*, 7397.

(57) Cermak, I.; Forderer, M.; Cermakova, I.; Kalhofer, S.; Stopka-Ebeler, H.; Monninger, G.; Kratschmer, W. *J. Chem. Phys.* **1998**, *108*, 10129

(58) Monninger, G.; Förderer, M.; Gurtler, P.; Kalhofer, S.; Petersen, S.; Nemes, L.; Szalay, P. G.; Kratschmer, W. *J. Phys. Chem. A* **2002**, *106*, 5779.

(59) Thompson, K. R.; Dekock, R. L.; Weltner, W. Jr. *J. Am. Chem. Soc.* **1971**, *93*, 4688.

(60) Vala, M.; Chandrasekhar, T. M.; Szczepanski, J.; Van Zee, R.; Weltner, W., Jr. *J. Chem. Phys.* **1989**, *90*, 595.

(61) Szczepanski, J.; Vala, M. *J. Chem. Phys.* **1993**, *99*, 7371.

(62) Szczepanski, J.; Ekern, S.; Chapo, C.; Vala, M. *Chem. Phys.* **1996**, *211*, 359.

(63) Lapinski, L.; Vala, M. *Chem. Phys. Lett.* **1999**, *300*, 195.

(64) Shen, L. N.; Graham, W. R. M. *J. Chem. Phys.* **1989**, *91*, 5115.

(65) Shen, L. N.; Withey, P. A.; Graham, W. R. M. *J. Chem. Phys.* **1991**, *94*, 2395.

(66) Kranze, R. H.; Withey, P. A.; Rittby, C. M. L.; Graham, W. R. M. *J. Chem. Phys.* **1995**, *103*, 6841.

(67) Kranze, R. H.; Rittby, C. M. L.; Graham, W. R. M. *J. Chem. Phys.* **1996**, *105*, 5313.

(68) Wang, S. L.; Rittby, C. M. L.; Graham, W. R. M. *J. Chem. Phys.* **1997**, *107*,

6032.

(69) Wang, S. L.; Rittby, C. M. L.; Graham, W. R. M. *J. Chem. Phys.* **1997**, *107*, 7025.

(70) Wang, S. L.; Rittby, C. M. L.; Graham, W. R. M. *J. Chem. Phys.* **2000**, *112*, 1457.

(71) Ding, X. D.; Wang, S. L.; Rittby, C. M. L.; Graham, W. R. M. *J. Chem. Phys.* **2000**, *112*, 5113.

(72) Miki, M.; Wakabayashi, T.; Momose, T.; Shida, T. *J. Phys. Chem.* **1996**, *100*, 12135.

(73) Freivogel, P.; Grutter, M.; Forney, D.; Maier, J. P. *Chem. Phys*. **1997**, *216*, 401.

(74) Presilla-Marquez, J. D.; Sheehy, J. A.; Mills, J. D.; Carrick, P. G.; Larson, C. W. *Chem. Phys. Lett.* **1997**, *274*, 439.

(75) Presilla-Marquez, J. D.; Harper, J.; Sheehy, J. A.; Carrick, P. G.; Larson, C. W. *Chem. Phys. Lett.* **1999**, *300*, 719.

(76) Tam, S.; Macler, M.; Fajardo, M. E. *J. Chem. Phys.* **1997**, *106*, 8955.

(77) Ott, A. K.; Rechtsteiner, G. A.; Felix, C.; Hampe, O.; Jarrold, M. F.; Van Duyne, R. P.; Raghavachari, K. *J. Chem. Phys.* **1998**, *109*, 9652.

(78) Rechtsteiner, G. A.; Felix, C.; Ott, A. K.; Hampe, O.; Van Duyne, R. P.; Jarrold, M. F.; Raghavachari, K. *J. Phys. Chem. A* **2001**, *105*, 3029.

(79) Moazzen-Ahmadi, N.; Thong, J. J.; Mckellar, A. R. W. *J. Chem. Phys.* **1994**, *100*, 4033.

(80) van Orden, A.; Provencal, R. A.; Keutsch, F. N.; Saykally, R. J. *J. Chem. Phys*. **1996**, *105*, 6111.

(81) Giesen, T. F.; Berndt, U.; Yamada, K. M. T.; Fuchs, G.; Schieder, R.; Winnewisser, G.; Provencal, R. A.; Keutsch, F. N.; Van Orden, A.; Saykally, R. J. *Chem. Phys. Chem* **2001**, *2*, 242.

(82) Neubauer-Guenther, P.; Giesen, T. F.; Berndt, U.; Fuchs, G.; Winnewisser, G. *Spectrochim. Acta Part A* **2003**, *59*, 431.

(83) Balfour, W. J.; Cao, J. Y.; Prasad, C. V. V.; Qian, C. X. W. *J. Chem. Phys.* **1994**, *101*, 10343.

(84) Motylewski, T.; Vaizert, O.; Giesen, T. F.; Linnartz, H.; Maier, J. P. *J. Chem. Phys.* **1999**, *111*, 6161.

(85) Linnartz, H.; Vaizert, O.; Motylewski, T.; Maier, J. P. *J. Chem. Phys.* **2000**, *112*, 9777.

(86) Boguslavskiy, A. E.; Ding, H.; Maier, J. P. *J. Chem. Phys.* **2005**, *123*, 034305.

(87) Boguslavskiy, A. E.; Maier, J. P. *J. Chem. Phys.* **2006**, *125*, 094308.

(88) Maier, J. P.; Boguslavskiy, A. E.; Ding, H.; Walker, G. A. H.; Bohlender, D. A. *Astrophys. J*. **2006**, *640*, 369.

(89) Ding, H.; Maier, J. P. *J. Phys.Conf. Ser.* **2007**, *61*, 252.

(90) Boguslavskiy, A. E.; Maier, J. P. *Phys. Chem. Chem. Phys.* **2007**, *9*, 127.

(91) Giesen, T. F.; Van Orden, A. O.; Cruzan, J. D.; Provencal, R. A.; Saykally, R. J.; Gendriesch, R.; Lewen, F.; Winnewisser, G. *Astrophys. J*. **2001**, *551*, L181.

(92) Gendriesch, R.; Pehl, K.; Giesen, T.; Winnewisser, G.; Lewen, F. *Z. Naturforsch.* **2003**, *58a*, 129.

(93) Začs, L. *Astrosphys. Space Sci.* **1997**, *251*, 289.

(94) Maier, J. P.; Lakin, N. M.; Walker, G. A. H.; Bohlender, D. A. *Astrophys. J*

2001, *553*, 267.

(95) Maier, J. P.; Walker, G. A. H.; Bohlender, D. A. *Astrophys. J.* **2004**, *602*, 286.

(96) Maier, J. P.; Walker, G. A. H.; Bohlender, D. A. *Astrophys. J.* **2002**, *566*, 332.

(97) Magers, D. H.; Harrison, R. J.; Bartlett, R. J. *J. Chem. Phys.* **1986**, *84*, 3284.

(98) Watts, J. D.; Gauss, J.; Stanton, J. F.; Bartlett, R. J. *J. Chem. Phys.* **1992**, *97*, 8372.

(99) Raghavachari, K.; Whiteside, R. A.; Pople, J. A. *J. Chem. Phys.* **1986**, *85*, 6623.

(100) Raghavachari, K.; Binkley, J. S. *J. Chem. Phys.* **1987**, *87*, 2191.

(101) Martin, J. M. L.; Francois, J-P.; Gijbels, R. *J. Chem. Phys.* **1989**, *90*, 3403.

(102) Martin, J. M. L.; Francois, J.-P.; Gijbels, R. *J. Chem. Phys.* **1990**, *93*, 8850.

(103) Martin, J. M. L.; Francois, J.-P.; Gijbels, R. *J. Chem. Phys.* **1991**, *94*, 3753.

(104) Martin, J. M. L.; Francois, J.-P.; Gijbels, R. *J. Chem. Phys.* **1991**, *95*, 9420.

(105) Parasuk, V.; Almlof, J. *J. Chem. Phys.* **1989**, *91*, 1137.

(106) Liang, C.; Schaefer, H. F. *Chem. Phys. Lett.* **1990**, *169*, 150.

(107) Liang, C.; Schaefer, H. F. *J. Chem. Phys.* **1990**, *93*, 8844.

(108) Ortiz, J. V.; Zakrzewski, V. G. *J. Chem. Phys.* **1994**, *100*, 6614.

(109) Hutter, J.; Luthi, H. P.; Diederich, F. *J. Am. Chem. Soc.* **1994**, *116*, 750.

(110) Schmatz, S.; Botschwina, P. *Chem. Phys. Lett.* **1995**, *235*, 5.

(111) Martin, J. M. L.; Taylor, P. R. *Chem. Phys. Lett.* **1995**, *240*, 521.

(112) Martin, J. M. L.; Elyazal, J.; Francois, J.-P. *Chem. Phys. Lett.* **1995**, *242*, 570.

(113) Martin, J. M. L.; Taylor, P. R. *J. Chem. Phys.* **1995**, *102*, 8270.

(114) Martin, J. M. L.; Taylor, P. R. *J. Phys. Chem.* **1996**, *100*, 6047-6056.

(115) Martin, J. M. L.; Schwenke, D. W.; Lee, T. J.; Taylor, P. R. *J. Chem. Phys.*

1996, *104*, 4657.

(116) Martin, J. M. L.; El-Yazal, J.; Francois, J.-P. *Chem. Phys. Lett.* **1996**, *252*, 9.

(117) Ohno, M.; Zakrzewski, V. G.; Ortiz, J. V.; von Niessen, W. *J. Chem. Phys.* **1997**, *106*, 3258.

(118) Valdes, E. A.; De La Mora, P.; Castro, M.; Keller, J. *Int. J. Quantum Chem.* **1997**, *65*, 867.

(119) Hanrath, M.; Peyerimhoff, S. D.; Grein, F. *Chem. Phys.* **1999**, *249*, 121.

(120) Muhlhauser, M.; Froudakis, G. E.; Hanrath, M.; Peyerimhoff, S. D. *Chem. Phys. Lett.* **2000**, *324*, 195.

(121) Muhlhauser, M.; Froudakis, G. E.; Peyerimhoff, S. D. *Chem. Phys. Lett.* **2001**, *336*, 171.

(122) Grein, F.; Franz, J.; Hanrath, M.; Peyerimhoff, S. D. *Chem. Phys.* **2001**, *263*, 5.

(123) Muhlhauser, M.; Froudakis, G. E.; Peyerimhoff, S. D. *Phys. Chem. Chem. Phys.* **2001**, *3*, 3913.

(124) Hanrath, M.; Peyerimhoff, S. D. *Chem. Phys. Lett.* **2001**, *337*, 368.

(125) Cao, Z. X.; Muhlhauser, M.; Hanrath, M.; Peyerimhoff, S. D. *Chem. Phys. Lett.* **2002**, *351*, 327.

(126) Giuffreda, M. G.; Deleuze, M. S.; Francois, J.-P.; Trofimov, A. B. *Int. J. Quantum Chem.* **2001**, *85*, 475.

(127) Jo, C.; Lee, K. *J. Korean Phys. Soc.* **2002**, *41*, 200.

(128) Baranovski, V. I. *Chem. Phys. Lett.* **2005**, *408*, 429.

(129) Vala, M.; Chendrasekhar, T. M.; Szczepanski, J.; Pellow, R. *J. Mol. Struct*. **1990**, *222*, 209.

(130) Szczepanski, J.; Ekern, S.; Vala, M. *J. Phys. Chem.* **1995**, *99*, 8002.

(131) Fulara, J.; Riaplov, E.; Batalov, A.; Shnitko, I.; Maier, J. P. *J. Chem. Phys.* **2004**, *120*, 7520.

(132) Fulara, J.; Shnitko, I.; Batalov, A.; Maier, J. P. *J. Chem. Phys.* **2005**, *123*, 044305.

(133) Scuseria, G. E. *Chem. Phys. Lett.* **1991**, *176*, 27.

(134) Watts, J. D.; Stanton, J. F.; Gauss, J.; Bartlett, R. J. *J. Chem. Phys.* **1991**, *94*, 4320.

(135) Schnell, M.; Muhlhauser, M.; Froudakis, G. E.; Peyerimhoff, S. D. *Chem. Phys. Lett.* **2001**, *340*, 559.

(136) Haubrich, J.; Muhlhauser, M.; Peyerimhoff, S. D. *Phys. Chem. Chem. Phys.* **2002**, *4*, 2891.

(137) Haubrich, J.; Muhlhauser, M.; Peyerimhoff, S. D. *J. Mol. Spectrosc.* **2004**, *228*, 31.

(138) Gillery, C.; Rosmus, P.; Werner, H. J.; Stoll, H.; Maier, J. P. *Mol. Phys.* **2004**, *102*, 2227.

(139) Giuffreda, M. G.; Deleuze, M. S.; Francois, J.-P. *J. Phys. Chem. A* **1999**, *103*, 5137.

(140) Deleuze, M. S.; Giuffreda, M. G.; Francois, J.-P.; Cederbaum, L. S. *J. Chem. Phys.* **1999**, *111*, 5851.

(141) Deleuze, M. S.; Giuffreda, M. G.; Francois, J.-P.; Cederbaum, L. S. *J. Chem. Phys.* **2000**, *112*, 5325.

(142) Deleuze, M. S.; Giuffreda, M. G.; Francois, J.-P. *J. Phys. Chem. A* **2002**, *106*,

5626.

(143) Diaz-Tendero, S.; Martin, F.; Alcami, M. *J. Phys. Chem. A* **2002**, *106*, 10782.

(144) Orlova, G.; Goddard, J. D. *Chem. Phys. Lett.* **2002**, *363*, 486.

(145) Duncan, M. A.; *Int. J. Mass Spectro*. **2000**, *200*, 545.

(146) Duncan, M. A.; *Int. Rev. Phys. Chem.* **2003**, *2*, 407.

(147) Yeh, L. I.; Okumura, M.; Myers, J. D.; Price, J. M.; Lee, Y. T. *J. Chem. Phys.* **1989**, *91*, 7319.

(148) Okumura, M.; Yeh, L. I.; Myers, J. D.; Lee, Y. T. *J. Phys. Chem.* **1990**, *94*, 3416.

(149) Ebata, T.; Fujii, A.; Mikami, N. *Int. Rev. Phys. Chem.* **1998**, *17*, 331.

(150) Bieske, E. J.; Dopfer, O. *Chem. Rev.* **2000**, *100*, 3963.

(151) Robertson, W. H.; Johnson, M. A. *Ann. Rev. Phys. Chem.* **2003**, *54*, 173.

CHAPTER 4

THE EFFECTS OF NOBLE METAL ION DOPING ON CARBON CLUSTERS

4.1 ABSTRACT

Noble metal carbide cluster cations ($M_2C_n^+$, M = Cu, Au) are produced by laser vaporization in a pulsed molecular beam and detected with time-of-flight mass spectrometry. Copper carbides favor the formation of clusters with an odd number of carbons, while the gold carbides show marked drops in ion intensity after clusters with 3, 6, 9, and 12 carbons, suggesting enhanced stability for these sizes. Clusters are mass selected and photodissociated at 355 nm. Small copper carbide clusters with an odd number of carbons fragment by losing the entire carbon cluster, while those with an even number of carbons show significant loss of neutral C_3. This even odd alternation, with the even clusters having mixed fragments, holds true for sizes as larger as CuC_{30}^+. No loss of C_2 is observed for even the largest sizes studied, indicating that fullerene formation does not occur. The gold carbide photodissociation data closely resembles that of the copper, with even clusters primarily losing C_3 and odd ones losing the entire carbon cluster. Comparisons to known carbon cluster ionization potentials gives insight into the structure of the detected carbon fragments for some sizes. DFT calculations performed on $CuC_{3\text{-}11}^+$ clusters allow comparisons of the energetics of isomers likely present in our experiment and metal – carbon dissociation energies help explain the even odd alternation in the fragmentation channels.

4.2 INTRODUCTION

Mixed clusters of transition metals with carbon have generated considerable interest over the years for their importance in such areas as varied as ceramic materials, catalysis, astrophysics, surface science, and for their unusual models of chemical bonding.[1-5] The structures of small metal carbides are thought to form linear and cyclic structures, similar to clusters of pure carbon, which have been studied much more extensively.[6-8] However, the extent to which the presence of a metal ion affects the structure and energetics of these small systems is not well characterized. Experimental investigations into the reactions of metal ions with hydrocarbons lead to the discovery of a unique class of three dimensional metal carbide structures called metallo-carbohedrenes, or "met-cars," along with cubic analogues known as metal carbide "nanocrystals."[8-11] Large carbon clusters such as fullerenes are also known to bind metals to form metallofullerenes, with endohedral,[12,13] exohedral,[13-16] or networked[17] configurations of the metal atoms possible. Understanding the structure and bonding in small model systems of this type can help to elucidate the electronic structure and properties of the bulk material. Photodissociation studies of noble metal (Cu, Au) carbide cations, as described here, provide one method for studying the structures and stabilities of these species in the gas phase.

The earliest experiments on mixed metal carbon molecules utilized the high temperature Knudsen effusion oven mass spectrometric technique to record ionization efficiency curves, generate appearance potentials, and estimate dissociation energies, heats of formation, and atomization energies of small carbide clusters.[18-22] Berkowitz and

co-workers[18] predominately observed the formation of the dicarbide and tetracarbide species and ascribed to the C_2 moiety a pseudo-oxygen atom character, in comparison to results from metal oxide experiments. Later experiments showed the formation of larger MC_3^+, MC_5^+, and MC_6^+ species, but with ion intensities considerably smaller than for the MC_2^+ and MC_4^+ clusters.[22] Secondary ion mass spectrometry (SIMS) has also been used to study both anions and cations produced from fast atom bombardment of bulk metal carbide samples.[23] Carbides of early transition metals favor clusters with even numbers of carbon atoms, while later transition metals favor those with odd numbers of carbon atoms. This is attributed to differences in the electronic structures of the metal atoms, including both electronegativity and occupation of the metal d orbitals used in complexation with carbon.

In 1992, Castleman and co-workers first reported the discovery of metallo-carbohedrenes, commonly called met-cars.[8] These clusters, formed by reacting methane or other hydrocarbon gases with a laser generated plasma of metal atoms, were found to have a very specific stoichiometry of 8 metal atoms and 12 carbon atoms. Additional studies by Duncan and co-workers revealed the larger cubic nanocrystal structure consisting of 14 metal atoms and 13 carbon atoms.[9] Fragmentation of met-cars has been studied by photodissociation,[9,24] CID,[25] and metastable decay.[26] Ion mobility[27] and photoelectron[28] spectroscopy experiments, along with numerous theoretical studies,[11, 29-32] have helped reveal the structures of both met-cars and nanocrystals. Infrared multi-photon ionization spectroscopy with a tunable free electron laser was used to measure the infrared spectra[33] of these species, confirming the cubic rock salt lattice structure for the nanocrystal and leading the assignment of the 21 μm line seen in stellar atmospheres to

titanium carbide nanocrystals.[34] While met-cars have generated intense scientific interest over the years, other types of mixed transition metal carbon clusters have been studied less extensively.

Mass spectrometry has been used to study metal carbides from oven sources,[35] laser photolysis of organometallic vapor,[36] or laser vaporization sources.[37-42] Most of these studies have focused on the early transition metals, especially the group 3A elements (Sc, Y, La). Castleman and co-workers reacted acetylene with copper vapor and reported the formation of cations that were either rich in copper or with nearly equal copper-carbon stoichiometric ratios, depending on the concentration of the reactant gas.[35] As with the metal oven vapor experiments, C_2 units were favored in the cluster formation. Duncan and co-workers later generated mixed species of carbon with bismuth, antimony, nickel, cobalt, and copper by laser vaporization of carbon samples coated with these metals.[40] While many different sizes were formed in these conditions, $M_n(C_3)_m^+$ (n = 1,2: m = 1,2,3 etc.) clusters were prominent in the mass spectra for all metals studied, consistent with a high abundance of C_3 in carbon plasmas.[6,7,43] Gibson reacted hydrocarbons and halocarbons with Au_n^+ (n = 1- 7) clusters from a laser ablation source and produced gold carbides of the form $Au_nC_m^+$.[41] In addition to the experiments on met-cars mentioned above,[21] ion mobility has been used in experiments focused on smaller metal carbides as well as on the formation of larger metallofullerenes.[44]

Neutral diatomic transition metal carbide molecules have been studied spectroscopically by laser induced fluorescence,[45-48] resonant two photon ionization,[49] dispersed fluorescence,[50] and millimeter wave spectroscopy.[51] Studies of larger neutral metal-carbon species are much more limited. Graham and co-workers have recorded

vibrational spectra of neutral clusters of carbon with germanium, titanium, chromium, cobalt, and nickel in argon matrices.[52] Metha and co-workers studied tantalum carbides with multiphoton ionization.[53] More recent work from that group measured the ionization potentials (IPs) for Ta_3C_{1-3} and Ta_4C_{1-4} and found them to be in the region of 5 – 6 eV.[53] Good agreement with DFT calculations show that experimentally determined IPs can be used to confirm theoretical structures for species of this type.

Anionic metal carbides have also been studied in the gas phase by photoelectron spectroscopy,[54-57] ion mobility,[58] and Fourier transform ion cyclotron resonance mass spectrometry (FTMS) coupled with CID.[36] Photoelectron spectroscopy experiments of first row transition metals with C_2 showed the bonding to be mostly ionic, and the species may be pictured nominally as $M^{2+}C_2^{2-}$.[54b] For C_3 bound to first row transition metals the bonding was found to be similar to that of C_2, but with a smaller degree of charge transfer from the metal to the carbon.[54c]

Theoretical studies on metal carbide clusters are numerous. As mentioned above, an extensive amount of computational work has been conducted specifically on met-cars.[11,23-26] Smaller clusters have been considered as possible building blocks for met-cars and have thus generated considerable interest from that perspective.[11] As with the experimental work, much of the theoretical work on metal carbides consists of studies of the early transition metals scandium,[11,58-60] yttrium,[11,61,62] and lanthanum.[11,61,63,64] In the course of studying met-cars, theoretical investigations of small titanium,[11,65-68] vanadium,[11,69,70] and niobium[11,71,72] carbide clusters have also been conducted. Small clusters of iron,[11,68,73-75] cobalt,[76] nickel,[11,68,77,78] and tantalum[79] with carbon have also received theoretical attention, while Hall and co-workers have examined palladium[80] and

platinum[80] carbide cations to investigate linear and cyclic isomers. Recently, Largo and co-workers have applied density functional theory (DFT) to a variety of neutral and ionic clusters of the type $MC_n^{-/0/+}$ (M = Sc,[60] Ti,[67] V,[70] Zn;[81] n = 1-8), also studying both the linear and cyclic structures. Diatomic neutral carbides of the 3d,[82,83] 4d,[84a] and 5d[84b] transition metals have been the subject of studies analyzing the changes in the bonding as d electrons are added going across the periodic table. Largo and co-workers have additionally looked at the neutral[85a] and cationic[85b] dicarbides of the first row transition metals in order to study the structure and bonding in these systems. Theoretical work on the noble metal carbides is extremely sparse. Carbohedrene structures of copper[86] and cubic clusters of copper, silver, and gold[87] have been studied. Pyykkö and co-workers[88] and Peterson and co-workers[89] have studied small gold carbides in the larger context of examining gold cluster chemistry. Finally, a cage structure with a tetrahedral C_5 radical surrounded by a spherical Au_{12} layer has been proposed by Naumkin.[90]

Dissociation of clusters can be a useful tool to help elucidate structures and gain insight into bonding in systems where spectroscopic information is lacking. Many mass spectrometry experiments on pure carbon, conducted under a variety of different conditions, have shown very interesting cluster distributions.[91-98] Unfortunately, simple mass spectrometry studies have proved decidedly inconclusive about structures and energetics. Therefore techniques including mass selected photodissociation,[99-103] collision induced dissociation,[101,104] and metastable ion decay[105,106] have been used in conjunction with mass spectrometry to study the fragmentation behavior of carbon clusters. They are now well known to favor the elimination of C_3 in the small size regime and C_2 as fullerenes.[99-106]

Recently, our group has studied metal-oxide,[107] silicon-carbide,[108] and metal-silicon[109] clusters by photodissociation. The silicon carbides fragment by loss of mixed $Si_nC^{+/0}$, indicating the silicon – carbon bonding is stronger than silicon – silicon bonding. The metal silicon clusters, however, fragment predominately by losing the metal atom, suggesting a structure of an exposed metal atom on the surface of a silicon cluster. Photodissociation[9,18] and CID[19] experiments were also conducted on carbide clusters with multiple metals in the course of studying met-cars. To our knowledge, the only previous study of the growth and fragmentation of transition metal carbide clusters with a single metal atom is an FTMS study of tantalum carbide cations produced by laser vaporization.[39a] The ion distributions produced in this experiment are similar to those seen from metal oven sources, in that TaC_2^+ and TaC_4^+ are the most prominent. Collision induced dissociation of these ions resulted in the loss of neutral C_3 as the major fragmentation channel for all of the smaller sizes, consistent with a metal ion attached to a carbon chain. As mentioned above pure carbon clusters are well known to fragment by loss of the extremely stable C_3 unit.[99-106]

Many questions remain about the structures and bonding of small metal carbide clusters. Almost no experimental information exists on the carbides of the noble metals, and only a few theoretical studies address species of this type. The effect of a noble metal ion doped into a carbon cluster is largely unknown. The present study applies mass spectrometry and laser photodissociation techniques to copper and gold carbides. Cluster formation and fragmentation patterns, coupled with DFT calculations, give insight into structures and the types of bonding present in these systems.

4.3 EXPERIMENTAL

The laser vaporization source coupled to a pulsed molecular beam machine used to study these clusters has been described previously.[9,40,107-109] Briefly, coatings of copper and gold are prepared on 0.5 inch carbon rods (Glass Supply) in a vacuum deposition chamber, in which ~0.3 grams of metal is resistively heated and then vaporized. The carbon rod is rotated to ensure an even coating of the metal.

In the source chamber of the molecular beam machine, the second harmonic (532 nm) of a Spectra Physics Nd:YAG laser (Quanta Ray GCR-11) is used to vaporize the rotating and translating rod. Helium (60 psi backing pressure) is pulsed with a series 9 General Valve through the sample rod holder. The laser ignites a plasma and the mixed metal-carbon cations are grown directly in this plasma. In experiments where larger clusters are studied, a growth channel 0.5 inches long with a diameter of 5 mm is attached to the rod holder to promote aggregation. The molecular beam is skimmed into a differentially pumped chamber, where cations are pulse extracted into a reflectron time-of-flight mass spectrometer. For photodissociation experiments, the cluster of interest is mass selected by pulsing deflection plates. The mass selected ion packet is then excited by the third harmonic (355 nm) of an Nd:YAG laser (Spectra Physics DCR-3) in the turning region of the reflectron. The photofragments are reaccelerated in the reflectron, mass separated in the second flight tube, and detected with an electron multiplier tube and a digital oscilloscope (LeCroy 9310 A). Photodissociation studies were performed at laser powers between 6 and 50 mJ/pulse with an unfocused laser spot with an area approximately 1 cm^2.

To learn about the structure and energetics in the small copper carbide clusters, geometry optimizations were performed using density functional theory (DFT) computations with the Gaussian 03W program.[110] The Becke-3-Lee-Yang-Parr (B3LYP)[111,112] functional was used with the 6-311+G(d,p)[113] basis set for the carbon atoms and the LanL2DZ[114,115] basis set, containing effective core potential, for the copper. This method has been applied recently by Largo and co-workers on a variety of metal carbon systems.[60,70] Their work has shown that the B3LYP method has reasonable success in predicting ground states and lowest lying excited states when compared to more computationally expensive methods such as QCISD or CCSD(T). The minimum energy structures, energies, and vibrational frequencies were computed for copper carbides $CuC_{3\text{-}11}^{+}$ and their corresponding neutral species, and these data are reported in the Supporting Information.

4.4 RESULTS AND DISSCUSSION

Figure 4.1 shows mass spectra collected for a mixed sample of carbon coated with copper. The upper trace shows the mass spectrum for a copper coated carbon rod in a rod holder, while the lower trace shows the mass spectrum when a 0.5 inch long, 5 mm diameter growth channel is attached to the rod holder. Both the mass spectra in Figure 4.1 show a preference for forming mixed carbide clusters with an odd number of carbon atoms. This is especially evident in the upper trace, when no growth channel is used. In that mass spectrum, even numbered carbides are present only in small intensities, and the alternation in the abundances between the even and odd numbered clusters is dramatic.

The lower trace, using the growth channel, still shows some enhancement of the odd numbered species, but the degree of alternation is much less prominent and the even numbered clusters are present in reasonable intensity. Additionally, in both mass spectra pure carbon cations are produced in significant quantities, as expected from the relative amount of carbon to copper present in the plasma vapor. Carbon aggregates with itself very efficiently, and with the use of the growth channel pure carbon clusters out to the size of C_{60}^{+} are produced. The growth of the desired mixed metal carbide species thus depends on maximizing the amount of metal compared to the amount of carbon. The relative concentration of the metal can be roughly controlled by adjusting the rate of the rotation of the sample rod. Rotating the rod quickly provides a fresh surface of metal for ablation with each laser shot, thus increasing the amount of metal in the vapor. This leads to an increase in the abundance of mixed metal carbide peaks in the mass spectrum. Conversely, rotating the sample rod slowly increases the relative concentration of carbon in the plasma and favors the formation of pure carbon cations. The mass spectra in Figure 4.1 were collected with a fairly fast rod rotation speed. At slower speeds pure carbon clusters completely dominate the mass spectrum, with very little formation of the copper carbides. The use of the growth channel does allow for the formation of much larger mixed carbide and pure carbon species, as the lower trace of Figure 4.1 shows.

For the mixed carbides present in Figure 4.1, the doublet seen for each cluster size in the mass spectrum is due to the copper isotopes which are resolved at the lower end of the mass range studied in this experiment. It is interesting to note that by far the largest peak in the mass spectrum (excluding the atomic ion, not shown), corresponds to the CuC_3^{+} (hereafter 1/3) cluster. In fact, the 1/1 and 1/2 ions are completely absent

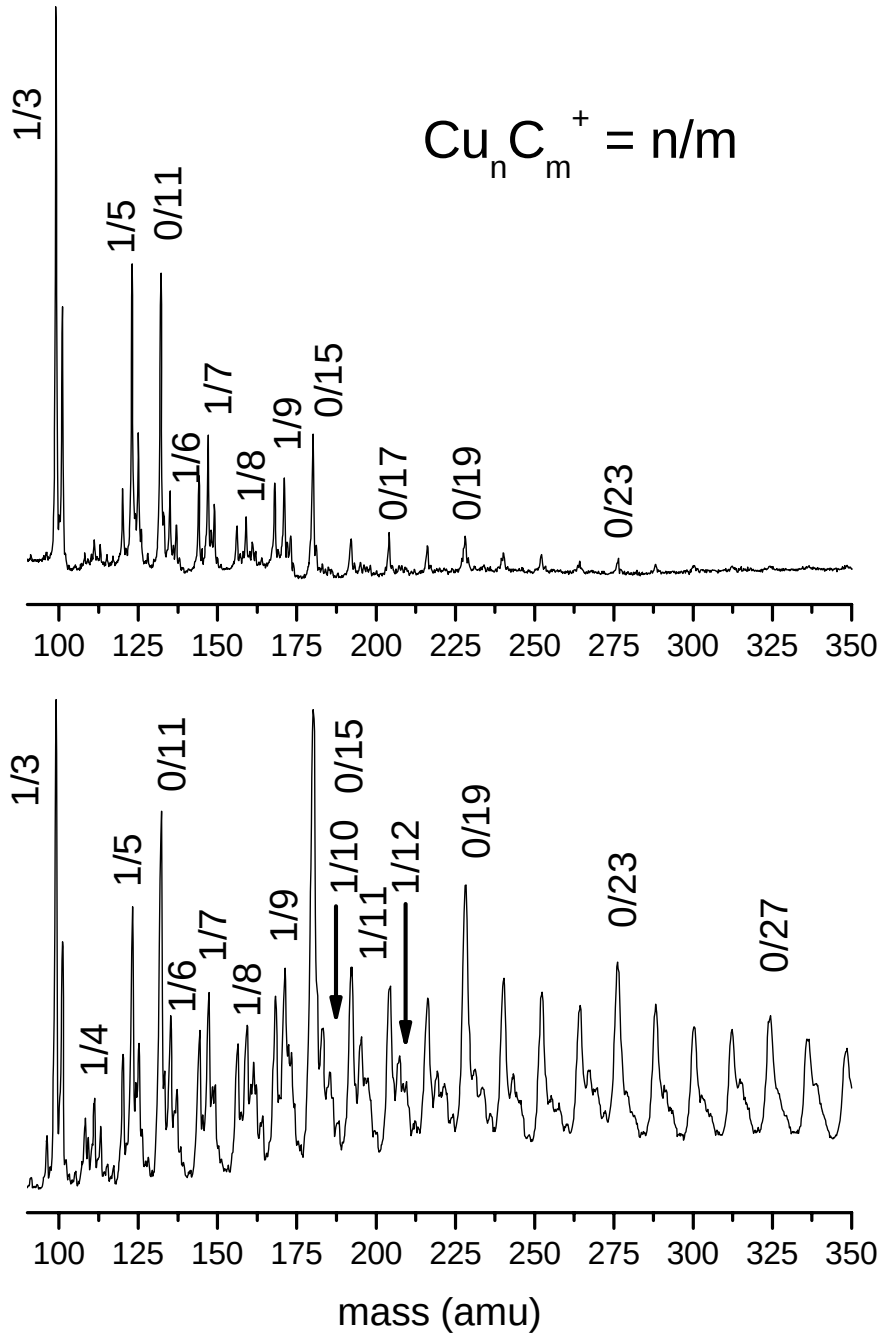

Figure 4.1: Mass spectrum of copper carbide clusters formed in a helium expansion. The upper trace shows the cluster distribution from an expansion out of a rod holder. The lower trace shows the cluster distribution with a 0.5 inch growth channel attached to the end of the rod holder.

from the mass spectrum. This is true under all experimental conditions. Even in the lower trace, where the growth channel promotes the formation of larger clusters, 1/3 is the largest peak in the mass spectrum.

Several previous gas phase mass spectrometry studies on copper carbide clusters have been conducted. Yamada and Castleman used a gas aggregation source that reacted copper vapor with acetylene (C_2H_2) gas dissociated over a hot filament and reported clusters with near stoichiometric ratios of metal to carbon.[35] That experiment favored the formation of clusters with multiple copper atoms and an even number of carbon atoms. The copper concentration was evidently extremely high in their source as pure copper clusters as large as Cu_{21}^+ were observed. In fact the smallest mixed carbide they observed was 3/2, whereas we observe no species with multiple copper atoms regardless of experimental conditions. Additionally, they saw only clusters containing even numbers of carbon atoms. As mentioned above, however, the carbon source in their experiment was C_2H_2 gas, so the formation of carbide species with carbon atoms in multiples of two is perhaps not surprising. In a later study, Reddic and Duncan used laser vaporization to produce copper carbide clusters in a mass spectrometer, utilizing experimental conditions very similar to ours.[40] In that experiment the 1/3 cluster size was prominent, while 1/1 and 1/2 were not seen, consistent with our results. Like our experiment, that experiment also saw significant clustering of pure carbon which provided competition for growing mixed metal carbides. Notably, they did not see the even odd alternation in signal intensities for the copper carbides observed in our experiment, and in fact they saw a slight enhancement for the 1/10 cluster, which we do not see.

The appearance of the mass spectra of the copper carbides is also clearly different from that seen previously in studies of pure carbon cations. This suggests that, even though carbon is present in significantly higher concentration than the copper, carbon clusters are not simply forming in their usual distribution and then binding a metal to form carbides. Previous mass spectrometry experiments on carbon cations have shown enhanced abundances for C_3^+, C_7^+, C_{11}^+, C_{15}^+, and C_{19}^+.[91-94,95,98] The nascent distribution for the neutrals has proven difficult to measure but C_3, C_{10}, C_{12}, and C_{14} are thought to be prominent.[43,95,97] While we do observe the C_{11}^+, C_{15}^+, and C_{19}^+ with the expected enhanced abundances, neither the cation nor the neutral series seen previously correspond to the metal carbon clusters present here with the greatest intensity. The presence of copper in the laser plasma seems to be affecting the growth of the mixed clusters and their distribution.

Very recently, high level ab initio calculations on carbon clusters[43] showed that small species with an odd number of atoms (C_3, C_5, C_7, C_9) have linear $^1\Sigma_g^+$ ground states, while those with an even number of carbon atoms (C_4, C_6,C_8) have cyclic ^1A_g or $^1A_1'$ ground states, with $^3\Sigma_g^-$ linear states lying higher in energy. The cumulenic bonding (:C=C···C=C:) in the linear singlet states leads to lone pairs of electrons on the ends of the chains that may be available for a dative type bond with the copper ion. The cyclic singlet or linear triplet states would not have these electron pairs available for bonding, which may explain the absence of the CuC_n^+ (n = even) clusters in the upper trace. This is also consistent with the lack of mixed carbides larger than CuC_9^+ in that mass spectrum, despite the presence of larger pure carbon clusters. C_{10} and larger clusters favor cyclic structures by a substantial amount of energy,[6,7] and the ring isomers may not

efficiently form clusters with copper. This is also in good agreement with the observation from ion mobility studies that linear carbon chains are more reactive than the cyclic structures.[116]

In the lower trace, however, the use of the growth channel helps to keep the local concentration of metal in the plasma relatively high. If cluster growth is controlled by kinetics rather than energetics, the copper ion may interact with a carbon species that has not yet relaxed to its ground state. The higher energy linear structures would then be populated, and the higher reactivity of the linear isomer allows it to bind a copper ion before the entire complex is cooled in the expansion. This may be an explanation for the greater intensity of the n = even clusters and for the formation of the much larger mixed carbides seen in the lower trace of Figure 4.1.

Figure 4.2 shows the mass spectrum collected for a carbon rod coated with gold. Pure carbon and mixed gold carbide clusters are both produced. The pure carbon distribution is peaked at C_{11}^+ (not shown), and the carbon clusters seen in the region of the mass spectrum shown in Figure 4.2 are small peaks seen between the carbide peaks. The mass spectrum shown was collected without a growth channel. When a growth channel is used the intensity of the carbon clusters is so great that the mixed metal carbide peaks are not seen in any appreciable intensity. As with the copper, the gold-carbon 1/3 is the biggest mixed metal carbon peak in the mass spectrum, but both 1/1 and 1/2 are present here, if only in small amounts. After 1/3, the 1/5 and 1/6 are the most abundant carbide peaks in the mass spectrum. Clusters with two gold atoms and multiple carbons are also formed, behavior not seen in the copper experiments. The 2/3 and 2/6 are the biggest peaks of this type. The gold carbides do not show the same even odd

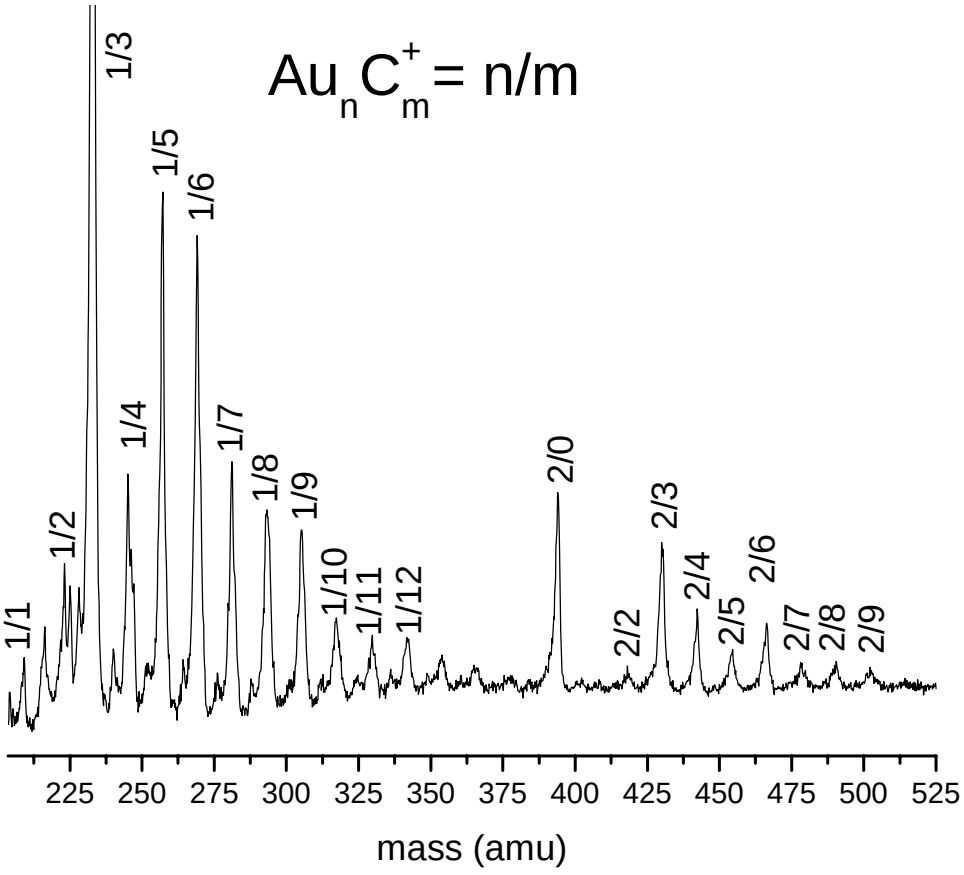

Figure 4.2: Mass spectrum of gold carbide clusters formed in a helium expansion.

alternation in intensity seen in the copper carbides. In fact, they display a sudden decrease in intensity after mixed clusters with 3, 6, 9, and 12 carbon atoms. Again, the appearance of the mass spectrum is very different than that seen for pure carbon cations, so the presence of the gold in the laser plasma changes the cluster distribution.

To our knowledge, only one previous mass spectrometry study on gold carbides exists. In the course of studying the reactions of laser ablated gold cations with hydrocarbons and halocarbons, Gibson observed the formation of small gold carbide species. He saw no formation of AuC_n^+ clusters, apparently because Au^+ is not reactive enough to catalyze dehydrogenation and dehalogenation reactions.[41] The gold dimer cation, however, as well as larger gold cation clusters, was reactive with the various precursor molecules. Carbon atom and the carbon dimer attached to gold clusters were the most common reaction products, but carbides as big as 3/7 were made under certain conditions. As mentioned above, in our gold experiments, as opposed to copper, we do see some formation of the 1/1, 1/2, and 2/2 species. This is consistent with Gibson's results, indicating that if C_1 and C_2 are present, they can bind to gold ions. The carbide clusters produced by laser vaporization in the mass spectrometer were then mass selected and photodissociated to explore their structure and bonding.

Figures 4.3 – 4.8 show photodissociation mass spectra for many of the copper and gold carbides studied, and additionally the major fragmentation channels for all clusters studied are collected in Table 4.1. The photodissociation data is accumulated by monitoring the mass spectrum when the photodissociation laser is on and again when the laser is off. The two mass spectra are subtracted from each other, generating a difference mass spectrum of the selected cluster. The downward going peak in the

photodissociation mass spectra represent depletion of the parent ion, while the positive going peaks show the appearance of fragments. The integrated areas of the fragment peaks should theoretically be exactly equal to the area of the parent depletion peak. As can be seen in Figures 4.3 - 4.5, the depletion of the parent ion is greater than the appearance of the fragments for some cluster sizes. Mass discrimination in our instrument due to ion focusing effects prevents the simultaneous detection of both parent and fragment ions with equal sensitivity, and in some cases all of the daughter ions are not detected. For selected photodissociation mass spectra the parent ion is presented off scale so that the fragment ions may be shown in greater detail. Additionally, because the bonding in these carbide species is expected to be strong, multiphoton absorption will likely be required to fragment these species in some cases.

Figure 4.3 shows the photodissociation mass spectra for small CuC_n^+ (n = 5-10) carbides. They clearly display different fragmentation behavior depending on the number of carbon atoms present in the cluster. Species with an odd number of carbon atoms (1/5, 1/7, 1/9) show the elimination of the entire carbon cluster as a neutral leaving group and the appearance of the copper cation as the sole charged fragment. This suggests a carbon cluster with an attached copper ion. As mentioned above, the ground states of the n = odd clusters of pure carbon are linear chains, which are known to be the more reactive structure for carbon species. These fragmentation products are also consistent with the expected binding energies of copper carbide species. In the case of the diatomics, the fragmentation energies have been calculated to be 5.8 eV for C_2[117] and 2.54 eV for CuC.[83] The dissociation energies for the ions have been calculated to be 4.7 eV[117] for C_2^+ and 2.02 eV for CuC^+.[83] Thus for both the neutrals and the ions, the

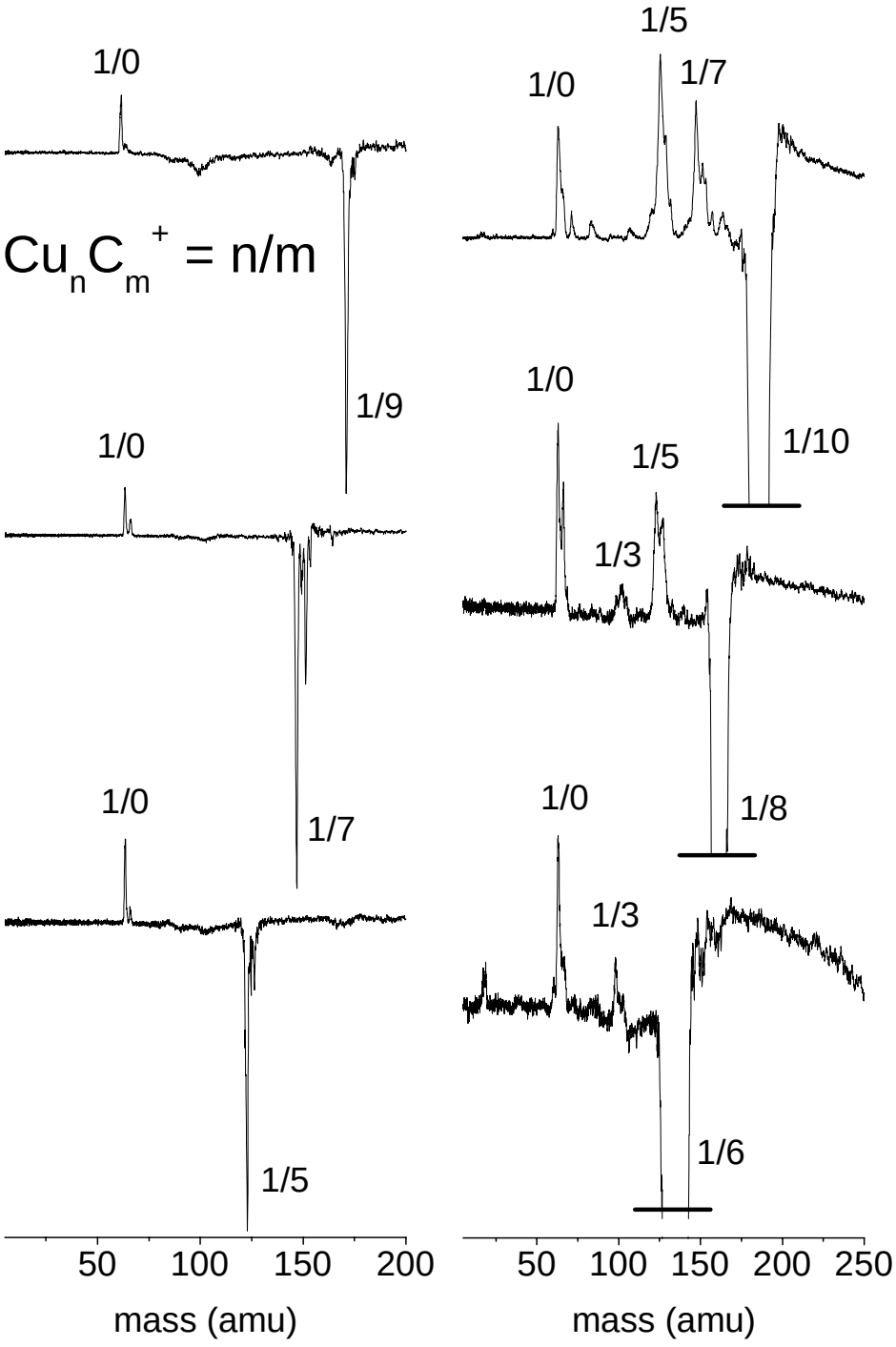

Figure 4.3: Photodissociation mass spectra of copper carbide clusters $CuC_{5\text{-}10}^+$ at 355 nm.

calculations show stronger bonding between two carbon atoms than between a carbon atom and a copper atom (or ion). Of course, because of changes in electronic structure as size increases, these dissociation energies cannot necessarily be extrapolated to the larger clusters. For example, the dissociation energy of CuC_2 has been calculated to be 3.42 eV for the linear isomer and 3.71 eV for the cyclic isomer,[85a] while the values for CuC_2^+ are 1.57 eV and 1.52 eV respectively.[85b] In general, however, fragmenting a copper-carbon bond should be a lower energy process than fragmenting a carbon-carbon bond. The dissociation energy of C_9^+ into $C_6^+ + C_3$, for example, has been measured by CID to be 5.7 eV,[104] considerably higher than that expect for a metal carbon bond. In photodissociation experiments of this type the weakest bond is expected to break first, which here would be the bond between the metal ion and the carbon. The fact that the charge stays on the metal upon fragmentation is also expected, as the ionization potential (IP) of a copper atom is 7.73 eV,[118] while the IP's of small carbon clusters are ~8.8 eV and higher.[43]

Figure 4.3 also shows the photodissociation mass spectra for the even numbered 1/6, 1/8, and 1/10 clusters. The largest fragment for each of these species is the copper atomic ion, which, as explained above for the n = odd sizes, suggests a carbon cluster with an attached copper atom. What is noticeably different for the n = even versus n = odd clusters, however, is the appearance of mixed metal carbide fragments. 1/6 fragments to 1/3, 1/8 fragments to 1/5 and 1/3, and 1/10 fragments to 1/7 and 1/5. By mass conservation, the neutral leaving group must be C_3 and C_5 units, respectively. As mentioned above, the predicted energetics for clusters of this size would favor the breaking of the copper carbon bond, as is seen for the n = odd species. The loss of

carbon units upon photoexcitation suggests that the simple picture of a metal ion bound to the end of a linear carbon chain is incomplete. C_3 is known to be a very stable neutral species[43] and is the common fragmentation product from dissociation of carbon clusters this size.[99,104] C_5 is also a common fragmentation channel for pure carbon clusters, but is only a significant loss channel for larger sizes, becoming important at C_{15}^+.[99] Its appearance in the dissociation of the 1/8 and 1/10 suggests that in this size regime the copper binds to the carbon much more strongly than expected. It should also be noted here that that for some clusters (1/10, for example), small peaks present in the background correspond to fragmentation of pure carbon species that were not rejected completely by the mass selection and were still present in the reflectron together with the desired ion. Laser timing studies show that these peaks are not from the cluster of interest.

The appearance of mixed fragments for these clusters may also reflect the enhanced stability of 1/3, 1/5, and 1/7 as cations, which is also seen in the mass spectra. This process may be driven by the fact that simultaneously losing neutral C_3 or C_5 and forming 1/3, 1/5, or 1/7 are together energetically favorable. Another possible structure for 1/6 and 1/8 is the metal ion attached to two separate C_3 units or one C_3 and one C_5 unit. These structures seem unlikely and copper would not be expected to form multiple bonds. However, as mentioned above, C_3 and C_5 are known to be stable neutral fragments. The photodissociation data alone cannot confirm either structure.

Figure 4.4 shows photodissociation mass spectra for the 1/11, 1/12, and 1/13 copper carbide clusters. The fragmentation behavior for the 1/11 shows a marked break from what was observed for the smaller n = odd species. A fragment peak corresponding

to the copper cation is seen, as before, but here it is present only in very small intensity. Instead, the two peaks that dominate the fragmentation are 1/8, corresponding to loss of neutral C_3, and 0/11, corresponding to loss of neutral copper atom. The loss of neutral C_3 was seen before only for the species with an even number of carbon atoms. Its appearance here suggests that for this cluster, breaking a carbon – carbon bond is at least comparable in energy to breaking the carbon – copper bond. As described above for the n = even species, this is somewhat surprising based on the expected carbon copper bond energies. Additionally, the formation of the 1/8 is the first time a mixed cluster fragment with an even number of carbon atoms is seen. The previous mixed fragments all had an odd number of carbons. Those mixed fragments, 1/3, 1/5, and 1/7, all also corresponded to the peaks with enhanced abundances in the mass spectrum, possibly indicating that they have enhanced stability as ions. Here, however, the 1/8 is formed, which was not especially abundant in the mass spectrum. Apparently the tendency to lose C_3 from this cluster is strongly favored energetically and proceeds even if the mixed carbide cation formed does not contain an odd number of carbons.

The other sudden change in fragmentation behavior seen for the 1/11 is the appearance of C_{11}^+ as the biggest fragment peak in the mass spectrum. This is the first species for which a pure carbon cation fragment is seen. Previous mass spectrometry and dissociation experiments on pure carbon clusters have repeatedly recognized C_{11}^+ as a prominent peak, possibly due to enhanced stability, a low IP, or both.[6,7] The appearance of a C_{11}^+ dissociation product here necessarily means that the IP of the fragment detected in the experiment is lower than that of copper atom, which is 7.73 eV.[118] The IP of C_{11} has been measured by charge transfer bracketing (CTB) to be 7.45 eV,[119] and by vacuum

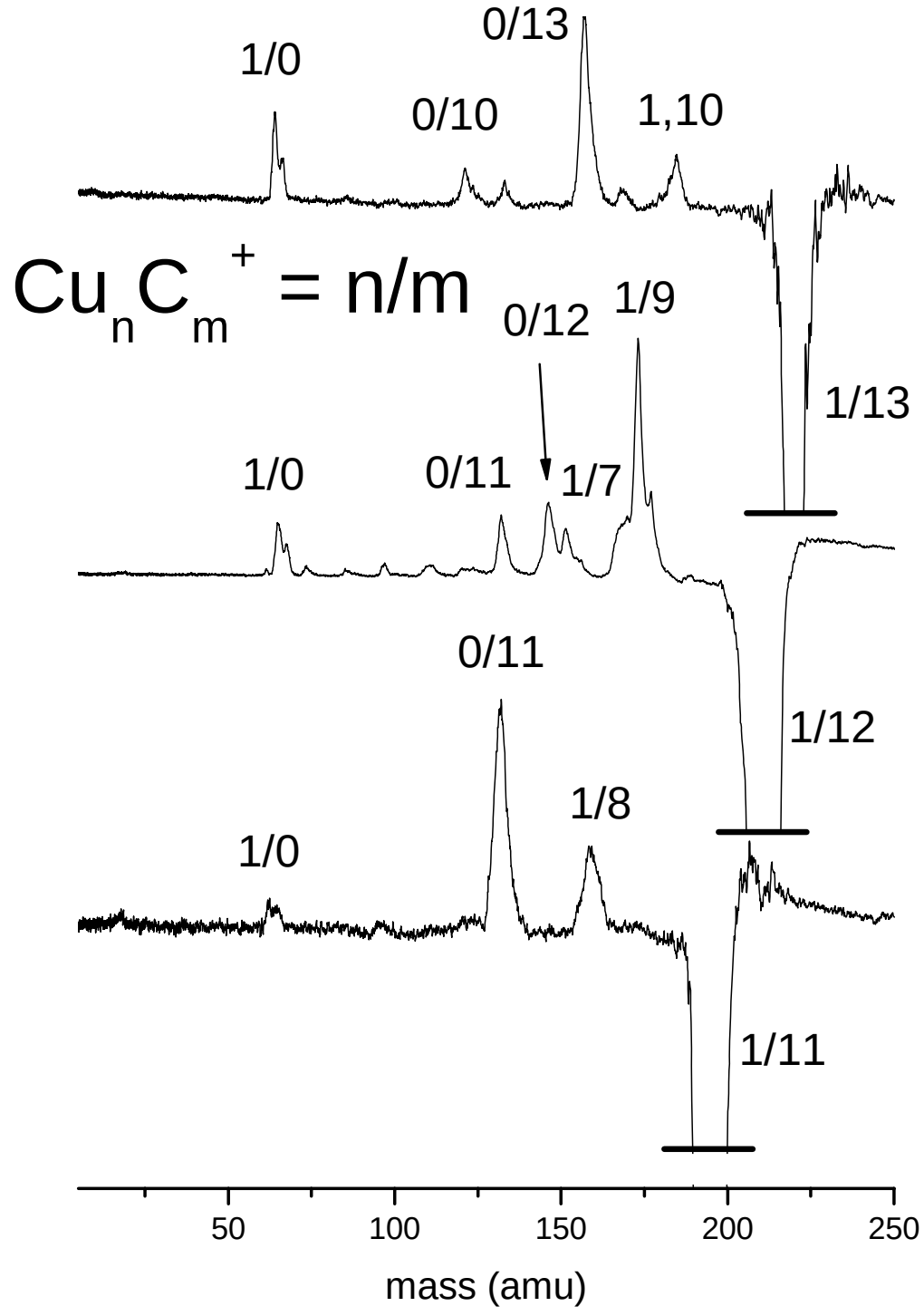

Figure 4.4: Photodissociation mass spectra of copper carbide clusters $CuC_{11\text{-}13}^+$ at 355 nm

ultraviolet photoionization (VUV-PI) to be 9.4 eV.[43] DFT calculations found an IP of 7.6 eV for the cyclic structure and 8.6 eV for the linear structure,[120] indicating that the discrepancy between the two experimental values was due to the measurement of the cyclic isomer in the CTB study and the linear isomer in the VUV-PI study. In this case, the C_{11}^+ species we observe as a fragment has an IP consistent with that of only the cyclic isomer. Small carbon clusters are known to have many low lying excited electronic states, and population in these states has been shown to cause their photoionization thresholds to be detected at values lower than the true IP.[43] This possibility cannot be ruled out here, and thus the assignment of a cyclic structure to the observed C_{11}^+ fragment cannot be made with absolute certainty. Also, rearrangement of a cluster's structure may occur upon laser excitation and subsequent dissociation, so this experiment does not confirm unequivocally that the 1/11 parent is the ring isomer with a copper atom bound to it. With the above caveats in mind, however, the data does seem to suggest that at least some of the clusters in the beam likely lose cyclic C_{11}^+ upon fragmentation. This is also in good agreement with the results of ion mobility experiments on pure carbon cations,[116] which found only one isomer, predicted to be cyclic, for $C_{11\text{-}20}^+$.

The 1/12 fragmentation proceeds largely as expected when compared to the smaller even clusters, with loss of C_3 and C_5 to form 1/9, and 1/7, respectively. Also, like the 1/11, it shows some appearance of C_{12}^+, which indicates that the IP of this fragment must be lower than that of copper, using the argument given above. The IP of C_{12} has been measured by CTB[119] and VUV-PI[43] to be in the neighborhood of 8.5 eV, and DFT predicts the IPs of both the linear and cyclic isomers to be in this range.[120] Thus no assignment of the structure of this fragment is possible. The 1/12 also appears unique in

that it loses CuC to form C_{11}^+. This may be due to the fact that C_{11}^+ seems to have a special stability compared to other carbon clusters, although the literature disagrees quite significantly about this point. Additionally, previous experiments have observed the loss of both C_1 and C_2 as minor (but important) fragmentation channels for C_{12}^+, possibly because of excess internal energy in the some fraction of the ion distribution.[103b] Thus the appearance of the C_{11}^+ fragment peak from the 1/12 is not as anomalous as it first appears.

The fragmentation for the 1/13 is very similar to that seen for the 1/11. It loses C_3 to leave the 1/10, or loses copper atom to form C_{13}^+. In this case, the results of the CTB[119] and VUV-PI,[43] when compared to the DFT calculations,[120] seem to show an IP of around 9.3 eV for the linear species and 8.09 eV for the cyclic isomer of the pure carbon cluster. Because the IP of the cyclic structure is much closer to the IP of copper atom than the linear isomer, and because at this size regime the cyclic structures of carbon are strongly favored over the linear isomers, it is tempting to assign a cyclic structure to our observed C_{13}^+ fragment. Again, this is consistent with ion mobility measurements which only detected the cyclic isomer for clusters in this size regime.[116]

Figure 4.5 shows mass spectra of the 1/14, 1/15, 1/16, and 1/20 copper carbide clusters. Again, the fragmentation behavior observed here shows the similar even- odd alternation seen for the smaller clusters. The 1/15 shows primarily fragmentation to the C_{15}^+ with only a small appearance of the mixed 1/12 fragment. As mentioned above, C_{15}^+ has been repeatedly seen in previous experiments as an abundant cluster size for carbon cations, suggesting enhanced stability. For this fragment, again with comparison to the

IPs of carbon clusters measured by CTB[119] and VUV-PI[43] experiments and predicted by DFT calculations,[120] the isomer observed in our experiment is likely cyclic.

For species with an even number of carbons (including 1/18, not shown), the loss of neutral copper to leave the entire carbon cluster cation is seen, and only for the 1/16 is this not the dominant fragment channel. All of the n = even clusters in this size range also show the loss of neutral C_3 to leave a mixed carbide fragment with an odd number of carbon atoms, which was seen before for the smaller even numbered species. Interestingly, the 1/14 (by loss of C_3) and the 1/16 (by loss of C_5) fragment to the 1/11, and 1/16 especially shows the formation of C_{11}^+. As mentioned above, C_{11}^+ is known to be an abundant cluster in mass spectra of carbon, and it has indeed been seen as a sizable photofragment from C_{12}, C_{14}, and C_{16},[99] so its appearance as a fragment from these clusters in our experiment is not surprising.

Dissociation of this type was also seen, to some extent, in the only other transition metal carbide fragmentation study of which we are aware for clusters of this size. McElvany and Cassady made tantalum carbide ions by laser vaporization of a variety of different materials containing metal and carbon.[39a] They produced clusters in the same size regime as those in our experiment, and fragmented them with CID. They saw the loss of neutral C_3 as the dominant fragment channel for most of the species smaller than n = 9. This dissociation process was justified by comparison to the fragmentation energies of the other group V metals (V, Nb) to carbon, which are ~6 eV. In this case the metal-carbon bond is stronger than the carbon – carbon bond, so the loss of C_3 is the expected fragment just as from a pure carbon speceis. As described above, the bonding between noble metals and carbon is expected to be much weaker than this, but we still observe the

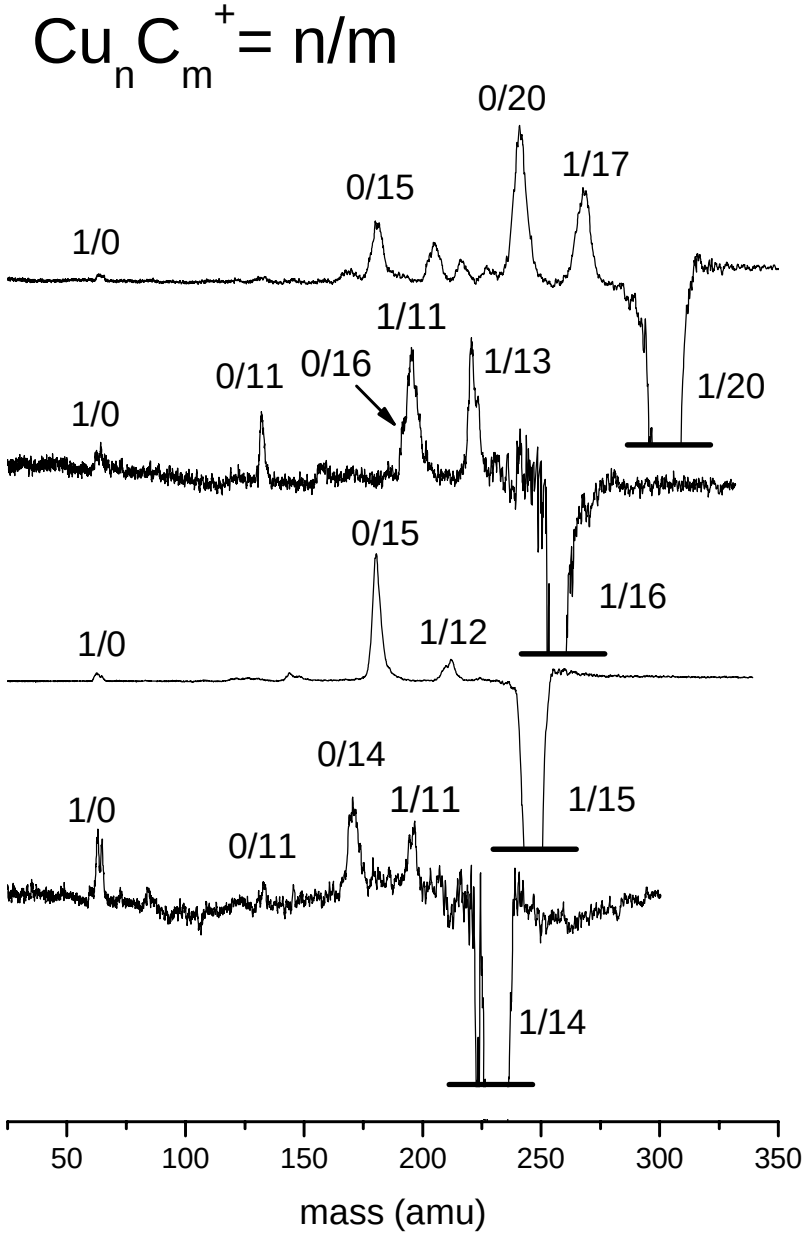

Figure 4.5: Photodissociation mass spectra of copper carbide clusters $CuC_{14\text{-}16,20}^+$ at 355 nm.

loss of C_3 from many cluster sizes. Additionally, the only large cluster for which the loss of the entire carbon species was observed in their experiment was TaC_{10}^+ losing neutral C_{10}. They also observed the loss of C_{10} from other larger sizes. In our experiment, on the other hand, we see the loss of the entire carbon cluster as either a neutral or cation as a possible fragmentation channel for every species studied. The loss of neutral C_{10} observed by McElvany for numerous larger clusters is never observed in our data. Carbon has been demonstrated in the past to form different isomers depending on the cluster growth conditions,[6,7,43] and tantalum clearly displays different bonding to carbon than the noble metals, so some differences in our experiments are not surprising. The fact that C_3 is a common leaving group for many cluster sizes studied in both experiments shows the extremely high stability of this species and its propensity as a favorable fragmentation product from a variety of metal carbide species.

The photodissociation behavior of the metal carbides in this size regime can also be compared to a previous study on the photodissociation of MSi_n^+ clusters (M = Ag, Au, and Cr).[109] In that study the most common fragmentation channel was loss of the metal atom, which would be expected for an intact silicon cluster which had bound metal to its surface. For the $CrSi_{15}^+$ and $CrSi_{16}^+$, however, the major loss channel was elimination of silicon atom. The interpretation of this was a metal atom encapsulated inside the silicon cluster, which was supported by several theoretical studies. Another possibility that was suggested, however, was a surface bound metal that with a particularly strong metal – silicon bond. In our metal carbide experiments the three dimensional structures favored by silicon are not likely. It thus seems likely that the photodissociation reveals a metal atom attached to an intact carbon cluster, and the even odd alternation in the

fragmentation patterns represents a different bonding paradigm rather than a dramatic change in the overall structure of the species.

Figure 4.6 shows the photodissociation mass spectra of the 1/27 and 1/28 copper carbides. The dominant fragmentation channel for both of these species is the loss of a neutral copper atom to leave a charged carbon cluster. However, the even odd alternation in fragmentation behavior seen in the smaller clusters is still present. The 1/28 and the 1/30 (not shown), with an even number of carbon atoms, shows some fragmentation by loss of C_3 to form the mixed 1/25 or 1/27. The 1/27, however, with an odd number of carbon atoms, shows no formation of mixed clusters upon fragmentation. Thus it appears that even in these large sizes the metal-carbon binding is stronger in species with an even number of carbons. The subsequent fragment peaks observed closely correspond to the dissociation channels seen previously for pure carbon clusters of this size, in that C_3 and C_5 are the loss channels.[6,7,100,105] The fact that C_3 loss is favored in subsequent fragmentation events also suggests that these are not metal- fullerene species. Fullerenes are known to fragment by the loss of C_2 or C_1 rather than the more stable C_3 because it preserves the integrity of the fullerene sphere.[100,105] This behavior is clearly not seen here. Fullerenes are not expected to readily form at sizes smaller than C_{32}, and are not the dominant isomer until~C_{50}.[100,105,116] Additionally, the C_{11}^+, C_{15}^+, C_{19}^+, and C_{23}^+ peaks tend to stand out among the other fragments, consistent with the dissociation of pure carbon clusters of this size, even at very low laser powers.[6,7,100,116]

Figure 4.7 shows the photodissociation mass spectra of the 1/36 and 1/43 copper carbide clusters. Both of these species fragment by the loss of copper atom to give charged fragments of pure carbon. The subsequent fragmentation of the carbon clusters

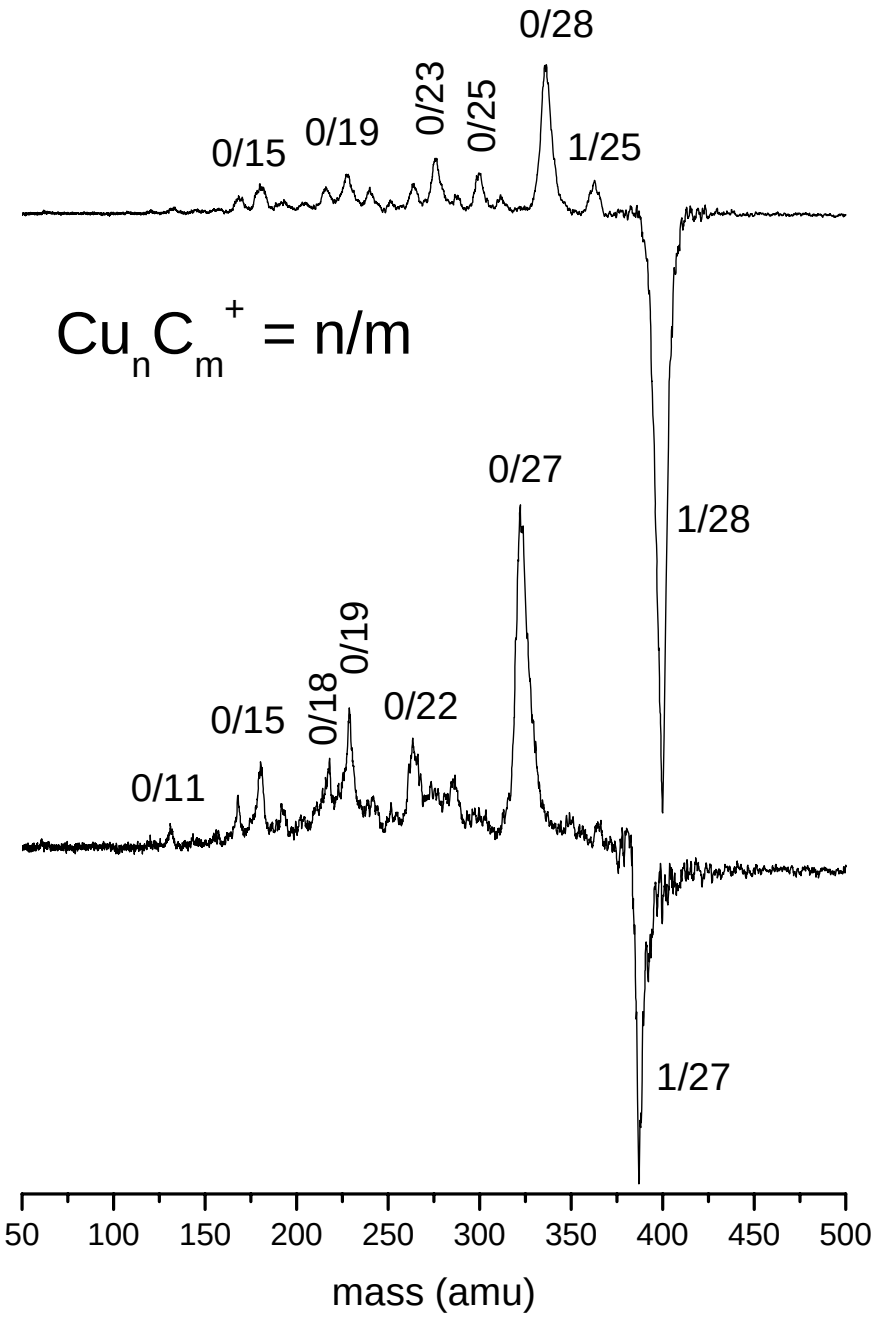

Figure 4.6: Photodissociation mass spectra of copper carbide clusters $CuC_{27,28}^+$ at 355 nm.

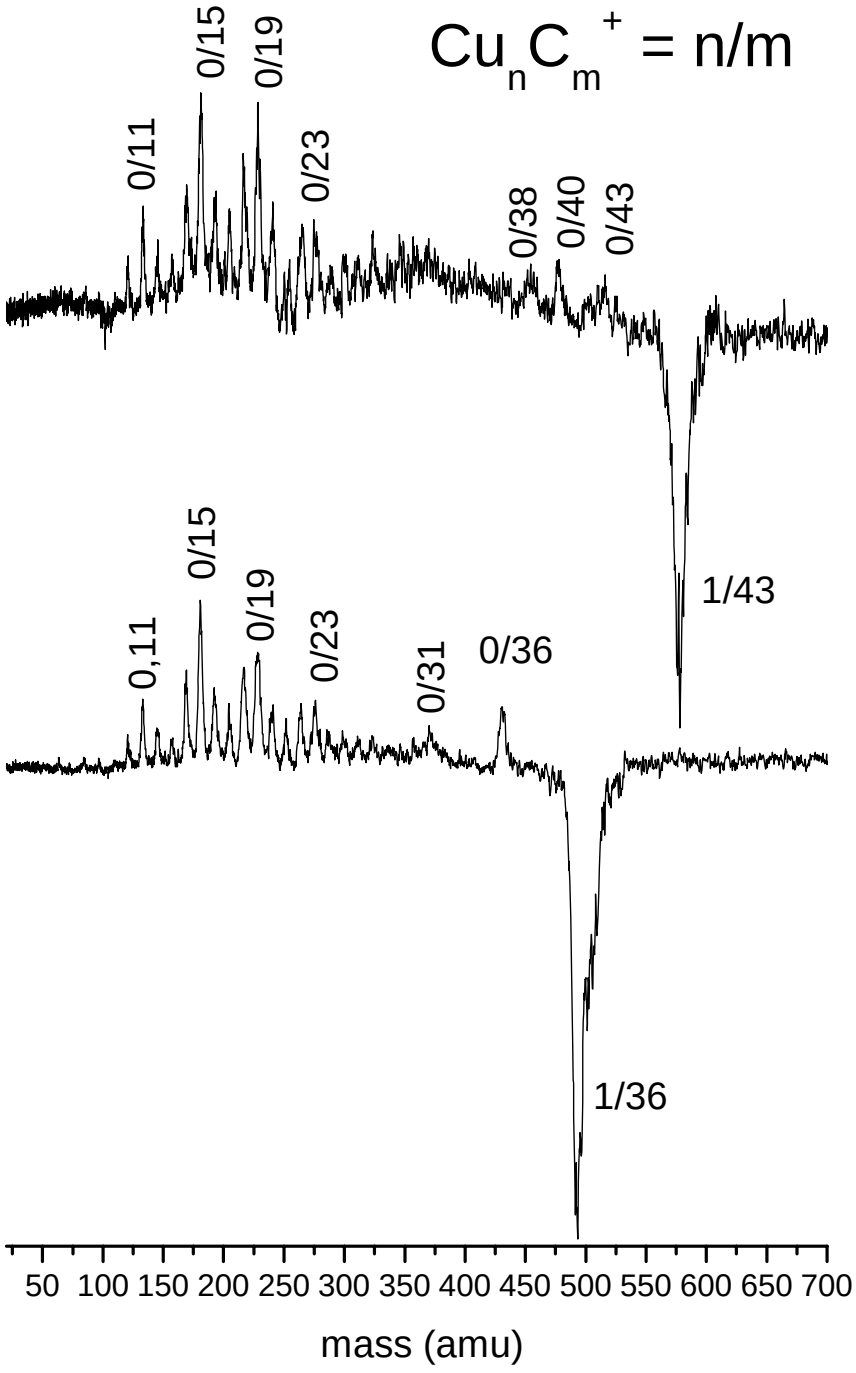

Figure 4.7: Photodissociation mass spectra of copper carbide clusters $CuC_{36,43}^+$ at 355 nm.

proceeds as expected, with losses of both C_3 and C_5 observed. Very few fragmentation products in the size range of about 30 carbon atoms is observed, consistent with the previous observations of Smalley and co-workers from photodissociation experiments of large carbon and fullerene clusters.[100] Around C_{27}^+, peaks are observed again at essentially every carbon cluster mass, and as before the C_{11}^+, C_{15}^+, C_{19}^+, and C_{23}^+ peaks are the most prominent. Again, because we do not see any loss of C_1 or C_2 units, we conclude that the peaks here do not represent metals bound to fullerenes. Additionally it should be noted that 1/36, which contains an even number of carbon atoms, does not show any loss of C_3 to form a mixed carbide fragment. Apparently at this large size the metal – carbon bond has become weak enough that it always breaks, or alternatively the 1/33 species, which would be produced by loss of C_3, is not stable enough to make this fragmentation channel active.

Figure 4.8 shows the photodissociation mass spectra for the gold carbides 1/4 – 1/9. The small species show fragmentation patterns similar to that of the small copper carbide clusters. As can be seen in Table 4.1, the 1/3, 1/4, and 1/5 for both metals fragment by loss of C_3, C_4, and C_5 neutrals respectively to leave only the metal cation. Likewise the 1/6 for both metals fragments either by losing C_3 to form the 1/3 or by losing C_6 to leave the metal cation, although for gold the loss of C_3 is the favored dissociation channel while for copper the loss of C_6 is greater. Only at the 1/7 cluster size do significant differences emerge between the copper and the gold carbides.

For the gold 1/7 species, breaking of the metal-carbon bond to leave gold cation is the dominant dissociation channel, but there is some formation of the 1/4 mixed fragment by loss of C_3. This is somewhat different from the dissocation observed for the copper

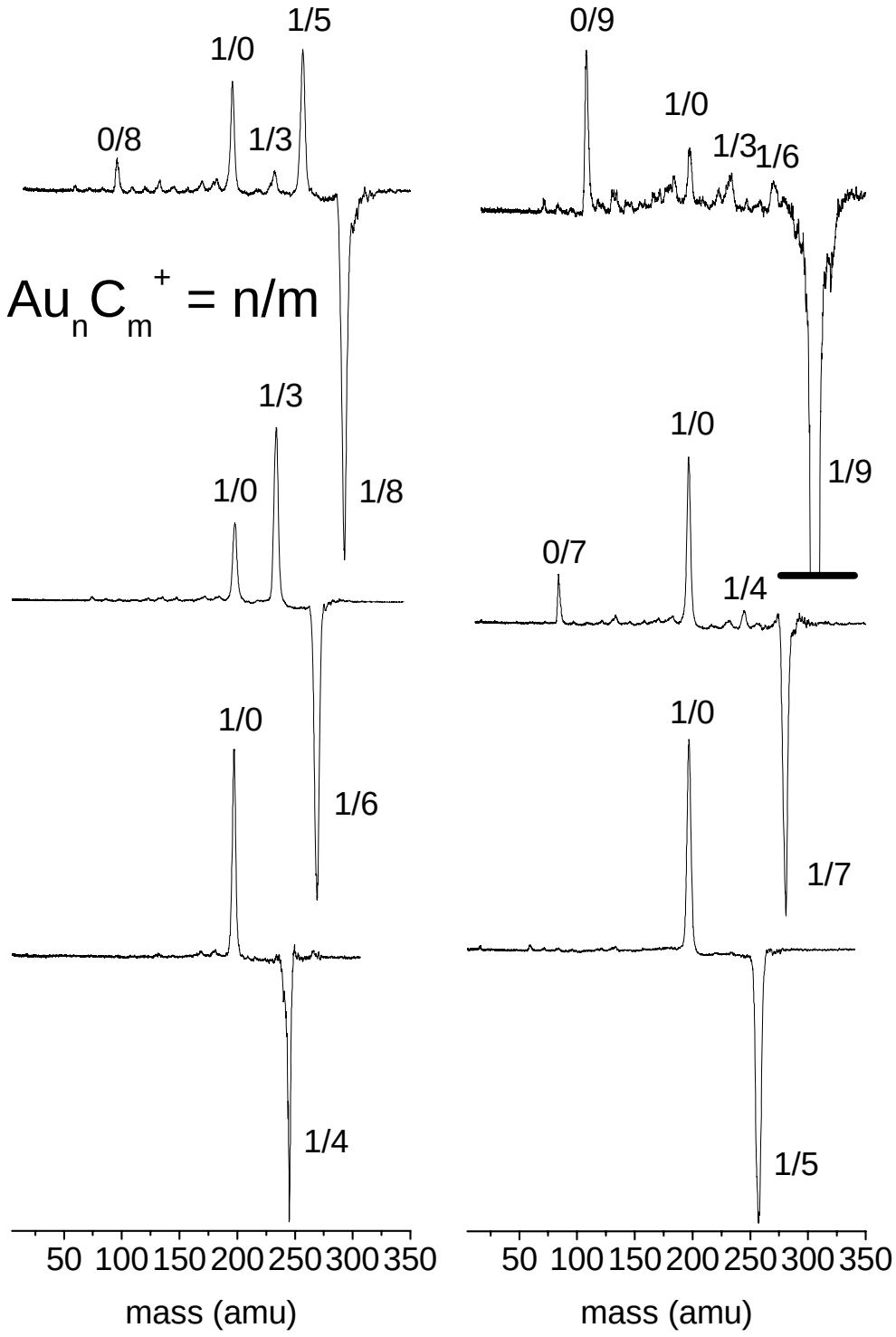

Figure 4.8: Photodissociation mass spectra of gold carbide clusters $AuC_{4\text{-}9}^+$ at 355 nm.

1/7, which simply fragmented to Cu^+. The first size for which this type of behavior was seen in a copper carbide cluster with an odd number of carbon atoms was the 1/11. The gold 1/7 also has a fragment of C_7^+. Because this fragment keeps the charge upon dissociation it must have a lower IP than gold atom, which is 9.225.[118] Interestingly, this behavior was also initially seen in the copper carbides for the 1/11 species. High level ab initio calculations performed on C_7 found the IP of the cyclic isomer to be 9.1 eV and the linear isomer to be 10.4 eV.[43] These values, when compared to experimental values of 8.09 eV from CTB[119] and 10.1 eV from VUV-PI[43] experiments, show that the CTB experiment was likely measuring the cyclic structure, while the VUVPI experiment was measuring the linear isomer. We are most likely detecting the cyclic isomer of C_7^+, although, as explained above, rearrangement of the cluster structure is possible in the photodissociation process, so this experiment does not prove any particular cluster structure before dissociation. Comparison to the ion mobility results for C_7^+ shows that the cyclic isomer is found in slightly higher intensity than the linear one, but both structures are significantly populated.[116]

The gold 1/8 dissociation mass spectra shown in Figure 4.8 is very similar to the copper 1/8 dissociation data, showing the mixed 1/5 and 1/3 fragments, as well as significant production of the bare metal cation. This formation of the mixed carbide fragments is again somewhat surprising. The gold carbon diatomic molecule has been predicted by theory to contain one of the strongest known bonds to gold,[88,89] and the calculated bond length of 1.764 Å supports the possibility of a multiple bond between gold and carbon.[88] Despite the possibility of a strong bond between gold and carbon, even in the neighborhood of 3.5 eV,[88,89] the bonding is still expected to be weaker than

that for pure carbon clusters. CID has measured the dissociation energy of C_7^+ at 6.3 eV and C_8^+ to be 5.3 eV.[101,104] Dissociation by loss of C_3 to leave a mixed fragment thus suggests that the gold has a strong effect on the bonding of the carbon species. The C_8^+ cluster is also a fragment from 1/8. Because the IP of both the linear and cyclic isomer of C_8 have been calculated to lie below the IP of gold, an assignment of the structure of this fragment is not possible.

The fragmentation of the 1/9 gold carbide is similar to the 1/7. It shows some formation of mixed clusters by loss of successive C_3 units to form 1/6 and 1/3 fragments. It should be noted that the gold carbide mass spectrum showed a drop off in intensity for sizes *after* the 1/3, 1/6, 1/9, 1/12, 2/3, 2/6, and 2/9 clusters, perhaps indicating enhanced stability for species with $Au_{1,2}C_{3n}^+$ stoichiometries. This fact, coupled with the loss of the stable C_3 unit, probably explains the presence of the mixed fragments here. The dominant peaks, however, correspond to Au^+ and C_9^+, which closely resembles the fragmentation seen in the 1/7. Based on the same IP arguments made for the other clusters from comparisons to the CTB,[119] VUV-PI,[43] and ab initio[43] IP values, we believe that the C_9^+ fragment observed is the cyclic isomer.

Theoretical Results

To investigate the stability and energetics of various isomers which may be present in these experiments, DFT calculations were performed by B. Bandyopadhyay on the copper carbide species 1/3 – 1/11 to determine stable structures. We have also calculated the binding energies for the linear cation species 1/3 -1/6. Most of the

previous theoretical work on the noble metal carbides has focused on diatomic and triatomic species.[82-85,88,89] Hall and co-workers have previously studied palladium and platinum carbide cations using the B3LYP functional with the LANL2DZ basis set on the metal found that for both metals the linear chains were the lowest energy isomer up to the size MC_9^+.[80] At larger sizes closed ring (metal bound to two atoms of a cyclic carbon cluster), open ring (metal incorporated into a carbon ring), and one-carbon ring (metal bound to one atom of a cyclic carbon cluster) structures were all found to be stable. The lowest energy isomer varied with both the metal and the cluster size. The stability of the cyclic structures for clusters with 10 carbon atoms is not surprising, however, because pure carbon clusters are known to be energetically favored as rings beginning at C_{10}, due to the reduction of the ring strain in larger species.[6,7,116] Recently Largo and co-workers, using the B3LYP functional with the LANL2DZ basis set on the metal, extensively studied the vanadium doped carbon clusters, examining both linear and cyclic structures for neutral, cationic, and anionic species.[70] They also found stable linear structures for all sizes, but only for the 5-7 sizes was the linear isomer lowest in energy. A fan-type cyclic structure was the lower energy structure for the 1/2 and 1/4 clusters, while the 1/3 and 1/8 favored the open ring isomer with the vanadium incorporated into a cyclic carbon unit. The bonding of copper to carbon will likely be different from the metals studied before, but the metal carbide geometries identified as stable by these previous studies were used to guide our present theoretical investigations.

The lowest energy isomer for each carbide cation studied is shown in Figure 4.9. A complete summary of the results for all the calculations performed is available in the Supporting Information. The lowest energy structure for most of the cluster studied is

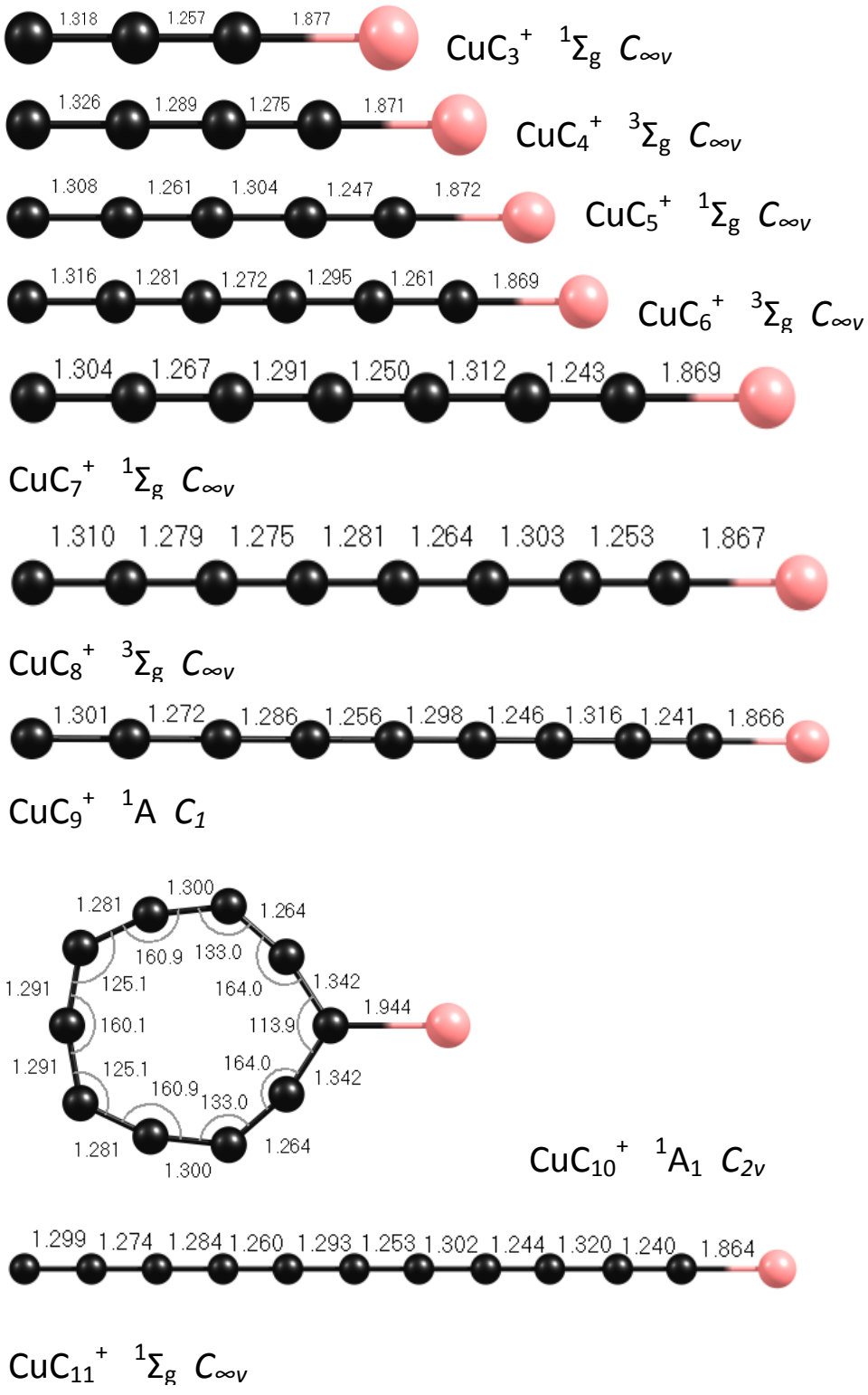

Figure 4.9: Predicted structures of the lowest energy isomers of copper carbide clusters $CuC_{3\text{-}11}^{+}$ using DFT (B3LYP functional with 6-311+G(d,p) basis set on carbon and LanL2DZ basis set on copper

a linear carbon chain with a copper atom attached to the end. In all of the species studied the metal carbon bond is the longest bond in the cluster, on the order of 1.87 Å. This is very close to the bond lengths found for the metal-carbon bonds in the V, Pt, and Pd carbides, all of which were 1.85 – 2.0 Å.[70,80]

An even – odd alternation is present in the both the structures and the multiplicities of the linear clusters. The odd numbered ones are $^1\Sigma_g$ states (1/9 is ^{1}A), while the even numbered ones are all $^3\Sigma_g$ states. The odd numbered species show acetylenic (·C≡C–C···C≡C·) type bonding with alternating longer and shorter bonds along the carbon chain. The even numbered clusters, however, show more cumulenic (:C=C···C=C:) type bonding with a considerably smaller alternation in bond lengths between carbon atoms. The two exceptions to the lowest energy isomer being linear are the 1/9, which is slightly bent (C_1 symmetry), and the 1/10. The 1/10 notablely favors a closed carbon ring structure with the copper bound to a single carbon by 20.64 kcal/mol over the linear chain isomer. This closed ring structure is a $^1A_1$ state with C_{2v} symmetry. In the terminology of Hall and co-workers, which we have adopted here, this is called the one-carbon ring.[80] As noted above, the C_{10} cluster has been repeatedly seen to be more stable as a cyclic ring rather than a linear chain,[6,7,116] so finding the 1/10 cluster here to favor a cyclic structure is not surprising.

Trends can also be seen when examining the lowest energy cyclic structures, which are found, with the notable exception of the 1/10 cluster, to be higher in energy than the linear isomers. However, even with cooling from the supersonic expansion, high internal energies of 1 eV or more are still possible, especially in smaller species where internal energy may not be efficiently quenched. Thus examining the higher energy

cyclic isomers is still useful, and indeed even - odd alternations are seen in the lowest energy cyclic isomers of copper carbides as well. Examining only the even clusters, starting with the 1/4 and continuing through the 1/10, the lowest energy cyclic isomer is always the one-carbon ring. The 1/4 is a $^3A_1$ state and the 1/6 is a $^1A_1$, both with C_{2v} symmetry, the 1/8 is a $^1A'$ state, with C_s symmetry, and the 1/10 is a $^1A_1$ state with C_{2v} symmetry. The metal – carbon bond lengths in all of these species are on the order of 1.91 – 1.93 Å. The 1/3 cluster size appears to lie outside the observed even odd trend, and the only stable cyclic isomer is the one-carbon ring, a $^3A'$ state with C_s symmetry. For the odd clusters larger than the 1/3, however, the lowest energy cyclic isomer is the open ring, which corresponds to the metal inserted into a carbon ring. The metal - carbon bonds are much longer than the carbon - carbon bonds, as expected, and range in length from 1.881 Å for the 1/11 to 2.062 Å for the 1/5. For the 1/5, 1/9, and 1/11 clusters, the open ring isomer is a $^1A_1$ state, while the 1/7 is a $^1A'$ state. Additionally, even though the 1/11 is found to be more stable as a linear chain, the open ring isomer is only 8.75 kcal/mol higher in energy, by far the smallest linear – cyclic energy difference of any of the species studied. This is most likely due to the increased size of the cluster reducing the ring strain in the cyclic isomer.

While these computations show interesting differences between the even and odd numbered clusters for both the linear and cyclic isomers, and the photodissociation data do indeed show remarkable differences in the fragmentation patterns for even and odd numbered clusters, the structures themselves do not necessarily reveal the source of the differences in fragmentation behavior. To gain more insight into this issue, copper – carbon dissociation energies were computed for the linear isomers for the 1/3 - 1/6. The

results here also display a rather dramatic even odd alternation and do in fact help to explain the fragmentation data. The 1/3 and 1/5 were found to have a metal – carbon dissociation energy of 2.35 eV and 2.87 eV respectively. This is well below the expected carbon – carbon bond energy, which is 5 – 7 eV depending on the cluster size. Thus the fragmentation of these speciess by the loss of copper ion, which we observe, is in agreement with the theory. For the 1/4 and 1/6, however, the metal – carbon dissociation energies are calculated to be 7.00 eV and 7.21 eV, respectively. When compared to the dissociation energies for pure carbon clusters (5 - 7 eV), the observed loss of C_3 from the even numbered speciess to leave behind mixed carbon metal cationic fragments makes sense. This, combined with the fact that C_3 loss from an even numbered cluster leaves behind the 1/3, 1/5, 1/7, or 1/9 species which are seen as stable in the mass spectrum, satisfactorily explains the even odd alternation in fragmentation patterns observed in this experimental investigation.

4.5 CONCLUSIONS

Copper and gold carbide cluster cations produced by laser vaporization have been investigated with time-of-flight mass spectrometry, mass-selected photodissociation, and density functional theory. The mass spectral data for the copper carbides is extremely different from that seen previously for pure carbon clusters. Here a dramatic alternation in cluster intensities is seen, and species with an odd number of carbon atoms are much more abundant. This is possibly due to a higher level of reactivity for the singlet ground states of the odd cluster sizes as compared to the triplet ground states in the even clusters.

The mass spectrum of the gold carbides show drops in ion intensity after clusters with 3, 6, 9, and 12 carbons, suggesting they have enhanced stability.

The photodissociation data for the copper carbides also shows differences between even and odd clusters. For the small sizes, the odd numbered species fragment by loss of the entire neutral carbon cluster, while the even numbered species show significant loss of C_3 to leave behind mixed metal carbide charged fragments. The stoichiometries of these fragments correspond to the odd numbered clusters observed to be abundant in the mass spectrum. This even odd alternation in fragmentation behavior is observed, in varying degrees, in clusters as large as 1/30. The gold carbide fragmentation closely follows that of the copper carbides, with the even species favoring loss of C_3 to leave mixed fragments and the odd species favoring the loss of the entire intact carbon cluster. For larger carbides of both copper and gold, the IPs of some carbon cluster fragments are low enough that upon dissociation they keep the charge and a neutral metal is lost. The structures of certain carbon fragments can then be identified based on comparisons to the known IPs of the linear and cyclic isomers. Loss of C_2 is never seen as a fragmentation channel for any of the clusters studied here, indicating that fullerene formation is not occurring, even in the largest cluster sizes.

DFT calculations were conducted to investigate the various isomers possible for the copper carbide clusters of the size 1/3 – 1/11. The results showed that the ground state for all the clusters, with the notable exception of 1/10, was a linear carbon chain with the copper on the end. The computations also showed even odd alternations in the electronic structure, as the linear isomers of the even species were all triplets, while the odd species were all singlets. Examination of the lowest lying cyclic isomers also showed

an even odd difference. The even clusters all formed a one-carbon ring, in which the copper is attached to a single carbon of a closed carbon ring. The overall ground state of the 1/10 cluster was found to be the one-carbon ring. The odd clusters, on the other hand, all had an open ring structure, in which the metal is incorporated into the ring, as the lowest energy cyclic isomer.

Metal – carbon dissociation energies were calculated for the linear 1/3 – 1/6 species, and a dramatic difference between the even and odd clusters was seen. The odd ones have metal- carbon dissociation energies less than 3 eV, while the even ones have dissociation energies 7.00 eV and greater. This enormous difference in dissociation energy explains the alternation observed in the photodissociation data. For the odd clusters, breaking the metal – carbon bond is a lower energy process than breaking a carbon – carbon bond, so this fragmentation channel is favored. For the even numbered clusters, however, the metal – carbon bond is evidently much stronger. Breaking a carbon – carbon bond in these species is energetically competitive with or even favored over breaking the metal – carbon bond. Additionally, C_3 elimination from an even cluster leaves behind an odd numbered mixed fragment, which were suggested by the mass spectral data to be more stable. These two factors combined explain the differences in the observed fragmentation channels. The measurement of infrared spectra for both carbon and carbide cluster cations would be very useful in confirming the structures proposed here and may lead to further insight into of the effect of noble metal doping on the structures of carbon clusters.

Table 4.1: The stoichiometries of major noble metal carbide cluster photofragments ($M_nC_m^+$ = *n/m*) detected using 355 nm. The fragments listed in bold were the most prominent.

Parent Cation Cluster	**Fragment Ions**	
	Cu	**Au**
1/3	**Cu^+**	**Au^+**
1/4	**Cu^+**	**Au^+**
1/5	**Cu^+**	**Au^+**
1/6	1/3, **Cu^+**	**1/3**, Au^+
1/7	**Cu^+**	1/4, **Au^+**, 0/7
1/8	1/5, 1/3, **Cu^+**	**1/5**, 1/3, 1/0, 0,8
1/9	**Cu^+**	1/6, 1/3, **Au^+**, 0/9, 0/7, 0/6, 0/5
1/10	1/7, **1/5**, Cu^+	
1/11	1/8, **0/11**, Cu^+	
1/12	**1/9**, 1/7, 0/12, 0/11, Cu^+	
1/13	1/10, **0/13**, 0,10, Cu^+	
1/14	1/11, **0/14**, 0/11, Cu^+	
1/15	1/12, **0/15**, 0/12, Cu^+	
1/16	**1/13**, 1/11, 0/16, 0/11, Cu^+	
1/18	1/15, **0/18**, 0/15, 0,13, Cu^+	
1/20	1/17, **0/20**, 0/19, 0/18, 0/17, 0/15, Cu^+	
1/27	**0/27**, 0/24, 0/22, 0/19, 0/18, 0/16, 0/15, 0/14, 0/11	
1/28	1/25, **0/28**, 0/25, 0/23, 0/19, 0/15	
1/30	1/27, **0/30**, 0/28 - 0/14	
1/36	0/36, 0/31, 0/23 – 0/10 (**0/15 most intense**)	
1/43	0/43, 0/40, 0/38, 0/27, 0/23 – 0/10 (**0/19, 0/15 most intense**)	

4.6 REFERENCES

(1) Oyama, S. T., Ed. *The Chemistry of Transition Metal Carbides and Nitrides***;** Blackie: Glasgow, 1996.

(2) Oyama, S. T. *Catal. Today* **1992**, *15*, 179.

(3) Johansson, L. I. *Surf. Sci. Rep.* **1995**, *21*, 177.

(4) Furimsky, E. *App. Catal. A* **2003**, *240*, 1.

(5) Cataldo, F. *Int. J. Astrobiol.* **2003**, *2*, 51.

(6) Weltner, Jr., W.; Van Zee, R. J. *Chem. Rev.* **1994**, *89*, 1713.

(7) Van Orden, A.; Saykally, R. J. *Chem. Rev*. **1998**, *98*, 2313.

(8) (a) Guo, B. C.; Kerns, K. P.; Castleman, A. W. Jr. *Science* **1992**, *255*, 1411. (b) Guo, B. C.; Wei, S.; Purnell, J.; Buzza, S.; Castleman, A. W. Jr. *Science* **1992**, *256*, 515. (c) Wei, S.; Guo, B. C.; Purnell, J.; Buzza, S.; Castleman, A. W. Jr. *Science* **1992**, *256*, 818. (d) Guo, B. C.; Castleman, A. W. Jr. *Advances in Metal and Semiconductor Clusters*; JAI Press: London, 1994; Vol. 2. (e) Leskiw, B. D.; Castleman, A. W. Jr. *C. R. Physique* **2002**, *3*, 251.

(9) (a) Pilgrim, J. S.; Duncan, M. A. *J. Am. Chem. Soc.* **1993**, *115*, 6958. (b) Pilgrim, J. S.; Duncan, M. A. *J. Am. Chem. Soc.* **1993**, *115*, 9724. (c) Pilgrim, J. S.; Duncan, M. A. *Advances in Metal and Semiconductor Clusters*; JAI Press: London, 1995; Vol. 3. (d) Duncan, M. A. *J. Clust. Sci* **1997**, *8*, 239.

(10) (a) Yeh, C. S.; Afzaal, S.; Lee, S. A.; Byun, Y. G.; Freiser, B. S. *J. Am. Chem. Soc.* **1994**, *116*, 8806. (b) Yeh, C. S.; Byun, Y. G.; Afzaal, S.; Kan, S. Z.; Lee, S.; Freiser, B. S.; Hay, P. J. *J. Am. Chem. Soc.* **1995**, *117*, 4042. (c) Byun, Y. G.;

Yeh, C. S.; Xu, Y. C.; Freiser, B. S. *J. Am. Chem. Soc.* **1995**, *117*, 8299. (d) Byun, Y. G.; Lee, S. A.; Kan, S. Z.; Freiser, B. S. *J. Phys. Chem* **1996**, *100*, 14281.

(11) Rohmer, M. M.; Benard, M. *Chem. Rev.* **2000**, *100*, 495.

(12) (a) Weiss, F. D.; Elkind, J. L.; O'Brien, S. C.; Curl, R. F.; Smalley, R. E. *J. Am. Chem. Soc.* **1988**, *110*, 4464. (b) Chai, Y.; Guo, T.; Jin, C.; Haufler, R. E.; Chibante, L. P. F.; Fure, J.; Wang, L.; Alford, J. M.; Smalley, R. E. *J. Phys. Chem.* **1991**, *95*, 7564.

(13) McElvany, S. W. *J. Phys. Chem.* **1992**, *96*, 4935.

(14) Roth, L. M.; Huang, Y.; Schwedler, J. T.; Cassady, C. J.; Ben-Amotz, D.; Kahr, B.; Freiser, B. S. *J. Am. Chem. Soc.* **1991**, *113*, 6298.

(15) Balch, A. L.; Olmstead, M. M. *Chem. Rev.* **1998**, *98*, 2123.

(16) Lee, K.; Song, H.; Park, J. T. *Acc. Chem. Res.* **2003**, *36*, 78.

(17) Clemmer, D. E.; Hunter, J. M.; Shelimov, K. B.; Jarrold, M. F. *Nature* **1994**, *372*, 248.

(18) Chupka, W. A.; Berkowitz, J.; Giese, C. F.; Inghram, M. G. *J. Phys. Chem.* **1958**, *62*, 611.

(19) De Maria, G.; Guido, M.; Malaspina, L.; Pesce, B. *J. Chem. Phys.* **1965**, *43*, 4449.

(20) Vander Auwera-Mahieu, A.; Drowart, J. *Chem. Phys. Lett.* **1967**, *1*, 311.

(21) Kohl, F. J.; Stearns, C. A. *J. Phys. Chem.* **1970**, *74*, 2714.

(22) (a) Haque, R.; Gingerich, K. A. *J. Chem. Phys.* **1981**, *74*, 6407. (b) Gupta, S. K.; Nappi, B. M.; Gingerich, K. A. *J. Phys. Chem.* **1981**, *85*, 971. (c) Pelino, M.;

Haque, R.; Bencivenni, L.; Gingerich, K. A. *J. Chem. Phys.* **1988**, *88*, 6534. (d) Meloni, G.; Thomson, L. M.; Gingerich, K. A. *J. Chem. Phys.* **2001**, *115*, 4496.

(23) (a) Leleyter, M.; Ortoli, S.; Joyes, P. *Sur. Sci.* **1981**, *106*, 293. (b) Leleyter, M.; Joyes, P. *Sur. Sci.* **1985**, *156*, 800. (c) Leleyter, M. *J. Phys. II France* **1991**, *1*, 1179.

(24) (a) Pilgrim, J. S.; Duncan, M. A. *J. Am. Chem. Soc.* **1993**, *115*, 4395. (b) Pilgrim, J. S.; Duncan, M. A. *Int. J. Mass Spect. Ion Proc.* **1994**, *138*, 283. (c) Pilgrim, J. S.; Brock, L. R.; Duncan, M. A. *J. Phys. Chem* **1995**, *99*, 544.

(25) (a) Kerns, K. P.; Guo, B. C.; Deng, H. T.; Castleman, A. W. Jr. *J. Chem. Phys.* **1994**, *101*, 8529. (b) Kerns, K. P.; Guo, B. C.; Deng, H. T.; Castleman, A. W. Jr. *J. Phys. Chem.* **1996**, *100*, 16821.

(26) (a) Wei, S.; Guo, B. C.; Purnell, J.; Buzza, S. A.; Castleman, A. W. Jr. *J. Phys. Chem.* **1993**, *97*, 9559. (b) Purnell, J.; Wei, S.; Castleman, A. W. Jr. *Chem. Phys. Lett.* **1994**, *229*, 105. (c) Stairs, J. R.; Davis, K. M.; Castleman, A. W. Jr. *J. Chem. Phys.* **2002**, *117*, 4371.

(27) (a) Bowers, M. T. *Acc. Chem. Res.* **1994**, *27*, 324. (b) Lee, S.; Gotts, N. G.; von Helden, G.; Bowers, M. T. *Science* **1995**, *267*, 999.

(28) (a) Wang, L. S.; Li, S.; Wu, H. *J. Phys. Chem.* **1996**, *100*, 19211. (b) Li, S.; Wu, H.; Wang, L. S. *J. Am. Chem. Soc.* **1997**, *119*, 7417.

(29) Zhang, Q.; Lewis, S. P. *Chem. Phys. Lett.* **2003**, *372*, 836.

(30) (a) Hou, H.; Muckerman, J. T.; Liu, P.; Rodriguez, J. A. *J. Phys. Chem. A* **2003**, *107*, 9344. (b) Liu, P.; Rodriguez, J. A. *J. Chem. Phys.* **2003**, *120*, 5414. (c) Liu, P.; Rodriguez, J. A.; Muckerman, J. T. *J. Chem. Phys.* **2004**, *121*, 10321.

(31) Martinez, J. I.; Castro, A.; Rubio, A.; Poblet, J. M.; Alonso, J. A. *Chem. Phys. Lett.* **2004**, *389*, 292.

(32) (a) Varganov, S. A.; Gordon, M. S. *Chem. Phys.* **2006**, *326*, 97. (b) Varganov, S. A.; Dudley, T. J.; Gordon, M. S. *Chem. Phys. Lett.* **2006**, *429*, 49.

(33) (a) van Heijnsbergen, D.; von Helden, G.; Duncan, M. A.; van Roij, A. J. A.; Meijer, G. *Phys. Rev. Lett.* **1999**, *83*, 4983. (b) von Helden, G.; van Heijnsbergen, D.; Duncan, M. A.; Meijer, G. *Chem. Phys. Lett.* **2001**, *333*, 350. (c) van Heijnsbergen, D.; Duncan, M. A.; Meijer, G.; von Helden, G. *Chem. Phys. Lett.* **2001**, *349*, 220.

(34) von Helden, G.; Tielens, A. G. G. M.; van Heijnsbergen, D.; Duncan, M. A.; Hony, S.; Waters, L. B. F. M.; Meijer, G. *Science* **2000**, *288*, 313.

(35) Yamada, Y.; Castleman, A. W. Jr. *Chem. Phys. Lett.* **1993**, *204*, 133.

(36) Jin, C.; Haufler, R. E.; Hettich, R.L.; Barshick, C. M.; Compton, R. N.; Puretzky, A. A.; Dem'yanenko, A. V.; Tuinman, A. A. *Science* **1994**, *263*, 68.

(37) Dietze, H. J.; Becker, S. *Int. J. Mass Spectrom. and Ion Process*. **1988**, *82*, 47.

(38) (a) Teghil, R.; Giardini-Guidoni, A.; Piccirillo, S.; Mele, A.; Polla-Mattiot, F. *Appl. Sur. Sci.* **1990**, *46*, 220. (b) Mele, A.; Giardini-Guidoni, A.; Teghil, R. *Proc. Indian Acad. Sci. (Chem. Sci.)* **1993**, *105*, 715. (c) Teghil, R.; D'Alessio, L.; Zaccagnino, M.; Marotta, V.; Ferro, D.; De Maria, G. *Appl. Sur. Sci.* **2001**, *173*, 233.

(39) (a) McElvany, S. W.; Cassady, C. J. *J. Phys. Chem.* **1990**, *94*, 2057. (b) Cassady, C. J.; McElvany, S. W. *J. Am. Chem. Soc.* **1990**, *112*, 4788.

(40) Reddic, J. E.; Duncan, M. A. *Chem. Phys. Lett.* **1997**, *264*, 157.

(41) Gibson, J. K. *J. Vac. Sci. Technol. A* **1998**, *16*, 653.

(42) Zhang, R.; Achiba, Y.; Fisher, K. J.; Gadd, G. E.; Hopwood, F. G.; Ishigaki, T.; Smith, D. R.; Suzuki, S.; Willett, G. D. *J. Phys. Chem. B.* **1999**, *103*, 9450.

(43) Belau, L.; Wheeler, S. E.; Ticknor, B. W.; Ahmed, M.; Leone, S. R.; Allen, W. D.; Schaefer, H. F. III; Duncan, M. A. *J. Am. Chem. Soc.* **2007**, *129*, 10229.

(44) (a) Clemmer, D. E.; Shelimov, K. B.; Jarrold, M. F. *J. Am. Chem. Soc.* **1994**, *116*, 5971. (b) Clemmer, D. E.; Jarrold, M. F. *J. Am. Chem. Soc.* **1994**, *116*, 8841. (c) Shelimov, K. B.; Clemmer, D. E.; Jarrold, M. F. *J. Phys. Chem.* **1995**, *99*, 11376. (d) Shelimov, K. B.; Jarrold, M. F. *J. Phys. Chem.* **1995**, *99*, 17677. (e) Shelimov, K. B.; Jarrold, M. F. *J. Am. Chem. Soc.* **1996**, *118*, 1139. (f) Shelimov, K. B.; Clemmer, D. E.; Jarrold, M. F. *J. Chem. Soc., Dalton Trans.* **1996**, *5*, 567.

(45) (a) Steimle, T. C.; Jung, K. Y.; Li, B. –Z. *J. Chem. Phys.* **1995**, *102*, 5937. (b) Beaton, S. A.; Steimle, T. C. *J. Chem. Phys.* **1999**, *111*, 10876,

(46) Balfour, W. J.; Cao, J.; Prassad, C. V. V.; Qian, C. X. W. *J. Chem. Phys.* **1995**, *103*, 4046.

(47) Barnes, M.; Merer, A. J.; Metha, G. F. *J. Chem. Phys.* **1995**, *103*, 8360.

(48) Adam, A. G.; Peers, J. R. D. *J. Mol. Spec.* **1997**, *181*, 24.

(49) (a) Brugh, D. J.; Morse, M. D. *J. Chem. Phys.* **1997**, *107*, 9772. (b) Brugh, D. J.; Ronningen, T. J.; Morse, M. D. *J. Chem. Phys.* **1998**, *109*, 7851. (c) Langenberg, J. D.; DaBell, R. S.; Shao, L.; Dreessen, D.; Morse, M. D. *J. Chem. Phys.* **1998**, *109*, 7863. (d) Langenberg, J. D.; Shao, L.; Morse, M. D. *J. Chem. Phys.* **1999**, *111*, 4077. (e) Sickafoose, S. M.; Smith, A. W.; Morse, M. D. *J. Chem. Phys.* 2002, **116**, 993. (f) Brugh, D. J.; Morse, M. D. *J. Chem. Phys.* **2002**, *117*, 10703.

(g) Lindholm, N. F.; Hales, D. A.; Ober, L. A.; Morse, M. D. *J. Chem. Phys.* **2004**, *121*, 6855.

(50) DaBell, R. S.; Meyer, R. G.; Morse, M. D. *J. Chem. Phys.* **2001**, *114*, 2938.

(51) (a) Allen, M. D.; Pesch, T. C.; Ziurys L. M. *Ap. J.* **1996**, *472*, L57. (b) Brewster, M. A.; Ziurys, L. M. *Astrophys. J.* **2001**, *559*, L163. (c) Sheridan, P. M.; Ziurys, L. M.; Hirano, T. *Astrophys. J.* **2003**, *593*, L141.

(52) (a) Robbins, D. L.; Rittby, C. M. L.; Graham, W. R. M. *J. Chem. Phys.* **2001**, *114*, 3570. (b) Robbins, D. L.; Chen, K. C.; Rittby, C. M. L.; Graham, W. R. M. *J. Chem. Phys.* **2004**, *120*, 4664. (c) Gonzalez, E.; Rittby, C. M. L.; Graham, W. R. M. *J. Chem. Phys.* **2006**, 125, 044550. (d) Bates, S. A.; Rittby, C. M. L.; Graham, W. R. M. *J. Chem. Phys.* **2006**, 125, 074506. (e) Kinzer, R. E. Jr.; Rittby, C. M. L.; Graham, W. R. M. *J. Chem. Phys.* **2006**, 125, 074531. (f) Bates, S. A.; Rhodes, J. A.; Rittby, C. M. L.; Graham, W. R. M. *J. Chem. Phys.* **2007**, *127*, 064506. (g) Kinzer, R. E.; Rittby, C. M. L.; Graham, W. R. M. *J. Chem. Phys.* **2008**, *128*, 064312.

(53) (a) Heaven, M. W.; Stewart, G. M.; Buntine, M. A.; Metha, G. F. *J. Phys. Chem. A* **2000**, *104*, 3308. (b) Dryza, V.; Addicoat, M. A.; Gascooke, J. R.; Buntine, M. A.; Metha, G. F. *J. Phys. Chem. A* **2005**, *109*, 11180.

(54) (a) Wang, X. B.; Ding, C. F.; Wang, L. S. *J. Phys. Chem.* A **1997**, *101*, 7699. (b) Li X.; Wang, L. S. *J. Chem. Phys.* **1999**, *111*, 8389. (c) Wang, L. S.; Li, X. *J. Chem. Phys.* **2000**, *112*, 3602. (d) Zhai, H. J.; Wang, L. S.; Jena, P.; Gutsev, G. L.; Bauschlicher, C. W. Jr. *J. Chem. Phys.* **2004**, *120*, 8996. (e) Alexandrova, A. N.; Boldyrev, A. I.; Zhai, H. J.; Wang, L. S. *J. Phys. Chem. A* **2005**, *109*, 562.

(55) (a) Suzuki, S.; Kohno, M.; Shiromaru, H.; Achiba, Y.; Kietzmann, H.; Kessler, B.; Gantefor, G.; Eberhardt, W. *Z. Phys. D* **1997,** *40*, 407. (b) Kohno, M.; Suzuki, S.; Shiromaru, H.; Kobayashi, K.; Nagase, S.; Achiba, Y.; Kietzmann, H.; Kessler, B.; Gantefor, G.; Eberhardt, W. *J. Electron Spec. and Rel. Phen.* **2000,** *112*, 163.

(56) Tono, K.; Terasaki, A.; Ohta, T.; Kondow, T. *J. Chem. Phys.* **2002**, *117*, 7010.

(57) Knappenberger, K. L. Jr.; Jones, C. E. Jr.; Sobhy, M. A.; Iordanov, I.; Sofo, J.; Castleman, A. W. Jr. *J. Phys. Chem. A* **2006**, *110*, 12814.

(58) von Helden, G.; Gotts N. G.; Maitre, P.; Bowers, M. T. *Chem. Phys. Lett.* **1994** *227*, 601.

(59) Roszak,S.; Majumdar, D.; Balasubramanian, K. *J. Chem. Phys.* **2002**, *116*, 10238.

(60) (a) Redondo, P.; Barrientos, C.; Largo, A. J. *Phys. Chem. A* **2005**, *109*, 8594. (b) Redondo, P.; Barrientos, C.; Largo, A. *J. Phys. Chem. A* **2006**, *110*, 4057.

(61) Strout, D. L.; Hall, M. B. *J. Phys. Chem*. **1996**, *100*, 18007.

(62) Puzzarini, C.; Peterson, K.A. *J. Chem. Phys.* **2005**, *122*, 084323.

(63) Roszak, S.; Balasubramanian, K. *J. Chem. Phys.* **1997**, *106*, 158.

(64) Strout, D. L.; Hall, M. B. *J. Phys. Chem. A* **1998**, *102*, 641.

(65) (a) Sumathi, R; Hendrickx, M. *J. Phys. Chem. A* **1998**, *102*, 7308. (b) Sumathi, R.; Hendrickx, M. *J. Phys. Chem. A* **1998**, *102*, 4883.

(66) Bauschlicher, C. W. Jr. *Theor. Chem. Acc*. **2003**, *110*, 153.

(67) (a) Rayón, V. M.; Redondo, P.; Barrientos, C.; Largo, A. *Chem. Phys. Lett.* **2006**, *422*, 289. (b) Largo, L.; Cimas, A.; Redondo, P.; Rayón, V. M.; Barrientos, C. *Chem. Phys.* **2006**, *330*, 431.

(68) Sosa, R. M.; Gardiol, P.; Beltrame, G. *Int. J. Quantum Chem.* **1997**, *65*, 919.

(69) Majumdar, D.; Roszak, S.; Balasubramanian, K. *J. Chem. Phys.* **2003**, *118*, 130.

(70) (a) Redondo, P.; Barrientos, C.; Largo, A. *J. Chem. Theory Comput.* **2006**, *2*, 885. (b) Redondo, P.; Barrientos, C.; Largo, A. *J. Mol. Struct. (THEOCHEM)* **2006**, *769*, 225. (c) Redondo, P.; Barrientos, C.; Largo, A. *Int. J. Mass Spectrom.* **2007**, *263*, 101.

(71) (a) Dai, D.; Roszak, S.; Balasubramanian, K. *J. Phys. Chem.* **2000**, *104*, 5861. (b) Dai, D.; Roszak, S.; Balasubramanian, K. *J. Phys. Chem.* **2000**, *104*, 9760.

(72) Harris, H.; Dance, I. *J. Phys. Chem. A* **2001**, *105*, 3340.

(73) Noya, E. G.; Longo, R. C.; Gallego, L. J. *J. Chem. Phys.* **2003**, *119*, 11130.

(74) Ryzhkov, M.; Ivanovskii, A. L.; Delley, B. T. *Chem. Phys. Lett.* **2005**, *404*, 400.

(75) Harris, H. H.; Dance, I. G. *Polyhedron* **2007**, *26*, 250.

(76) Arbuznikov, A. V.; Hendrickx, M. *Chem. Phys. Lett.* **2000**, *320*, 575.

(77) Froudakis, G. E.; Mühlhäuser, M.; Andriotis, A. N.; Menon, M. *Phys. Rev. B* **2001**, *64*, 241401.

(78) Longo, R. C.; Alemany, M. M. G.; Fernández, B.; Gallego, L. J. *Phys. Rev. B* **2003**, *68*, 167401.

(79) Roszak, S.; Balasubramanian, K. *J. Chem. Phys.* **1997**, *106*, 4008.

(80) (a) Strout, D. L.; Miller III, T. F.; Hall, M. B. *J. Phys. Chem. A* **1998**, *102*, 6307. (b) Miller III, T. F.; Hall, M. B. *J. Am. Chem. Soc* **1999**, *121*, 7389.

(81) Barrientos, C.; Redondo, P.; Largo, A. *J. Chem. Theory Comput.* **2007**, *3*, 657.

(82) Gutsev, G. L.; Andrews, L.; Bauschlicher, C. W. Jr. *Theor. Chem. Acc.* **2003**, *109*, 298.

(83) Harrison, J. F. *Chem. Rev.* **2000**, *100*, 679.

(84) (a) Wang, J.; Sun, X.; Wu, Z. *Chem. Phys. Lett.* **2006**, *426*, 141. (b) Wang, J.; Sun, X.; Wu, Z. *J. Cluster Sci.* **2006**, *426*, 141.

(85) (a) Rayón, V. M.; Redondo, P.; Barrientos, C.; Largo, A. *Chem. Eur. J.* **2006**, 12, 6963. (b) Rayón, V. M.; Redondo, P.; Barrientos, C.; Largo, A. *J. Phys.Chem. A.* **2007**, *111*, 6345.

(86) Dance, I. J. *Am. Chem. Soc.* **1993**, *115*, 11052.

(87) Li, S. F.; Xue, X.; Jia, Y.; Zhao, G.; Zhang, M.; Gong, X. G. *Phys. Rev. B.* **2006**, *73*, 165401.

(88) (a) Barysz, M.; Pyykkö, P. *Chem. Phys. Lett.* **1998**, *285*, 398. (b) Pyykkö, P.; Patzschke, M.; Suupere, J. *Chem. Phys. Lett.* **2003**, *381*, 45. (c) Pyykkö, P. *Angew. Chem. Int. Ed.* **2004**, *43*, 4412. (d) Pyykkö, P. *Inorg. Chim. Acta* **2005**, *358*, 4113.

(89) Puzzarini, C.; Peterson, K. A. *Chem. Phys.* **2005**, *311*, 177.

(90) Naumkin, F. Phys. *Chem. Chem. Phys.* **2006**, *8*, 2539.

(91) Rohlfing, E. A.; Cox, D. M.; Kaldor, A. *J. Chem. Phys.* **1984**, *81*, 3322.

(92) (a) Kroto, H. W.; Heath, J. R.; O'Brien, S. C.; Curl, R. F.; Smalley, R. E. *Nature* **1985**, *318*, 162. (b) Curl, R. F.; Smalley, R. E. *Science* **1988**, *242*, 1017.

(93) Hahn, M. Y.; Honea, E. C.; Paguia, A. J.; Schriver, K. E.; Camarena, A. M.; Whetten, R. L. *Chem. Phys. Lett.* **1986**, *130*, 12.

(94) Rohlfing, E. A. *J. Chem. Phys.* **1990**, *93*, 7851.

(95) (a) Kaizu, K.; Kohno, M.; Suzuki, S.; Shiromaru, H.; Moriwaki, T.; Achiba, Y. *J. Chem. Phys.* **1997**, *106*, 9954. (b) Moriwaki, T.; Kobayashi, K.; Osaka, M.; Ohara, M.; Shiromaru, H.; Achiba, Y. *J. Chem. Phys.* **1997**, *107*, 8927.

(96) Choi, Y.-K.; Im, H.-S.; Jung, K.-W. *Int. J. Mass Spectrom.* **1999**, *189*, 115.

(97) (a) Wakabayashi, T.; Momose, T.; Shida, T. *J. Chem. Phys.* **1999**, *111*, 6260. (b) Kato, Y.; Wakabayashi, T.; Momose, T. *J. Chem. Phys.* **2003**, *118*, 5390.

(98) Bae, C. H.; Park, S. M. *J. Chem. Phys.* **2002**, *117*, 5347.

(99) (a) Geusic, M. E.; Jarrold, M. F.; McIlrath, T. J.; Bloomfield, L. A.; Freeman, R. R.; Brown, W. L. *Z. Phys. D: At., Mol. Clusters* **1986,** 3, 309. (b) Geusic, M. E.; McIlrath, T. J.; Jarrold, M. F.; Bloomfield, L. A.; Freeman, R. R.; Brown, W. L. *J. Chem. Phys.* **1986,** 84, 2421. (c) Geusic, M. E.; Jarrold, M. F.; McIlrath, T. J.; Freeman, R. R.; Brown, W. L. *J. Chem. Phys.* **1987,** 86, 3862.

(100) O'Brien, S. C.; Heath, J. R.; Curl, R. F.; Smalley, R. E. *J. Chem. Phys.* **1988**, *88*, 220.

(101) Sowa, M. B.; Hintz, P. A.; Anderson, S. L. *J. Chem. Phys.* **1991**, *95*, 4719.

(102) Bouyer, R.; Roussel, F.; Monchicourt, P.; Perdix, M.; Pradel, P. *J. Chem. Phys.* **1994,** 100, 8912.

(103) (a) Pozniak, B.; Dunbar, R. C. *Int. J. Mass Spectrom. Ion Processes* **1994**, *133*, 97. (b) Pozniak, B. P.; Dunbar, R. C. *Int. J. Mass Spectrom. Ion Processes* **1997,** 165/166, 29.

(104) Sowa-Resat, M. B.; Hintz, P. A.; Anderson, S. L. *J. Phys. Chem.* **1995**, *99*, 10736.

(105) (a) Radi, P. P.; Bunn, T. L.; Kemper, P. R.; Molchan, M. E.; Bowers, M. T. *J. Chem. Phys.* **1988**, *88*, 2809. (b) Radi, P. P.; Hsu, M. T.; Brodbelt-Lustig, J.; Ricon, M.; M. E.; Bowers, M. T. *J. Chem. Phys.* **1990**, *92*, 4817.

(106) (a) Gluch, K.; Matt-Leubner, S.; Echt, O.; Concina, B.; Scheier, P.; Mark, T. D. *J. Chem. Phys.* **2004**, *121*, 2137. (b) Concina, B.; Gluch, K.; Matt-Leubner, S.; Echt, O.; Scheier, P.; Mark, T. D. *Chem. Phys. Lett.* **2005**, *407*, 464.

(107) (a) France, M. R.; Buchanan, J. W.; Robinson, J. C.; Pullins, S. H.; Tucker, J. L.; King, R. B.; Duncan, M. A. J. *Phys. Chem. A* **1997**, *101*, 6214. (b) Molek, K. S.; Jaeger, T. D.; Duncan, M. A. J. Chem. Phys. 2005, 123, 144313. (c) Molek, K. S.; Reed, Z. M.; Ricks, A. M.; Duncan, M. A. *J. Phys. Chem. A* **2007**, *111*, 8080. (d) Reed, Z. A.; Duncan, M. A. *J. Phys. Chem. A*, in press. (e) Molek, K. S.; Anfuso-Cleary, C.; Duncan, M. A. *J. Phys. Chem. A*, in press.

(108) Ticknor, B. W.; Duncan, M. A. *Chem. Phys. Lett.* **2005**, *405*, 214.

(109) Jaeger, J. B.; Jaeger, T. D.; Duncan, M. A. *J. Phys. Chem. A.* **2006**, *110*, 9310.

(110) Frisch, M. J. et al., *Gaussian 03 (Revision B.02)*; Gaussian, Inc.: Pittsburgh, PA, 2003.

(111) Becke, A. D. *J. Chem. Phys.* **1993**, *98*, 5648.

(112) Lee, C.; Yang, W.; Parr, R. G. *Phys. Rev. B* **1988**, *37*, 785.

(113) Krishnan, R.; Binkley, J. S.; Seeger, R.; Pople, J. A. *J. Chem. Phys.* **1980**, *72*, 650.

(114) Dunning, T.H.; Hay, P. J. *Methods of Electronic Structure Theory*, Vol. 2, H. F. Schaefer, ed., Plenum Press, **1977**.

(115) (a) Hay, P. J.; Wadt, W. R. *J. Chem. Phys.* **1985,** *82*, 270. (b) Hay, P. J.; Wadt, W. R. *J. Chem. Phys.* **1985,** *82*, 284. (c) Hay, P. J.; Wadt, W. R. *J. Chem. Phys.* **1985,** *82*, 299.

(116) von Helden, G.; Hsu, M. T.; Gotts, N.; Bowers, M. T. *J. Phys. Chem.* **1993**, *97*, 8182.

(117) Raghavachari, K.; Binkley, J. S. *J. Chem. Phys.* **1987**, *87*, 2191.

(118) Lias, S. G. "Ionization Energy Evaluation" in *NIST Chemistry WebBook*, NIST Standard Reference Database Number 69, Eds. P.J. Linstrom and W.G. Mallard, June 2005, National Institute of Standards and Technology, Gaithersburg MD. (http://webbook.nist.gov).

(119) (a) Bach, S. B. H.; Eyler, J. R. *J. Chem. Phys.*1990, 92, 358. (b) Ramanathan, R.; Zimmerman, J. A.; Eyler, J. R. *J. Chem. Phys.* **1993**, *98*, 7838.

(120) Giuffreda, M. G.; Deleuze, M. S.; Francois, J. P. *J. Phys. Chem. A* **1999**, *103*, 5137.

CHAPTER 5

PHOTODISSOCIATION OF SIZE SELECTED SILICON CARBIDE CLUSTER CATIONS

5.1 ABSTRACT

Small clusters of silicon carbide ($Si_nC_m^+$, n = 3-10, m = 1-2) are produced by laser vaporization in a pulsed molecular beam and detected with time-of-flight mass spectrometry. Specific clusters are mass selected and photodissociated at 355 nm. Si_3C^+ is especially abundant in the mass spectrum, and is also a common fragment from larger clusters, suggesting that it has higher relative stability compared to other species. The smaller clusters ($Si_{3-5}C^+$) predominately fragment by loss of a neutral Si atom, while the larger clusters ($Si_{7-10}C^+$) lose neutral Si_2C and Si_3C, which are concluded to be stable neutral leaving groups. Energetics and bonding are discussed using ionization potentials and binding energies.

5.2 INTRODUCTION

Small clusters of carbon[1-3] and silicon[3] have been extensively studied for many years, both as model systems to study the fundamentals of chemical bonding and for their astrophysical relevance.[4,5] Even though the two elements are members of the IVA family on the periodic table, their bonding is extremely different. Carbon forms linear chains at small sizes and rings at larger sizes, while silicon favors three-dimensional structures with multiple single bonds per atom.[3] Both elements are relatively common in outer space and species containing carbon and silicon atoms have been identified in stellar and interstellar media.[6,7] In the laboratory, laser photodissociation[8-11] and collision induced dissociation (CID)[12,13] experiments have revealed important energetic information about

these clusters. Fourier transform ion cyclotron resonance mass spectrometry has also been used to bracket the ionization potentials of small carbon clusters.[14] Recently, Maier and co-workers[15] recorded the electronic and infrared absorption spectra of the C_6^+ ion in a neon matrix, the first spectroscopic study of a pure carbon cation chain larger than the dimer. To our knowledge, no spectroscopic study of any cationic silicon cluster has ever been conducted. Numerous theoretical studies[16-19] have examined these species, however, complementing experiment by helping to identify structural and energetic information for the elemental clusters. Just as pure clusters of carbon and silicon have generated considerable interest over the years, mixed silicon carbides are likewise interesting, but species of this type have been studied much less extensively. In this investigation small clusters of silicon carbide are studied by ultraviolet laser photodissociation of mass-selected cations.

Silicon carbide clusters have been previously studied with mass spectrometry,[20-22] optical spectroscopy,[23-25] photoelectron spectroscopy,[26,27] and theory.[28-31] Some of these studies have led to the discovery of various small silicon carbide molecules in space.[7] Most of the experimental efforts have focused on the neutral or anionic clusters, with relatively few experiments and no spectroscopy on the small cations. Photodissociation of large, mass selected, cationic silicon carbide clusters up to the size of heterofullerenes has been observed by Pellarin and co-workers[32] in a study that focused on species with near 1:1 stoichiometries of silicon to carbon. However, photodissociation has not been systematically applied to the smaller silicon carbide clusters (<10 atoms).

Photodissociation has been used extensively to study the elemental clusters of carbon[8-10] and silicon,[11] as well as the related metal-carbon,[33-39] metal-silicon,[40] and

metal-oxide clusters.[41-45] Especially for clusters in the small size regime, photodissociation can be an informative technique for elucidating structural and bonding information. It can be used to determine relative stabilities, identifying both stable cations produced as fragments from the dissociation of larger clusters and stable neutrals, inferred from mass conservation, that occur as common leaving groups. In the present study, we report on the production and photodissociation of silicon carbide clusters in a molecular beam. These experiments help to provide insight into the energetics and bonding of these species by comparison to known and calculated ionization potentials (IP's) and binding energies, and they reveal new stable cation and neutral clusters.

5.3 EXPERIMENTAL

The experimental setup for production and fragmentation of these clusters has been described previously.[33-46] Briefly, the third harmonic (355 nm) of a Spectra Physics Nd:YAG laser (Quanta Ray GCR-11) is used to vaporize a rotating and translating silicon rod (ESPI 99.999% purity). A 1 mm Series 9 General Valve pulses either pure helium or a mix of up to 10% methane in helium at 300 μsec and a backing pressure of 50 psi. The carbon source for this experiment is the methane in the mixed expansion or carbon contamination of the silicon rod, probably from pump oil, in the pure helium expansion. The vaporization ignites a plasma and the mixed silicon-carbon clusters are grown in a 1.5 inch long, 4 mm diameter channel, before being cooled by supersonic expansion into the source chamber. The molecular beam is then skimmed into the differentially pumped mass spectrometer chamber. Cations present in the molecular beam are pulse extracted

into the reflectron time-of-flight mass spectrometer. For photodissociation experiments, the cluster size of interest is mass selected by pulsed deflection plates before entering the reflectron. The ions are then excited with the third harmonic (355 nm) of a Spectra Physics Nd:YAG laser (Spectra Physics DCR-3) in the turning region of the reflectron. Laser excitation of the clusters occurs, and if enough energy is absorbed they will undergo photodissociation. Mass separation of the fragments is achieved by flight time through the second drift tube. The clusters are detected with an electron multiplier tube and a digital oscilloscope (LeCroy 9310A). Data are transferred from the digital scope to a computer via an IEEE-488 interface. The photodissociation experiments use 15-40 mJ/pulse of unfocused laser light in a spot size of roughly 1 cm^2.

5.4 RESULTS AND DISCUSSION

Figure 5.1 shows the mass spectrum produced from the laser vaporization of a silicon rod. The upper trace shows the cluster distribution when a 10% methane mix is seeded into the helium expansion, while the lower trace shows the distribution in a pure helium expansion. High abundances of cluster sizes SiC_2^+, Si_3C^+, Si_4C^+, and Si_7C^+, with very few species of other sizes and stoichiometries present in the background, are seen in from the expansion seeded with methane. The Si_3C^+ and Si_7C^+ sizes are especially prominent in the mass spectrum, possibly indicating enhanced stability for these clusters. The pure helium expansion, shown in the lower trace, produces a smoother distribution of both $Si_nC_m^+$ clusters and Si_n^+ clusters. It is not surprising that the methane expansion

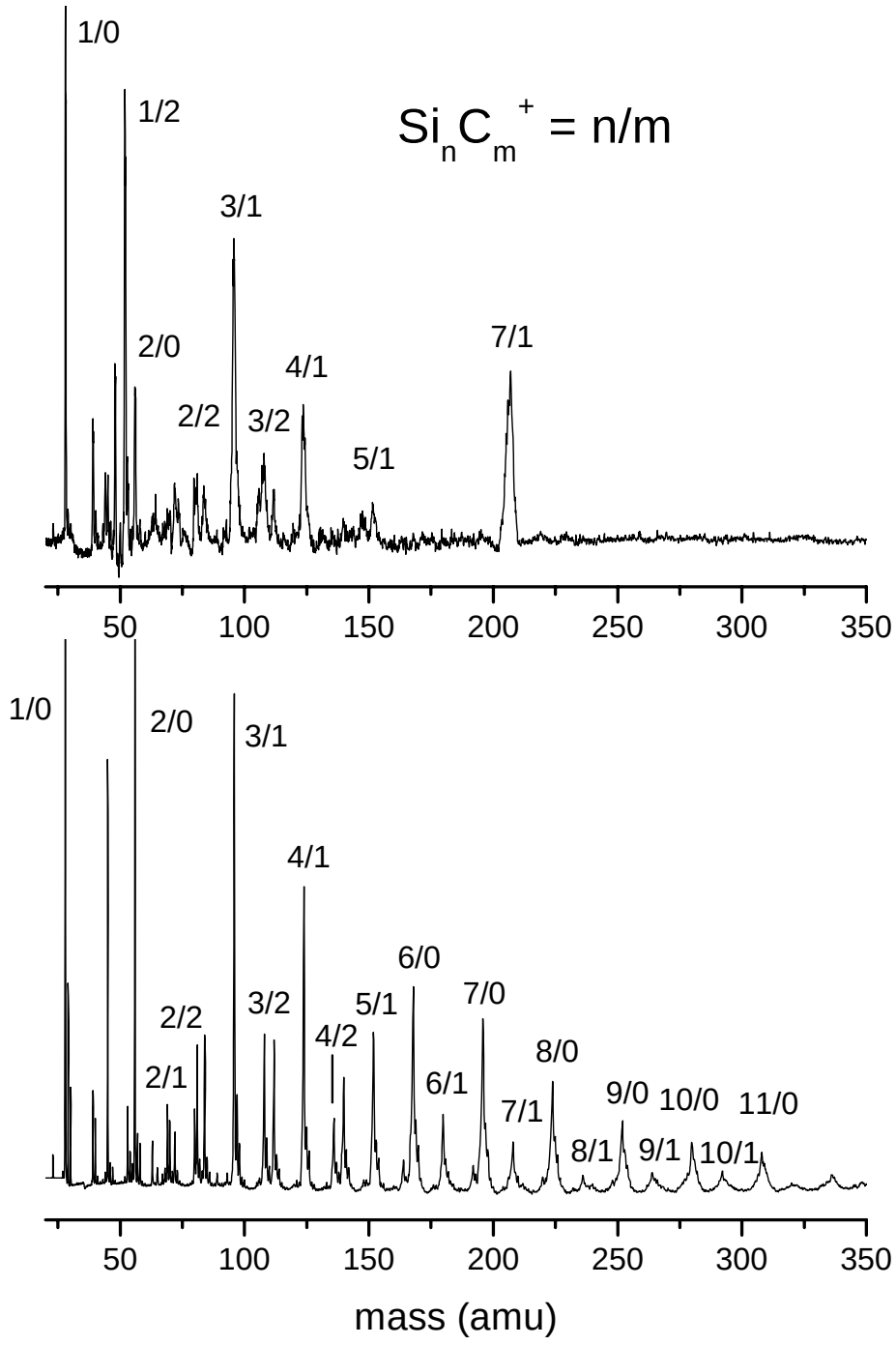

Figure 5.1: Mass spectrum of silicon carbide clusters produced by laser vaporization of a silicon rod in an expansion of helium seeded with 10% methane (upper trace) and in a pure helium expansion.

favors production of especially stable clusters of silicon carbide for a couple of reasons. First, the methane expansion has a high carbon concentration compared to the pure helium expansion, where the carbon source is background impurities of pump oil. Because of the relatively high amount of carbon in the methane expansion, clusters of pure silicon are not observed under these conditions. Second, dissociating the methane to grow clusters requires more energetic laser plasma conditions, resulting in warmer growth conditions than the pure helium expansion. As the clusters grow in the hotter plasma they have higher internal energy. Species with greater stability are more likely to survive the hotter growth conditions, explaining the abundance of certain masses. Although some of the smaller species present here had been previously observed in mass spectrometry studies,[20-23,32] the enhanced abundance of Si_3C^+ and Si_7C^+ has not been reported in any of the prior experimental investigations conducted on silicon carbide.

The cluster distribution produced by the pure helium expansion in the lower trace of Figure 5.1 shows the formation of both pure silicon clusters and silicon carbides. Two series of silicon carbide clusters are seen, with the stoichiometries Si_nC^+ and $Si_nC_2^+$. The cluster distribution is peaked at Si_3C^+, but otherwise no unusual abundances of specific mass peaks are seen under these colder, carbon deficient conditions. Thus, under both warm, carbon rich conditions, and colder, silicon rich conditions, the Si_3C^+ species appears as one of the most dominate peak in the mass spectrum, suggesting special stability for this particular cluster. Notably, no other cluster size, including the Si_7C^+, which was dominant in the mass spectrum shown in the upper trace, stands out here.

The Si_3C^+ species was seen before in mass spectrometry experiments, but it was not previously recognized as an especially stable cluster.[22,23] Earlier experiments were

typically conducted using SiC samples rather than a pure silicon rod as ablation targets, leading to much higher concentrations of carbon in those experiments. Carbon clusters much more efficiently than silicon because of higher bond energies. For example, C_3 has a predicted dissociation energy of 4.23 eV, [16] while the dissociation energy of Si_3 has been predicted to be 2.57 eV.[17] The fact that we produce clusters containing multiple silicon atoms with either one or two carbon atoms implies that the carbon concentration, even in the 10% methane expansion, is extremely low in our experiments. We attribute the differences in our mass spectra compared with previous work to this fact.

The clusters were mass selected and photodissociated to gain additional insight into their structure and bonding. Table 5.1 displays all the parent ions dissociated and shows their major photofragments. Figures 5.2-5.4 show the fragmentation patterns for many of the clusters examined in this study. The data are accumulated by monitoring the fragment ion appearance when the laser is on versus when the laser is off. This generates a difference mass spectrum of the selected cluster. The negative going peak in each photodissociation mass spectra represent depletion of the parent ion, while the positive going peaks show appearance of charged fragments. The third harmonic (355 nm, 3.49 eV photon energy) of an unfocused YAG laser was used in the dissociation, with power ranging between 15-40 mJ/pulse, depending on the cluster size. Previous experience in our lab suggests that multiphoton absorption is likely under these conditions. High laser powers are necessary to measure significant fragmentation of these clusters, which is consistent with high dissociation energies (3-4 eV per atom), predicted by theory.[28,30] The Si_2C^+ and $Si_2C_2^+$ clusters are present in the mass spectrum with good intensity, but when mass selected they did not photodissociate, even at high laser power. Thus they

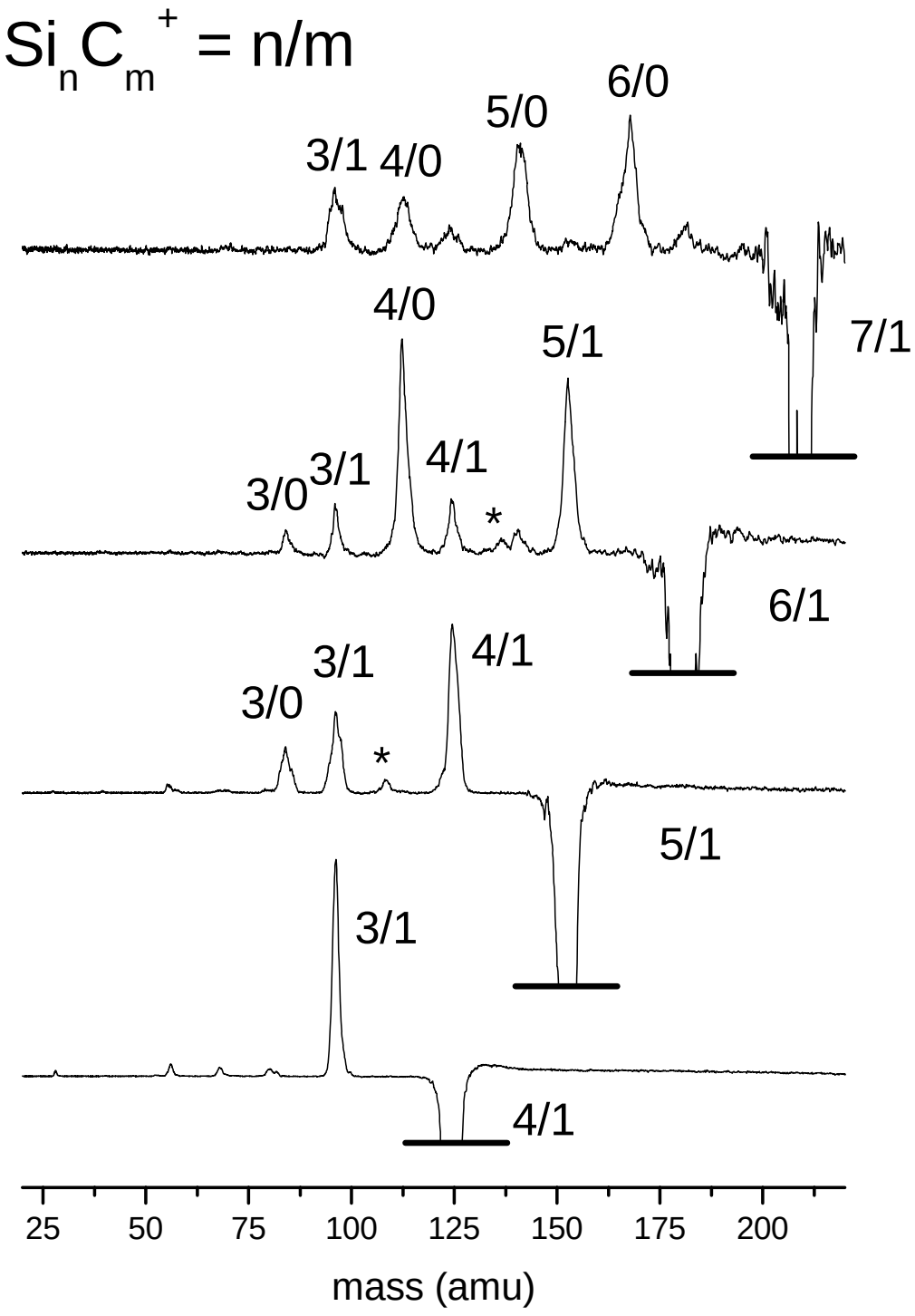

Figure 5.2: Photodissociation mass spectra of $Si_{4-7}C^+$ clusters at 355 nm.

either do not absorb at the 355 nm wavelength or they are too strongly bound to fragment even with multiphoton absorption conditions in the experiment. We do observe photofragmentation with reasonable intensity for the larger ions under similar dissociation conditions. The peaks marked with asterisks in both Figures 5.2 and 5.3 correspond to fragments from larger clusters which were not totally deflected out of the ion beam upon mass selection and thus were still present in the reflectron when the dissociation laser intersected the ion beam. Laser timing studies definitively proved that those peaks are not from the parent cluster of interest.

Table 5.1 and Figure 5.2 show that the small Si_nC^+ clusters have similar tendencies in their fragmentation behavior. Si_4C^+ fragments to Si_3C^+ by elimination of a neutral silicon atom. Si_5C^+ fragments to Si_4C^+ (by loss of Si atom), Si_3C^+, and Si_3^+ (by inferred loss of neutral Si_2C). Si_6C^+ fragments to Si_5C^+ by loss of Si atom, and to Si_4^+, corresponding to the loss of neutral Si_2C. Additionally, small amounts of Si_3C^+ and Si_4C^+ are also produced. Thus all of these small clusters lose a neutral silicon atom, but this channel suddenly decreases in importance for Si_7C^+. Si_3C^+ is also a common fragment for all of the $Si_{4\text{-}7}C^+$ clusters. This is not surprising if, as argued above based on the mass spectral data, Si_3C^+ has enhanced stability over other silicon carbide species. As cluster size increases, loss of Si_2C becomes a more prominent fragment channel, leading to fragments of Si_3^+, Si_4^+, and Si_5^+ from Si_5C^+, Si_6C^+, and Si_7C^+ respectively.

The fragmentation of Si_7C^+ shows behavior markedly different than that observed in the smaller clusters. Notably, the signal for the photodissociation of that cluster size is worse than for any other silicon carbide speceis studied here and higher lasers powers were necessary to see any fragmentation, indicating that this ion is much harder to

dissociate. This is consistent with the mass spectral data suggesting enhanced stability for this cluster size. Additionally, the biggest fragment from Si_7C^+ is Si_6^+, which corresponds to a loss of neutral SiC. No other cluster fragments in this way. However, previous photodissociation experiments on pure silicon cations have shown that Si_6^+ is a common fragment.[10-11] Thus the appearance of the Si_6^+ fragment probably corresponds to the known stability of that species. The formation of Si_5^+, corresponding to loss of Si_2C neutral, and Si_3C^+, are again seen as major fragments. The fragmentation of the Si_7C^+ parent ion then also reflects the relative stability of these species.

Figure 5.3 shows photodissociation mass spectra for some of the larger cluster sizes, and again the loss of neutral Si_2C is a major fragmentation channel. For Si_9C^+ and $Si_{10}C^+$ loss of neutral Si_3C is also seen. Si_6^+ is a common fragment for all these species, and as discussed above in relation to Si_7C^+, is well known as a common fragment of pure silicon.[10-11] It is interesting, however, that only for the Si_8C^+ size is this the dominate fragment, and there it also corresponds to the loss of neutral Si_2C. The larger clusters favor the loss of neutral Si_2C and Si_3C. It appears, then, that the loss of Si_2C and Si_3C are favored fragmentation channels over the formation of Si_6^+. Si_7C^+ is not seen as a fragment of any parent ion studied here, and additionally Si_3C^+ is only observed as a minor component, likely from sequential dissociation of fragment ions. Apparently these stable cations are not favored dissociation channels when the Si_2C and Si_3C neutrals can be formed.

Figure 5.4 shows photodissociation mass spectra for $Si_{3\text{-}4}C_2^+$. The fragmentation patterns here most closely resemble those of the smaller $Si_{3\text{-}6}C^+$ clusters, where neutral silicon atom is the major leaving group. The $Si_4C_2^+$cluster does show some loss of

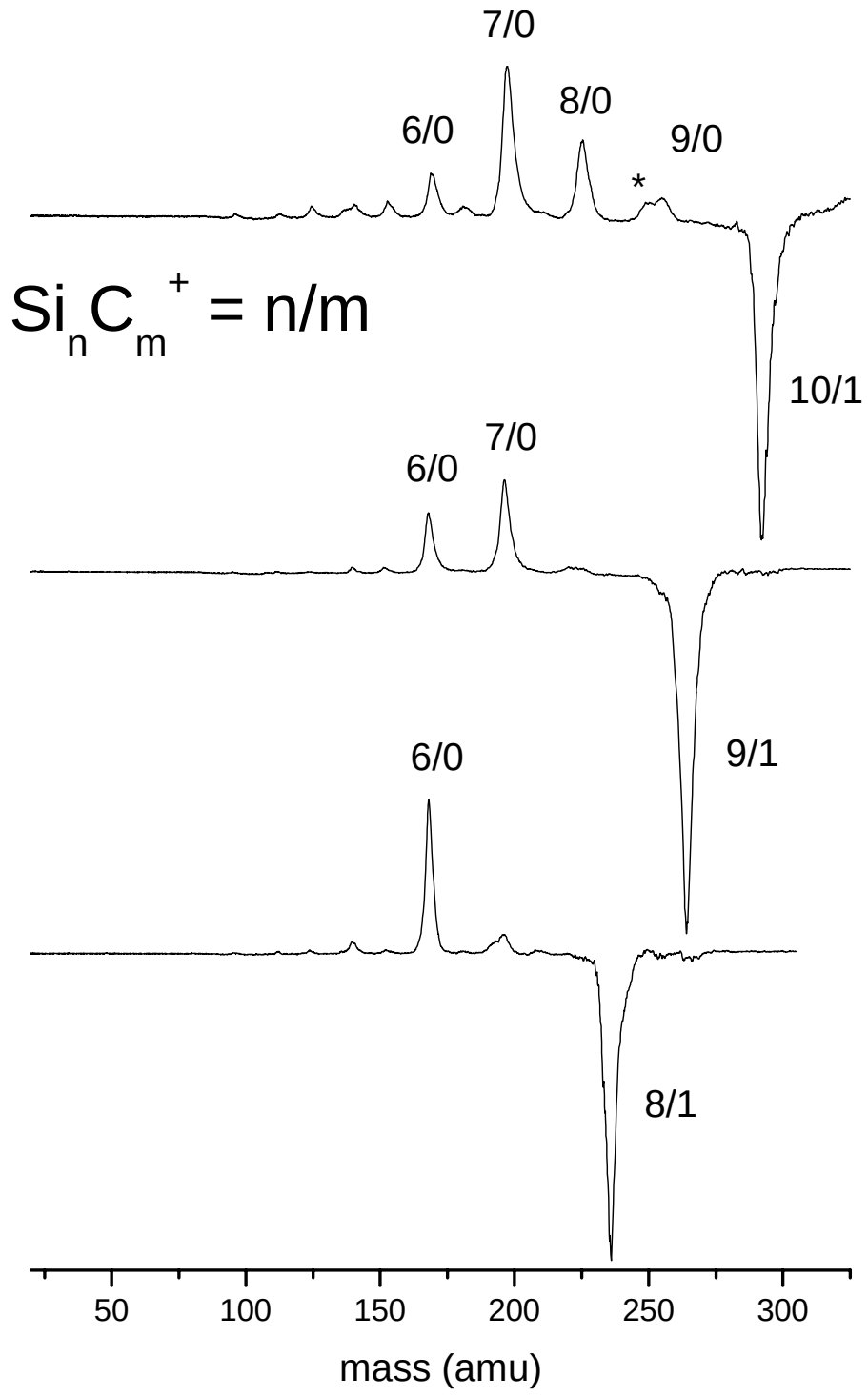

Figure 5.3: Photodissociation mass spectra of $Si_{8\text{-}10}C^+$ clusters at 355 nm.

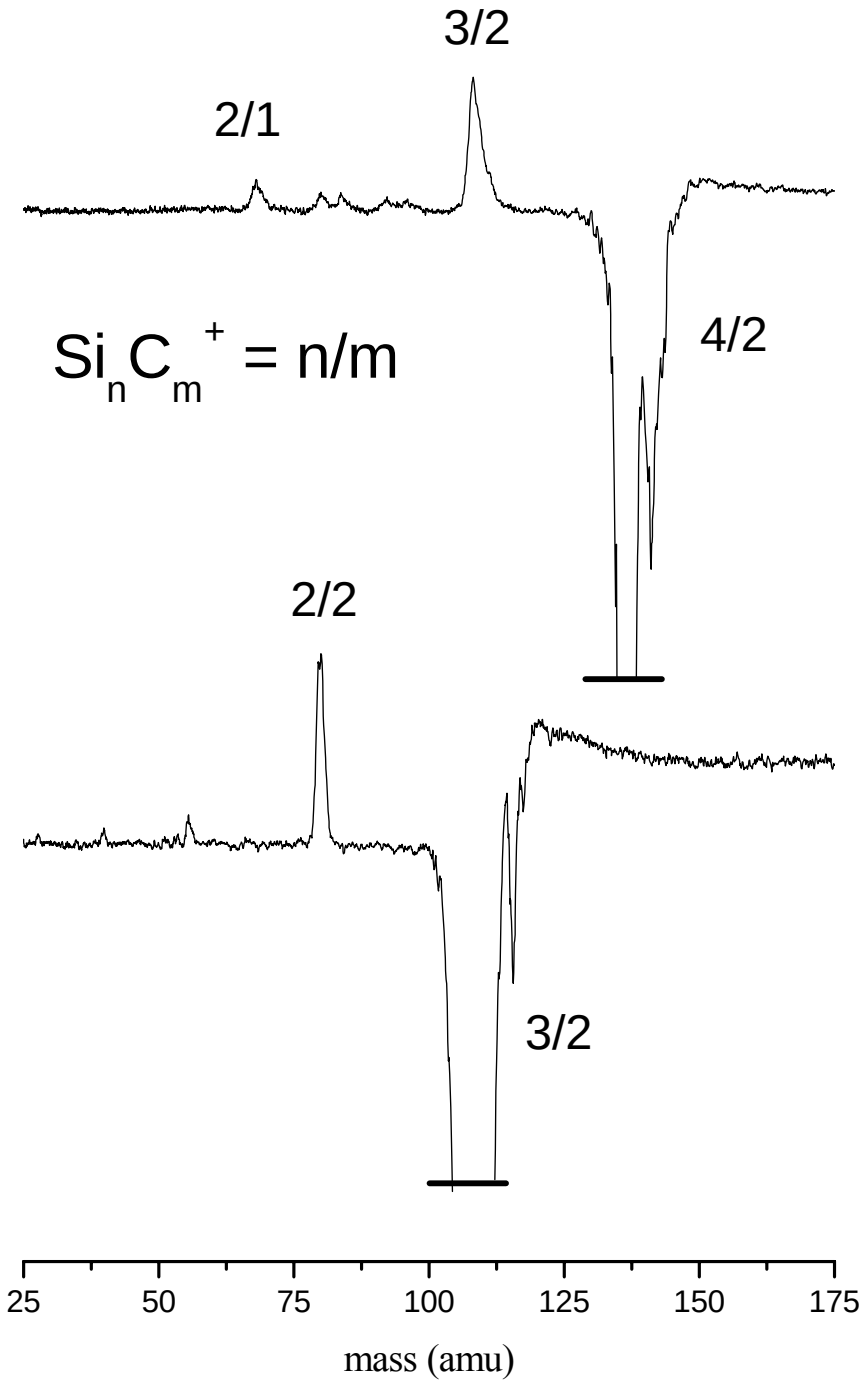

Figure 5.4. Photodissociation mass spectra of $Si_{3\text{-}4}C_2^+$ clusters at 355 nm.

neutral Si_2C, but it is a relatively minor channel. As can be clearly seen in Figure 5.4, the depletion of the parent ion intensity is much greater than the appearance of the fragments. Mass discrimination in our instrument due to ion focusing effects prevents the simultaneous detection of both parent and fragment ions with equal sensitivity, and in some cases all of the daughter ions are not detected.[33] For selected photodissociation mass spectra the parent ion is presented off scale so that the fragment ions may be shown in greater detail.

The photofragmentation data for these silicon carbide clusters can be used to investigate their energetics and bonding. Table 5.2 shows experimental and theoretical IP's and binding energies for some small carbon and silicon species. Exact energetics cannot be determined due to the absence of reliable thermochemical data for these clusters. Useful insight may still be gained when the known IP's and binding energies are examined. Taking the Si_4C^+ parent ion as an example, the following fragmentation channels are possible:

$$Si_4C^+ \rightarrow Si_3C^+ + Si \quad (1)$$

$$Si_4C^+ \rightarrow Si_3C + Si^+ \quad (2)$$

$$Si_4C^+ \rightarrow Si_4 + C^+ \quad (3)$$

$$Si_4C^+ \rightarrow Si_4^+ + C \quad (4)$$

$$Si_4C^+ \rightarrow Si_2 + Si_2C^+ \quad (5)$$

$$Si_4C^+ \rightarrow Si_2^+ + Si_2C \quad (6)$$

These possible fragmentation channels represent three pairs differing only in the fragment that carries the charge. In ion photodissociation experiments such as this the positive charge will generally remain on the fragment with the lower IP. Using the data

collected in Table 5.2, several of these reactions may be immediately ruled out based on this fact. When comparing channels (3) and (4), (3) is unlikely to occur based on ionization potential differences. Carbon (IP = 11.26 eV),[47] is unlikely be eliminated as a cation and leave behind neutral Si_4 (IP = 7.6 eV).[47] A similar IP argument may be used to reject (5) as compared to (6), where the IP is lower for Si_2 (7.5 eV)[17] than for Si_2C (9.1 eV).[29] Comparing channels (1) and (2) suggests that (2) is favored because the IP of Si_3C (8.2 eV)[29] is believed to be greater than that of Si (8.15 eV).[46] Figure 2 shows very conclusively, however, that channel (1) is observed and that the major fragment of the Si_4C^+ cluster is Si_3C^+. This is understandable, however, because the only IP data available for Si_3C is calculated and has considerable uncertainty. The actual IP of Si_3C may still be within the error bars predicted by the calculation,[29] but is still probably lower than 8.15 eV. Based on these arguments from the known energetics, channels (1), (4), and (6) are considered the most likely.

Examining the dissociation energies for the remaining possible channels can also help to explain the observed fragmentation behavior. Channel (4) is unlikely because of the binding energies for the diatomic molecules SiC and Si_2, which should provide a reasonable approximation for the strength of Si-Si and Si-C bonds in all of these clusters. Again, Table 2 shows that Si_2 has a binding energy per atom of ~ 1.61 eV,[48] which is less than the Si-C binding energy per atom of 2.32 eV.[48] On average, the expected binding energies are greater for mixed carbides than for pure silicon clusters. Channel (4) is unlikely to occur because it breaks silicon-carbon bonds before silicon-silicon bonds. Between channel (1) and (6), (6) seems to be more likely because both of the fragments

are molecular. However, channel (1) is actually observed. This strongly attests to the high stability of the Si_3C^+ species.

The same general explanation of the fragmentation patterns, as outlined specifically for Si_4C^+, can be applied to all of these silicon carbide clusters, although even less specific energetic and bonding information is available for larger species. However, the observed trend of the elimination of Si_2C as a neutral to leave behind charged silicon clusters (Si_3^+, Si_4^+, Si_5^+, etc.) is consistent with silicon clusters having lower IP's (e.g. Si_3 = 7.9 eV)[17] than that calculated for the Si_2C leaving group (9.1 eV).[29] Seeing Si_2C as a common fragment of the larger clusters is also consistent with its special stability as a neutral. The photodissociation data of Pellarin et al. also observed Si_2C and Si_3C as major neutral leaving groups[32] for a number of larger silicon carbides. The loss of neutral Si atom and the appearance of the Si_3C^+ fragment that we see in the smaller clusters have not been previously reported.

The stabilities of certain silicon carbide species observed in this study have implications for astrophysics. Molecules and ions of carbon and silicon have already been observed in space, and other species containing these elements have been suggested as likely interstellar molecules.[4-7] Molecules and ions in space are constantly bombarded by deep ultraviolet light, and thus must exhibit high photo-stability to survive. The Si_3C^+ and Si_7C^+ species observed here show enhanced stability and might be good candidates to exist under interstellar conditions. Likewise, Si_2C, Si_3C, and Si_3C^+ are all common fragments from a variety of silicon carbides, and maybe produced in space by photodecomposition of larger carbide clusters or even dust grains containing both carbon and silicon. Radio astronomy has already detected several neutral silicon carbide species

(SiC_2, SiC_3, and SiC_4) ,[7] and based on this study Si_2C and Si_3C^+ are worth further consideration as potential interstellar molecules. The lack of spectroscopic data on these species, especially the ions, is presently a barrier to their possible detection in space.

5.5 CONCLUSIONS

$Si_{3-10}C^+$ and $Si_{3-4}C_2^+$ clusters have been produced in a supersonic molecular beam by laser vaporization. From the mass spectra, Si_3C^+ and Si_7C^+ appear to be especially stable ions. Mass selected clusters are then studied by photodissociation. For the $Si_{3-5}C^+$ and $Si_{3-4}C_2^+$ clusters, loss of neutral silicon atom is the major fragment channel. The appearance of Si_3C^+ is a common fragment for the $Si_{4-7}C^+$ clusters as well. For cluster sizes $Si_{6-7}C^+$, both the loss of silicon atom and the loss of neutral Si_2C are competing fragmentation channels, while the appearance of Si_6^+ fragment from the Si_7C^+ parent is attributed to the known stability of that species. In the largest species studied here, $Si_{8-10}C^+$, neutral Si_2C and Si_3C are the dominant leaving groups. A rudimentary analysis of the possible fragmentation channels using the available ionization potentials and binding energies for some of these clusters allows for a reasonable explanation of the observed photodissociation data. Consistent with theoretical predictions, the mixed bonding between silicon and carbon in these clusters appears stronger than silicon-silicon bonding. The IP of Si_3C is suggested to be less than that of the silicon atom (8.15 eV),[47] while the IP for Si_2C is suggested to be greater than that of Si_3^+ (7.9 eV).[17] In the future, spectroscopy of these ionic clusters could help to definitively determine their structure

and energetics, and the study of the Si_3C^+ and Si_2C species could prove especially interesting targets for astrophysics.

Table 5.1: Major Cation Fragments Observed From Photodissociation (355 nm) of Mass Selected Silicon Carbide Clusters.

Parent	**Major Cation Fragments**
Si_3C^+	Si_2C^+
Si_4C^+	Si_3C^+
Si_5C^+	Si_4C^+, Si_3C^+, Si_3^+
Si_6C^+	Si_3C^+, Si_4C^+, Si_4^+, Si_3C^+, Si_3^+
Si_7C^+	Si_6^+, Si_5^+, Si_4^+, Si_3C^+
Si_8C^+	Si_6^+
Si_9C^+	Si_6^+, Si_7^+
$Si_{10}C^+$	Si_6^+, Si_7^+, Si_8^+
$Si_3C_2^+$	$Si_2C_2^+$
$Si_4C_2^+$	$Si_3C_2^+$, Si_2C^+

Table 5.2: Experimental and Theoretical Ionization Potentials and Binding Energies Per Atom of Small Silicon and Carbon Atoms and Molecules.

species	Ionization Potential in eV	Binding Energy per atom in eV
C	11.26[a]	na
Si	8.15[a]	na
C_2	12.1[b]	2.9[b], 3.11[c]
Si_2	7.5[d]	1.61[c], 1.59[d]
C_3	11.4[b], 12.97 +/- 0.1[e]	4.23[b], 4.58[f]
Si_3	7.9[d]	2.57[d]
C_4	10.5[b], 12.54 +/- 0.35[e]	4.33[b]
Si_4	7.6[d]	3.21[d]
SiC	8.9[g], 8.9 +/- 0.2[h]	2.32[c], 2.01[i]
SiC_2	9.7[g]	4.26[f], 4.26[i]
Si_2C	9.1 +/- 0.2[h]	3.65[f], 3.90[i]
Si_3C	8.2 +/- 0.2[h]	3.86[i]

[a]Ref. 47, [b]Ref. 16, [c]Ref. 48, [d]Ref. 17, [e]Ref. 14, [f]Ref. 28, [g]Ref. 31, [h]Ref. 29, [i]Ref. 30

5.6 REFERENCES

(1) Weltner, Jr., W.; Van Zee, R. J. *Chem. Rev.* **1994**, *89*, 1713.

(2) Van Orden, A.; Saykally, R. J. *Chem. Rev*. **1998**, *98*, 2313.

(3) Johnson, R. L. *Atomic and Molecular Clusters*; Taylor and Francis: New York, 2002.

(4) Tielens, A. G. G. M.; Snow, T. P., Eds. *The Diffuse Interstellar Bands*; Kluwer: Dordrecht, The Netherlands, 1995.

(5) Hartquist, T. W.; Williams, D. A., Eds. *The Molecular Astrophysics of Stars and Galaxies*; Oxford University Press: New York, 1998.

(6) Thaddeus, P.; McCarthy, M. C. *Spectrochimica Acta A.* **2001,** *57A*, 757.

(7) McCarthy, M. C.; Gottlieb, C. A.; Thaddeus, P. *Molec. Phys.*, **2003**, *101*, 697.

(8) Geusic, M. E.; Jarrold, M. F.; McIlrath, T. J.; Freeman, R. R.; Brown, W. L. *J. Chem. Phys.* **1987,** 86, 3862.

(9) Pozniak, B.P.; Dunbar, R.C. *Int. J. Mass Spectrom. Ion Processes* **1997**, *165/166*, 299.

(10) Bloomfield, L. A.; Freeman, R. R.; Brown, W. L. *Phys. Rev. Lett.* **1985**, *54*, 2246.

(11) Zhang, Q. L.; Liu, Y.; Curl, R. F.; Tittel, F. K.; Smalley, R. E. *J. Chem. Phys.* **1987**, *88*, 1670.

(12) Sowa-Resat, M. B.; Hintz, P. A.; Anderson, S. L. *J. Phys. Chem.* **1995**, *99*, 10736.

(13) Jarrold, M. F.; Bower, J. E. *J. Phys. Chem.* **1988**, *92*, 5702.

(14) Ramanathan, R.; Zimmerman, J. A.; Eyler, J. R. *J. Chem. Phys.* **1993**, *98*, 7838.

(15) Fulara, J.; Riaplov, E.; Batalov, A.; Shnitko, I.; Maier, J. P. *J. Chem. Phys.* **2004**, *120*, 7520.

(16) Raghavachari, K.; Binkley, J. S. *J. Chem. Phys.* **1987**, *87*, 2191.

(17) Raghavachari, K.; Logovinsky, V. *Phys. Rev. Lett.* **1985**, *55*, 2853.

(18) Raghavachari, K. *J. Chem. Phys.* **1986**, *84*, 5672.

(19) Raghavachari, K.; Rohlfing, C. M. *J. Chem. Phys.* **1988**, *89*, 2219.

(20) Schmude, Jr., R. W.; Gingerich, K. A. *J. Phys. Chem. A* **1997**, *101*, 2610.

(21) Kimura, T.; Nakamura, T.; Ishikawa, K.; Kokai, F.; Koga, Y. *Chem. Phys. Lett.* **2001**, *340*, 296.

(22) Nam, S. H.; Park, S. M. *J. Appl. Phys.* **2004**, *95*, 8425.

(23) Presilla-Márquez, J. D.; Graham, W. R. M. *J. Chem. Phys.* **1990**, *93*, 5424.

(24) Van Order, A.; Giesen, T. F.; Provencal, R. A.; Hwang, H. J.; Saykally, R. J. *J. Chem. Phys.* **1994**, *101*, 10237.

(25) McCarthy, M. C.; Apponi, A. J.; Gottlieb, C. A.; P. Thaddeus *Ap. J.* **2000**, *538*, 766.

(26) Nakajima, A.; Taguwa, T.; Nakao, K.; Gomei, M.; Kishi, R.; Iwata, S.; Kaya, K. *J. Chem. Phys.* **1995**, *103*, 2051.

(27) Duan, X.; Burggraf, L.W.; Weeks, D. E.; Davico, G. E.; Schwartz, R. L.; Lineberger, W.C. *J. Chem. Phys.* **2002**,*116*, 3601.

(28) Deutsch, P.W.; Curtiss, L. A. *Chem. Phys. Lett.* **1994**, *226*, 387.

(29) Boldyrev, A. I.; Simons, J.; Zakrzewski, V.G.; von Niessen, W. *J. Phys. Chem.* **1994**, *98*, 1427.

(30) Erkoç, Ş.; Tüker, L. *Physica E* **2000**, *8*, 50.

(31) Li, G.; Tang, Z. *J. Phys. Chem. A* **2003**, *107*, 5317.

(32) Pellarin, M.; Ray, C.; Mélinon, P.; Lermé, J.; Vialle, J. L.; Kéghélian, P.; Perez, A.; Broyer, M. *Chem. Phys. Lett.* **1997**, *277*, 96.

(33) Cornett, D. S.; Peschke, M.; Laihing, K.; Cheng, P. Y.; Willey, K. F.; Duncan, M. A. *Rev. Sci. Instrum.* **1992**, *63*, 2177.

(34) Pilgrim, J. S.; Duncan, M. A. *J. Am. Chem. Soc.* **1993**, *115*, 4395.

(35) Pilgrim, J. S.; Duncan, M. A. *J. Am. Chem. Soc.* **1993**, *115*, 6958.

(36) Pilgrim, J. S.; Duncan, M. A. *J. Am. Chem. Soc.* **1993**, *115*, 9724.

(37) Pilgrim, J. S.; Duncan, M. A. *Int. J. Mass Spect. Ion Proc.* **1994**, *138*, 283.

(38) Pilgrim, J. S.; Brock, L. R.; Duncan, M. A. *J. Phys. Chem* **1995**, *99*, 544.

(39) Duncan, M.A. *J. Clust. Sci.* **1997**, *8*, 239.

(40) Ticknor, B. W.; Bandyopadhyay, B.; Duncan, M. A. *J. Phys. Chem. A* to be submitted.

(41) Jaeger, J. B.; Jaeger, T. D.; Duncan, M. A. *J. Phys. Chem. A.* **2006**, *110*, 9310.

(42) France, M. R.; Buchanan, J. W.; Robinson, J. C.; Pullins, S. H.; Tucker, J. L.; King, R. B.; Duncan, M. A. J. *Phys. Chem. A* **1997**, *101*, 6214.

(42) Molek, K. S.; Jaeger, T. D.; Duncan, M. A. J. Chem. Phys. 2005, 123, 144313.

(44) Molek, K. S.; Reed, Z. M.; Ricks, A. M.; Duncan, M. A. *J. Phys. Chem. A* **2007**, *111*, 8080.

(45) Reed, Z. A.; Duncan, M. A. *J. Phys. Chem. A*, in press.

(46) Molek, K. S.; Anfuso-Cleary, C.; Duncan, M. A. *J. Phys. Chem. A*, in press.

(47) Lias, S.G. "Ionization Energy Evaluation" in NIST Chemistry WebBook, NIST Standard Reference Database Number 69**,** Eds. P.J. Linstrom and W.G. Mallard, March 2003, National Institute of Standards and Technology, Gaithersburg MD, 20899 (http://webbook.nist.gov).

(48) Huber, K.P.; Herzberg, G. *Constants of Diatomic Molecules*; Van Nostrand Reinhold: New York, 1979.

CHAPTER 6

PHOTOIONIZATION THRESHOLDS OF SMALL CARBON CLUSTERS: TUNABLE VACUUM ULTRAVIOLET EXPERIMENTS

6.1 ABSTRACT

Small neutral carbon clusters (C_n, n = 2 – 15) produced in a laser vaporization molecular beam source are studied by vacuum ultraviolet (VUV) photoionization mass spectrometry using tunable VUV light from the Advanced Light Source (ALS) at the Lawrence Berkeley National Laboratory. The mass spectra, recorded by single photon ionization at different energies, reveal the distribution of neutral carbon clusters grown from a laser vaporization source. The experiment shows C_3 to be the most abundant species produced in the laser plasma, while even numbered clusters C_{10}, C_{12}, and C_{14} show greater relative intensity than other sizes. Ionization threshold spectra are recorded from 8 – 12 eV for $C_{4\text{-}15}$, and comparison to theory allows the assignment of isomeric structures for some cluster sizes. The data are inconclusive for $C_{4\text{-}6}$ due to unquenched excited electronic states. The larger clusters, however, appear to be free of this complication. Here, the data suggests the presence primarily of a linear structure for C_7, C_9, C_{11}, and C_{13}, and of a cyclic structure for C_{10}.

6.2 INTRODUCTION

Small clusters of carbon have been extensively studied,[1-11] both as model systems to examine the fundamentals of chemical bonding as well as for their prominence in astrochemical[9-12] and combustion processes.[13] Fullerenes and nanotubes are grown out of carbon plasmas, so characterizing the gas phase composition of carbon vapor would aid in the understanding of how such structures form.[3,4,14,15] As described in Chapter 3 of

this dissertation, however, the experimental measurement of the nascent distribution of neutral carbon clusters produced in a laser vaporization source has been extremely problematic. Detecting clusters with mass spectrometers requires some ionization mechanism, which then raises questions about the dependence of the ionization cross sections on cluster size, as well as the energy dependence of ionization potentials (IPs) and electron affinities (EAs). The ionization process may also lead to fragmentation events, which further confuses the situation. The use of tunable vacuum ultraviolet (VUV) light from the Advanced Light Source (ALS) allows us to measure ionization thresholds and to study neutral distributions of carbon clusters produced in a pulsed laser vaporization source. Comparison to high level ab initio predictions of ionization potentials for linear and cyclic structures of allows the assignment of the isomer present in the experiment for some cluster sizes.

Mass spectrometry has been used extensively to study carbon clusters.[16-23] Various experiments made on these species have identified certain sizes with enhanced abundances in the mass spectrum, which has led to speculation that they may have greater relative stability. Fullerenes, and specifically C_{60}, are the most notable examples of this,[2-4,17] but it is seen for smaller clusters as well. Complications from ionization methods employed, variations in ionization cross sections with energy and cluster size, and potential fragmentation events, however, make conclusions about relative stability tenuous at best. Experiments on mass selected ions avoid these problems by directly studying fragmentation channels and dissociation energies of specific cluster sizes. Numerous groups have used photodissociation,[23-27] metastable ion decay,[28,29] and collision induced dissociation[25,30] techniques on carbon clusters. It is now well known

that elimination of C_3 is the major fragmentation channel for small cations. Fullerenes, however, lose C_2 from even numbered clusters, or C atom from odd numbered ones, because these dissociation channels maintain the closed spherical geometry that stabilizes them.[24] Determination of the true neutral cluster distribution produced by laser ablation sources remains an open experimental issue, however. Charge-transfer bracketing experiments have measured the ionization potentials of small carbon clusters, finding values in the range of 8 – 13 eV.[31] This indicates that for recent photoionization experiments conducted with 118 nm (10.5 eV) light from Nd:YAG laser ninth harmonic generation,[32,33] single photon ionization of all cluster sizes is not possible. Even at this high photon energy, multiphoton absorption will still be necessary to ionize some cluster sizes, possibly resulting in fragmentation. Higher energy VUV light, such as available from the ALS, could overcome this limitation.

The issue of isomers in carbon clusters is also a long standing question.[1,5] Many theoretical studies have been performed on both the neutral[34-49] and charged species.[50-61] Most investigations agree that odd numbered clusters have linear ground states while the even numbered ones have cyclic ground states. Many of the neutral species have been studied by gas phase[1,5,62-64] and matrix isolation[1,5,65-70] spectroscopy. Anions have been studied with resonance-enhanced photodetachment spectroscopy,[5,71-73] photoelectron spectroscopy,[5,74-76] and matrix isolation infrared spectroscopy.[77] Spectroscopic data on the cations is limited to a couple of recent studies by Maier and co-workers on matrix isolated $C_{6\text{-}9}^{+}$.[78] Ion mobility experiments have found both linear and cyclic isomers possible up to C_{10}^{+}, but only cyclic rings are present at larger sizes,[79,80] in agreement with the energetics predicted by most of the available theory. However, the isomers probed in

the spectroscopic studies have not always been those predicted by theory to be the lowest energy structures. Specifically, linear isomers have been detected for clusters as large as C_{21} (the neutral and anion),[63] well above the size regime where cyclic isomers should be strongly favored.

Significant differences in ionization potentials between linear and cyclic geometries are predicted to exist for some cluster sizes.[47,55,56,89] Systematically examining the ionization potentials (IPs) as a function of size for small, neutral carbon clusters offers one method for identifying the isomers present in an experiment and studying the bonding and electronic structure in these clusters. The Advanced Light Source (ALS) allows photoionization mass spectrometry utilizing tunable vacuum ultraviolet (VUV) light in the 8 – 15 eV region of the spectrum. Recent photoionization studies of C_3[81] and the metal oxide diatomics FeO and CuO[82] have shown the successful coupling of a pulsed laser vaporization cluster source to the quasi-continuous output of the ALS. In the present study small neutral carbon clusters produced in a pulsed molecular beam laser ablation source are ionized and photoionization efficiency curves from 8 – 12 eV show the onset of ionization for the clusters up to C_{15}. The results are interpreted by comparing the experimental ionization thresholds to IPs predicted by high level ab initio theory.[89] This investigation provides the best current measurement of the size distribution and isomeric structures of neutral carbon clusters produced by a laser vaporization source.

6.3 EXPERIMENTAL

Carbon clusters are produced in a high repetition rate pulsed-nozzle laser vaporization source and photoionized with vacuum ultraviolet light (VUV) from the Advanced Light Source (ALS), tunable from 8-13 eV. The details of the experiment are somewhat different from those described in Chapter 2 of this dissertation, so a more detailed explanation is given here. These experiments use the 3 m monochromator at the Chemical Dynamics Beamline of the ALS.[83] The molecular beam produced by the pulsed laser ablation source is collimated by a 1 mm skimmer cone and passes into a differentially pumped chamber, where the beam is intersected by the VUV output of the ALS. Photoionization occurs in the source region of a reflectron time-of-flight mass spectrometer (R.M. Jordan Co.), where resulting ions are mass analyzed and detected. The experimental apparatus has been described in detail elsewhere.[81,82]

The experiment requires the coupling of the pulsed cluster source to the quasi-continuous (500 MHz) VUV light from the ALS. This is accomplished by utilizing a high repetition rate source. A rotating and translating 1/2 inch carbon rod (Glass Supply, 99.9%) is ablated with focused 532 nm light from a pulsed Nd:YAG laser (Coherent Infinity) operating at 100 Hz. Typical ablation conditions utilize 5 – 10 mJ/pulse of laser energy, focused to a 1.5 mm spot. A piezo-electric valve pulsing the helium carrier gas is synchronized with the laser. The ablation creates a plasma and the clusters are grown and then cooled via supersonic expansion. Ions produced directly from the laser plasma are rejected by deflection plates located before the skimmer cone, which allow only the

neutral clusters in the beam to pass into the mass spectrometer chamber. The beam is intersected with the light from the ALS in the ion source region of the mass spectrometer. The VUV output of the ALS is quasi-continuous, so the acceleration plates of the mass spectrometer are pulsed at the arrival time of the cluster beam and any ions produced by photoionization from absorption of VUV are extracted from the beam into the mass spectrometer. The ions are then separated by flight time and detected by a microchannel plate, and the signal is collected with a multichannel scaler card (FAST Comtec 7886). The VUV is tuned and mass spectra are collected at each step. The experiment generates low signal levels, requiring extensive averaging. Low resolution scans were collected with an ALS step size of 0.2 eV, while higher resolution scans used 0.05 eV steps. At every step the mass spectra were averaged for 8000 laser shots. Photoionization efficiency spectra (PIEs) for each cluster size were generated by extracting ion intensity in each mass channel versus photon energy. Multiple scans were collected, and the PIEs reported are the average of two or three of the best scans, determined by source stability.

6.4 RESULTS AND DISSCUSSION

Figure 6.1 shows mass spectra collected at the photon energies of 10.0 eV (upper trace) and 12.0 eV (lower trace). Experimental conditions of the cluster source and the mass spectrometer were identical for both measurements. Differences in the two mass spectra correspond exclusively to differences in the photon energy. Clusters out to a size of at least C_{15} are observed, along with peaks corresponding to acetone (an impurity from

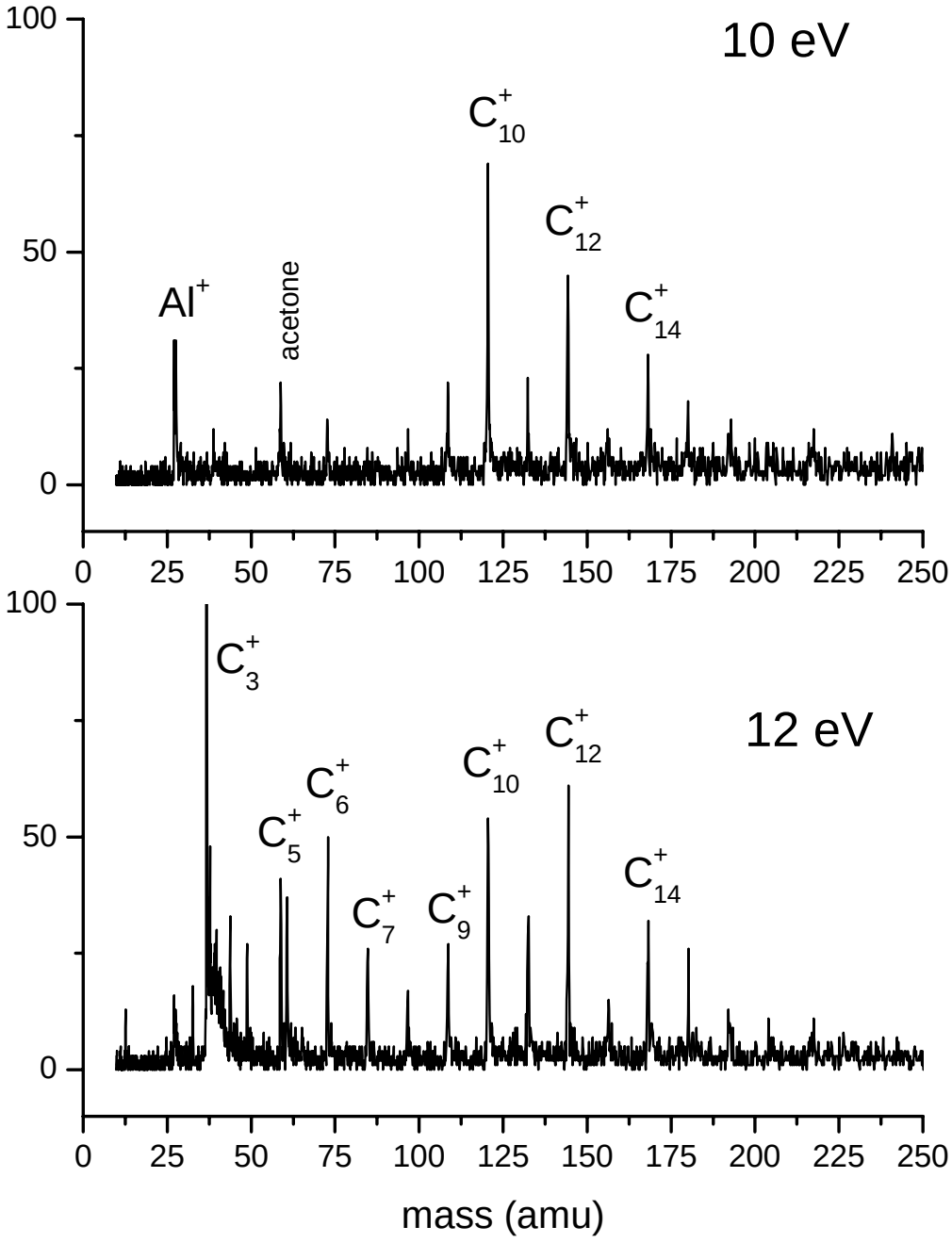

Figure 6.1: The mass spectra measured at the photon energies of 10.0 and 12.0 eV. The tail apparent just after C_3 is due to impurity masses in this region, including potassium (39 amu) and some C_3H_n species.

the gas line) and aluminum, vaporized from the rod holder. At the lower photon energy, C_{10}^+, C_{12}^+, and C_{14}^+ are prominent, while smaller cluster sizes are completely absent. At the higher photon energy of 12.0 eV, however, new peaks are detected, corresponding to C_3^+, C_5^+, C_6^+,and C_7^+. This result is consistent with the expected trend of decreasing IP with increasing cluster size. 10.0 eV is apparently above the IP for C_{10} and larger clusters (as confirmed below), while only at the 12.0 eV photon energy do the smaller clusters appear. Additionally, C_3^+ is the dominant peak in the mass spectrum at the 12.0 eV photoionization energy. The ionization threshold for C_3 has been measured previously to be 11.61 eV,[81] consistent with its absence at 10.0 eV and appearance at 12.0 eV. The photoionization mass spectra at both wavelengths shows that in the higher size range, clusters with an even number of carbons (n = 10, 12, 14) are more prominent than the odd numbered ones. This is consistent with previous experiments conducted in other laboratories, which used 10.5 eV light to photoionize neutral carbon clusters.[32,33] Those experiments also detected smaller carbon species, notably C_3^+, at the lower photon energy. Its presence in those experiments, well below its known IP (11.61 eV),[81] was attributed to photoionization out of metastable excited states of C_3 populated in the beam. The lack of such a signal here indicates that in our experiment, population in excited states high enough to cause ionization at such low photon energies is quenched before the clusters are probed.

Figure 6.2 shows the mass spectrum measured at the photon energy of 12.6 eV. New peaks corresponding to water and molecular oxygen impurities are detected, consistent with their known IPs of 12.6 eV and 12.1 eV, respectively.[84] The relative intensities of the larger carbon clusters remains essentially the same as at the longer

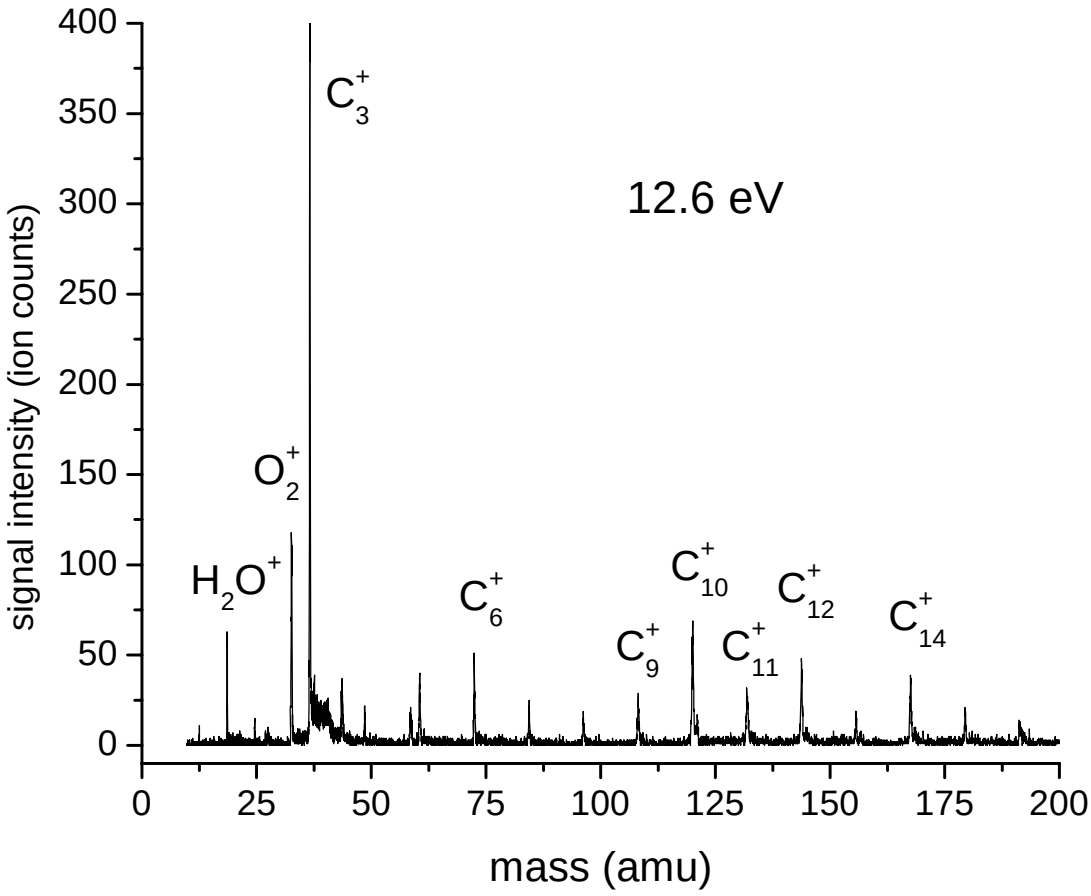

Figure 6.2: Mass Spectrum measured at the photon energy of 12.6 eV.

wavelengths, with the even numbered clusters still showing enhanced abundance. The most notable difference between the mass spectrum collected at 12.0 eV and that collected at 12.6 eV, however, is the dramatic fourfold increase in the intensity of the C_3 mass peak, which dominates the mass spectrum. In some photoionization experiments, the relative intensity of mass peaks may vary with photon energy due to multiphoton absorption and subsequent fragmentation. However, the VUV photon flux from the ALS is too low for multiphoton absorption. This result thus indicates that the photoionization cross section of C_3 is wavelength dependent. A previous experimental study on the energy dependence of the photoionization cross section of C_3 observed an increase after 12.5 eV,[81] which would explain the increase in intensity observed in our experiment at 12.6 eV. A second issue to consider is the possibility that photofragmentation of larger clusters is creating intensity in the C_3^+ mass channel. As illustrated in Chapter 3 of this thesis, carbon clusters of certain sizes, most prominently C_5^+ and C_6^+, may indeed fragment to C_3^+. The dissociation energies for these species have been measured by CID to be 6.0 and 5.2 eV,[30] respectively. Fragmentation processes would then not contribute to intensity in the C_3^+ mass channel until at approximately 5 eV above the ionization threshold of these clusters. Their thresholds have been measured, as shown below, to be 9.5 – 10.0 eV. Single photon ionization followed by subsequent fragmentation is unlikely to occur at photon energies below about 14 eV for these species. Larger carbon clusters are known to fragment by elimination of neutral C_3,[23-30] but we are detecting an increase in the C_3^+ signal. The intensity of the C_3^+ peak must then be due to the high abundance of the neutral C_3 molecule present in the beam and the energy dependence of its photoionization cross section.

The relative intensity of C_3^+ compared to other clusters detected in this experiment suggests that C_3 is produced in high abundance in our source. Previous work has shown that C_3 is very abundant in carbon vapor, and as described in Chapter 3 of this dissertation and elsewhere, C_3 is a very stable fragment from small carbon clusters.[23-30] This experiment represents the first time that photoionization, with photon energies high enough to ensure single photon ionization of the entire neutral cluster distribution, has been used to detect carbon clusters produced by a laser vaporization source. Interestingly, C_2^+ is not detected in any appreciable intensity, even at the highest photon energies utilized in this experiment. The IP of C_2 is believed to lie below 12.1 eV,[84,85] so it should be detected at the 12.6 eV photon energy if it was present in the laser ablation vapor. The fact that we do not detect significant amounts of it suggests that it is not present in high density. The relative abundance of C_2 versus C_3 has serious implications for the growth of both fullerenes and nanotubes, which may be grown in laser vaporization sources similar to this, although the growth of nanotubes requires an additional catalyst. The most current theoretical models for the condensation and growth of these species assume that C_2, not C_3, is the most abundant species present in carbon vapor.[15] The findings here call that very much into question, and at the very least suggest that more experimental and theoretical attention should be paid to this issue.

Threshold ionization measurements were made for the clusters by tuning the energy of the ALS and collecting mass spectra, like those shown in Figures 6.1 and 6.2, at every step. High resolution scans used energy step sizes of 0.05 eV, while lower resolution scans were stepped at 0.2 eV. For sizes where both high and low resolution data were collected, the appearance of the photoionization efficiency curves are

essentially the same, and the higher resolution data was always used when available. The PIEs measured for all clusters are available in the Supporting Information of reference 89. Representative examples are presented here.

Figures 6.3 and 6.5 - 6.10 show PIE curves for C_4, C_5, C_6, C_7, C_9, and C_{10}, respectively, generated by scanning the ALS energy and recording mass spectra at each photon energy. The figures are the average of multiple ALS energy scans, and the error bars show the standard error associated with this averaging. The inset of each figure shows how the ionization threshold is extracted. A linear fit line determines the average baseline prior to the onset of the ionization signal, and another linear fit shows the ionization signal rising out of the background. The intersection of these two lines is the experimental ionization threshold for the given cluster, with an uncertainty estimated to be ± 0.1 eV. The experimental values for each cluster, determined in this way, are collected in Table 6.1. Because the thresholds for most clusters represent small signals rising slowly out of the background, extensive averaging and a multiple scans are used to ensure the measured onset of ionization is reproducible. All the PIE spectra show a significant drop in signal intensity at 11.8 eV due to the use of an argon gas filter. The filter is necessary to block higher harmonics that are generated simultaneously with the VUV used in the experiment,[83] but at this energy it causes a decrease in transmitted VUV light and thus a decrease in detected ionization signal. Additionally, some of the spectra show small dips in signal intensity around 10.5 and 11.2 eV which are attributed to momentary instability in the cluster source while scanning at these energies. The thresholds measured here, excluding C_3, all fall between 8.4 and 10.35 eV, with a trend of decreasing threshold energy with increasing cluster size observed. The C_3 PIE has been

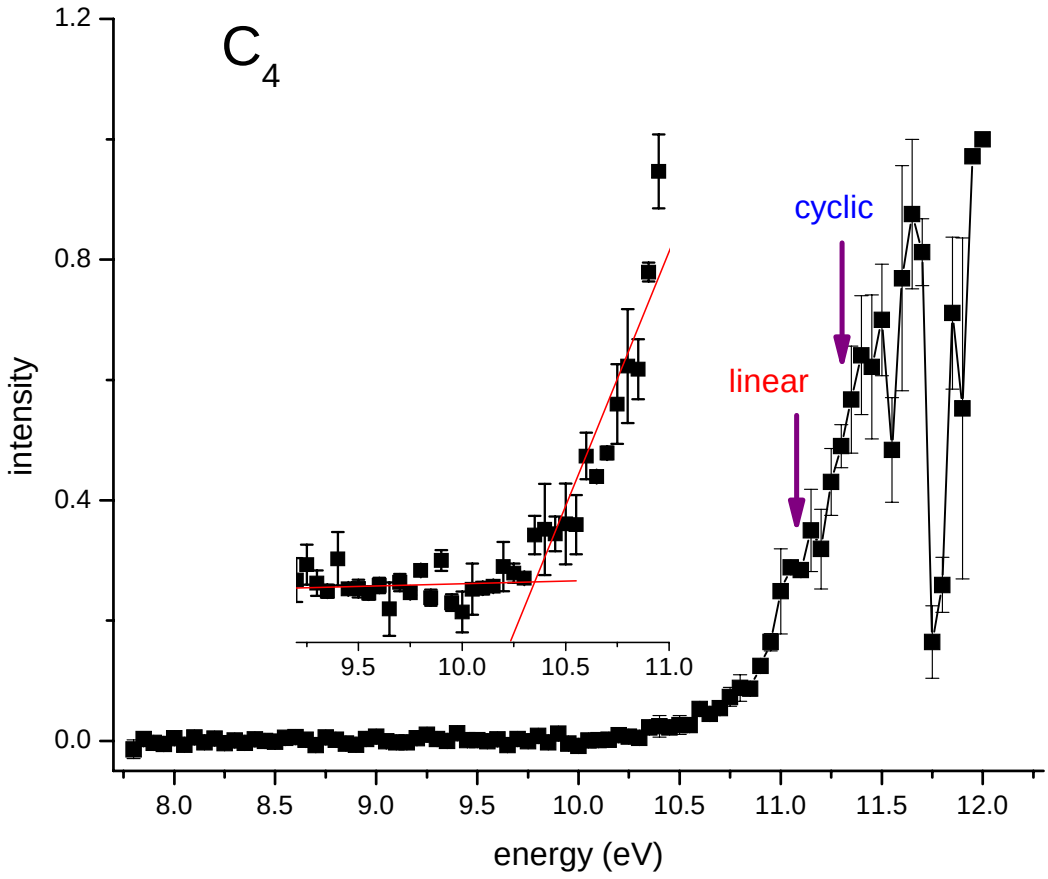

Figure 6.3: Photoionization efficiency curve in the threshold region for C_4. The arrows show the positions of the calculated vertical IP for the two different isomers. The blue lettering indicates the isomer computed to be more stable, and the red lettering indicates the less stable one.

measured previously in a similar experiment and the threshold was reported to be 11.61 eV,[81] consistent with our observations here. That study represents the only previous measurement of photoionization thresholds for carbon clusters, however. Ionization potentials of carbon species have been measured previously by both charge transfer bracketing[31] and electron impact ionization,[86] however. These data are also collected in Table 6.1. Agreement between the charge transfer bracketing (CTB) and the threshold photoionization (TPI) data is rather poor for most clusters. Only the n = 6, 10, 12, and 14 sizes have values that agree within the error bars of the two experiments. Electron impact ionization (EI) also measures IPs somewhat higher than our TPI values. Several serious differences exist between these experiments, however, especially the energy dependence of the ionization method utilized and the source of the clusters upon which the measurements are being made.

As described above, the TPI data measured here rely on small signals rising gradually out of the baseline. Thus the very real possibility exists that the actual ionization potentials lie at energies lower than the values reported here because the ion signal at the threshold was below our detectable level. Frank – Condon factors may also influence the measurements here, causing the thresholds to be detected at energies above the adiabatic ionization potential (IP_a). The IP_a is the minimum energy between the ground state of the neutral and the cation, while the vertical ionization potential (IP_v) is the most probable transition from the neutral ground state to the cation ground state of the same geometry. The thresholds measured in this experiment are expected to lie somewhere between these two values, and thus should be considered only as upper limits to the true IP_a. The CTB and EI experiments each suffer from related problems due to

the energy efficiencies of the ionization methods employed, and may also be said to measure upper limits of the IP_a.

An added complication to each of these experiments is the issue of internal energy in the clusters studied, which may cause ionization to be observed at energies below the IP_a. Unquenched energy in vibrational and rotational degrees of freedom is unlikely to significantly affect the measured thresholds.[87] However, as described in Chapter 3 of this dissertation, carbon clusters are known to have many low lying excited electronic states which may be populated despite the collisional cooling employed.[81,88] Ionization out of such unrelaxed metastable excited states would then be detected at significantly lower photon energy than the true ground state IP.

A final issue in the measurement of ionization potentials for all three experiments is the role of isomers in carbon clusters. Linear chains and cyclic rings are both possible for these clusters, with the relative amounts governed by the energy and the entropy present in the systems. The linear isomers are favored by entropy, and thus high temperatures should increase the relative amount of this structure. As shown below, the linear and cyclic isomers are expected to have different IPs, and the most stable geometry will not always be the same for the neutrals and the cations. The TPI and EI[86] experiments both start with neutral clusters, but the CTB makes measurements on mass selected cations.[31] This complicates the comparison of the various experiments and necessitates an evaluation of the experiments on an individual basis for each cluster size.

To aid in this experimental investigation of the photoionization behavior of small carbon clusters, we engaged in a collaboration with Steven Wheeler, working under the direction of Dr. Wesley Allen and Professor H. F. Schaefer at the Center for

Computational Chemistry at the University of Georgia. Steven performed high level ab intio calculations on cluster sizes $C_{4\text{-}10}$. The details of the computations are described in reference 89. Briefly, the geometric structures were optimized at the CCSD(T) level with cc-pVTZ ($C_{4\text{-}8}$, C_{10}), or cc-pVDZ (C_9) basis sets, and focal point extrapolations were applied to both neutral and cation species to determine adiabatic and vertical ionization potentials. The values are listed in Table 6.1, along with the summary of the experimental results for each cluster size. This computational study also investigated the relative energies of the linear and cyclic isomers for both the neutral and cationic species. These values are tabulated in Table 2 of reference 89. The results of these computations are referenced as necessary in the following discussion of the experimental results for each cluster size.

C_4. Previous work on the C_4 and C_4^+ clusters has shown that the linear and cyclic structures for both species lie close in energy. Only the linear neutral has been detected by spectroscopically,[5,7-9,62] however. Ion mobility experiments identified the linear cation,[79] and photoelectron experiments on the linear anion have characterized multiple excited states of the neutral.[76] The recent ab initio calculations[89] predict the cyclic structure to lie lower in energy for both the neutral (1.1 kcal/mol) and cation (3.4 kcal/mol). The focal point extrapolated IPs are very close for both isomers, with the cyclic (IP_a/IP_v = 10.9/11.3 eV) values encompassing the linear ones (IP_a/IP_v = 11.0/11.1 eV).[89] Because the two isomers are predicted to lie so close in energy, the effect of entropy was investigated by calculating free energy versus temperature for the two isomers, using vibrational frequencies predicted in a previous theoretical study.[34] The result of the calculation is depicted graphically in Figure 6.4, and reveals that the free

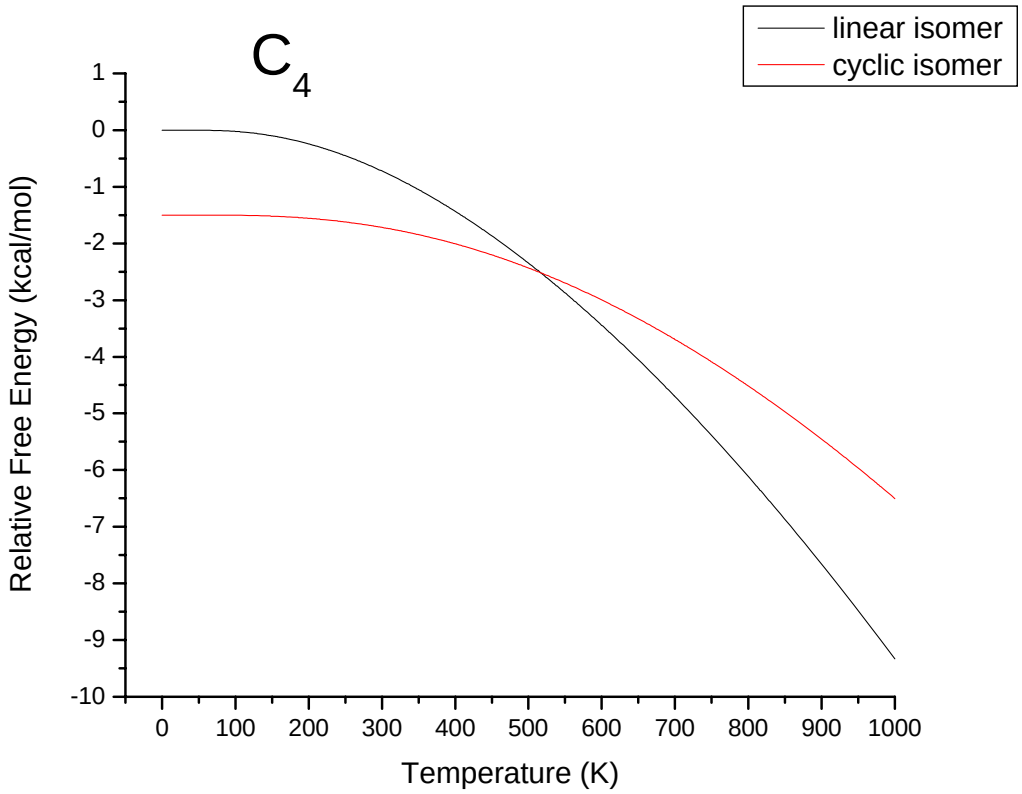

Figure 6.4: Free energy versus temperature calculated for the linear and cyclic isomers of the C_4 cluster, using vibrations predicted in reference 34.

energy of the two isomers is the same at approximately 500 K. This is well within the temperature range expected in our clusters. As described in Chapter 3 of this dissertation, carbon clusters produced in laser vaporization sources such as this can contain significant internal energy, and the collisional cooling from the supersonic expansion may fail to completely quench it. Thus in the conditions present in this experiment both the linear and cyclic isomers are likely to be present.

Figure 6.3 shows that the experimental ionization threshold for C_4 is 10.35 eV, almost 1 eV below the predictions for either isomer. Population in excited vibrational or rotational states cannot account for an energy difference this large, and thus the possibility of excited electronic states must be considered. As mentioned above, photoelectron spectroscopy of the linear anion has mapped out numerous low lying excited states in the neutral species.[76] In respect to the $^1\Sigma_g$ ground state, these experiments found a $^1\Delta_g$ state at 0.33 eV and a $^1\Sigma_g^+$ state at 0.93 eV. Population in both of these states would be metastable versus emission to the ground state due to symmetry restrictions, and they lie in the correct energy range to explain the discrepancies between the predicted IPs and the measured thresholds. For the cyclic isomer, theory predicts a metastable triplet state 0.9 eV above the ground singlet state. Thus both isomers may have population in excited states which would account for the lower ionization threshold measured for C_4. This, coupled with the fact that essentially no difference in the IP's for the linear and cyclic isomers is predicted by theory, allows us to make no conclusion about the isomers present in the experiment.

Our measured threshold for C_4 is also low when compared to the IP obtained by the CTB experiment (12.54 eV).[31] Due to the complications of excited state population

in our TPI experiment a direct comparison cannot be made. However, the CTB experiment is also in poor agreement with the theoretical predictions, and thus the question of its accuracy is open as well. The EI experiment generated a value of 11.9 ± 0.5, which is closer to the theoretical values. A very recent theoretical work studied the ground and low lying excited states for isomers of both C_4 and C_4^+, with the goal of interpreting the PIE spectrum of C_4.[88] This work concluded that ionization channels from multiple excited states, in several different isomers, are possible, consistent with our conclusion that the presence of populated excited states lowers the observed threshold value compared to the prediction of theory.

C_5. Theoretical work on the C_5 and C_5^+ clusters has shown the linear isomer to be much lower in energy for both the neutral and the cation.[1,5,89] The neutral species has been studied in numerous spectroscopy experiments,[1,5,7-9,62] but the ion has mainly been studied with ion mobility, which only detected one structure, assigned to the linear species.[79] Because of this, and the fact that entropy effects would favor a linear chain over a cyclic ring, we expect the linear isomer to be most prevalent in the experiment. The IPs predicted by the focal point extrapolations are IP_a/IP_v = 11.4/11.4 eV for the linear isomer and IP_a/IP_v = 10.4/10.8 eV cyclic isomer.[89] As shown in Figure 6.5, the measured photoionization threshold for C_5 is 9.9 eV, lower than that predicted for either isomer. Thus, as with C_4, the possibly of excited electronic states must be considered. The photoelectron spectrum of the anion did not reveal any low lying states in the neutral molecule,[76] but theory has found triplet states lying 1.2 – 1.3 eV above the ground state.[47] Population in these states would be metastable to relaxation down to the singlet ground state, and thus could create a lowering in the observed ionization threshold. Inspection of

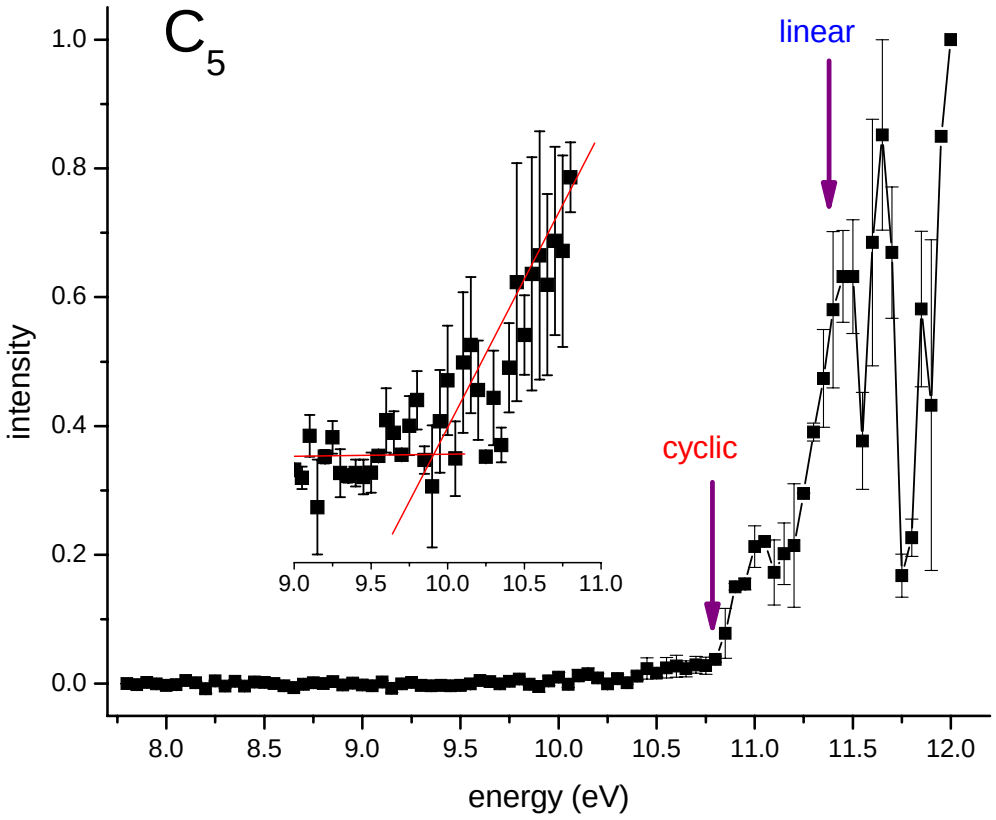

Figure 6.5: Photoionization efficiency curve in the threshold region for C_5. The arrows show the positions of the calculated vertical IP for the two different isomers. The blue lettering indicates the isomer computed to be more stable, and the red lettering indicates the less stable one.

the threshold spectrum does show very small signals indicating the onset of ionization at 9.9 eV, and then a dramatic increase in photoionization efficiency at 10.5 eV, which is very near the predicted IP for the cyclic isomer. Thus the threshold detected at low energy may represent population in excited states, and the increase at 10.5 eV may be from the ionization of clusters from the ground state. Again, our threshold is low when compared to the IP measured by CTB (12.26 eV),[31] but that value is also in poor agreement with the theoretical predictions. The IP measured by the EI experiment, however, is 11.4 ± 0.5 eV,[86] which lies very close to the IP predicted for the linear species.

C_6. The ground state structure of the C_6 cluster has proven more difficult to determine than that of C_5. Early theoretical studies found the linear isomer to be lower in energy,[1,5] but later work predicted a cyclic D_{3h} structure for the neutral and a cyclic C_{2v} structure for the cation.[7,89] Both isomers of the neutral[1,5,7,69] and cation[79] have been detected spectroscopically, while ion mobility only detected one structure, which was assigned to the linear isomer.[79] Here again we investigated the effects of entropy and temperature on the free energy of the two isomers in the same manner described above for C_4. The results of this show that at 1100 K the free energy of the two isomers will be similar. This temperature seems high, but as described in Chapter 3 of this dissertation, carbon clusters produced from a laser ablation source such as this may still contain significant internal energy. Thus both isomers may be present in the experiment.

Figure 6.6 shows the threshold ionization spectrum collected for C_6. Theory predicts IP values of IP_a/IP_v = 9.9/10.0 eV for the linear isomer and IP_a/IP_v = 10.2/10.6 eV for the cyclic species.[89] Our measured value of 9.45 eV is again below both of these

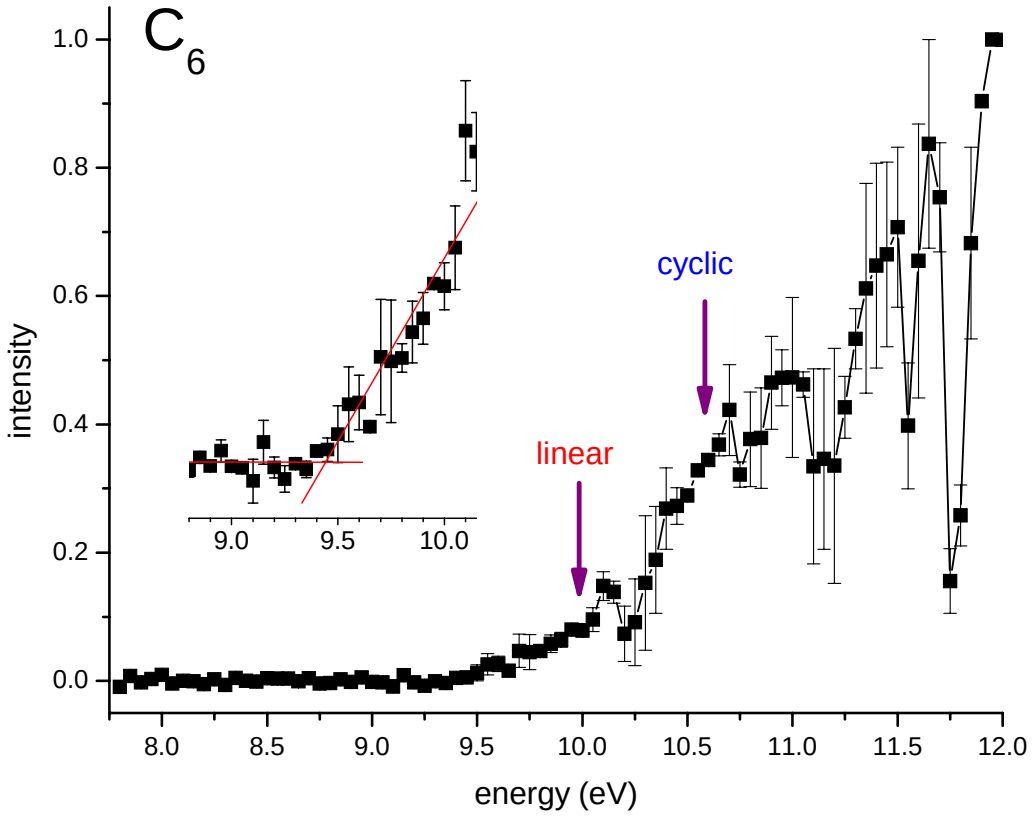

Figure 6.6: Photoionization efficiency curve in the threshold region for C_6. The arrows show the positions of the calculated vertical IP for the two different isomers. The blue lettering indicates the isomer computed to be more stable, and the red lettering indicates the less stable one.

predictions, and again excited electronic states are considered. Photoelectron spectroscopy has located a $^1\Delta_g$ state at 0.166 eV[76] which would be metastable to the $^3\Sigma_g^-$ ground state, and theory has predicted other states at similar energy.[1] Thus unquenched excited states may again explain the low IP measured for this cluster. The CTB experiment found an IP of 9.7 ± 0.2 eV,[31] very close to that predicted for the linear isomer. Ion mobility experiments found only a linear structure for the cation,[79] which is the species the CTB probed.

C_7. Theoretical work on C_7 has suggested that the neutral species is most stable as a linear chain, while the cation prefers a cyclic C_{2v} structure.[89] The linear neutral has been studied spectroscopically,[1,5,7] and both isomers of the cation have been isolated in rare gas matrices.[78b] Additionally, ion mobility identified both isomers of the cation.[79] Figure 6.7 shows the photoionization efficiency spectrum of C_7, which gives an experimental threshold of 10.1 eV. The predicted IPs are IP_a/IP_v = 8.4/9.1 eV for the cyclic species and IP_a/IP_v = 10.4/10.4 eV for the linear species.[89] This represents the first time that an experimental threshold is found to be higher than the value predicted for one of the isomers (the cyclic isomer), and is in fact only slightly lower than that predicted for the linear species. For this cluster size, then, the data is consistent with the presence of the linear species in our experiment. The CTB experiment, in contrast, measured an IP of 8.09 eV.[31] As mentioned above, however, that experiment starts with mass selected cations, and thus is likely probing the cyclic structure, while our TPI experiment starts with neutral species, which should be linear. In fact, the CTB ionization potential (8.09 eV) is close to the predicted value for the cyclic species (IP_a = 8.4 eV).

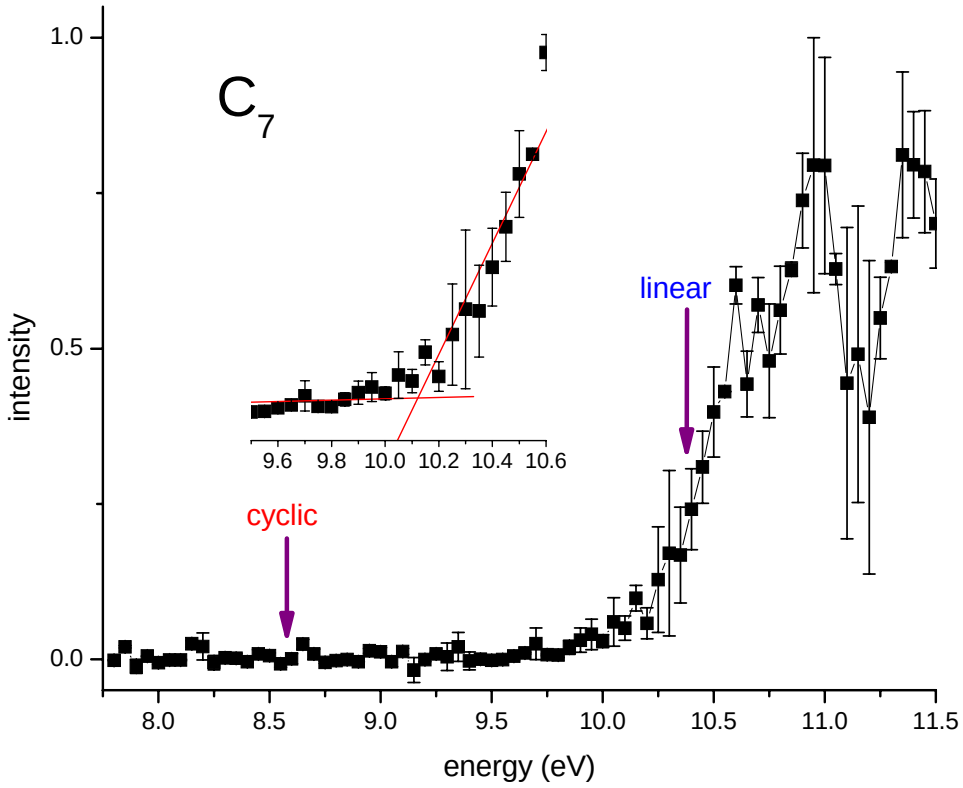

Figure 6.7: Photoionization efficiency curve in the threshold region for C_7. The arrows show the positions of the calculated vertical IP for the two different isomers. The blue lettering indicates the isomer computed to be more stable, and the red lettering indicates the less stable one.

C_8. The lowest energy structure of C_8 is predicted to be cyclic,[89] but spectroscopy in matrices have detected both the cyclic and linear isomers of the neutral[1,5,7,67-69] and cation.[78b] Ion mobility experiments on the cations have also found both isomers, but the cyclic structure was determined to be more stable.[79] The experimental threshold, derived from the photoionization efficiency spectrum shown in Figure 6.8, is 9.15 ± 0.1 eV. The predicted ionization potentials for this cluster are IP_a/IP_v = 9.2/9.3 ± 0.2 eV for the linear species and IP_a/IP_v = 8.8/9.0 ± 0.2 eV for the cyclic species.[89] Thus the experimental value falls with the error bars of both of the predicted IPs, preventing a definitive assignment of the isomer detected here. The IP derived from the CTB experiment is 8.76 eV ± 0.1 eV, which is in close agreement with the predicted value for the cyclic isomer.[31]

C_9. Much like C_7, the C_9 cluster is predicted to have a linear ground state as a neutral, while the cation favors a cyclic structure.[89] The linear neutral has been detected in several spectroscopic investigations,[1,5,7-9,62] and the linear cation has been studied by electronic spectroscopy in a rare gas matrix.[78b] Figure 6.9 shows the PIE curve for C_9, from which an experimental threshold of 9.4 eV was determined. The predicted ionization potentials for this cluster are IP_a/IP_v = 9.6/9.6 eV for the linear isomer and IP_a/IP_v = 8.4/8.8 eV for the cyclic isomer.[89] The experimental value is much higher than the predicted value for the cyclic structure, and only slightly lower than the value predicted for the linear isomer. Thus the data is consistent with the presence of predominately the linear isomer in our experiment, which should be favored by both entropy and energy. The charge-transfer bracketing experiment measured an IP of 8.76 eV,[31] which is close to that predicted for the cyclic structure. Again, that experiment

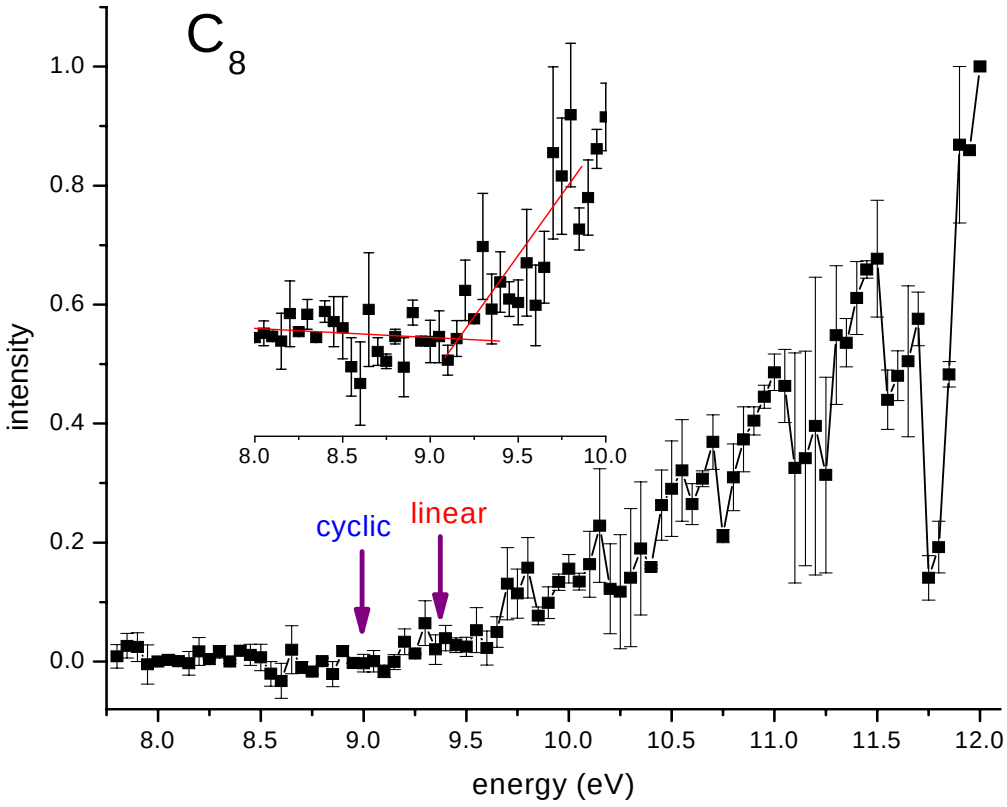

Figure 6.8: Photoionization efficiency curve in the threshold region for C_8. The arrows show the positions of the calculated vertical IP for the two different isomers. The blue lettering indicates the isomer computed to be more stable, and the red lettering indicates the less stable one.

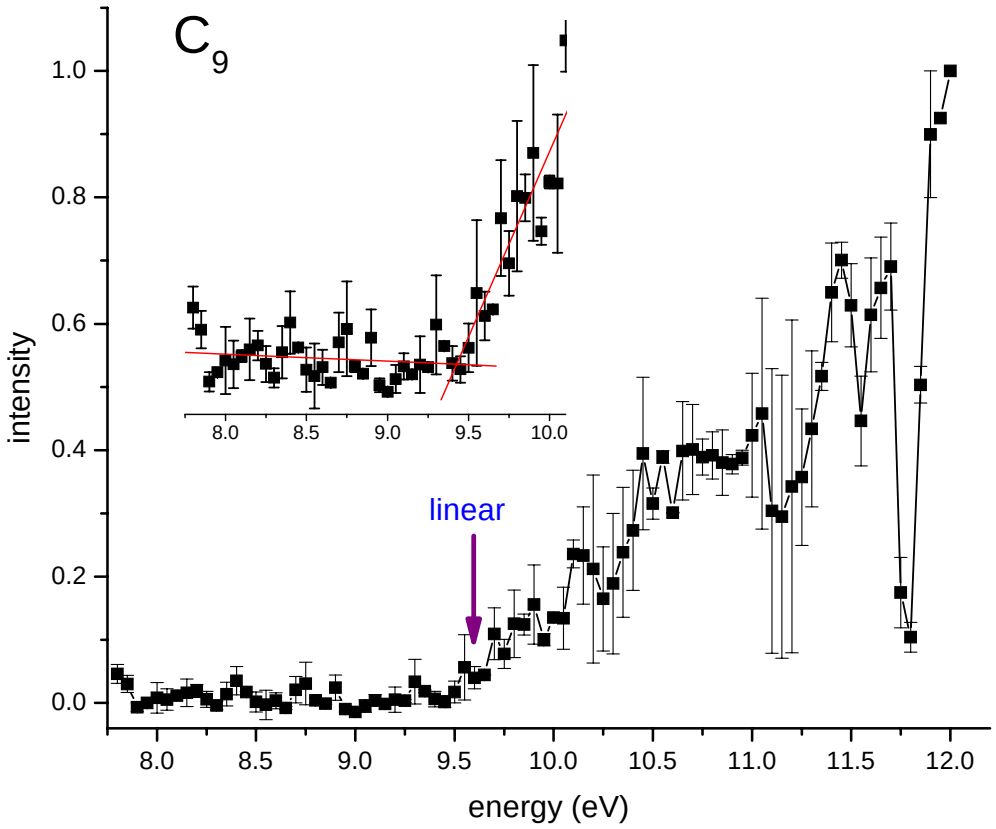

Figure 6.9: Photoionization efficiency curve in the threshold region for C_9. The arrows show the positions of the calculated vertical IP for the two different isomers. The blue lettering indicates the isomer computed to be more stable, and the red lettering indicates the less stable one.

makes measurements on cations, and the lowest energy structure of C_9^+ is thought to be cyclic.

C_{10}. The C_{10} cluster marks the first cluster size for which the ground state of both the neutral and the cation is predicted by theory to be cyclic.[1,5,7,89] The energy difference between the two isomers is significant here, computed to be 70.6 and 60.0 kcal/mol for the neutral and the cation, respectively.[89] The linear species has been detected by infrared spectroscopy in matrices and in the gas phase.[1,5,7-9,64] The only measurement on the cyclic species is an electronic transition measured in a matrix.[69] No spectroscopy exists on the cation, but ion mobility studies only detected the cyclic isomer.[79] The predicted IPs for this cluster are IP_a/IP_v = 8.8/8.8 eV for the linear structure and IP_a/IP_v = 9.2/9.5 eV for the cyclic structure.[107] The PIE spectrum, shown in Figure 6.10, gives an experimental threshold of 9.2 eV. This value very closely matches the theoretical prediction for the cyclic cluster, and is consistent with the presence of mainly this isomer in the experiment, as expected from the energetics. The CTB experiment measured an IP of 9.08 eV,[31] slightly lower than our value but also seemingly consistent with the cyclic structure.

C_{11} to C_{15}. Theory for larger cluster sizes finds both linear and cyclic isomers to be stable, but the ground state for clusters in this size regime is always predicted to be cyclic by significant amounts of energy for both neutrals and cations.[1,5] Many spectroscopy experiments have studied these clusters, however, and interestingly, most have detected only the linear isomers,[1,5-9,63,68-70] although cyclic isomers of C_{12} and C_{14} have recently been studied by electronic spectroscopy.[69] Ion mobility experiments have detected only the cyclic isomer for the cations of this size.[79] The threshold values

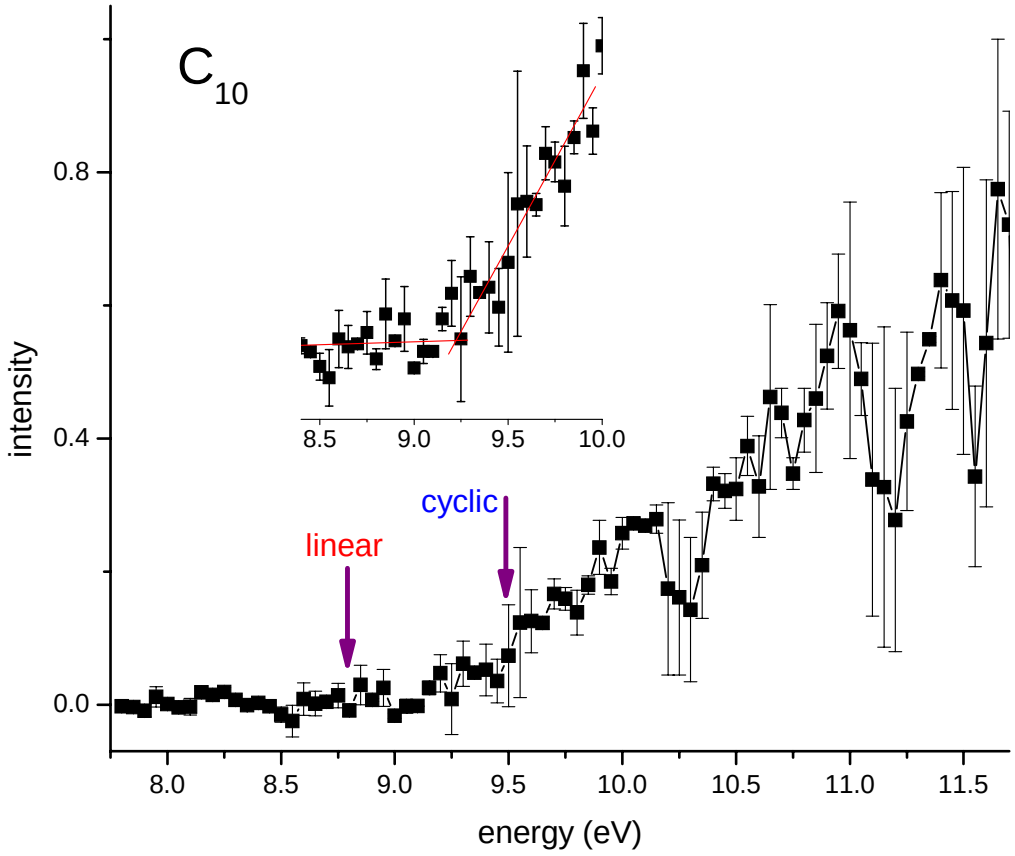

Figure 6.10: Photoionization efficiency curve in the threshold region for C_{10}. The arrows show the positions of the calculated vertical IP for the two different isomers. The blue lettering indicates the isomer computed to be more stable, and the red lettering indicates the less stable one.

from our experiment for clusters of this size are presented in Table 6.1, and the full PIE spectra are contained in the Supporting Information of reference 89. Focal point calculations could not be completed for these larger clusters, and thus the theoretical data available for these systems is limited to a study by Guiffreda et al.[55a] This work used density functional theory (DFT) with the B3LYP functional and the cc-pVDZ basis set to estimate the IPs of carbon clusters up to C_{19}. For the smaller clusters, the IPs generated by DFT are 0.2 – 0.5 eV lower than those from the focal point extrapolation method. Assuming that this trend continues at the larger sizes, some estimates of the expected IPs can be made. The DFT values for C_{11} (7.6 eV for the cyclic isomer and 8.6 eV for the linear isomer)[55a] can then be estimated to be about 8 eV and 9 eV, respectively. Our experimental value of 9.4 eV thus likely indicates the presence of the linear structure, while CTB value of 7.45 eV probably indicates the cyclic structure is present in that experiment.[31] Similar estimates can be made for $C_{12\text{-}15}$. Our experimental values for these clusters are: C_{12} = 8.4 eV; C_{13} = 9.3 eV; C_{14} = 8.7 eV; and C_{15} = 8.9 eV. Comparison to the predicted DFT values, shifted up by 0.2 – 0.5 eV, show that in our experiment, the measured threshold for C_{13} possibly corresponds to the linear isomer and C_{14} to the cyclic isomer.

Comparisons to the charge-transfer bracketing[31] values can also be made. As mentioned above, that experiment starts with cations, which are expected to strongly favor cyclic structures in this size range. Thus the assumption is made that the CTB experiment was measuring that isomer. The experimental thresholds of C_{13} and C_{15}, much like C_{11} described above, are considerably larger than the CTB values, and thus might indicate the presences of the linear isomers for those clusters in our experiment, which

was also suggested by the comparison to the values from DFT. For C_{12} and C_{14}, however, the IPs from the two experiments are similar. The TPI experiment measures 8.4 eV and 8.70 eV for the two clusters, while the CTB experiment measures 8.5 eV and 8.52 eV, respectively. Because the ionization potentials determined from both experiments are similar, they are likely measuring the same isomer, which we suggest here is the cyclic structure. Again, this also supports the conclusion drawn from the DFT comparison of a cyclic C_{14} cluster.

Figure 6.11 summarizes the experimental ionization thresholds for all the carbon clusters measured in the experiment, as well as the theoretical values predicted by the focal point extrapolation method.[89] The black squares are the experimental data. The blue (solid) symbols indicate the more stable isomer and the red (open) symbols indicate the less stable isomer, while the circles and rectangles represent the cyclic and linear isomers respectively. The experimental thresholds for C_{4-6} lie below the calculated values, but C_{7-10}, however, lie in line with the theory, allowing assignments of the structures for some cluster sizes. As outlined above, the low values measured for the ionization thresholds for the small clusters is attributed to population in excited electronic states. This excited state problem seems not to affect the larger clusters, which all have measured thresholds that lie within the predicted values for the linear and cyclic isomers.

The difference in behavior between the smaller and larger clusters can be rationalized by examining how clusters are grown and collisionally cooled. Carbon – carbon bonds are known to be strong, at least 4 – 5 eV,[30] and so all the clusters have significant condensation energy which may not be completely quenched by collisions with the helium gas in the expansion. Inefficient cooling of the clusters would leave

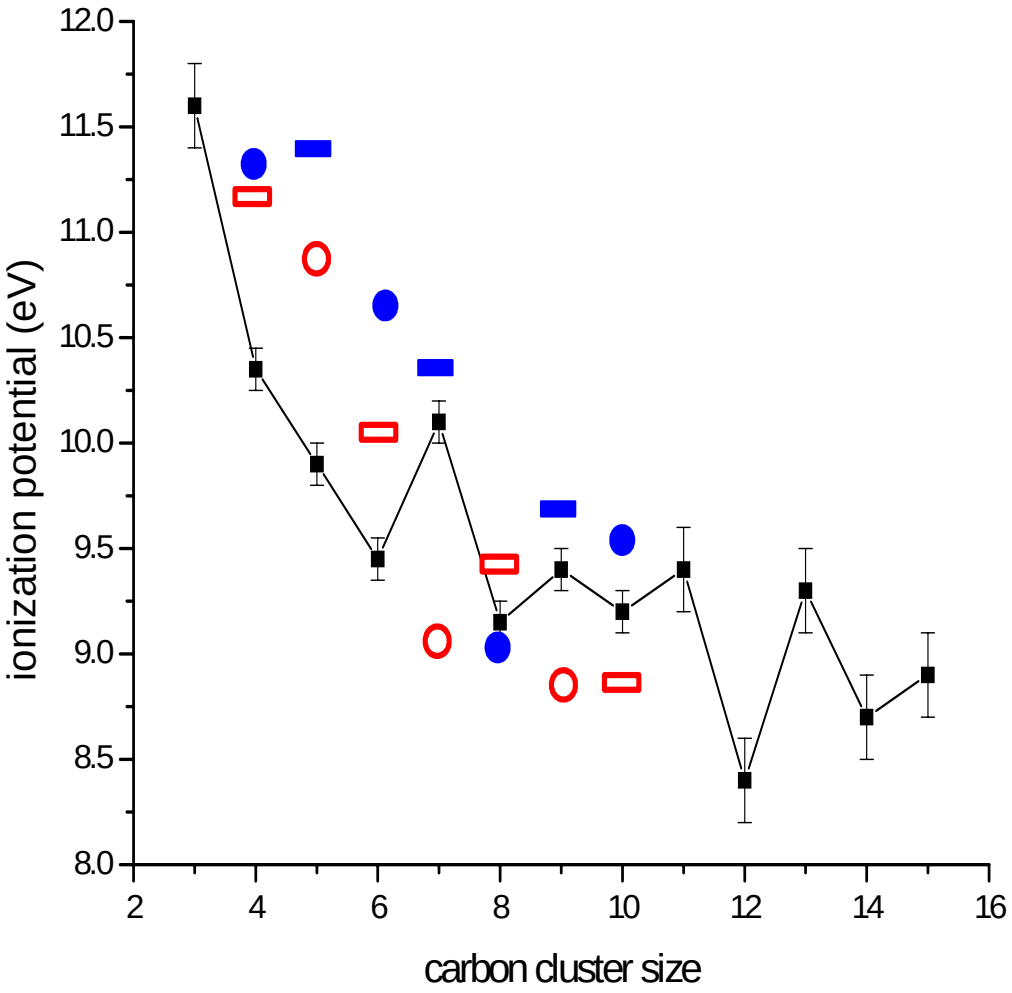

Figure 6.11: The ionization thresholds measured for these carbon clusters as a function of size compared to theoretical predictions. The blue (solid) or red (open) colors of the symbols indicate the vertical IP values for the more or less stable structures, respectively. The circle or rectangle indicates cyclic or linear species.

them with excess vibrational and electronic energy. Vibrational energy is unlikely to significantly affect the ionization potential,[87] but population in electronic excited states would cause ionization at photon energies below the true ionization potential. Excited electronic states would be populated initially in both small and large clusters, but are they are apparently relaxed more efficiently in the larger clusters. The excited states in the larger clusters will likely lie at lower energies than those in the smaller ones, and thus would be easier to relax through collisions with the helium. Also, the larger clusters will have a higher density of states than the smaller ones. This makes nonradiative processes such as internal conversion and intersystem crossing more efficient for relaxing excess electronic energy. The efficiency of these processes will affect the lifetimes of metastable excited states. Apparently these relaxation processes, due to the low density of states in the small clusters, are slow enough that they survive to influence the experiment.

6.6 CONCLUSIONS

This work reports the first investigation of the photoionization thresholds of small neutral carbon clusters, larger than C_3, using tunable VUV light from the Advanced Light Source. Clusters are produced in a molecular beam by pulsed laser vaporization, and the neutrals are studied by photoionization mass spectrometry. C_3^+ is observed to be an especially abundant in the mass spectrum at photon energies above its ionization potential, which is attributed to the high density of C_3 present in the carbon vapor produced by the laser ablation. C_2^+, however, even above the ionization potential of C_2,

was not detected in any appreciable quantity. This finding has implications for theoretical models of the growth of fullerenes and nanotubes, which currently assume C_2 to be a major species involved.[15] For the larger clusters, C_{10}^+, C_{12}^+, and C_{14}^+ were seen in the greatest intensity, similar to previous observations from photoionization at 118 nm.[32,33]

Additionally, photoionization efficiency spectra were measured for $C_{4\text{-}15}$. Comparison to new theoretical results, which optimized geometries at the CCSD(T) level with the cc-pVTZ basis set and then used focal point extrapolation to predict ionization potentials,[89] as well as previous DFT calculations,[55a] allows for the assignment of the isomers probed in the experiment for some cluster sizes. The data for $C_{4\text{-}6}$ are inconclusive due to unquenched excited states. For the larger odd numbered species, C_7, C_9, C_{11}, and C_{13}, the data suggests primarily the presence of the linear isomer. C_{10}, and possibly larger even numbered clusters, seem to show evidence for the cyclic isomer.

The results of this experiment show that a pulsed molecular beam cluster source can be successfully coupled to the quasi-continuous output of the Advanced Light Source. The tunable vacuum ultraviolet light available from the ALS will be useful in making ionization measurements of other cluster systems with high IPs where experimental data are lacking. The development of a new cluster source, currently underway, should aid in the production of clusters with much greater signal intensity, which would permit higher resolution measurements to be made on these systems. Additionally, the new source should grow clusters with lower internal energies by more effective cooling, allowing more accurate data to be collected.

Table 6.1: Photoionization Thresholds Measured Here Compared to the Predictions of Theory for Ionization Potentials and to Previous IP Values Determined from Charge Transfer and Electron Impact Experiments

cluster size	expt. threshold (eV)	focal point[a] IP_a/IP_v	charge transfer expt. IP[b]	electron impact expt. IP[c]
3	11.6 ± 0.2	----------	12.97 ± 0.1	----------
4	10.35 ± 0.1[d]	11.3 (cyclic) ± 0.1 11.1 (linear) ± 0.1	12.54 ± 0.35	11.9 ± 0.5
5	9.9 ± 0.1[d]	11.4 (linear) ± 0.2 10.8 (cyclic)± 0.2	12.26 ± 0.1	11.4 ± 0.5
6	9.45 ± 0.1[d]	10.0 (linear) ± 0.1 10.6 (cyclic) ± 0.1	9.7 ± 0.2	
7	10.1 ± 0.1	8.6 (cyclic) ± 0.1 10.4 (linear) ± 0.1	8.09 ± 0.1	
8	9.15 ± 0.1	9.0 (cyclic) ± 0.1 9.3 (linear) ± 0.1	8.76± 0.1	
9	9.4 ± 0.1	9.6 (linear) ± 0.1	8.76± 0.1	
10	9.2 ± 0.1	9.5 (cyclic) ± 0.1 8.8 (linear) ± 0.1	9.08 ± 0.1	
11	9.4 ± 0.2		7.45 ± 0.1	
12	8.4 ± 0.2		8.50 ± 0.1	
13	9.3 ± 0.2		8.09 ± 0.1	
14	8.7 ± 0.2		8.52 ± 0.1	
15	8.9 ± 0.2		7.2 ± 0.3	

[a] Ref. 89, [b]Ref. 31, [c]Ref. 86, [d]These threshold values are believed to be lower than the true ionization potentials because of the presence of unquenched excited states.

6.6 REFERENCES

(1) Weltner, W., Jr.; Van Zee, R. J. *Chem. Rev*. **1989**, *89*, 1713.

(2) Kroto, H. W.; Allaf, A. W.; Balm, S. P. *Chem. Rev.* **1991**, *91*, 1213.

(3) Billups, W. E.; Ciufolini, M. A. *Buckminsterfullerenes*; VCH Publishers: New York, 1993.

(4) Dresselhaus, M. S.; Dresselhaus, G.; Eklund, P. C. *Science of Fullerenes and Carbon Nanotubes*; Academic Press: San Diego, CA, 1996.

(5) Van Orden, A.; Saykally, R. J. *Chem. Rev.* **1998**, *98*, 2313.

(6) Lifshitz, C. *Int. J. Mass Spectrom.* **2000**, *200*, 423.

(7) Weltner, W., Jr.; Van Zee, R. J. *J. Mol. Struct.* **1990**, *222*, 20.

(8) Maier, J. P. *J. Phys. Chem. A* **1998**, *102*, 3462.

(9) Kirkwood, D. A.; Linnartz, H.; Grutter, M.; Dopfer, O.; Motylewski, C. T.; Pachkov, M.; Tulej, M.; Wyss, M.; Maier, J. P. *Faraday Discuss.* **1998**, *109*, 109.

(10) Maier, J. P.; Walker, G. A. H.; Bohlender, D. A. *Astrophys. J.* **2004**, *602*, 286.

(11) Thaddeus, P.; McCarthy, M. C. *Spectrochim. Acta A* **2001**, *57A*, 757.

(12) Hartquist, T. W., Williams, D. A., Eds. *The Molecular Astrophysics of Stars and Galaxies*; Clarendon Press: Oxford, 1998.

(13) Gardiner, W. C. *Combustion Chemistry*; Springer-Verlag: New York, 1984.

(14) Strout, D. L.; Scuseria, G. E. *J. Phys. Chem.* **1996**, *100*, 6492.

(15) (a) Zheng, G.; Irle, S.; Elstner, M.; Morokuma, K. *J. Phys. Chem. A* **2004**, *108*, 3182. (b) Irle, S.; Zheng, G.; Wang, Z.; Morokuma, K. *J. Phys. Chem. B* **2006**, *110*, 14531.

(16) Rohlfing, E. A.; Cox, D. M.; Kaldor, A. *J. Chem. Phys.* **1984**, *81*, 3322.

(17) Kroto, H. W.; Heath, J. R.; O'Brien, S. C.; Curl, R. F.; Smalley, R. E. *Nature* **1985**, *318*, 162. (b) Curl, R. F.; Smalley, R. E. *Science* **1988**, *242*, 1017.

(18) Hahn, M. Y.; Honea, E. C.; Paguia, A. J.; Schriver, K. E.; Camarena, A. M.; Whetten, R. L. *Chem. Phys. Lett.* **1986**, *130*, 12.

(19) Rohlfing, E. A. *J. Chem. Phys.* **1990**, *93*, 7851.

(20) Moriwaki, T.; Kobayashi, K.; Osaka, M.; Ohara, M.; Shiromaru, H.; Achiba, Y. *J. Chem. Phys.* **1997**, *107*, 8927.

(21) Choi, Y.-K.; Im, H.-S.; Jung, K.-W. *Int. J. Mass Spectrom.* **1999**, *189*, 115.

(22) Bae, C. H.; Park, S. M. *J. Chem. Phys.* **2002**, *117*, 5347.

(23) (a) Geusic, M. E.; Jarrold, M. F.; McIlrath, T. J.; Bloomfield, L. A.; Freeman, R. R.; Brown, W. L. *Z. Phys. D: At., Mol. Clusters* **1986**, *3*, 309. (b) Geusic, M. E.; McIlrath, T. J.; Jarrold, M. F.; Bloomfield, L. A.; Freeman, R. R.; Brown, W. L. *J. Chem. Phys.* **1986**, *84*, 2421. (c) Geusic, M. E.; Jarrold, M. F.; McIlrath, T. J.; Freeman, R. R.; Brown, W. L. *J. Chem. Phys.* **1987**, *86*, 3862.

(24) O'Brien, S. C.; Heath, J. R.; Curl, R. F.; Smalley, R. E. *J. Chem. Phys.* **1988**, *88*, 220.

(25) Sowa, M. B.; Hintz, P. A.; Anderson, S. L. *J. Chem. Phys.* **1991**, *95*, 4719.

(26) Bouyer, R.; Roussel, F.; Monchicourt, P.; Perdix, M.; Pradel, P. *J. Chem. Phys.* **1994**, *100*, 8912.

(27) (a) Pozniak, B. P.; Dunbar, R. C. *Int. J. Mass Spectrom. Ion Processes* **1997**, *165/166*, 299. (b) Pozniak, B.; Dunbar, R. C. *Int. J. Mass Spectrom. Ion Processes* **1994**, *133*, 97.

(28) Radi, P. P.; Bunn, T. L.; Kemper, P. R.; Molchan, M. E.; Bowers, M. T. *J. Chem. Phys.* **1988**, *88*, 2809.

(29) (a) Gluch, K.; Matt-Leubner, S.; Echt, O.; Concina, B.; Scheier, P.; Mark, T. D. *J. Chem. Phys.* **2004**, *121*, 2137. (b) Concina, B.; Gluch, K.; Matt-Leubner, S.; Echt, O.; Scheier, P.; Mark, T. D. *Chem. Phys. Lett.* **2005**, *407*, 464.

(30) Sowa-Resat, M. B.; Hintz, P. A.; Anderson, S. L. *J. Phys. Chem.* **1995**, *99*, 10736.

(31) (a) Bach, S. B. H.; Eyler, J. R. *J. Chem. Phys.* **1990**, *92*, 358. (b) Ramanathan, R.; Zimmerman, J. A.; Eyler, J. R. *J. Chem. Phys.* **1993**, *98*, 7838.

(32) Kaizu, K.; Kohno, M.; Suzuki, S.; Shiromaru, H.; Moriwaki, T.; Achiba, Y. *J. Chem. Phys.* **1997**, *106*, 9954.

(33) (a) Wakabayashi, T.; Momose, T.; Shida, T. *J. Chem. Phys.* **1999**, *111*, 6260. (b) Kato, Y.; Wakabayashi, T.; Momose, T. *J. Chem. Phys.* **2003**, *118*, 5390.

(34) (a) Magers, D. H.; Harrison, R. J.; Bartlett, R. J. *J. Chem. Phys.* **1986**, *84*, 3284. (b) Watts, J. D.; Gauss, J.; Stanton, J. F.; Bartlett, R. J. *J. Chem. Phys.* **1992**, *97*, 8372.

(35) (a) Raghavachari, K.; Whiteside, R. A.; Pople, J. A. *J. Chem. Phys.* **1986**, *85*, 6623. (b) Raghavachari, K.; Binkley, J. S. *J. Chem. Phys.* **1987**, *87*, 2191.

(36) (a) Martin, J. M. L.; Francois, J-P.; Gijbels, R. *J. Chem. Phys.* **1989**, *90*, 3403. (b) Martin, J. M. L.; Francois, J.-P.; Gijbels, R. *J. Chem. Phys.* **1990**, *93*, 8850. (c) Martin, J. M. L.; Francois, J.-P.; Gijbels, R. *J. Chem. Phys.* **1991**, *94*, 3753. (d) Martin, J. M. L.; Francois, J.-P.; Gijbels, R. *J. Chem. Phys.* **1991**, *95*, 9420.

(37) Parasuk, V.; Almlof, J. *J. Chem. Phys.* **1989**, *91*, 1137.

(38) (a) Liang, C.; Schaefer, H. F. *Chem. Phys. Lett.* **1990**, *169*, 150. (b) Liang, C.; Schaefer, H. F. *J. Chem. Phys.* **1990**, *93*, 8844.

(39) Ortiz, J. V.; Zakrzewski, V. G. *J. Chem. Phys.* **1994**, *100*, 6614.

(40) Hutter, J.; Luthi, H. P.; Diederich, F. *J. Am. Chem. Soc.* **1994**, *116*, 750.

(41) Schmatz, S.; Botschwina, P. *Chem. Phys. Lett.* **1995**, *235*, 5.

(42) (a) Martin, J. M. L.; Taylor, P. R. *Chem. Phys. Lett.* **1995**, *240*, 521. (b) Martin, J. M. L.; Elyazal, J.; Francois, J.-P. *Chem. Phys. Lett.* **1995**, *242*, 570. (c) Martin, J. M. L.; Taylor, P. R. *J. Chem. Phys.* **1995**, *102*, 8270. (d) Martin, J. M. L.; Taylor, P. R. *J. Phys. Chem.* **1996**, *100*, 6047. (e) Martin, J. M. L.; Schwenke, D. W.; Lee, T. J.; Taylor, P. R. *J. Chem. Phys.* **1996**, *104*, 4657.

(43) Martin, J. M. L.; El-Yazal, J.; Francois, J.-P. *Chem. Phys. Lett.* **1996**, *252*, 9.

(44) Ohno, M.; Zakrzewski, V. G.; Ortiz, J. V.; von Niessen, W. *J. Chem. Phys.* **1997**, *106*, 3258.

(45) Valdes, E. A.; De La Mora, P.; Castro, M.; Keller, J. *Int. J. Quantum Chem.* **1997**, *65*, 867.

(46) (a) Hanrath, M.; Peyerimhoff, S. D.; Grein, F. *Chem. Phys.* **1999**, *249*, 121. (b) Muhlhauser, M.; Froudakis, G. E.; Hanrath, M.; Peyerimhoff, S. D. *Chem. Phys. Lett.* **2000**, *324*, 195. (c) Muhlhauser, M.; Froudakis, G. E.; Peyerimhoff, S. D. *Chem. Phys. Lett.* **2001**, *336*, 171. (d) Grein, F.; Franz, J.; Hanrath, M.; Peyerimhoff, S. D. *Chem. Phys.* **2001**, *263*, 55. (e) Muhlhauser, M.; Froudakis, G. E.; Peyerimhoff, S. D. *Phys. Chem. Chem. Phys.* **2001**, *3*, 3913. (f) Hanrath, M.; Peyerimhoff, S. D. *Chem. Phys. Lett.* **2001**, *337*, 368. (g) Cao, Z. X.;

Muhlhauser, M.; Hanrath, M.; Peyerimhoff, S. D. *Chem. Phys. Lett.* **2002**, *351*, 327.

(47) Giuffreda, M. G.; Deleuze, M. S.; Francois, J.-P.; Trofimov, A. B. *Int. J. Quantum Chem.* **2001**, *85*, 475.

(48) Jo, C.; Lee, K. *J. Korean Phys. Soc.* **2002**, *41*, 200.

(49) Baranovski, V. I. *Chem. Phys. Lett.* **2005**, *408*, 429.

(50) Martin, J. M. L.; Francois, J. P.; Gijbels, R. *J. Chem. Phys.* **1990**, *93*, 5037.

(51) Scuseria, G. E. *Chem. Phys. Lett.* **1991**, *176*, 27.

(52) Watts, J. D.; Stanton, J. F.; Gauss, J.; Bartlett, R. J. *J. Chem. Phys.* **1991**, *94*, 4320.

(53) (a) Schnell, M.; Muhlhauser, M.; Froudakis, G. E.; Peyerimhoff, S. D. *Chem. Phys. Lett.* **2001**, *340*, 559. (b) Haubrich, J.; Muhlhauser, M.; Peyerimhoff, S. D. *Phys. Chem. Chem. Phys.* **2002**, *4*, 2891. (c) Haubrich, J.; Muhlhauser, M.; Peyerimhoff, S. D. *J. Mol. Spec.* **2004**, *228*, 31.

(54) Gillery, C.; Rosmus, P.; Werner, H. J.; Stoll, H.; Maier, J. P. *Mol. Phys.* **2004**, *102*, 2227.

(55) (a) Giuffreda, M. G.; Deleuze, M. S.; Francois, J.-P. *J. Phys. Chem. A* **1999**, *103*, 5137. (b) Deleuze, M. S.; Giuffreda, M. G.; Francois, J.-P.; Cederbaum, L. S. *J. Chem. Phys.* **1999**, *111*, 5851. (c) Deleuze, M. S.; Giuffreda, M. G.; Francois, J.-P.; Cederbaum, L. S. *J. Chem. Phys.* **2000**, *112*, 5325. (d) Deleuze, M. S.; Giuffreda, M. G.; Francois, J.-P. *J. Phys. Chem. A* **2002**, *106*, 5626.

(56) Diaz-Tendero, S.; Martin, F.; Alcami, M. *J. Phys. Chem. A* **2002**, *106*, 10782

(57) Orlova, G.; Goddard, J. D. *Chem. Phys. Lett.* **2002**, *363*, 486.

(58) Schmatz, S.; Botschwina, P. *Int. J. Mass Spectrom. Ion Processes* **1995**, *150*, 621.

(59) Cao, Z. X.; Peyerimhoff, S. D.; Grein, F.; Zhang, Q. *J. Chem. Phys.* **2001**, *115*, 2062.

(60) Lepine, F.; Allouche, A. R.; Baguenard, B.; Bordas, C.; Aubert-Frecon, M. *J. Phys. Chem. A* **2002**, *106*, 7177.

(61) Giuffreda, M. G.; Deleuze, M. S.; Francois, J.-P. *J. Phys. Chem. A* **2002**, *106*, 8569.

(62) (a) Motylewski, T.; Vaizert, O.; Giesen, T. F.; Linnartz, H.; Maier, J. P. *J. Chem. Phys.* **1999**, *111*, 6161. (b) Linnartz, H.; Vaizert, O.; Motylewski, T.; Maier, J. P. *J. Chem. Phys.* **2000**, *112*, 9777. (c) Boguslavskiy, A. E.; Maier, J. P. *J. Chem. Phys.* **2006**, *125*, 094308.

(63) Wyss, M.; Grutter, M.; Maier, J. P. *Chem. Phys. Lett.* **1999**, *304*, 35.

(64) (a) Giesen, T. F.; Berndt, U.; Yamada, K. M. T.; Fuchs, G.; Schieder, R.; Winnewisser, G.; Provencal, R. A.; Keutsch, F. N.; Van Orden, A.; Saykally, R. J. *Chem. Phys. Chem.* **2001**, *2*, 242. (b) Neubauer-Guenther, P.; Giesen, T. F.; Berndt, U.; Fuchs, G.; Winnewisser, G. *Spectrochim. Acta, Part A* **2003**, *59*, 431.

(65) (a) Cermak, I.; Forderer, M.; Cermakova, I.; Kalhofer, S.; Stopka-Ebeler, H.; Monninger, G.; Kratschmer, W. *J. Chem. Phys.* **1998**, *108*, 10129. (b) Monninger, G.; Forderer, M.; Gurtler, P.; Kalhofer, S.; Petersen, S.; Nemes, L.; Szalay, P. G.; Kratschmer, W. *J. Phys. Chem. A* **2002**, *106*, 5779.

(66) Lapinski, L.; Vala, M. *Chem. Phys. Lett.* **1999**, *300*, 195.

(67) Presilla-Marquez, J. D.; Harper, J.; Sheehy, J. A.; Carrick, P. G.; Larson, C. W.

Chem. Phys. Lett. **1999**, *300*, 719.

(68) (a) Wang, S. L.; Rittby, C. M. L.; Graham, W. R. M. *J. Chem. Phys.* **2000**, *112*, 1457. (b) Ding, X. D.; Wang, S. L.; Rittby, C. M. L.; Graham, W. R. M. *J. Chem. Phys.* **2000**, *112*, 5113.

(69) (a) Grutter, M.; Wyss, M.; Riaplov, E.; Maier, J. P.; Peyerimhoff, S. D.; Hanrath, M. *J. Chem. Phys.* **1999**, *111*, 7397. (b) Boguslavskiy, A. E.; Maier, J. P. *Phys. Chem. Chem. Phys.* **2007**, *9*, 127.

(70) (a) Ott, A. K.; Rechtsteiner, G. A.; Felix, C.; Hampe, O.; Jarrold, M. F.; Van Duyne, R. P.; Raghavachari, K. *J. Chem. Phys.* **1998**, *109*, 9652. (b) Rechtsteiner, G. A.; Felix, C.; Ott, A. K.; Hampe, O.; Van Duyne, R. P.; Jarrold, M. F.; Raghavachari, K. *J. Phys. Chem. A* **2001**, *105*, 3029.

(71) Tulej, M.; Kirkwood, D. A.; Maccaferri, G.; Dopfer, O.; Maier, J. P. *Chem. Phys.* **1998**, *228*, 293.

(72) (a) Ohara, M.; Suwa, M.; Ishigaki, T.; Shiromaru, H.; Achiba, Y.; Kratschmer, W. *J. Chem. Phys.* **1998**, *109*, 1329. (b) Ohara, M.; Kasuya, D.; Shiromaru, H.; Achiba, Y. *J. Phys. Chem. A* **2000**, *104*, 8622.

(73) (a) Lakin, N. M.; Pachkov, M.; Tulej, M.; Maier, J. P.; Chambaud, G.; Rosmus, P. *J. Chem. Phys.* **2000**, *113*, 9586. (b) Lakin, N. M.; Guthe, F.; Tulej, M.; Pachkov, M.; Maier, J. P. *Faraday Discuss.* **2000**, *115*, 383.

(74) Kohno, M.; Suzuki, S.; Shiromaru, H.; Moriwaki, T.; Achiba, Y. *Chem. Phys. Lett.* **1998**, *282*, 330.

(75) Fromherz, R.; Gantefor, G.; Shvartsburg, A. A. *Phys. Rev. Lett.* **2002**, *89*, 083001.

(76) (a) Arnold, D. W.; Bradforth, S. E.; Kitsopoulos, T. N.; Neumark, D. M. *J. Chem. Phys.* **1991**, *95*, 8753. (b) Xu, C.; Burton, G. R.; Taylor, T. R.; Neumark, D. M. *J. Chem. Phys.* **1997**, *107*, 3428. (c) Frischkorn, C.; Bragg, A. E.; Davis, A. V.; Wester, R.; Neumark, D. M. *J. Chem. Phys.* **2001**, *115*, 11185.

(77) Szczepanski, J.; Hodyss, R.; Vala, M. *J. Phys. Chem. A* **1998**, *102*, 8300.

(78) (a) Fulara, J.; Riaplov, E.; Batalov, A.; Shnitko, I.; Maier, J. P. *J. Chem. Phys.* **2004**, *120*, 7520. (b) Fulara, J.; Shnitko, I.; Batalov, A.; Maier, J. P. *J. Chem. Phys.* **2005**, *123*, 044305.

(79) (a) von Helden, G.; Hsu, M. T.; Kemper, P. R.; Bowers, M. T. *J. Chem. Phys.* **1991**, *95*, 3835. (b) von Helden, G.; Hsu, M. T.; Gotts, N.; Bowers, M. T. *J. Phys. Chem.* **1993**, *97*, 8182. (c) von Helden, G.; Gotts, N. G.; Bowers, M. T. *J. Am. Chem. Soc.* **1993**, *115*, 4363. (d) von Helden, G.; Gotts, N. G.; Bowers, M. T. *Chem. Phys. Lett.* **1993**, *212*, 241. (e) von Helden, G.; Palke, W. E.; Bowers, M. T. *Chem. Phys. Lett.* **1993**, *212*, 247. (f) Gotts, N. G.; von Helden, G.; Bowers, M. T. *Int. J. Mass Spectrom. Ion Processes* **1995**, *149/150*, 217.

(80) (a) Hunter, J. M.; Fye, J. L.; Roskamp, E. J.; Jarrold, M. F. *J. Phys. Chem.* **1994**, *98*, 1810. (b) Shvartsburg, A. A.; Hudgins, R. R.; Dugourd, P.; Gutierrez, R.; Frauenheim, T.; Jarrold, M. F. *Phys. Rev. Lett.* **2000**, *84*, 2421.

(81) Nicolas, C.; Shu, J. N.; Peterka, D. S.; Hochlaf, M.; Poisson, L.; Leone, S. R.; Ahmed, M. *J. Am. Chem. Soc.* **2006**, *128*, 220.

(82) Metz, R. B.; Ahmed, M.; Leone, S. R. *J. Chem. Phys.* **2005**, *123*, 114313.

(83) Heimann, P. A.; Koike, M.; Hsu, C. W.; Blank, D.; Yang, X. M.; Suits, A. G.;

Lee, Y. T.; Evans, M.; Ng, C. Y.; Flaim, C.; Padmore, H. A. *Rev. Sci. Instrum.* **1997**, *68*, 1945.

(84) NIST Chemistry WebBook, NIST Standard Reference Database Number 69, June 2005 (http://webbook.nist.gov/chemistry/).

(85) Reid, C. J.; Ballantine, J. A.; Andrews, S. R.; Harris, F. M. *Chem. Phys.* **1995**, *190*, 113.

(86) Benedikt, J.; Agarwal, S.; Eijkman, D.; Vandamme, W.; Creatore, M.; van de Sanden, M. C. M. *J. Vac. Sci. Technol. A* **2005**, *23*, 1400.

(87) Ruscic, B. *Res. Adv. Phys. Chem.* **2000**, *1*, 39.

(88) Hochlaf, M.; Nicolas, C.; Poisson, L. *J. Chem. Phys.* **2007**, *127*, 014310.

(89) Belau, L.; Wheeler, S. E.; Ticknor, B. W.; Ahmed, M.; Leone, S. R.; Allen, W. D.; Schaefer, H. F., III; Duncan, M. A. *J. Am. Chem. Soc.* **2007**, *129*, 10229.

CHAPTER 7

CONCLUSIONS

Clusters of carbon, noble metal carbides, and silicon carbide are produced in a laser vaporization pulsed nozzle cluster source and investigated with time-of-flight mass spectrometry and mass-selected photodissociation. The photoionization behavior of neutral carbon clusters with tunable vacuum ultraviolet light is also reported. The results of these studies give insight into the structures, energetics, and bonding that occur in these novel systems.

Carbon clusters have been produced by laser ablation at 532 nm and studied by mass spectrometry in numerous investigations, and the results presented here are entirely consistent with previous work.[1,2] The carbon cations produced in our experiments show the expected enhanced abundance for sizes corresponding to 4n -1 carbon atoms (C_3^+, C_7^+, C_{11}^+, C_{15}^+, C_{19}^+). The dissociation behavior of carbon cations is also studied here. The clusters require multiphoton absorption to dissociate, consistent with the strong carbon – cabon bonding in these systems (5-7 eV).[3] The fragmentation patterns observed here at 355 nm are also consistent with previous work. Small clusters up to at least 20 atoms fragment predominately by the loss of neutral C_3. However, we report here for the first time the use use of tunable lasers to measure resonance enhanced photodissociation spectra of C_6^+ and C_8^+ from 620 – 660 nm. The dissociation of carbon clusters with red visible light has not been previously reported. The resonance enhanced fragmentation takes place on top of a wavelength independent fragmentation background, likely due to an internally hot fraction of the clusters. The background fragmentation, combined with the fact that carbon clusters are well known to have many allowed transitions to a number of low lying excited states,[4-7] greatly complicates the interpretation of the measured spectra. The reported spectra are thus not assigned to specific transitions. Interestingly,

however, both species showed an enhancement in the photodissociation yield very near the location of a well known diffuse interstellar band at 628.4 nm. This exciting result shows the promise that measuring high resolution gas phase spectra for carbon cations holds for comparison to astronomical data. A study of the infrared resonance enhanced photodissociation spectra of C_5^+ and C_7^+ yielded negative results, consistent with the expected high bond energies in these systems.

The measurement of both the electronic and infrared spectra of carbon cations will be facilitated by a cold source, currently under development in our lab. This source will precool the expansion gas and cool the sample rod holder, which should produce clusters with lower internal energy. The quenching of internal energy in the clusters may allow more sensitive detection of the resonance enhanced dissociation signal for carbon species at visible wavelengths. Concentrating a higher percentage of the cluster population in the electronic and vibrational ground state of the species should lead to better resolved transitions and less complicated spectra.

A cold source may also allow the use of the rare gas tagging technique,[8-12] which would aid in the measurement of infrared resonance enhanced photodissociation spectra. In this method, a weakly bound rare gas atom is attached to a cluster. Upon vibrational excitation, intramolecular vibrational redistribution leads to dissociation via elimination of the rare gas atom. The infrared spectrum is measured by monitoring the appearance of the rare gas atom fragment as a function of wavelength.

Another recent experimental advance in our laboratory is the acquisition of a $AgGaSe_2$ crystal, which extends the wavelength range of our infrared laser down to 650 cm^{-1}. Previously, only the wavelength range of 2000 – 4500 cm^{-1} was accessible. All

small carbon clusters are predicted to have infrared active vibrations in the wavelength range of the $AgGaSe_2$ crystal, so the tunability of the laser will no longer be an impediment to the measurement of infrared spectra for these species.

Carbon clusters doped with noble metal (Cu, Au) ions are produced in a pulsed nozzle laser vaporization source and mass analyzed in a reflectron time-of-flight mass spectrometer. Copper carbides favor the formation of species with an odd number of carbon atoms, while the gold carbides show a drop in ion signal after clusters with 3, 6, 9, and 12 carbons. The appearance of the mass spectra for both the copper and the gold carbides is significantly different from that of pure carbon clusters, which indicates that the presence of the metal ion is affecting the cluster distribution. These clusters are mass selected and photodissiciated with 355 nm light. An even odd alternation in fragmentation patterns is evident for both metals. Species with an odd number of carbons fragment by loss of the entire carbon cluster, while the even numbered ones show significant loss of C_3. This behavior is seen in clusters as big as CuC_{30}^+. Even for the largest cluster studied here, CuC_{43}^+, no loss of C_2 is observed, indicating that fullerene formation does not occur.

Because the metal – carbon bonding (2-4 eV)[13] is expected to be weaker than carbon – carbon (5-7 eV)[3] bonding, the elimination of C_3 to leave behind a mixed metal carbon fragment from any parent ion was initially surprising. We employed density functional theory to predict the lowest energy isomers and the dissociation energies for small ($CuC_{3\text{-}11}^+$) copper carbides. The results showed that for all clusters in this size regime, with the exception of CuC_{10}^+, the lowest energy isomer is a linear carbon chain with an attached metal ion. CuC_{10}^+, however, is a cyclic carbon cluster with the metal

ion attached to one of the carbons. These results of these predictions suggest that the presence of the metal ion does not significantly affect the structure of the carbon. It appears as if the carbon cluster forms in its preferred structure and then binds the metal to the end. The results of the dissociation energy calculations reveal a strong even odd alternation, consistent with the experimental results. The binding energy of linear CuC_3^+ and CuC_5^+ is found to be 2.35 eV and 2.87 eV, respectively. In the CuC_4^+ and CuC_6^+ clusters, the binding energy is predicted to be 7.00 eV and 7.21 eV, respectively. The even numbered species thus have dissociation energies predicted to be as high, or higher, than those of pure carbon clusters. This explains the fact that C_3 elimination from these clusters is a competitive fragmentation channel with metal ion elimination. The DFT predictions also show that the even clusters are triplet states while the odd ones are singlet states, which may explain the large differences in dissociation energy between the two species.

Future work on these species could examine additional examples of transition metals bound to carbon. The more reactive early transition metals may form quite different structures when clustered with carbon as compared to the noble metals. This has already been seen with metallocarbohedrenes, which form easily from the early transition metals but not with later transition metals or main group metals. Infrared spectroscopy, likely using the rare gas tagging method outlined above, would also be a sensitive experimental probe of the structure of these species. Cyclic and linear isomers of carbon are predicted to have different infrared active vibrations. The strong bonding to the metal displayed by the even numbered species would likely shift the vibrations

away from those found for pure carbon clusters, while the vibrations in the odd numbered ones, with weaker metal-carbon bonding, may be less perturbed.

Silicon carbide clusters of the form $Si_nC_m^+$ (n = 3-10, m = 1-2) are produced in a pulsed nozzle laser vaporization source and mass analyzed in a reflectron time-of-flight mass spectrometer. Si_3C^+ and Si_7C^+ are both seen in great intensity, perhaps indicating enhanced relative stability for these species. The ions are mass selected and photodissociated at 355 nm. These fragmentation studies reveal Si_3C^+ to be a common fragmentation product from several larger species. The larger clusters (Si_{8-10}^+) fragment by the elimination of both Si_2C and Si_3C, which indicates that these neutrals have high relative stability as well. Small silicon and carbon containing species of this type have been previously detected in astronomical searches, and the results of this investigation suggest that Si_3C^+, Si_2C, and Si_3C, all of which are stable and fragmentation products of larger silicon carbide clusters, would be interesting targets for astrophysics.

In experiments at the Advanced Light Source (ALS) at Lawerence Berkeley National Laboratory, neutral carbon clusters produced in a pulsed nozzle laser vaporization source are studied by vacuum ultraviolet (VUV) photoionization mass spectrometry. Mass spectra obtained at various photon wavelengths reveal for the first time the nascent distribution of carbon cluster neutrals produced in a laser ablation source. The results show that the density of C_3 in this experiment is extremely high, while no appreciable quantities of C_2 were detected. This finding has serious implications for theoretical models of fullerene growth, many of which presently assume high abundances of C_2 in laser plasmas.[14] Photoionization efficiency spectra were measured by stepping the ALS from 8.0 – 12.0 eV and recording mass spectra at every

photon wavelength. The ionization thresholds determined in this way are compared to previous charge-transfer bracketing[15] and electron impact ionization[16] experiments, as well as to high level ab initio calculations.[17] The results allow for the determination of the isomeric structure present in the experiment for some cluster sizes. C_7, C_9, C_{11}, and C_{13} are found to be present predominately as linear structures, while C_{10} is likely present in cyclic form, and possibly larger even numbered clusters as well.

The success of this experiment shows that a pulsed molecular beam cluster source can be coupled to a quasi-continuous light source such as the ALS. No other source offers tunable VUV light at the powers necessary for these types of experiments. Many other systems with high IPs can be studied in this way. Elemental clusters such as gold are known to have IPs in the range of the ALS, and have never been accurately measured before. The IPs of many metal oxide clusters are also in the 8 – 10 eV range, and would thus be ideal candidates for future studies. The development of an improved source, currently underway at the ALS, may allow for the realization of these goals.

7.1 REFERENCES

(1) Weltner, Jr., W.; Van Zee, R. J. *Chem. Rev.* **1994**, *89*, 1713.

(2) Van Orden, A.; Saykally, R. J. *Chem. Rev*. **1998**, *98*, 2313.

(3) Sowa-Resat, M. B.; Hintz, P. A.; Anderson, S. L. *J. Phys. Chem.* **1995**, *99*, 10736.

(4) (a) Schnell, M.; Muhlhauser, M.; Froudakis, G. E.; Peyerimhoff, S. D. *Chem.*

Phys. Lett. **2001**, *340*, 559. (b) Haubrich, J.; Muhlhauser, M.; Peyerimhoff, S. D. *Phys. Chem. Chem. Phys.* **2002**, *4*, 2891. (c) Haubrich, J.; Muhlhauser, M.; Peyerimhoff, S. D. *J. Mol. Spectrosc.* **2004**, *228*, 31.

(5) Gillery, C.; Rosmus, P.; Werner, H. J.; Stoll, H.; Maier, J. P. *Mol. Phys.* **2004**, *102*, 2227.

(6) Nicolas, C.; Shu, J. N.; Peterka, D. S.; Hochlaf, M.; Poisson, L.; Leone, S. R.; Ahmed, M. *J. Am. Chem. Soc.* **2006**, *128*, 220.

(7) Hochlaf, M.; Nicolas, C.; Poisson, L. *J. Chem. Phys.* **2007**, *127*, 014310.

(8) Duncan, M. A.; *Int. J. Mass Spectro*. **2000**, *200*, 545.

(9) Duncan, M. A.; *Int. Rev. Phys. Chem.* **2003**, *2*, 407.

(10) Yeh, L. I.; Okumura, M.; Myers, J. D.; Price, J. M.; Lee, Y. T. *J. Chem. Phys.* **1989**, *91*, 7319.

(11) Okumura, M.; Yeh, L. I.; Myers, J. D.; Lee, Y. T. *J. Phys. Chem.* **1990**, *94*, 3416.

(12) Ebata, T.; Fujii, A.; Mikami, N. *Int. Rev. Phys. Chem.* **1998**, *17*, 331.

(13) Gutsev, G. L.; Andrews, L.; Bauschlicher, C. W. Jr. *Theor. Chem. Acc.* **2003**, *109*, 298.

(14) (a) Zheng, G.; Irle, S.; Elstner, M.; Morokuma, K. *J. Phys. Chem. A* **2004**, *108*, 3182. (b) Irle, S.; Zheng, G.; Wang, Z.; Morokuma, K. *J. Phys. Chem. B* **2006**, *110*, 14531.

(15) (a) Bach, S. B. H.; Eyler, J. R. *J. Chem. Phys.* **1990**, *92*, 358. (b) Ramanathan, R.; Zimmerman, J. A.; Eyler, J. R. *J. Chem. Phys.* **1993**, *98*, 7838.

(16) Benedikt, J.; Agarwal, S.; Eijkman, D.; Vandamme, W.; Creatore, M.; van de

Sanden, M. C. M. *J. Vac. Sci. Technol. A* **2005**, *23*, 1400.

(17) Belau, L.; Wheeler, S. E.; Ticknor, B. W.; Ahmed, M.; Leone, S. R.; Allen, W. D.; Schaefer, H. F. III; Duncan, M. A. *J. Am. Chem. Soc.* **2007**, *129*, 10229.